Mercury Open Water Final Report for Compliance with the Delta Mercury Control Program

Executive Summary

Submitted August 31, 2020 by:

The Open Water Workgroup

The Open Water Mercury Technical and Modeling Workgroup

Executive Summary

Purpose of This Report

This report and its accompanying Technical Appendices, are submitted to the Central Valley Regional Water Quality Control Board by the Open Water Workgroup in fulfillment of open water reporting requirements for Phase 1 of the Delta Mercury Control Program (DMCP). The Workgroup consists of staff from the California Department of Water Resources (DWR), California State Lands Commission, Central Valley Flood Protection Board, United States Army Corps of Engineers, and United States Bureau of Reclamation.

Open water is defined in the DMCP as the methylmercury load that fluxes to the water column from sediments in open water habitats within channels and floodplains in the Delta and Yolo Bypass. Open water allocations encompass three activities: 1) water conveyance operations that may impact Delta in-channel methylmercury ([e.g., operations of the State Water Project and Federal Central Valley Project]; 2) production of methylmercury in the Yolo Bypass floodplain inundated by managed floodplain flows; and 3) regulatory or management oversight of activities proposed within open water areas. The DMCP lays out an implementation strategy for the control of methylmercury and total mercury in the Delta and Yolo Bypass.

The foundation of this report is based on a workplan and an accompanying technical memorandum approved by the Regional Board in February 2014. A characterization approach was approved due to the complexity of the system and the infeasibility of altering operations of the State and Central Valley Water Projects for control study purposes.

One goal of this project was to develop two mercury models for open water areas of the greater Delta and the Yolo Bypass. An existing proprietary mercury model, the Dynamic Mercury Cycling Model (D-MCM) (EPRI, https://www.epri.com/#/pages/product/3002002518/?lang=en-US, accessed 9/10/19) was applied to the Yolo Bypass. For mercury modeling of the remaining Delta system, the ability to simulate mercury and suspended/bed sediments was added to an existing DWR 1-D model, the Delta Simulation Model 2 (DSM2; https://water.ca.gov/Library/Modeling-and-Analysis/Bay-Delta-Region-models-and-tools/Delta-Simulation-Model-II, accessed 9/10/19). For the Yolo Bypass D-MCM, the parameter estimation software (PEST ++) (Model-Independent Parameter Estimation and Uncertainty Analysis; http://www.pesthomepage.org/, accessed on 7/6/20) software package was used to fine-tune the manual calibration, and optimize parameter estimates. DWR is in the process of making modeling data available publicly. When packaged for public release, DWR will publish model source code, executable files, and other information on the DSM2 website (https://water.ca.gov/Library/Modeling-and-Analysis/Bay-Delta-Region-models-and-tools/Delta-Simulation-Model-II, accessed 7/29/20). The Yolo Bypass D-MCM model source code is not available publicly. However, the approach to mercury cycling in D-MCM has been published (Harris and others, 2012, Hudson and others, 1994). In addition to Technical Appendix G, which provides details on model development, assumptions, calibration, and sensitivity runs, any model input and output information is available on specific request.

Because available mercury data for the Yolo Bypass was limited, a second project goal was to conduct field and laboratory studies to characterize and quantify major mercury and methylmercury sources and

flows using a geochemical mass balance approach. This information would provide critically needed parameterization data for the development of the Yolo Bypass D-MCM.

Sediment erosion studies provided the model with erosion values for different land-use types and sediment-water exchange flux experiments were used to estimate mercury diffusive flux into overlying waters for various land types. Vegetation senescence studies of pasture land in the Yolo Bypass during a flood event investigated MeHg contributions from decaying vegetation and led to possible approaches for a future Best Management Practices for pasture lands. Samples collected from import and export sites allowed mass balance calculations for the Yolo Bypass and provided data on the relative contributions of total, filter-passing, and particulate analytes. The mass balance information was not used directly by the model as sampling occurred outside of the modeled time period; however, it provided a valuable check on model patterns.

Key Highlights-Technical Studies in the Yolo Bypass

Over the course of the sampling period, the state of California experienced a severe drought in Water Years (WYs) 2013-2016, however WY 2017 was the second wettest year in a 122-year record. For the mass balance study, only one small event in 2014 and one larger event in 2016 was captured; nine events were sampled in 2017. Therefore, mass balance results focus on samples collected in WY 2017.

Mass balance sampling built upon previous sampling efforts by sampling unfiltered mercury (Hg) and methylmercury (uMeHg), filter-passing Hg (fHg) and MeHg (fMeHg) and particulate Hg (pHg) and MeHg (pMeHg). This allowed greater exploration of patterns associated with floodwater dynamics. This included examining MeHg and Hg dynamics by dividing the Yolo Bypass into two sections—the upper reach, from the top of the Fremont Weir to the stairsteps and the lower reach from the stairsteps to the base of Liberty Island (Figure EX-1).

Figure EX-1 Yolo Bypass Schematic Map
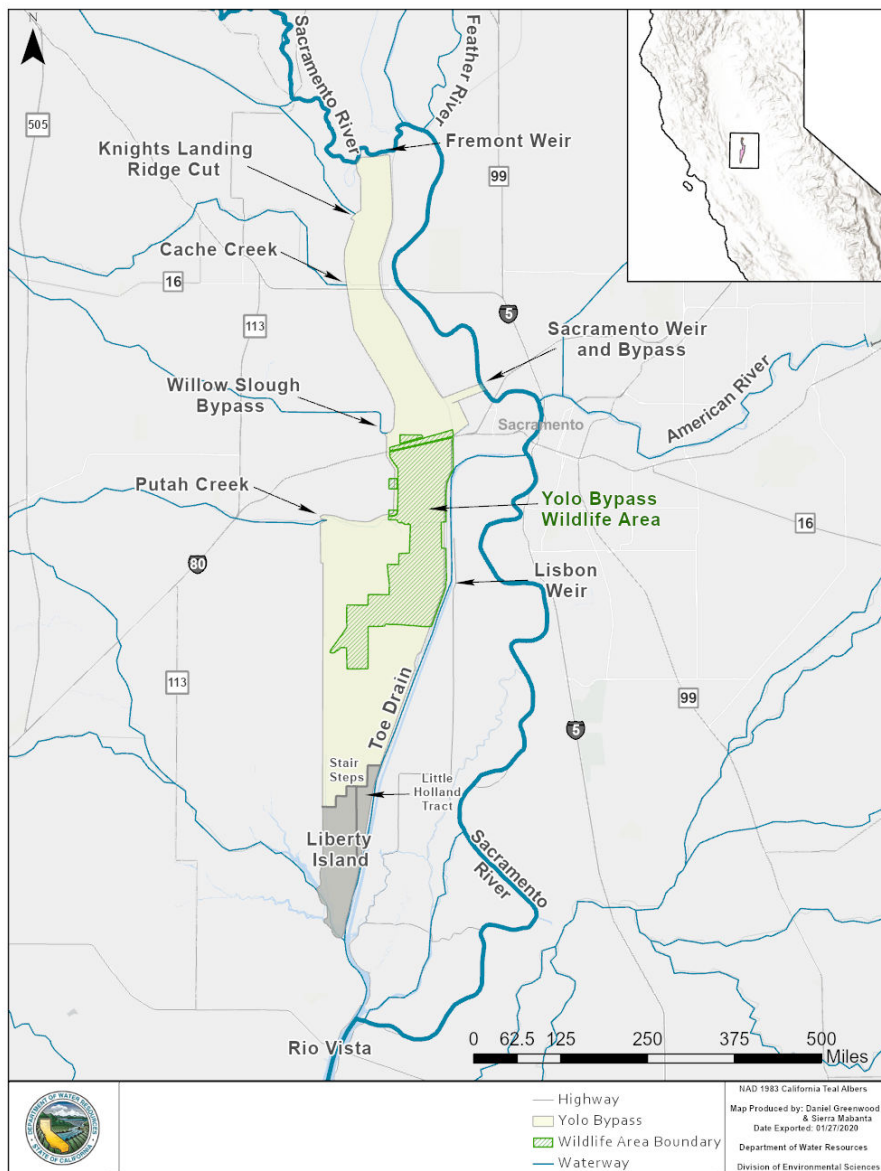
Mass balance work corroborated previous work that the Yolo Bypass was a net source of MeHg, but also showed that most of the generation of MeHg occurred in the upper reach of the Yolo Bypass. On average, the upper reach of the Yolo Bypass was a net sink for all fractions of Hg and a net source for all fractions of MeHg. The entire Yolo Bypass was a net sink for uHg and a net source for uMeHg (Figure EX-2). The upper reach between the inlets and the stairsteps supplied 79% of the total amount of MeHg produced within the Bypass, the majority being in the particulate form; the majority of Hg was also in the particulate form. When the Fremont Weir was spilling, it was the dominant tributary input of water flow and loads of all parameters to the Yolo Bypass, though some uncertainty in the individual load estimates impedes our ability to close with certainty the mass balance. Nevertheless, given this caveat, the mass balance shows reasonable closure, suggesting that the major loads have been identified.
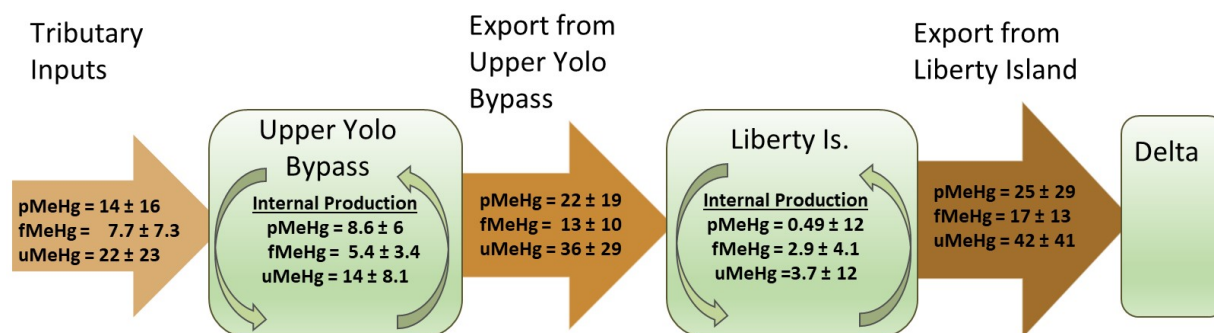
Figure EX-2 Mass Balance of MeHg (g/day) in the Yolo Bypass for WY 2017

Figure Notes: pMeHg = particulate methylmercury. fMeHg = filter-passing methylmercury. uMeHg = unfiltered methylmercury. Internal production fluxes were determined by averaging the net difference (output – input) determined for each individual sampling event. Thus, the average flux for the internal production does not simply represent the difference between the average output flux minus the average input flux.

Spatially, MeHg concentrations increased as water moved from the Fremont Weir in the north, to the stairsteps in the south. No such increase was observed for Hg or other analytes. Additionally, the quality of the MeHg changed as water moved from north to south, with more MeHg becoming associated with particles and the particles becoming more organic in nature.

Several notable temporal trends emerged. First, for samples collected from the Fremont Weir and Putah Creek, a first flush effect was observed for uMeHg concentrations. This was not observed at other tributaries. First, at Fremont Weir, increased loads in the first flush event were driven both by high flows and high concentrations. Second, at the Cache Creek Settling Basin (CCSB), the highest concentrations were observed at the lowest flows. The results at the CCSB mirrored those observed in a previous CalFed study (see Chapter 3 and Technical Appendix B, Foe and others, 2008). Third, over the course of the 2017 sampling season (from the beginning of January through the end of April 2017), the dominant fraction of MeHg changed from being predominantly filter-passing to predominantly particulate with time. Fourth, the quality of the MeHg appeared to shift from less organic to more organic as water moved south.

Of the 14 ± 8.1 g/day of net internal MeHg production observed in the upper reach of the Yolo Bypass (Figure EX-2), approximately 5.04 ± 1.56 g/day can be accounted for by open water sediment-water exchange flux of filter-passing methylmercury. Note that this sediment-water flux estimate was determined based on short duration (~ 1 day) experiments and therefore they may not represent the flux over a 4-month flood event, such as occurred in WY 2017. Additionally, a number of assumptions went into upscaling the experimental value to sediment-water flux for the full Yolo Bypass. Given these caveats, this estimate of open water sediment flux leaves approximately 9 g/day of internal methylmercury production within the upper Yolo Bypass unaccounted for, strongly suggesting that there is another unidentified internal source. Note that our experiments were unable to translate MeHg contributions from erosion or consider possible increased shear forces associated with post-first flush flooding events or resuspension and deposition of external sediment loads. Therefore, the contributions from these sources were not included and require further study. However, sediment erosion studies determined that there was little erosion associated with pasture lands, the largest land use in the Yolo Bypass, therefore this component was not added to our conceptual model of sources.

Mass balance patterns suggested that organics could be one source of the unaccounted 9 g/day of internal MeHg production in the upper reach. Vegetation senescence mesocosm experiments, simulating floodwater inundation of pasture lands (the largest managed vegetation source in the Yolo Bypass), consistently showed that disking vegetation into the sediment resulted in significantly less fMeHg production than sediments with standing rye grass vegetation.

Integrating the results from mass balance and sediment-water flux studies with the vegetation senescence experiments provided a conceptual model for the contributions of decaying vegetation to MeHg production under floodwater inundation. This suggested that vegetation senescence effectively balanced the internal production of uMeHg determined from the mass balance study (within the uncertainty of the load calculations).

Production of methylmercury in decaying emergent vegetation released an estimated 7.8 ± 1.8 g/day of filter-passing (3.0 ± 0.7 g/day) and particulate (4.8 ± 1.1 g/day) methylmercury to flood waters. The sum of pasture sediment-water flux of filtered (1.4 ± 0.8 g/day) and particulate methylmercury (2.2 ± 1.3 g/day), combined with the release of methylmercury from decaying vegetation, introduced 11.4 ± 7.8 g/day of methylmercury. Our work could not adequately quantify the pMeHg contributions of erosion, deposition, and resuspension of solids and could only estimate the pMeHg contributions from sediment-water exchange and vegetation senescence. The importance of pMeHg in the Yolo Bypass is not currently understood or quantified.

Our work also highlighted the distinction between fresh and senescent vegetation in producing MeHg. One vegetation senescence experiment estimated that fresh vegetation produced a higher flux of fMeHg to overlying water than the dry vegetation even though the fresh vegetation biomass was only 40% of the dried vegetation. This example illustrates the compounding difficulty of understanding the effects of removing vegetation via grazing and the potential differences associated with vegetation age/condition on MeHg production and the flux of fMeHg to overlying waters.

Vegetation senescence study results suggest that reducing the amount of standing winter vegetation may play an important role in reducing methylmercury loads. Removing the decaying vegetation in all the pasture lands of the Yolo Bypass, estimated to produce 1710 ± 560 g for the 2017 flood event, could decrease methylmercury loads more than the 833 g/year load reduction required by the DMCP. However, given the assumptions associated with experimental values, more study is required to fully quantify vegetation numbers.

Executive Summary

Key Highlights- Modeling Studies

An overview of key points and model capabilities is provided below in Table EX-1. While the model domains of the two models are provided in Figure EX-3.

Table EX-1 Synopsis of Key features of the Yolo Bypass D-MCM and Delta DSM2-Hg Model Analyses

	Yolo Bypass Mercury Model	Delta Mercury Model
Model name	Dynamic Mercury Cycling Model (D-MCM)	Delta Simulation Model version 2 (DSM2-Hg)
Forms of Mercury Modeled	Methylmercury Hg(II) Elemental mercury	Methylmercury Hg(II) Elemental mercury
Model Domain	Yolo Bypass from Fremont Weir to the base of Liberty Island Focused on areas upstream of stairsteps	Open water channels in the Sacramento - San Joaquin Delta between Sacramento, Vernalis and Martinez. Emphasis on results upstream of Chipps Island
Study Period	October 1996 to May 2012	Oct 1999 to July 2006
Time Step	Seconds to hours	15-minutes
Connection between Yolo Bypass and Delta	Simulated export of sediments, Hg(II) and MeHg from Yolo Bypass at stairsteps used as input to the Delta Hg model	Simulated export of sediments, Hg(II) and MeHg from Yolo Bypass at stairsteps used as input to the Delta Hg model
Potential Future Applications	Examine sensitivity of Delta Hg concentrations to changes in flows, climate, boundary concentrations, etc. Replicate historical conditions, fill data gaps, explore spatial patterns.	Scenario testing (options to reduce MeHg supply) Address data gaps using coordinated field and modeling studies Improved characterization of spatial and temporal patterns for Hg and MeHg cycling and supply in Delta Sensitivity of Delta Hg/MeHg concentrations to changes in flows, etc.

Note: future studies require other resources and may involve running other models, such as reservoir operations models

Figure EX-3 Model Domains for the Yolo Bypass and Delta Models and Inflow and Outflow Locations for the Delta Model. Inset shows location of data transfer at the stairsteps (bold red-line in insert) from the Yolo Bypass model to Delta Model.
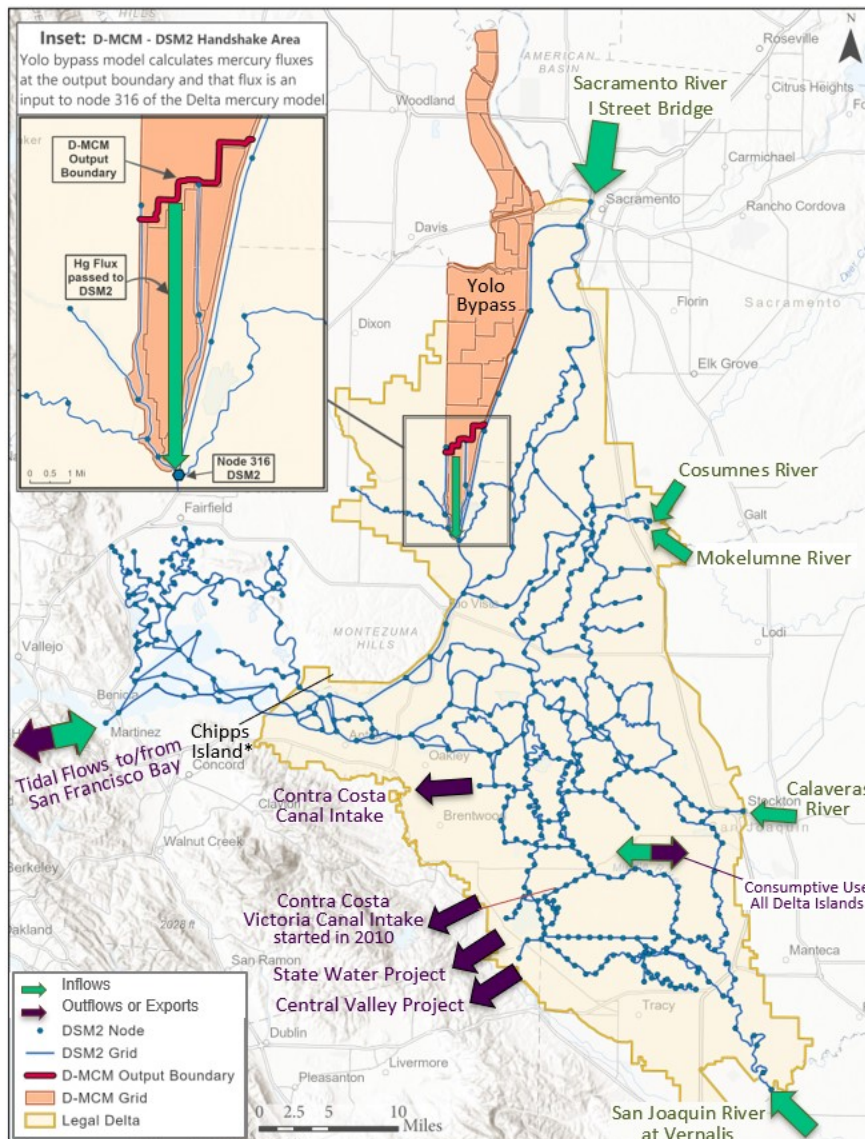
Yolo Bypass Model Results

The model estimated that the Yolo Bypass was a net source for uMeHg from October 1996-May 2012, via sediment production and the associated flux to overlying waters. Modeled uMeHg export loads at the stairsteps (all exports are reported at the stairsteps) were roughly twice the tributary load for the simulation period. The net load of MeHg to water passing through the Yolo Bypass, i.e. the difference between outflow and inflow fluxes, was approximately 1000 g/yr. Most of this net load occurred during the wet season, when more of the Yolo Bypass was flooded, and flows were greater. The Yolo Bypass model simulations in this study did not include WY 2017, so direct comparisons cannot be made between model results and the mass balance study. However, the model average for the same date range (January

11 – April 25), for years classified as wet (2017 was a wet year), was 18 g/day (range 11-32 g/day among these wet years). For the overall simulation period, the Yolo Bypass was a net trap for inorganic Hg, with 20% less exported at the stairsteps than was loaded from tributaries. Similarly, the Yolo Bypass was a net sink for sediment. Trapping efficiency tended to be greater in drier years.

The total amount of flow and the relative contributions of different water sources varied by an order of magnitude or more among the simulated years. For the simulation period, the Fremont Weir was the largest tributary contributor to water, suspended sediments, and uMeHg, followed by the CCSB. The Fremont Weir contributed approximately half of the uMeHg tributary load, followed by Cache Creek Settling Basin at approximately one third. Together, these two sources represented more than 80% of the total tributary uMeHg load for the simulation period. The CCSB was a slightly larger contributor of inorganic Hg, followed closely by the Fremont Weir (51% vs. 43%, respectively). However, the inorganic Hg load from the CCSB could be overestimated under high flow conditions. In wet years, the largest modeled external sources of suspended sediment were the Fremont Weir and the CCSB, with the Fremont Weir representing two thirds of the suspended sediment input to the Yolo Bypass. In wet years, contributions from the Knights Landing Ridge Cut were small, however, its importance increased in dry years, representing up to 90% of tributary sediment inputs. Direct atmospheric loading of inorganic Hg was small, less than three percent of tributary loads for the simulation period.

To examine potential MeHg reductions, nine simulations, developed in consultation with the Regional Board, were carried out to examine the sensitivity of model results to hypothetical 50% reductions to select model input values. Overall, the simulations reduced the predicted export of MeHg from less than 5% to roughly 20%. The largest decrease in MeHg exports (~20%) occurred by decreasing the conversion efficiencies of Hg(II) to MeHg in Yolo Bypass surface sediments. For some of the simulations, the lack of model response to various sensitivity reductions may have suggested that a simulation period of sixteen years was insufficient to observe a change in response. Simulated removal of all vegetation led to a reduction of approximately 60% in net MeHg production in Yolo Bypass sediments. However, surprisingly, removing vegetation by 50% resulted in less than a 5% decline in MeHg exports. These results reflect competing processes in the model, however, they may also reflect modifications required to allow the model to simulate vegetation effects, which may not fully capture real-world vegetation dynamics. Overall, the simulations and experimental evidence available suggest vegetation can have a strong influence on MeHg production in Yolo Bypass.

Delta Modeling Results

The model was calibrated for suspended sediments, Hg (II), and MeHg. Overall, the model calibration results reasonably fit observations of suspended solids, uHg(II), f(Hg (II), uMeHg, and fMeHg in Delta waters.

During the model study period, the Sacramento River was generally the largest inflowing source of uHg(II) and MeHg to the Delta (71% and 52% respectively). The relative importance of tributaries as sources of Hg and MeHg also varied from year to year. Yolo Bypass represented about one third of the external supply of MeHg to the Delta for the overall simulation period, but this ranged from 3-50% among the years simulated. Under some high-flow months, the Yolo Bypass was the largest external source of MeHg to the Delta. Annual freshwater inputs of uHg(II) and uMeHg each varied by approximately 6-fold for water years 2000-2006.

The largest simulated Delta outflows of uHg(II) and uMeHg were exports at Chipps Island (89% and 85% respectively). The Delta was simulated to be a net long-term sink for uHg(II) and uMeHg, exporting roughly half the inflowing load of uHg(II) and 80% of the inflowing uMeHg load (see Chapter 5).

The model was used to explore spatial and temporal patterns of concentrations for suspended sediments, uHg(II) and uMeHg for high, median, and low flow conditions during the Hg calibration period. For the highest flow in the Sacramento River and the Yolo Bypass, suspended sediment and uHg(II) concentrations were higher on the periphery of the Delta and lower in the Central Delta. This pattern was not evident for uMeHg. Similar patterns were not observed under median and low flows. These patterns represent one snapshot in time; further investigation would be required to see if these patterns are consistent under similar flow conditions.

Estimates of simulated open water sediment fluxes were similar to those developed for CalFed; the model estimated Delta open water sediment flux at 0.42 g/day compared to 0.48 g/day in a 2008 CalFed report (see Chapter 3 and Technical Appendix B, Foe and others, 2008).

Management Implications

Technical Studies

Managing vegetation as a key component of reducing winter internal Yolo Bypass methylation has important management considerations and provides a starting point for future open water control studies and development of Best Management Practices (BMPs).

Vegetation senescence experiments suggest that controlling above-ground vegetation mass may be an effective mechanism to control methylmercury production and release to overlying waters during a flood event. Disking vegetation into the soil appears to be a promising approach to reduce the internal production of MeHg in the Yolo Bypass. Controlling vegetative biomass by grazing gave mixed results. The dynamics between vegetation quality, quantity, and vegetation type requires further investigation before grazing as a BMP can be proposed. While not examined, selective flooding of pastures in the fall, prior to the winter flood season, may be another approach to reduce or remove the standing biomass of vegetation and reduce methylmercury production from vegetation during a flood event.

With any of these approaches, it is important to note that DWR is not a landowner in the Yolo Bypass, therefore any changes in land use practices are outside its jurisdiction and must be pursued by the Regional Water Quality Control Board. Any proposed BMP will need to be evaluated holistically within the full context of the environment that the BMP would be used. It is recommended that before additional studies are conducted, landowners and agencies, such as the Resource Conservation Districts, will need to be consulted to determine if the ecological and cost-benefit impacts, associated with potential land use management approaches, are reasonable or practical.

Much attention has been placed on the Cache Creek Settling Basin (CCSB) and its contributions of inorganic Hg and MeHg to the Yolo Bypass. However, our coarse estimates of MeHg mass generated from decaying vegetation suggests that reductions in vegetation biomass could substantially help with the Yolo Bypass load allocation reduction required in the DMCP.

Modeling Studies

Modeling frameworks were successfully developed for both the Yolo Bypass and the Delta. Comparison of simulated results to field observations suggest that the models are successfully reproducing patterns and trends, providing a meaningful, but coarser perspectives, rather than a tightly-constrained analysis. The analysis was constrained by a combination of limited data and knowledge gaps regarding some key processes operating in the Yolo Bypass. To extend the models' usefulness and to improve modeling results, additional data is needed to better characterize inflowing loads and within-system conditions in the Delta and the Yolo Bypass for a range of hydrologic conditions and a range of years. Needed data includes measurements of inorganic Hg and MeHg in unfiltered, particulate, and filtered phases in tributaries, the water column, and sediments of the Delta and the Yolo Bypass, as well as ancillary data such as water chemistry (e.g. suspended sediment concentrations, dissolved organic carbon, pH, temperature) and sediment characterization.

The dynamic nature of flow in the Delta and Yolo Bypass resulted in a high degree of variability in simulated uHg(II) and uMeHg concentrations, inflowing loads and export rates in the short term (e.g. daily) and longer term (e.g. annually). This has important implications when estimating present-day baseline loads, assigning load allocations, and monitoring for compliance with regulations in the future. A multi-year perspective is needed, designed to capture year to year variability, but with sufficient resolution to also capture short term variability (or not be biased by it), and show longer term systematic trends that might occur (e.g., via climate change). It is recognized that characterizing the spatial and temporal patterns in a system as large and heterogeneous as the Delta/Yolo Bypass is a large effort. A carefully coordinated program would be required, and options should be considered to use automated or surrogate sampling techniques where possible (e.g. continuous turbidity data to estimate suspended sediment concentrations). In the Yolo Bypass, the spatial coverage of sampling should reflect the various land uses and include vegetation-related parameters where appropriate.

Moving forward, the ability to model a variety of operational scenarios would be improved by developing a single publicly available hydrodynamic and Hg model for both the Delta and the Yolo Bypass. Additionally, given the important role that vegetation appears to play in MeHg production in the Yolo Bypass, model enhancements should include an improved treatment of vegetation where applicable. Since bioaccumulation in fish is the driver of the DMCP, consideration should be given to adding a bioaccumulation component to the model framework. Similarly, since model analysis indicated that tributary inflows have a strong influence on mercury concentrations in the Delta, consideration could be given to the merits and cons of a model analysis extending upstream and/or downstream of the legal Delta. However, the confidence associated with a model analysis carried out with improved tools would still be limited by the level of data currently available. Therefore, model refinements and data collection efforts need to occur in parallel.

Mercury Open Water Final Report for Compliance with the Delta Mercury Control Program

Chapter 1. Report Organization and Background

Submitted by the Open Water Workgroup

August 31, 2020

Mercury Open Water Final Report Preparers

The Open Water Workgroup

California Department of Water Resources — Division of Environmental Sciences

Carol DiGiorgio
David Bosworth

California State Lands Commission

Cynthia Herzog

Central Valley Flood Protection Board

Nancy Moritz
Itzia Rivera

U.S. Army Corps of Engineers

Cory Koger

U.S. Department of the Interior, Bureau of Reclamation

Michael Mosley
Jobaid Kabir

The Open Water Mercury Technical Workgroup

Pacific Northwest National Laboratory

Gary Gill

San Jose State University, Moss Landing Marine Laboratories

Wesley Heim
Mark Stephenson

U.S. Geological Survey — California Science Center

David Schoellhamer
Paul A. Work

The Open Water Mercury Modeling Workgroup

Reed Harris Environmental Ltd.

Reed Harris
David Hutchinson
Matt Gove
Cody Beals
Don Beals

California Department of Water Resources — Bay Delta Office

Prabhjot Sandhu
Ali Abrishamchi
Jamie Anderson
Hans Kim
Kevin He
En-Ching Hsu
Kijin Nam
Hari Rajbhandari
Min-Yen Yu
Tara Smith
Eli Ateljevich

U.S. Geological Survey — Upper Midwest Science Center

Randy Hunt

Mercury Open Water Final Report Acknowledgments

Mercury Open Water Final Report for Compliance with the Delta Mercury Control Program

Executive Summary

Chapter 1: Background and Report Organization

Chapter 2: Non-DWR Open Water Workgroup Activities

Chapter 3: Yolo Bypass Mercury Scientific Studies

Chapter 4: Yolo Bypass Mercury Modeling Studies

Chapter 5: Delta Mercury Modeling Studies

Chapter 6: Climate Change Impacts

Chapter 7: Conclusions-Management Implications

Technical Appendices

Technical Appendix A: Approved Modifications to Workplan/Technical Memorandum and Original Workplan and Technical Memorandum

Technical Appendix B: Yolo Bypass Mass Balance Study

Technical Appendix C: Sediment-water Exchange of Mercury and Monomethylmercury by Land Use Within the Yolo Bypass

Technical Appendix D: Gust Chamber Erosion Study

Technical Appendix E: Vegetation Studies-Investigations into the Role of Vegetation and Land Management Practices in Producing Monomethyl Mercury from Flooded Pasture Land in the Yolo Bypass

>   *Technical Appendix E1: Compilation of Supplementary Data for Technical Appendix E: Vegetation Studies*

Technical Appendix F: Sediment Sample Collection in the Yolo Bypass to Characterize Mercury, Methylmercury and Grain Size Distribution-Data Appendix

Technical Appendix G: Yolo Bypass Mercury and Methylmercury Modeling Studies

Technical Appendix H: Parameter Estimation Studies

Technical Appendix I: Delta Mercury and Methylmercury Modeling Studies

Technical Appendix J: Delta Suspended and Bed Sediment Modules

Contents

Tables

Figures

Acronyms and Abbreviations

|	
BMP	best management practice
CVRWQCB	Central Valley Regional Water Quality Control Board
Delta	Sacramento-San Joaquin Delta
D-MCM	Dynamic Mercury Cycling Model
DSM2	Delta Simulation Model 2
DWR	California Department of Water Resources
Hg	mercury
MeHg	methylmercury
PEST++	parameter estimation and uncertainty analysis
uHg	unfiltered mercury
Workgroup	Open Water Workgroup
Yolo Bypass D-MCM	Yolo Bypass Dynamic Mercury Cycling Model

Background

The Sacramento-San Joaquin Delta (Delta) is the largest estuary on the West Coast, consisting of 700 miles of sloughs and waterways. The major rivers that feed the system are the Sacramento, Mokelumne, Cosumnes, Calaveras, and San Joaquin rivers. Of these rivers only the Cosumnes flows into the Delta unobstructed by dams. The Delta receives the runoff from 40 percent (60,000 square miles) of California's land and is the hub of the State's two largest surface water delivery systems, the State Water Project and the federal Central Valley Project. During major flood events the Delta receives runoff from the Yolo Bypass, a 59,000-acre managed floodway that protects the city of Sacramento from floodwaters.

Since 1990, the Delta has been on the State Water Resources Control Board's list of impaired waters for mercury under section 303d of the Clean Water Act because of elevated fish tissue levels of mercury, which pose a risk for human and wildlife consumers. The sources of mercury contamination in the Delta and Yolo Bypass are complex; but, legacy mercury and gold mining within the watershed are considered large contributors to the mercury contamination observed in these areas today. Mercury was mined from naturally occurring deposits in California's Coast Range and was transported to the Sierra Nevada gold fields of the 1800s, where it was used to recover gold (Alpers and others 2005). In the gold fields, it is estimated that 10 million pounds of mercury was lost in placer mines, of which 80 percent to 90 percent were in the Sierra Nevada. In hardrock mines, where gold ore was crushed in stamp mills, approximately 3 million pounds of mercury was lost (Churchill 2000). The Feather River, as well as it's tributary watersheds (the Bear and the Yuba rivers) all drain areas associated with major legacy gold mining operations (Figure 1-1). The Sacramento River is the largest contributor of freshwater to the Delta system. During large storm events, it can also be the largest contributor of freshwater to the Yolo Bypass. Tributaries emptying into the Yolo Bypass also have their own source of legacy mercury contamination. For example, mercury mines are in the watershed of Cache Creek, which drains and empties into the Yolo Bypass via the Cache Creek Settling Basin (Cooke and Morris 2005).

Delta Mercury Control Program

Under the authority of the Clean Water Act and section 13240 of the Porter-Cologne Act, the California State Water Quality Control Board established a Sacramento/San Joaquin River Delta Total Maximum Daily Load (TMDL) and Delta Mercury Control Program as a result of Amendment No. R5-2010-0043 to the Water Quality Control Plan for the Sacramento and San Joaquin River Basins (Basin Plan). In November 2011, under the Delta Mercury Control Program (DMCP), the Central Valley Regional Water Quality Control Board (CVRWQCB) issued the California Department of Water Resources (DWR) a letter identifying DWR and several other State and federal agencies as causing or contributing to elevated levels of mercury (Hg) and/or methylmercury (MeHg) to the Delta or Yolo Bypass based on identified water and land use activities under each agency's jurisdiction. One source identified was open water which was defined in the DMCP as the MeHg load that fluxes to the water column from sediments in open water habitats within channels and floodplains in the Delta and Yolo Bypass (Central Valley Regional Water Quality Control Board 2011).

**Figure 1-1** Overview of Major Waterbodies in the Yolo Bypass and Greater Delta
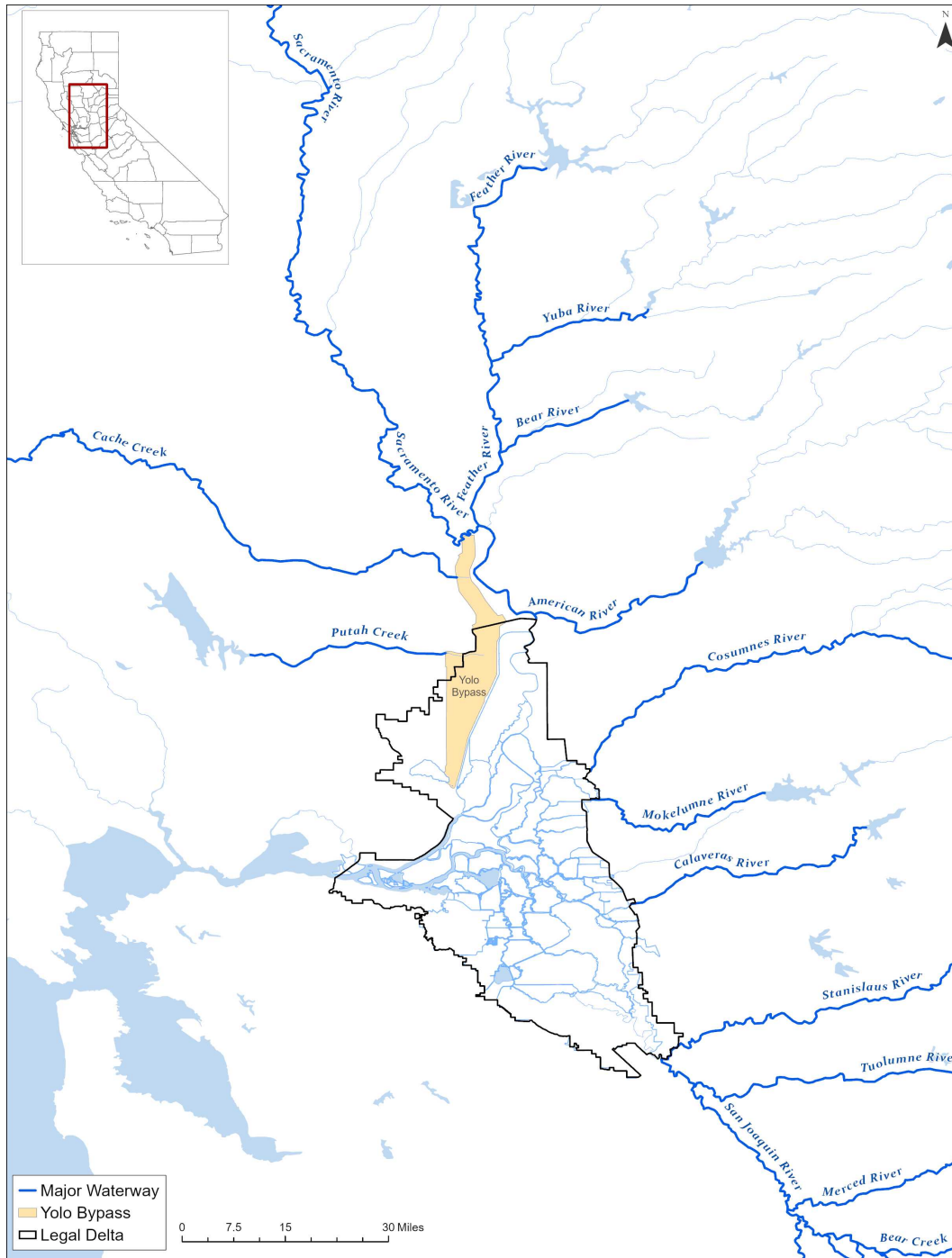
The legal Delta, and the Yolo Bypass when flooded, face significant MeHg contamination. As shown in Figure 1-2, large areas of the regulated area are out of compliance with the DMCP. Mandated reductions in MeHg from open water sediment flux for different regions of the Delta and the Yolo Bypass range from 0 percent to 82 percent (Table 1-1).

The DMCP lays out an implementation strategy for the control of MeHg and total unfiltered mercury (uHg). The regulation is designed to protect people eating one meal per week of trophic levels 3 and 4 Delta fish, plus some non-Delta (commercial market) fish (Central Valley Regional Water Quality Control Board 2011). As part of its implementation strategy, the DMCP requires regulated entities to conduct either control studies to evaluate existing (or new) control approaches to reducing MeHg, or characterization studies to provide information that could lead to new approaches to control MeHg. This report documents Department of Water Resources (DWR) scientific and modeling characterization studies and non-DWR Open Water Workgroup member's efforts to meet regulatory requirements associated with the open water portion of the DMCP.

Figure 1-2 **Methylmercury Compliance Areas for the Delta Mercury Control Program**
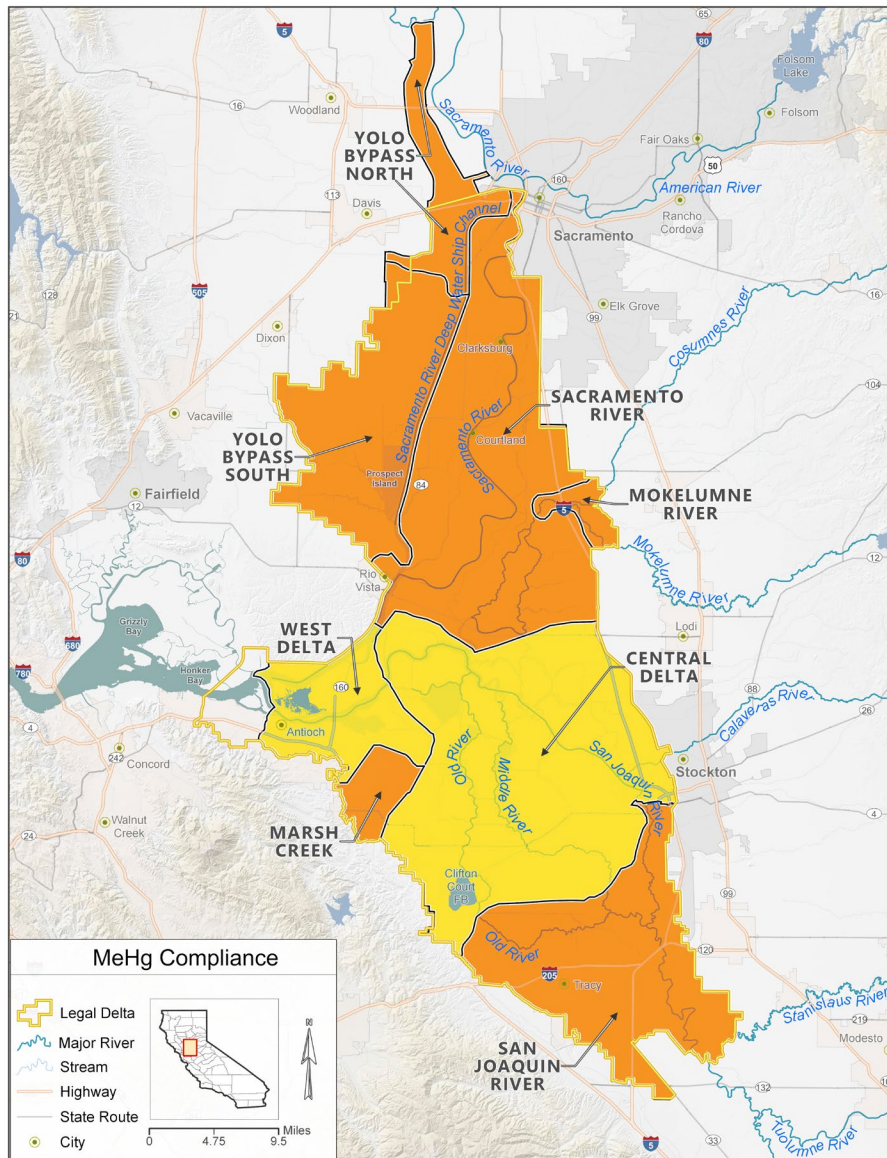
Table 1-1 Net Methylmercury Target Load Allocations (grams/year) and Necessary Percent Reductions to Meet Target Load Allocations for Open Water Areas of the Delta and Yolo Bypass

Open Water Area	Current Load	Allocation	Reduction
Central Delta	370	370	0%
Marsh Creek	0.18	0.03	82%
Mokelumne River	4.0	1.4	65%
Sacramento River	140	78	44%
San Joaquin River	48	17	65%
West Delta	190	190	0%
Yolo Bypass	100	22	78%

Note: Adapted from Table A, Attachment 1 to Resolution No. R5-2010-0043, (Central Valley Regional Water Quality Control Board 2011)

Overview of Activities

Open Water Workgroup

Affected stakeholders formed the Open Water Workgroup (Workgroup) to jointly address the open water portion of the Delta Mercury Control Program. Stakeholders consist of the State and federal agencies charged with reducing open water loads of MeHg. These agencies are: the State Lands Commission, DWR, the Central Valley Flood Protection Board, the U.S. Army Corps of Engineers and the U.S. Bureau of Reclamation.

In April 2013, the Workgroup submitted a workplan to the CVRWQCB. In response to comments a technical memo was submitted in October 2013. The technical memo revised originally proposed laboratory characterization studies to large-scale experimental ponds located in the Yolo Wildlife Area. In February 2014, the combined workplan and technical memo addendum was approved. The approved workplan and technical memo can be found in Technical Appendix A.

A characterization approach, as opposed to a control study, was approved because of the complexity of the system and the infeasibility of altering operations of the State and Central Valley Water Projects for control study purposes. The characterization studies consisted of field/technical studies and numerical modeling. Creation of an integrative model linking process-based studies, restoration activities, and monitoring was one long-term goal suggested by a panel of experts convened to advise the CALFED Bay-Delta Program on strategies and approaches to use to guide ecosystem restoration and management in the Hg contaminated Delta (Weiner and others 2003). DWR funded and led the technical and modeling studies summarized in the workplan/technical memo. Other Workgroup agencies focused on their areas of jurisdiction. Figure 1-3 provides an overview of how open water stakeholder activities fall within the overall DMCP regulation.

Open Water Characterization Studies
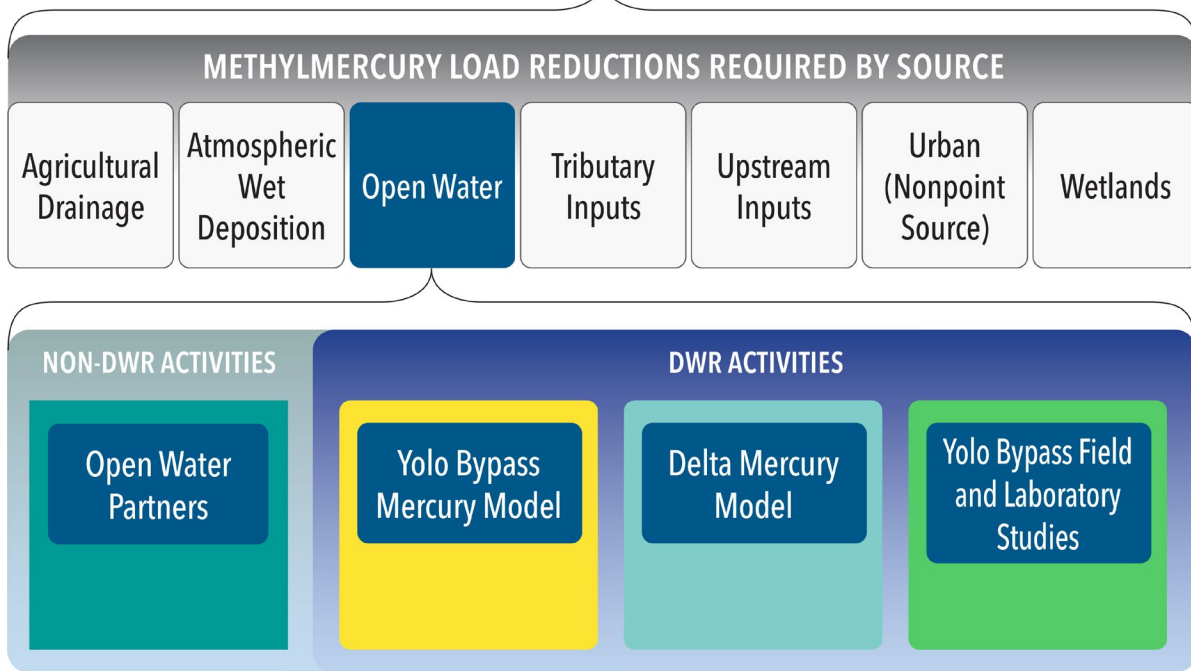
Field Characterization Studies

Models, in general, become more accurate and reliable when a significant abundance of data exists. Relative to the wealth of hydrodynamic and other water-quality data available for the Delta system,

Figure 1-3 Overview of the Open Water Workgroup Activities for Compliance with the Delta Mercury Control Program
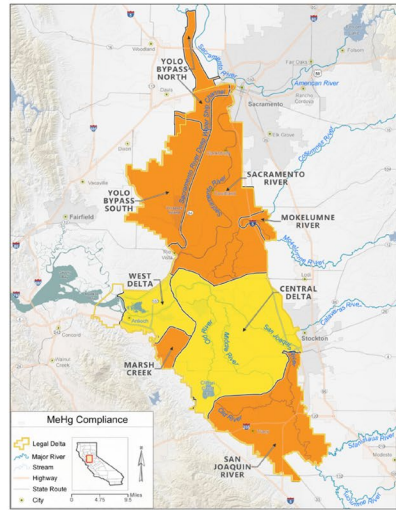
relatively little mercury and MeHg data exists; even less data is available for the Yolo Bypass. For example, comparatively little filtered or particulate MeHg data was available for the Yolo Bypass, yet the Yolo Bypass is a net producer of MeHg and can provide as much as 40 percent of the MeHg exported from the Sacramento basin when the Fremont weir is spilling (Foe and others 2008). As a result, field studies were conducted in the Yolo Bypass to meet model data needs and provide information for possible future best management practices (BMPs).

DWR contracted with several different groups and agencies in order to create and adapt new modeling tools for the Yolo Bypass and Delta, and to conduct field and laboratory studies for the Yolo Bypass. The Open Water Mercury Technical Workgroup consisted of researchers from the Moss Landing Marine Laboratory, who provided laboratory analysis and mercury technical support; the Pacific Northwest National Laboratory, who provided mercury, metals, and statistical technical support; and the U.S. Geological Survey, who conducted erosional studies. DWR scientists with the Mercury, Monitoring, and Evaluation Section were responsible for most sample collection, execution of some experimental studies, and statistical support. The Open Water Mercury Modeling Workgroup consisted of Reed Harris Environmental, Ltd. who developed a mercury module for the Delta and adapted a mercury model for use in the Yolo Bypass; the US. Geological Survey, who used the Parameter Estimation (PEST++) software package to refine manual model calibrations and bound model uncertainty; and DWR modelers with the Bay Delta Office, who provided in-house development of the suspended sediment module, animation tools used to visualize modeled results, and support for the consultant's development of the mercury and bed sediment modules in Delta Simulation Model 2 (DSM2).

The research teams focused on several data gaps identified for the Yolo Bypass Hg model. Sediment erosion studies provided the model with erosion values for different land-uses, while sediment-water flux experiments provided the model with diffusive flux from sediments of different land uses. Soil samples were used to provide starting Hg and MeHg soil concentrations for the model. The largest land use in the Yolo Bypass is pasture. To address this major land use, vegetation senescence experiments were conducted, and a vegetation component was added to the model. These studies permitted development of possible approaches for a future BMP for pasture lands. Samples collected from import and export sites of the Yolo Bypass allowed mass balance calculations for the system and provided data on the relative contributions of total, filtered, and particulate analytes. This information was not used directly by the model (sampling occurred outside of the modeled time period), but it provided a valuable check on model patterns.

The relationship between field characterization studies and Yolo Bypass modeling efforts are shown in Figure 1-5, while Table 1-2 shows the relationship between the research teams, the data gap addressed, and the appendices containing the full study write-ups. These technical appendices provide in-depth details on study design, methodology, and in-depth analysis of results. Data including Quality Control will be provided to staff of the Central Valley Regional Water Quality Control Board (CVRWQB). DWR staff are also working on publishing data to the Environmental Data Initiative (EDI) data portal.

Finally, following workplan/technical memorandum approval, the scope and approach of some studies evolved over time. This included returning to smaller scale mesocosm and laboratory-based approaches for many experimental studies, when the use of experimental ponds proved unfeasible, and reducing the scope of some studies because of time, safety, and resource constraints. But, modifications to study design remained consistent with the approved workplan/technical memorandum. The CVRWQCB staff were kept apprised of all changes. Modifications to the workplan/technical memorandum were approved by the CVRWQCB and are summarized in Technical Appendix A.

Model Development

At the time of model construction, there was no single hydrodynamic numerical model unifying the Delta and Yolo Bypass. After an evaluation of available modeling tools, two Hg models were developed to

characterize Hg dynamics in the Delta and Yolo Bypass. An existing proprietary mercury model, the Dynamic Mercury Cycling Model (D-MCM), was adapted for the Yolo Bypass (Electric Power Research Institute 2019). For the remainder of the Delta, mercury and sediment functions were added to DWR's DSM2, an existing, well-established 1-D model (California Department of Water Resources 2019), creating a final product known as DSM2-Hg. The full modeling domain of the two mercury models is shown in Figure 1-4.

For the Yolo Bypass model, following manual calibration, the PEST++ software package was used to fine-tune manual calibrations, optimize parameter estimates, and provide uncertainty analysis for sensitivity runs.

Figure 1-4 Domains for the Yolo Bypass D-MCM and Delta DSM2-Hg Models
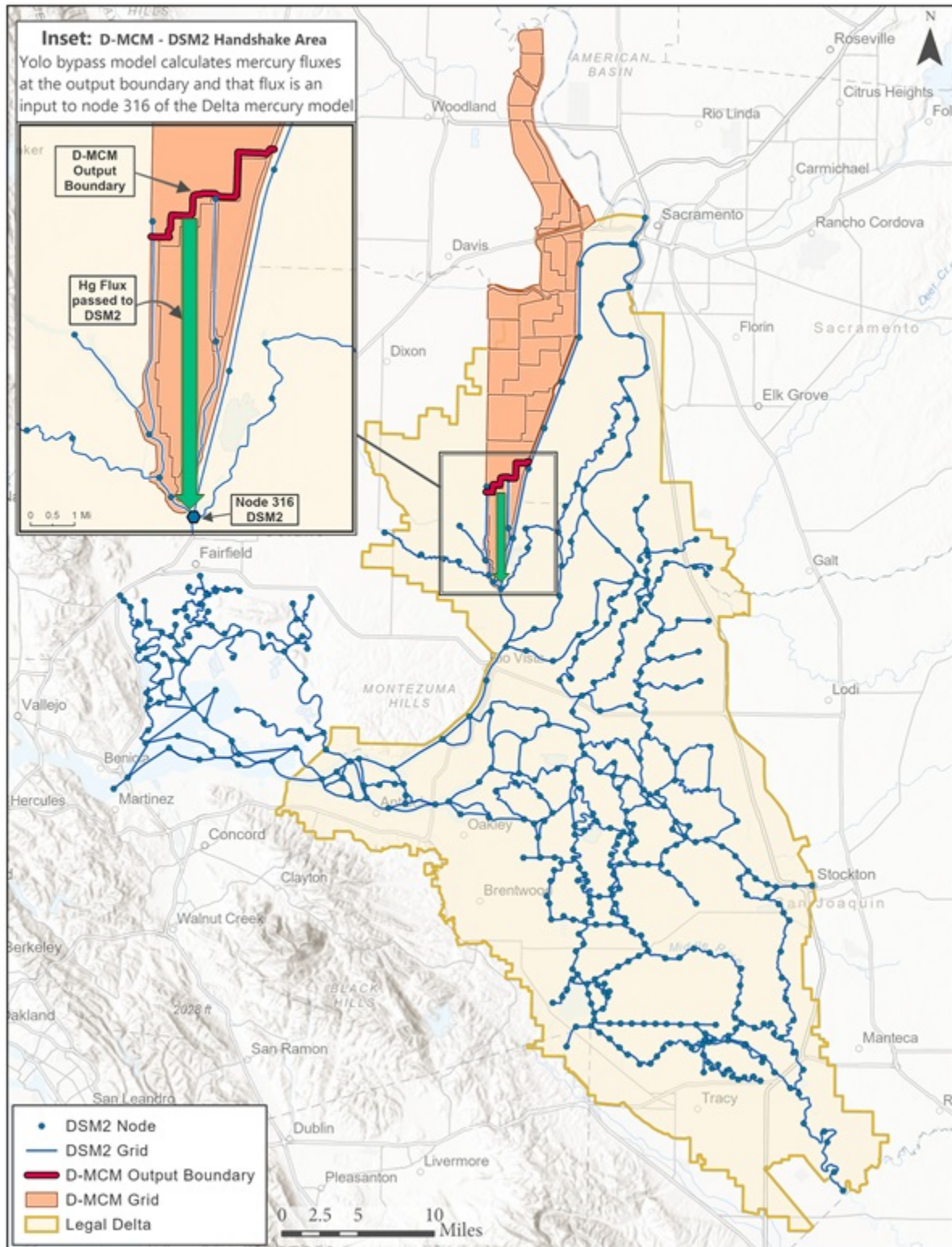
Notes: D-MCM = Dynamic Mercury Cycling Model, DSM2 = Delta Simulation Model 2

Model used for the Delta was the DSM2-Hg model and for the Yolo Bypass, the D-MCM model was adapted to the Yolo Bypass (Yolo Bypass D-MCM).

Table 1-2 **Relationship of Technical Studies to Yolo Bypass D-MCM Modelling Development**

Study	Model Data Gap	Research Team	Technical Appendix
Mass balance loading study (Yolo Bypass	Used as a check on model results and expanded upon CALFED mass load work by including collection of filter Hg and MeHg as well as samples collected below Liberty Island.	DWR	B
Sediment-water flux	Addressed Hg and MeHg flux from sediments of different land uses.	MLML	C
Gust chamber	Addressed soil erosion of different land uses under different flow velocities.	USGS	D
Vegetation Senescence	Addressed possible vegetation impacts associated with the largest actively managed land use and investigated possible BMPs.	DWR MLML	E & E1
Spatial soil sampling for mercury	Supplemented previous work (Heim and others 2010) to extend the spatial coverage of Hg and MeHg in soils of different land uses.	MLML DWR	F

Notes: BMPs = best management practices, CALFED = CALFED Bay-Delta Program, D-MCM = Dynamic Mercury Cycling Model, DWR = California Department of Water Resources, Hg = mercury, MeHg = methylmercury, MLML = Moss Landing Marine Laboratories, USGS = U.S. Geological Survey

Yolo Bypass Mercury Model Development

The objectives of the Yolo Bypass Dynamic Mercury Cycling Model (Yolo Bypass D-MCM) were to:

- Create a Hg and MeHg model for the Yolo Bypass that can predict fate and transport in the Yolo Bypass.
- Use the model to evaluate processes governing MeHg supply to the Yolo Bypass.
- Use the model to help evaluate whether there are operational changes or other strategies that can be implemented to reduce ambient MeHg concentrations in Yolo Bypass floodwaters.

The D-MCM v.4.0 is a proprietary Windows-based simulation model for personal computers and has been used to model Hg and MeHg biogeochemical cycling and bioaccumulation in a number of ecosystems including the Gulf of Mexico (Harris and others 2012). The model is a time dependent, mechanistic mass balance model for Hg cycling and bioaccumulation and is an extension of the D-MCM published by Hudson and others (1994). It simulates the cycling and fate of three major forms of mercury (methylmercury, inorganic Hg (II), and elemental mercury in aquatic systems. It is capable of simulating mercury for a wide range of 1-D to 3-D situations. Model compartments include one or more layers in the water column and sediments, macrophytes (where relevant), and a food web defined by the user. The

regulation required evaluation of open water sediment-water flux, as a result, only the sediment and water compartments of the model were used.

The D-MCM was adapted to the Yolo Bypass by creating a coarse resolution grid consisting of 47 cells defining the top eight land uses in the Yolo Bypass. Based on Hg and MeHg data availability, the period modeled was from October 1996 to May 2012. Hydrodynamics were provided by coupling the Yolo Bypass D-MCM to a TUFLOW hydrodynamic model developed to simulate flows for a separate DWR /USBR project in the Yolo Bypass (DOI/DWR, 2019). Outputs from the Yolo Bypass model at the downstream end of the domain provided boundary inputs for the Delta model (Figure 1-4). Figure 1-5 summarizes the different modeling components required to build the Yolo Bypass D-MCM. Technical Appendix G provides in-depth details on model assumptions and manual calibration results. Technical Appendix H provides details on the use of PEST++ for model calibration and sensitivity results. While D-MCM is a proprietary model the approach to mercury cycling in D-MCM has been published (Harris and others, 2012, Hudson and others, 1994). In addition to information in Technical Appendix G, any model input and output information, which is not proprietary are available on request.

Figure 1-5 Components Associated with the Adaptation of the D-MCM Model to the Yolo Bypass Including the Relationship Between the Model and Field/Lab Studies
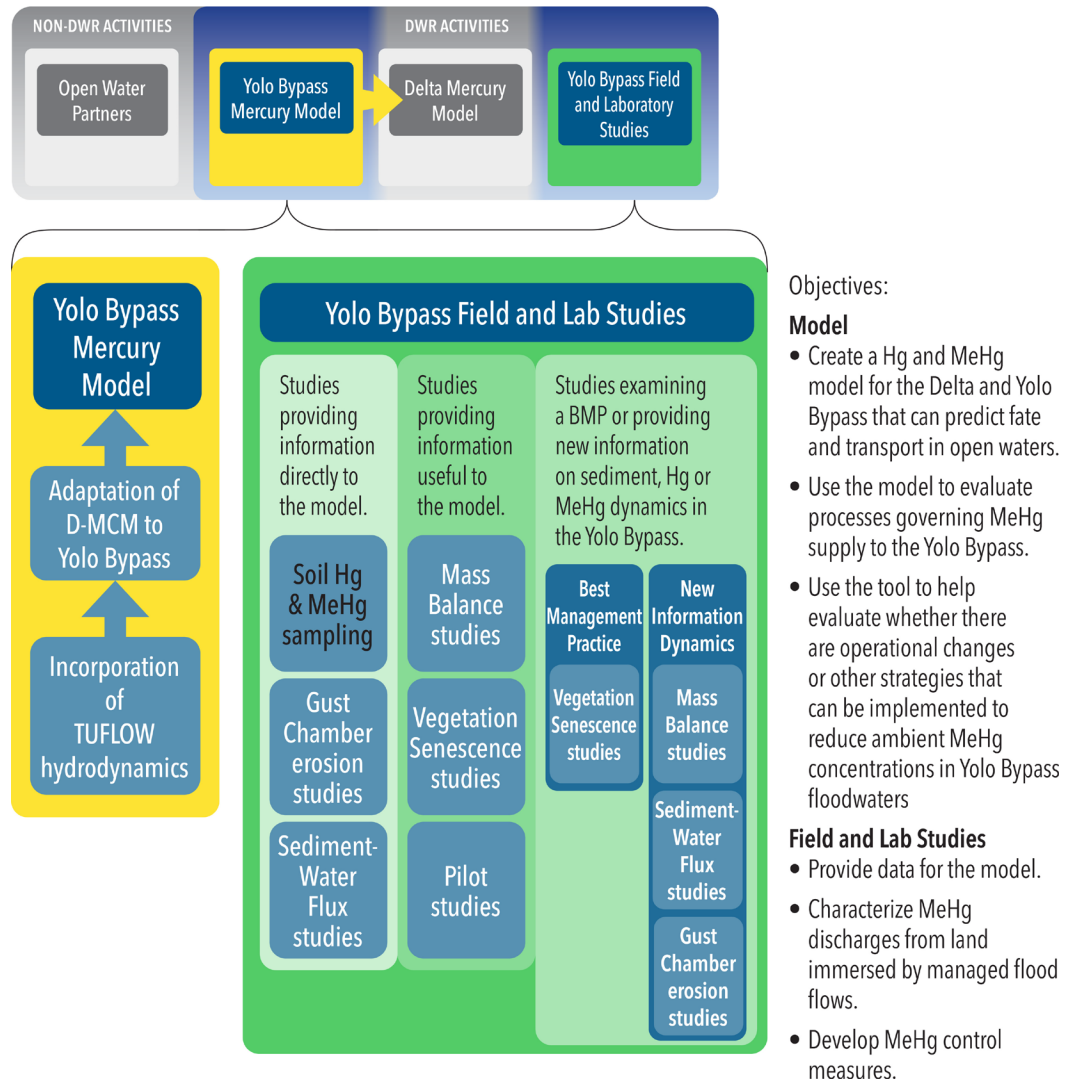
Notes: BMP = best management practice, D-MCM = Dynamic Mercury Cycling Model, DWR = California Department of Water Resources, Hg = mercury, MeHg = methylmercury

Delta Mercury Model Development

The Delta was modelled by integrating mercury and methylmercury production biogeochemistry into DWR's Delta Simulation Model 2-Mercury Model (DSM2-Hg). DSM2 also provided the hydrodynamics for the Delta. The DSM2-Hg model was created by adding equations for bed sediment, suspended sediment, and mercury as modules to DSM2. Yolo Bypass boundary fluxes from the Yolo Bypass D-MCM served as the Yolo Bypass input to DSM2-Hg (Figure 1-6).

The objectives of the DSM2-Hg model were to:

- Create a Hg and MeHg model for the larger Delta that can simulate fate and transport in the larger Delta system.

- Use the model to evaluate processes governing MeHg supply to the larger Delta.
- Use the model to help evaluate whether there are operational changes or other strategies that can be implemented to reduce ambient MeHg concentrations in the open waters of the larger Delta.

Figure 1-6 summarizes the different modules that were added to the DSM2 model. Similar to the Yolo Bypass D-MCM, the DSM2-Hg model simulates the cycling and fate of three major forms of mercury (methylmercury, inorganic mercury [II], and elemental mercury) in the water column. Tributary inputs and atmospheric deposition were inputted into the model which, in turn calculated open water sediment flux, photodegradation and water column concentrations. This effort provided the basic framework for mercury modeling. Based on the regulatory definition of the source of open water flux, the model focused on flux from the sediments and concentrations and loads of MeHg in the water. Technical Appendices I and J provide in-depth details on data sources, model assumptions, and calibration results for the mercury model and bed and suspended sediment models. When packaged for public release, DWR will publish model source code, executable files, and other information on the DSM2 website (DWR, 2020).

Figure 1-6 Components Associated with the Development of the DSM2-Hg Model.
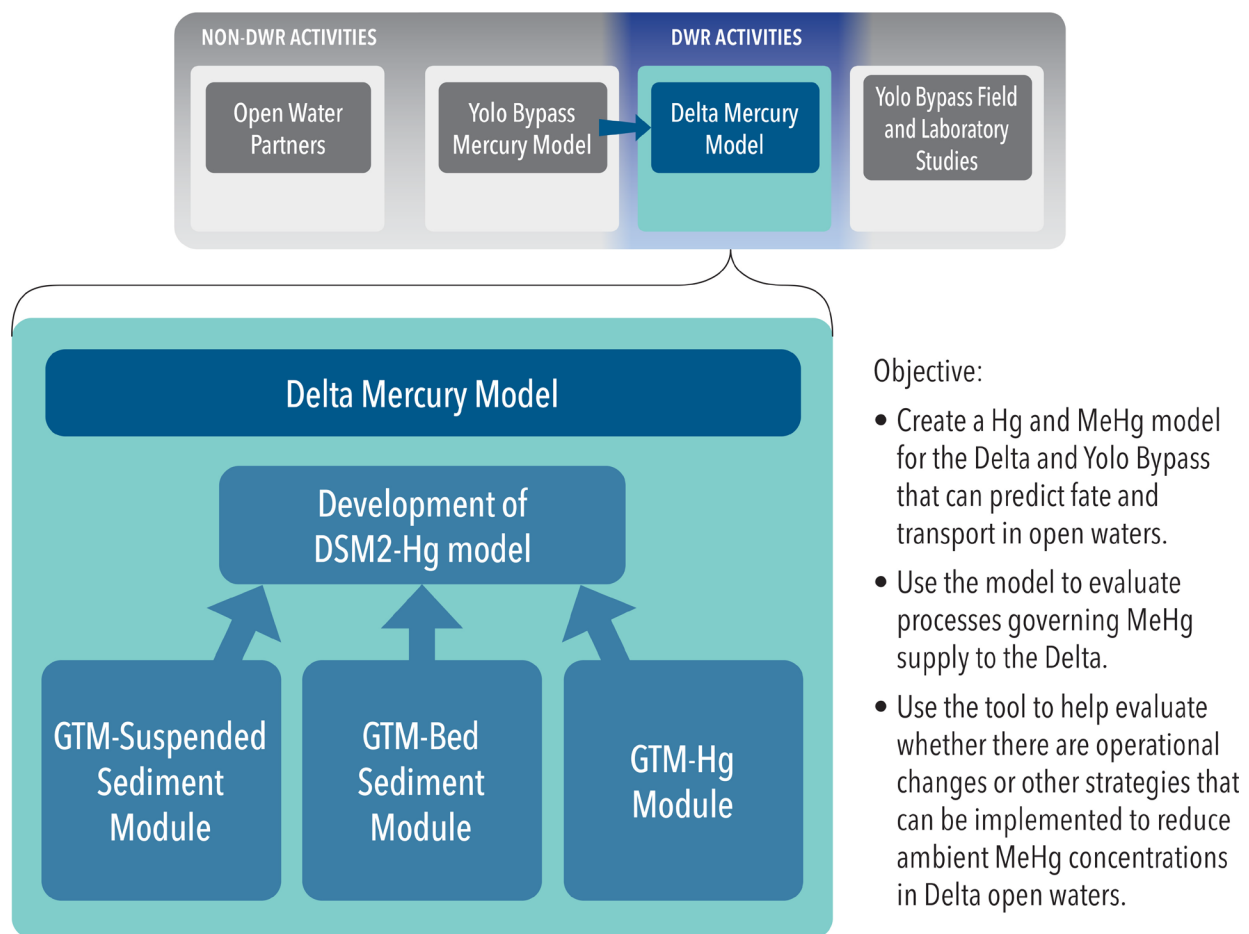
Notes: DSM2 = Delta Simulation Model 2, DWR = California Department of Water Resources, GTM = general transport model, Hg = mercury, MeHg = methylmercury

Workplan/Technical Memo Objectives and Hypotheses

Objectives

The four approved objectives as outlined in the workplan and the approach used to address each objective is summarized below.

1. Provide working models for Hg and MeHg supply, transport, and fate in the open waters of the Delta and Yolo Bypass.

   A. Objective 1 was addressed by creating Hg and MeHg models for the Delta and Yolo Bypass which provided a foundational platform for future mercury modeling improvements and questions. The models were calibrated manually and with PEST++ (Yolo Bypass D-MCM only) and can be used for sensitivity analyses and exploring hypotheses and scenarios. Creating the mercury model for the Delta included creating models for suspended sediment and bed sediment, which are also valuable tools for understanding sediment transport in the Delta.

2. Apply the models to identify processes governing MeHg supply to the Delta and Yolo Bypass.

   A. Objective 2 was addressed by conducting sensitivity runs with the Yolo Bypass D-MCM which helped identify key processes affecting MeHg supply. Sensitivity runs consist of holding all parameters constant, except the parameter of interest, and adjusting its contribution to determine its effects on MeHg production and transport. Discussion between DWR and CVRWQCB staff resulted in a suite of agreed upon sensitivity runs for the Yolo Bypass D-MCM. This approach allowed DWR to ask hypothesis-driven questions to examine which processes or inputs had the biggest impacts on modeled MeHg production. These hypothesis driven questions are listed in Table 1-3. As discussed, and approved by the CVRWQCB, sensitivity runs were not conducted for the DSM2-Hg model (Technical Appendix A).

3. Apply the models to examine the potential impacts of proposed operational changes in water management and flood conveyance in the Delta and Yolo Bypass on MeHg supply and compare to the total maximum daily load allocations.

   A. Objective 3 was met by conducting sensitivity runs. Sensitivity runs provided insights into how operational changes might affect MeHg production. For example, sensitivity runs adjusting MeHg outputs from the Cache Creek Settling Basin provides information on how MeHg outputs might change if operational modifications were made to the basin. Adjusting the amount of MeHg leaving the Yolo Bypass provides clues on the overall MeHg response to the Delta. Because of resource, time, and technical constraints, forecast scenarios proposed in the workplan were not conducted for the Yolo Bypass or the Delta. All changes were approved by the CVRWQCB (Technical Appendix A).

4. Use existing data to the extent possible, supplemented as needed, to meet Objectives 2 and 3. This includes collecting sample data in the Yolo Bypass and the laboratory to elucidate fundamental MeHg processes under flooding events.

   A. Objective 4 was addressed through field and laboratory studies. At the time of workplan approval, little MeHg data existed for the Yolo Bypass, relative to the Delta. As shown in

Figure 1-5, and discussed previously, field studies were conducted in the Yolo Bypass to provide data for the model so that modeling requirements could be met for Objective 2.

As discussed in the workplan/technical memo, field and laboratory studies were primarily conducted to provide needed information for the model. The mass balance, sediment-water flux, and Gust Chamber studies were not hypothesis driven. They either provided necessary data for identified model data gaps or were used by modelers as a check on observed modeling patterns. In the case of vegetation senescence experiments, study results filled an identified data gap in the model and were also hypothesis driven. Objectives for these studies are provided below.

B. **Mass-balance study**: (1) Quantify input, output, and net loads of unfiltered MeHg, uHg, and suspended particles during mini-flood events and periods of time when the bypass is flooded, (2) investigate the possible sources that contribute to within-bypass production of MeHg during floods, including evaluating filtered vs. particulate loads and correlations with ancillary parameters, and (3) evaluate load contributions from the east and west sides of the Yolo Bypass. In addition, the data from this study was used to validate results from the Yolo Bypass D-MCM developed by consultants for DWR. As discussed, and approved by the CVRWQCB, not all monitoring could be conducted due to lack of flooding and safety concerns (Technical Appendix A).

- **Sediment-water flux study**: (1) Provide flux rates, for filtered MeHg and Hg, for land use types found within the Yolo Bypass, and, (2) provide data useful to setting up and calibrating the D-MCM.
- **Gust Chamber study**: Quantify the erodibility of surface soils associated with different land uses modeled in the Yolo Bypass D-MCM model.
- **Vegetation senescence study**: (1) Address the role of vegetation in the internal production and cycling of MeHg in the Yolo Bypass, (2) conduct pilot experiments to test and validate methodologies for the larger scale studies, to help fill data gaps for the Yolo Bypass modelling effort, and, (3) develop information that could be used to help develop BMPs to reduce the production of MeHg and export loads from the upper reach of the Yolo Bypass.

Hypotheses

Sections 2.2.1 and 2.2.2 of the workplan lists suggested hypotheses to be addressed by the MeHg models. Based on feedback from the technical advisory committee, the technical memo refined these hypotheses. Within this framework, the CVRWQCB listed a number of questions in the technical memo. Based on the original hypotheses and questions listed in the workplan and technical memo, DWR and the CVRWQCB staff prioritized questions to create a final set of Yolo Bypass and Delta sensitivity analyses to examine drivers of interest but stay within the timeline and modeling constraints. Table 1-3 lists the sensitivity investigations associated with the Yolo Bypass D-MCM model. While not framed as hypotheses, the questions lead to logical hypotheses and modeled results associated with each question. As discussed with the CVRWQCB, time constraints prevented sensitivity runs for the Delta.

In the case of vegetation senescence experiments, there were both pilot-study and full-study hypotheses to help understand possible BMPs. Study results filled an identified data gap in the model and were also hypothesis driven.

The hypotheses tested in vegetation senescence pilot studies included:

- Plants are a more significant contributor to methylmercury production (release to overlying water) than sediments alone (without plants).
- Irrigated and non-irrigated pastures release different amounts of MeHg to overlying water.
- The duration of the senescence period is important to understanding the timing of the release or production of MeHg from the plant material. A lag period is likely to occur after a flood event before significant release or production is observed.
- Aeration of overlying water affects the release of MeHg to overlying water.

The hypotheses tested in vegetation senescence studies conducted in 2017, 2018, and 2019 were:

- Grazing land will lower MeHg releases to overlying flood water.
- Disking land will lower MeHg releases to overlying flood water.
- More vegetation results in more MeHg releases to overlying flood water.

Table 1-3 Sensitivity Questions Addressed by the D-MCM Yolo Bypass Model

Category	Parameter
Particle Related	Investigate sensitivity of simulated MeHg to changes in suspended sediment inputs to the Yolo Bypass. Begin by varying suspended sediment concentrations from the Cache Creek Settling Basin (CCSB).
External Inorganic Hg Loads	Investigate sensitivity of simulated MeHg to changes in inorganic Hg inputs from tributaries to the Yolo Bypass. Begin by varying CCSB inorganic Hg concentrations to the Yolo Bypass. Investigate sensitivity of simulated MeHg to changes in atmospheric inputs.
External MeHg Loads	Investigate sensitivity of simulated MeHg to changes in MeHg inputs from tributaries to the Yolo Bypass. Begin by varying CCSB MeHg concentrations to the Yolo Bypass.
Internal MeHg Loads	Investigate sensitivity of simulated MeHg to the rate of MeHg supply generated within the Yolo Bypass.
Influence of Vegetation	Investigate sensitivity of simulated MeHg to vegetation effects in the Yolo Bypass. Begin by reducing pasture or seasonal wet-land vegetated areas in the model.

Notes: D-MCM = Dynamic Mercury Cycling Model, Hg = mercury, MeHg = methylmercury

Report Organization

The open water final report consists of two stand-alone pieces. The first part of the report consists of an executive summary and 7 chapters. The second part consists of 12 technical appendices. The technical appendices provide additional in-depth, supporting material. The field and laboratory appendices include methods, sampling locations, statistical analyses, and quality assurance/quality control. The modeling appendices include model documentation, calibration, validation, and sensitivity runs.

Chapter 1 provides a high-level summary of the requirements and processes leading to the final products and orients the reader to the organization of the report.

Chapter 2 summarizes the actions undertaken by non-DWR Open Water Workgroup members, who, to the extent allowable by their regulatory authority, were required to direct project applicants, grantees, and loan recipients to apply to or consult with the CVRWQCB to ensure full compliance with the DMCP.

Chapters 3 summarizes technical results from scientific studies conducted in the Yolo Bypass. Technical appendices that support this chapter are: Technical Appendices A, B, C, D, D, E, E1 and F.

Chapter 4 summarizes modeling results for the Yolo Bypass. Technical appendices supporting this chapter are Technical Appendices G and H.

Chapter 5 summarizes findings associated with the development of a manually calibrated Delta Mercury Model. Technical appendices supporting this chapter are: Technical Appendices I and J

Chapter 6 provides information on the possible impacts associated with climate change and methylation factors in the Yolo Bypass and the Delta.

In Chapter 7, the report concludes with the possible management implications associated with the experimental and modeling results.

References

Alpers CN, Hunerlach MP, May JT, Hothem R. 2005. Mercury Contamination from Historical Gold Mining in California, USGS Fact Sheet 2005-3014. April 2005. https://pubs.usgs.gov/fs/old.2005/3014/pdf/fs2005_3014.pdf. Accessed: November 14, 2019.

California Department of Water Resources 2019. Viewed online at: https://water.ca.gov/Library/Modeling-and-Analysis/Bay-Delta-Region-models-and-tools/Delta-Simulation-Model-II. Accessed: September 10, 2019

Central Valley Regional Water Quality Control Board, 2011. Amendments to the Water Quality Control Plan for the Sacramento River and San-Joaquin Basins for the Control of Methylmercury and Total Mercury in the Sacramento-San Joaquin River Delta Estuary (Attachment 1 to Resolution NO. R5-2010-0043. Viewed online at: https://www.waterboards.ca.gov/centralvalley/water_issues/tmdl/central_valley_projects/delta_hg/2011_1020_deltahg_bpa.pdf. Accessed: August 22, 2019. Last updated: June 13, 2019.

Churchill RK. 2000. Contributions of Mercury to California's Environment from Mercury and Gold Mining Activities; Insights from the Historical Record, in Extended Abstracts for the US. S. EPA Sponsored Meeting, Assessing and Managing Mercury from Historic and Current Mining Activities, November 28-2000, San Francisco, California, Pages 33-36 and S35-S48.

Cooke J, Morris P. 2005. The Water Quality Control Plan for the Sacramento River and San Joaquin River Basins for the Control of Mercury in Cache Creek, Bear Cache Creek, Sulphur Creek, and Harley Gulch. Staff Report. October 2005.

DWR, 2020. DSM2: Delta Simulation Model II, California Department of Water Resources website https://water.ca.gov/Library/Modeling-and-Analysis/Bay-Delta-Region-models-and-tools/Delta-Simulation-Model-II. Accessed on July 29, 2020.

Foe C, Louie S, Bosworth D. 2008. Task 2. Methyl Mercury Concentrations and Loads in the Central Valley and Freshwater Delta, August 2008. In Transport, Cycling, and Fate of Mercury and Monomethyl Mercury in the San Francisco Delta and Tributaries: An Integrated Mass Balance Assessment Approach. CALFED Mercury Project Final Report, September 15, 2008.

Electric Power Research Institute 2019. Viewed online at: https://www.epri.com/#/pages/product/3002002518/?lang=en-US. Accessed: September 10, 2019

Harris RH, Pollman C, Hutchinson D, Landing W, Axelrad D. Morey SL, Dukhovskoy D, Vijayarghaven K. 2012. "A Screening Model Analysis of Mercury Sources, Fate and Bioaccumulation in the Gulf of Mexico." Environmental Research. Volume 119, Pages 53-63.

Heim WA, Newman A, Byington, A, Hughes B, Stephenson. 2010. Spatial Distribution of Total Mercury in the Yolo Bypass: Implications for Land Use Management of Mercury Contaminated Floodplains. Report to Chris Foe and the Central Valley Regional Water Quality Control Board. May 2010. 44 Pages.

Hudson FJM, Gherini SA, Watras CJ, Porcella DB, 1994. Modeling the Biogeochemical Cycle of Mercury in Lakes; The Mercury Cycling Model (MCM) and its Application to the MTL Study Lakes. In: Watras, C.J., Huckabee, J.W. (Eds.) Mercury Pollution-Integration and Synthesis CCRC Press Inc. Lewis Publishers.

US DOI, Bureau of Reclamation/DWR. 2019. Yolo Bypass Salmonid Habitat Restoration and Fish Passage, Final Environmental Impact Statement/Environmental Impact Report, Appendix D. May 2019. Available at: https://www.usbr.gov/mp/nepa/nepa_project_details.php?Project_ID=30484. Accessed July 20, 2020.

Weiner J.G, Gilmour CC, Krabbenhoft DP. 2003. Mercury Strategy for the Bay-Delta Ecosystem: A Unifying Framework for Science, Adaptive Management, and Ecological Restoration. Final Report to The California Bay Delta Authority for Contract 4600001642 between The Association of Bay Area Governments and the University of Wisconsin-La Crosse, December 31, 2013. 67 pps.

Mercury Open Water Final Report for Compliance with the Delta Mercury Control Program

Chapter 2. Non-DWR Open Water Workgroup Activities

Submitted by the Open Water Workgroup

August 31, 2020

Contents

List of Tables

List of Figures

Acronyms and Abbreviations

CDPH	California Department of Public Health
CSLC	California State Lands Commission
CVFPB	Central Valley Flood Protection Board
CVRWQCB	Central Valley Regional Water Quality Control Board
DMCP	Delta Mercury Control Program
DWR	California Department of Water Resources
Hg	mercury
MeHg	methylmercury
MERP	Mercury Exposure Reduction Program
Reclamation	U.S. Bureau of Reclamation
USACE	U.S. Army Corps of Engineers
USGS	U.S. Geological Survey

Introduction

This chapter focuses on activities undertaken by non-California Department of Water Resources (DWR) Open Water Workgroup members who, to the extent allowable by their regulatory authority, were required to direct project applicants, grantees, and loan recipients to apply to or consult with the Central Valley Regional Water Quality Control Board (CVRWQCB) to ensure full compliance with the Delta Mercury Control Program (DMCP). In addition to DWR, the Open Water Workgroup consists of the California State Lands Commission (CSLC), the Central Valley Flood Protection Board (CVFPB), the U.S. Army Corps of Engineers (USACE) and the U.S. Bureau of Reclamation (Reclamation).

California State Lands Commission

This section summarizes activities undertaken by the CSLC in compliance with the DMCP. In the workplan, CSLC agreed that as new leases are issued or come up for renewal, they will be examined to determine what modifications are necessary to address the mobilization and transport of sediment-bound mercury. The CSLC leases sovereign land for various purposes that are consistent with the Public Trust Doctrine. Some of these leases may include activities (e.g., dredging, riprap installation, spur dike removal) that contribute to the disturbance of streambed sediments.

Key Findings

- Leases within the DMCP area were identified and categorized. Very few leases were identified where activities could substantially contribute to the disturbance of streambed sediments.
- Environmental documents for proposed projects located within the DMCP area were reviewed and comments submitted that included a notice of potential mercury (Hg) or methylmercury (MeHg) contamination.
- Leases potentially applicable under the Mercury Exposure Reduction Program (MERP) (docks, marinas, etc.) were pulled into a list and shared with the California Department of Public Health (CDPH) to aid in the posting of advisory signs for the MERP. Seven signs were posted throughout the DMCP area from 2017 through 2018.

Participation Overview

The CSLC leases sovereign land for various purposes that are consistent with the Public Trust Doctrine. CSLC staff reviewed all current leases within the DMCP area and identified leases that had (or have) the potential to result in substantial sediment disturbance or release within the DMCP area. These leases could include activities such as dredging, riprap installation, or spur dike removal. Only three active leases met that criteria. Upon review of the leases, CSLC staff found that existing permits from other agencies, including USACE and the CVRWQCB, provided substantial protection during sediment-disturbing activities. To more effectively modify future leases to address the mobilization and transport of sediment-bound Hg, the CSLC has examined, and will continue to examine, current effective methodologies to strengthen existing best management practices or develop new control measures aimed at reducing the concentration of Hg and/or MeHg released into the Delta as the result of sediment disturbance.

From 2014 through 2018, CSLC staff also reviewed environmental documents provided by the State Clearinghouse for projects that have the potential to result in sediment disturbance or release within the

Delta or adjacent areas. CSLC staff incorporated specific comments addressing the potential for Hg and MeHg release to promote agency and public awareness. Examples of these projects include:

- Smith Canal Gate Project, San Joaquin County (SCH #2014062079).
- Delta Levee Investment Strategy, Sacramento and San Joaquin counties (SCH #2015052070).
- North Sacramento Streams, Sacramento River East Levee, and Related Flood Improvements Project, Sacramento, Yolo, Sutter and Solano counties (SCH #2014052038).
- San Joaquin River Parkway Sycamore Island Pond Isolation Project, Fresno and Madera counties (SCH #2015011041).
- Emergency Drought Barriers Project, Yolo, Sacramento, and Contra Costa counties (SCH #2015012048).
- Delta Emergency Facilities Improvement Project Refinements, San Joaquin and Solano counties (SCH #2014112056).
- I Street Bridge Replacement Project, Sacramento and Yolo counties (SCH #2014092069).
- Butte Slough Outfall Gates Rehabilitation Project, Sutter and Colusa counties (SCH #2014082018).
- Sherman Island "Little Baja and Manzo Ranch" Fish Release Sites Project, Sacramento County (SCH #2014052035).
- Decker Island Electrical Crossing Project, Sacramento and Solano counties (SCH #2014032039).
- Raley's Dock Replacement and Rice Mill Pier Rehabilitation Project, Yolo County (SCH #2014022054).
- Woodward Island Bridge Project (ferry ramp replacement), San Joaquin County (SCH #2016012065).
- San Francisco Bay to Stockton Navigation Improvement Study, San Joaquin County (SCH #2016032010).
- Twin Cities Road over Snodgrass Slough Bridge Replacement, Sacramento County (SCH #2016062064).
- Altamont Corridor Express Extension Lathrop to Ceres/Merced Project, San Joaquin, Stanislaus, and Merced counties (SCH #2018012014).
- Northwest Levee Improvements and Stone Road Seepage Reduction Project, Sacramento County (SCH #2018072062).

In addition, CSLC staff worked with CDPH to aid in the posting of fish consumption advisory signs throughout the Delta to promote safe Delta-fish consumption (Figure 2-1). The advisory signs, prepared by Open Water Workgroup partner DWR, were made available to CSLC staff in January 2017.

Figure 2-1 Example of Fish Consumption Advisory Posted at California State Lands Commission Lease Locations


In 2012, CSLC staff identified approximately 54 leases that could be candidates for the posting of advisory signs. Of these 54 leases, a 2017 review identified 19 priority locations that were found to be potentially viable for the first year of the posting effort. CSLC staff compiled information on those lease locations into a list and shared the information with CDPH, who incorporated the information into their posting database. On February 14, 2017, letters were sent to these locations requesting permission to post an advisory sign onsite. Although the goal was to post 19 signs, 12 planned locations either were not viable, the land owner did not approve the sign posting, or the signs were posted by other agencies because of miscommunication with CDPH. As listed in Table 2-1, seven signs have been posted to date. Figure 2-2 provides a map of the locations. Photographs are provided in Figures 2-3 through 2-7.

Table 2-1 Facilities with Leases held by the California State Lands Commission with Posted Fish Consumption Advisories

Facility	Address/ Global Positioning System Coordinates
Lighthouse Restaurant Resort and Marina	151 Brannan Island Road in Sacramento 38°06'21.1"N, 121°34'16.6"W
Isleton Public Access	101 Second Street in Isleton
Heidi's Outrigger Marina and Saloon	17641 Sherman Island East Levee Road in Rio Vista 38°06'50.2"N, 121°41'02.2"W
Rio Vista Boat Launch	Montezuma Street near Front Street in Rio Vista 38° 9'16.54"N, 121°41'24.87"W
Rio Vista Fishing Pier	Front Street near State Route 12 in Rio Vista 38° 9'35.78"N, 121°41'12.44"W
Suisun City Marina	800 Kellogg Street in Suisun City
Duck Island RV Park	16814 State Route 160 in Rio Vista 38° 8'35.68"N, 121°41'3.65"W

Figure 2-2 Locations of Posted Fish Consumption Warning Signs on Properties Leased by the California State Lands Commission
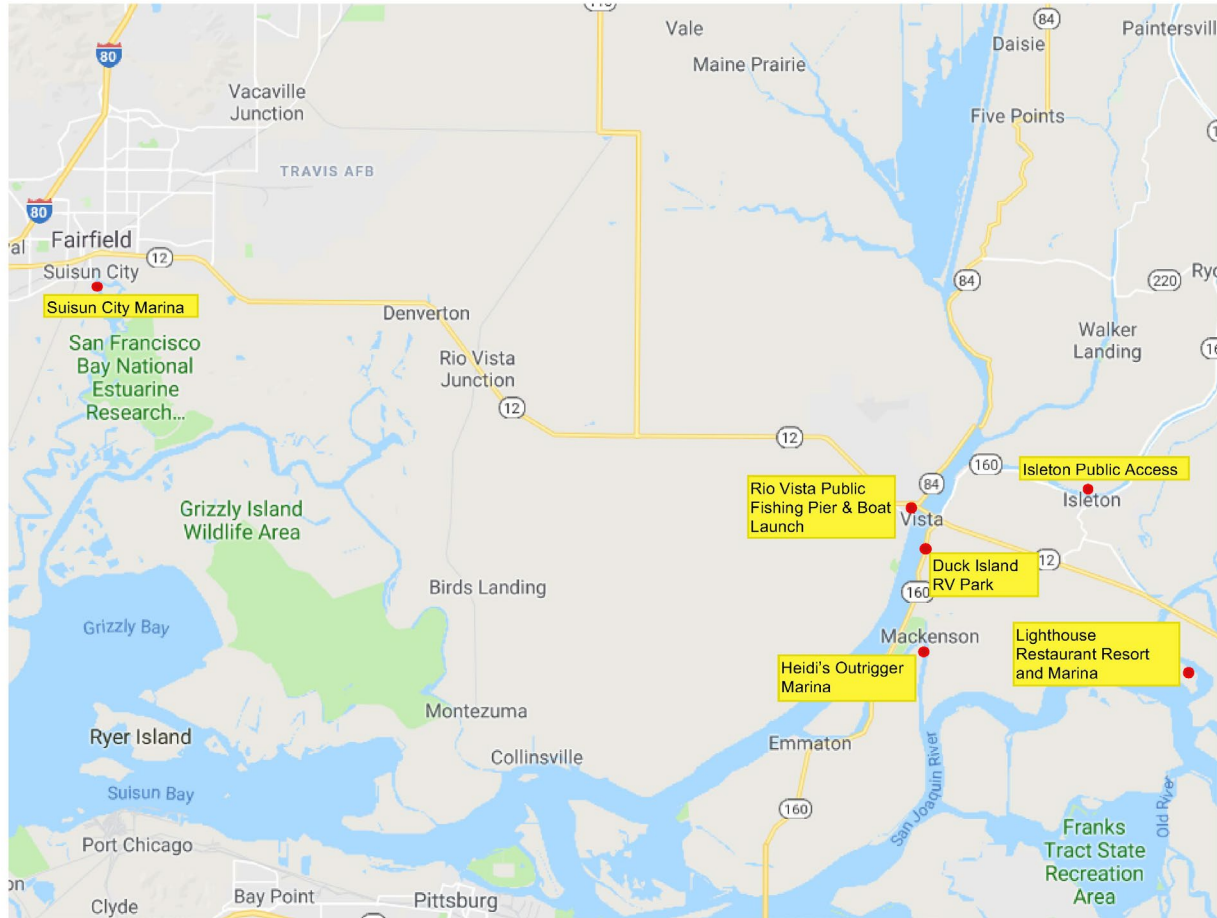
Figure 2-3 Photo and Location of Lighthouse Restaurant Resort and Marina

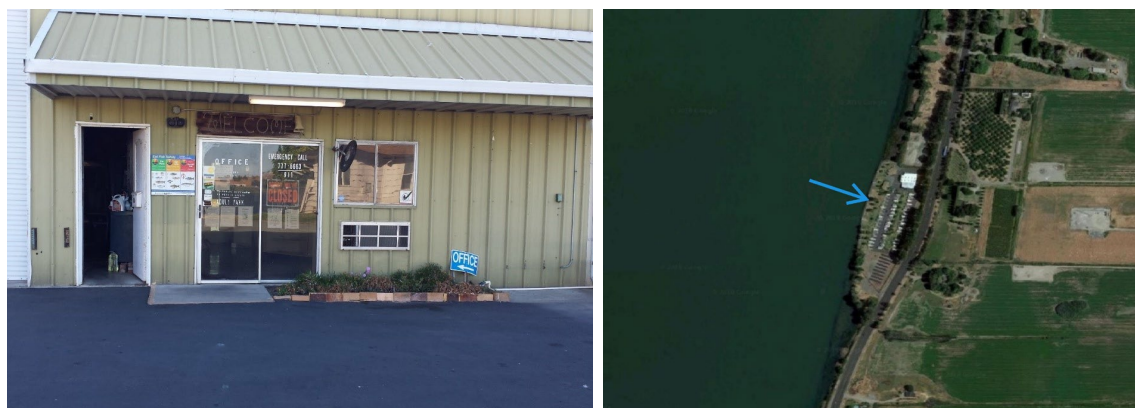**Figure 2-4 Photo and Location of Heidi's Outrigger Marina and Saloon**

Figure 2-5 Photo and Location of Rio Vista Boat Launch

Figure 2-6 Photo and Location of Rio Vista Fishing Pier

Figure 2-7 Photo and Location of Duck Island RV Park

Future Participation Efforts

CSLC staff will continue to look for ways to further emphasize the need to reduce sediment disturbance and subsequent MeHg release in the Delta. Future activities may include:

- Additional sign posting under the guidance of the CDPH.
- Inclusion of advisory pamphlets with new and renewed lease documents.
- Mass mailout of advisory pamphlets to leases within the DMCP area.
- Internal modification of procedures to automatically identify new leases within the DMCP area.

In addition, CSLC staff suggest increased communication between CDPH and sign-posting agencies to ensure that the agency assigned to post a sign to a particular location is able to fulfill that task.

Central Valley Flood Protection Board

The Central Valley Flood Protection Board (Board) is participating in the Delta Open Water Workgroup (workgroup) as a responsible entity because of its property, easements, and regulatory authority for the purpose of regulating flood control features. As stated in the workplan, the Board may act as a trustee agency under CEQA in reviewing projects that may mobilize and transport sediment-bound mercury.

The Board, as the non-federal sponsor of the State-federal flood control system in California's Central Valley issues encroachment permits for work that meets certain construction standards and will not be injurious to, or interfere with, the successful execution, function, or operation of the flood control system. The Board will examine each permit application to determine if project construction may result in the mobilization and transport of sediment and if project modifications are necessary pursuant to California Code of Regulations, Title 23, Sections 115, 116, and 121. In addition, a condition will be included in each permit within the DMCP area requiring the permittee to obtain or provide a waiver for the Clean Water Act Section 401 Water Quality Certification prior to commencement of project construction. It is anticipated that these requirements will ensure that any encroachment permits issued by the Board will be in compliance with the DMCP.

U.S. Army Corps of Engineers

In addition to working with the Delta Open Water Workgroup, USACE has been advancing mercury research in the Delta on several fronts. The paragraphs below provide a brief synopsis of the additional projects, with Hg components, occurring within the boundaries of the DMCP.

Lower Cache Creek Flood Control Project

USACE is resuming completion of the feasibility study for the Lower Cache Creek Project. The project proposes to provide flood protection for the City of Woodland, the local sponsor. USACE will finalize the feasibility study, determine the tentatively selected plan, complete the combined environmental impact statement/environmental impact report document, and produce the Chief of Engineers Report. Compliance with multiple total maximum daily loads for total Hg and MeHg will be coordinated between the local sponsor, DWR, and USACE. The Cache Creek system, including Clear Lake, has been historically impacted by active and abandoned gold rush era mercury mines, and is also impacted by the Sulphur Bank Mercury Mine Superfund site.

Delta Study

The USACE Chief of Engineers Report summarizing the recommended alternative and formally requesting funding has been received and sent to Congress. If funding is authorized, a Phase I environmental assessment and current condition sampling will be conducted to assist with placement design for use of dredged material for habitat restoration of a submerged Delta island called Big Break, near Antioch, California. An Hg control plan will also be produced to characterize current Hg and MeHg production as well as provide monitoring during and after restoration.

U.S. Bureau of Reclamation

Like USACE, Reclamation is participating in the Delta Open Water Workgroup in accordance with its authorizations to provide technical support when requested or necessary for the DMCP process. In addition to open water DMCP efforts, Reclamation, in collaboration with the U. S. Geological Survey (USGS), Bureau of Land Management, and Lawrence Berkeley National Laboratory, is funding and working on a three-year research project to develop a physically based watershed-scale model to simulate the effects of fire on the mobilization and transport of Hg and MeHg. The research partners selected the Cache Creek Watershed to develop and apply the model because previous USGS studies had collected hydrologic, mercury, sediment, and water-quality data necessary for such a model development. The hydrologic component of the model has been already calibrated for both pre- and post-fire conditions. Calibration of the sediment transport and completion of the Hg/MeHg fate and transport modules were completed in 2019. Reclamation is considering an application of the model in the Lake Berryessa watershed.

Mercury Open Water Final Report for Compliance with the Delta Mercury Control Program

Chapter 3. Yolo Bypass –Technical Studies

Submitted by the Open Water Mercury Technical Workgroup

Aug 31, 2020

Mercury Open Water Final Report

The Open Water Mercury Technical Workgroup

California Department of Water Resources
Division of Environmental Sciences
Carol DiGiorgio
David Bosworth

San Jose State University
Moss Landing Marine Laboratory
Wesley Heim,
Mark Stephenson (ret.)

Pacific Northwest National Laboratory
Marine Sciences Laboratory
Gary Gill, (ret.)

United States Geological Survey
California Science Center
David Schoellhamer.
Paul A. Work,

Acknowledgements

Contents

List of Figures

List of Tables

List of Acronyms and Abbreviations

BMP	Best Management Practice
CVRWQCB	Central Valley Regional Water Quality Control Board
CCSB	Cache Creek Settling Basin
Conc.	Concentration
Delta	Sacramento-San Joaquin Delta
D-MCM	Dynamic Mercury Cycling Model
DOC	Dissolved Organic Carbon
DMCP	Delta Mercury Control Program (DMCP)
DWR	(California) Department of Water Resources
EPA	Environmental Protection Agency
fHg	Filter-passing Mercury
fMeHg	Filter-passing Methylmercury
GIS	Geographic Information System
Hg	Mercury
KLRC	Knights Landing Ridge Cut
MeHg	Methylmercury
pHg	Particulate Mercury
pMeHg	Particulate Methylmercury
POC	Particulate Organic Carbon
tHg	Total Mercury (in sediment)
TOC	Total Organic Carbon
TSS	Total Suspended Solids
uHg	An unfiltered (aqueous) mercury (sample)
uMeHg	An unfiltered (aqueous) methylmercury (sample)
VSS	Volatile Suspended Solids
WY	Water Year(s)

Introduction - Technical Field Studies

The Delta Mercury Control Program (DMCP) requires the (California) Department of Water Resources (DWR) to reduce methylmercury (MeHg) open water sediment flux from areas out of compliance in the Delta and Yolo Bypass (See Chapter 1). A mercury mass balance biogeochemical modeling approach was approved to evaluate how hydrodynamic and other changes to the water flow system might impact open water sediment fluxes. At the time of the workplan's approval, mercury cycling and transport in the Yolo Bypass was not well understood, therefore technical studies were designed to provide critical input data to the Yolo Bypass Dynamic Mercury Cycling Model (D-MCM). The originally approved workplan relied upon large-scale, field-based studies to provide information for the model. However, the proposed studies had feasibility and funding constraints. Therefore, DWR discussed, and received approval from the (California) Central Valley Regional Water Quality Control Board (CVRWQCB) staff, to instead conduct laboratory and mesocosm studies to provide necessary information on mercury behavior with which to develop the mercury model for the Yolo Bypass.

The objective of this chapter is to summarize and provide key findings of interest to management and policy makers from the studies listed in Table 3-1**Error! Reference source not found.**. Stand-alone chapters for each of the laboratory and field studies are published in four Technical Appendices. In-depth details on study design, methodology as well as in-depth analysis of results can be found in the individual technical appendices. Data including QC, have been provided to staff of the CVRWQB. DWR staff are also working on publishing data to the Environmental Data Initiative (EDI) data portal.

Table 3-1 List of Summarized Open Water Yolo Bypass Technical Studies

Study	Description	Research Team[1]	Technical Appendix
Yolo Bypass Mass Balance Study	Information used to parameterize the mercury model. This study expands on previous CALFED investigations by determining MeHg in filtered and particulate fractions as well as extending sampling below Liberty Island.	DWR	B
Sediment-water Flux Study	Addressed Hg and MeHg fluxes from sediments of different land uses.	MLML	C
Gust Chamber Erosion Study	Addressed soil erosion of different land uses under different flow velocities.	USGS	D
Vegetation Senescence Study	Addressed possible vegetation impacts associated with the largest actively managed land use and investigated possible BMPs.	DWR MLML	E and E1

[1]DWR = California Department of Water Resources; MLML = Moss Landing Marine Laboratories; USGS = United States Geological Survey

Background

The Yolo Bypass

The Yolo Bypass is a 3-mile wide, 40 mile-long, 59,000-acre flood conveyance system that diverts flood waters from the Sacramento River around the City of Sacramento (Figure 3-1**Error! Reference source not found.**). The Yolo Bypass floods in roughly 7 out of 10 years with inundation occurring roughly between October and April. When completely flooded, the Yolo Bypass covers an area equal to about one-third the size of San Francisco and San Pablo Bays (Natural Resources Defense Council,https://www.nrdc.org/experts/monty-schmitt/building-rivers-yolo-bypass-hiding-plain-sight) and

can carry up to four times the flow of the Sacramento River's main channel during large floods (Suddeth Grimm and Lund, 2016). When fully inundated, the wetted area of the Sacramento-San Joaquin Delta system approximately doubles. The project design capacity is 343,000 cfs (DWR, https://water.ca.gov/LegacyFiles/newsroom/docs/WeirsReliefStructures.pdf, accessed 11/25/19).

The main input to the Yolo Bypass is at the 2-mile wide Fremont weir where water passively flows into the Yolo Bypass when the Sacramento river reaches 32 feet stage height (NAVD88 datum) or approximately 60,000 cfs. Additional tributaries into the Yolo Bypass include the Knight's Landing Ridge Cut (KLRC), the Cache Creek Overflow weir and low flow channel for the Cache Creek Settling Basin (CCSB), Willow Slough and Putah Creek (Figure 3-1). Depending on flood flows, the flood gates of the Sacramento weir can also be opened. In January 2017, a period captured by some of our studies, the Sacramento weir gates were opened for the first time in eleven years. The dominant hydrological feature at the southern end of the Yolo Bypass is Liberty Island, a 5,300-acre parcel of open water and wetland habitat that is tidally-influenced (fresh water) except during large floods in the Yolo Bypass. Just north of Liberty Island is the feature referred to as the Stairsteps drainage canals (Figure 3-1).

The use of the Yolo Bypass as a floodplain cannot be compromised, however, several spring-fall agricultural uses are compatible with maintaining the Yolo Bypass as an unimpeded floodplain. The Yolo Bypass is farmed, irrigated, left unmanaged, disked, mowed and grazed by cattle. Figure 3-2 shows the top land uses and their boundary cells used in the D-MCM model. Many technical studies in this chapter involved the Yolo Wildlife Area. The Yolo Wildlife Area is located within the Yolo Bypass and is managed by the California Department of Fish and Wildlife with the intent of restoring and managing a variety of wildlife habitats in the Yolo Bypass (Figure 3-1).

Figure 3-1 Yolo Bypass Schematic Map
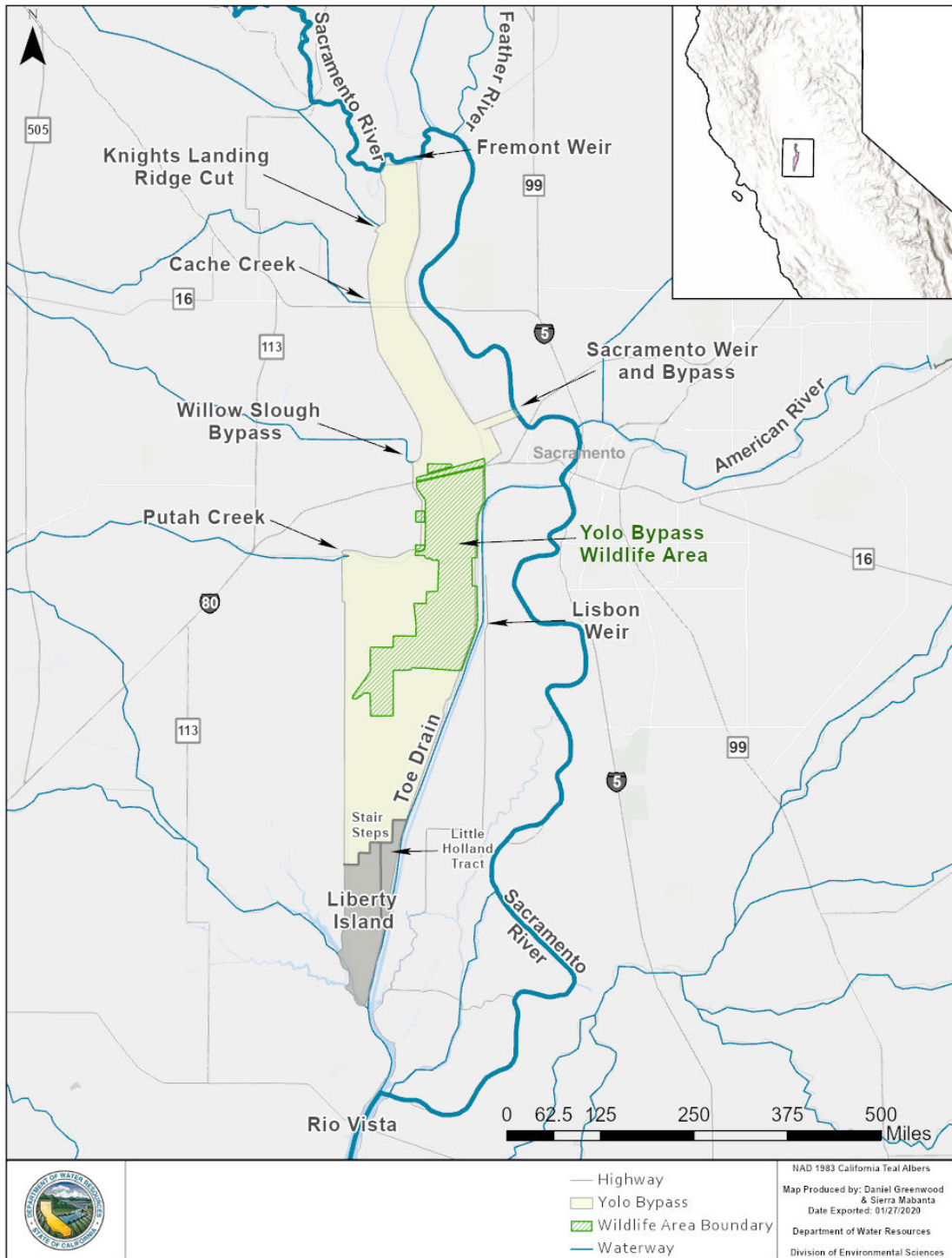
Figure 3-2 Land Uses in the Yolo Bypass as Delineated in the Yolo Bypass Dynamic Cycling Model.

Cell #	Land use
1	Fallow
2	Mixed/other
3	Water
4	Water
5	Water
6	Water
7	Water
8	Water
9	Water
10	Water
11	Water
12	Water
13	Water
14	White rice
15	Fallow
16	Mixed/other
17	Fallow
18	White rice
19	Wild rice
20	Wetland
21	Mixed/other
22	Fallow
23	White rice
24	Wild rice
25	Wetland
26	Wetland
27	Mixed/other
28	Wetland
29	Pasture
30	Pasture
31	Wetland
32	White rice
33	Wetland
34	Pasture
35	Tidal marsh
36	Tidal marsh
37	Mixed/other
38	Mixed/other
39	Pasture
40	Tidal marsh
41	Pasture
42	Water
43	Water
44	Water
45	Water
46	Water
47	Water

Program Goals

The main goal of this work was to provide critical information for model development. Toward this end, many of the report's technical studies evaluated needed parameters for different land uses and were not necessarily studies evaluating open water MeHg contributions as defined in the DMCP. Except for the Vegetation Senescence (VegSens) studies, field studies were used to provide data for the model and were not hypothesis driven, however, they did provide useful insights beyond providing data for the model. The technical studies significantly expanded on the earlier CALFED work and also allowed for an evaluation of Best Management Practices (BMP). The DMCP and additional work conducted for CALFED primarily looked at mercury and methylmercury in unfiltered samples (uHg and uMeHg, respectively). This current work expanded on this to include measurements of Hg and MeHg in filtered samples (fHg and fMeHg, respectively)[1] and estimates of Hg and MeHg in the particulate fraction (pHg and pMeHg, respectively). Understanding the patterns associated with individual fractions provides information on which fractions to target in future control studies. Additionally, the Yolo Bypass Mass Balance Study included sample collection below Liberty Island in addition to the inputs and exports at the Stairsteps. Collecting samples below Liberty Island provided a better estimate of the total loads exiting the Yolo Bypass into the Delta. Previous work had not included this lower reach.

Foe and others, (2008) documented that the Yolo Bypass, under large flood events, was a net internal producer of uMeHg. Understanding the source(s) of this internal production is a critical first step in assessing future BMP approaches. The sediment-water flux experiments provided flux values for the model, but also provided rough estimates of whether open water sediments could account for observed Yolo Bypass in-situ production. The VegSens studies looked at pasture vegetation inundated by floodwaters as another possible internal source of MeHg to the Yolo Bypass. Pasture was evaluated as this was the largest land use in the land use map developed for the Yolo Bypass model. This is a new source that has never been assessed. The vegetation studies were also designed to examine BMP's for pastureland to minimize in-situ production of MeHg and introduction into flood waters.

The following sections provide summaries of key highlights from the individual technical appendices.

---

[1] In this document, the term filtered or filter-passing mercury (fHg) and methylmercury (fMeHg) refers to the mercury or methylmercury passing through a 0.45-micron filter

Mass Balance Study - Import and Export Loads from the Yolo Bypass

Workplan Objectives

Objectives for the mass balance study were to: 1) quantify input, output, and net loads of Hg, MeHg (total filtered and particulate), and suspended particles (TSS) during periods of time when the Bypass is flooded; and 2) investigate the possible sources that contribute to within-Bypass production of MeHg during floods by evaluating filtered vs. particulate loads and correlations with ancillary parameters. A third objective of this study, not originally proposed in the Workplan, was to quantify the contribution of Liberty Island to the Hg and MeHg loads of the Yolo Bypass. The data from this study was also used to parameterize and validate the D-MCM developed by consultants to DWR. As discussed below, we were unable to pursue workplan objectives to compare mini-flood events to larger flood events. A mini-flood event was defined when flows in Knights Landing Ridge Cut, Cache Creek and/or Putah Creek are greater than the carrying capacity of their channels, resulting in local flooding, but no spillage over the Fremont weir. A major flood event was defined by the Sacramento River overtopping the Fremont Weir resulting in wide-scale flooding of the Yolo Bypass for days, weeks or months. As discussed in Technical Appendix A, safety concerns precluded collecting enough east-west transects across the Yolo Bypass to allow examination of the banded water mass contributions occurring in the flooded Yolo Bypass. Any changes associated with the original Workplan were discussed and approved by the Central Valley Regional Water Quality Control Board.

Sampling Locations

Water sampling locations from the major input and export sites are shown in Figure 3-3. Input samples were collected at Fremont Weir, Sacramento Weir (when it was open), the Knights Landing Ridge Cut (KLRC), Cache Creek Settling Basin (CCSB), and Putah Creek. Output samples were collected along the drainage canal known as the "Stairsteps" (Toe Drain, Liberty Cut, and Shag Slough). The stairsteps drainage canal is located immediately above Liberty Island. Additionally, during 8 sampling events in 2017 when an adequate volume of water was exiting the Yolo Bypass, samples were also collected from Cache and Miner Sloughs which are located downstream of Liberty Island. Sampling Cache and Miner Sloughs allowed us to divide the Yolo Bypass into upper and lower reaches. The upper reach encompasses the area receiving drainages from the inlets to the outlet at the stairsteps drainage canals which covers about two-thirds of the length of the Bypass. The lower reach encompasses the area from the stairsteps to below Liberty Island which is dominated by Liberty Island. Details on sample locations, sample dates, and other logistics are given in Technical Appendix B.

Figure 3-3 Mass Balance Study Sampling Locations in the Yolo Bypass
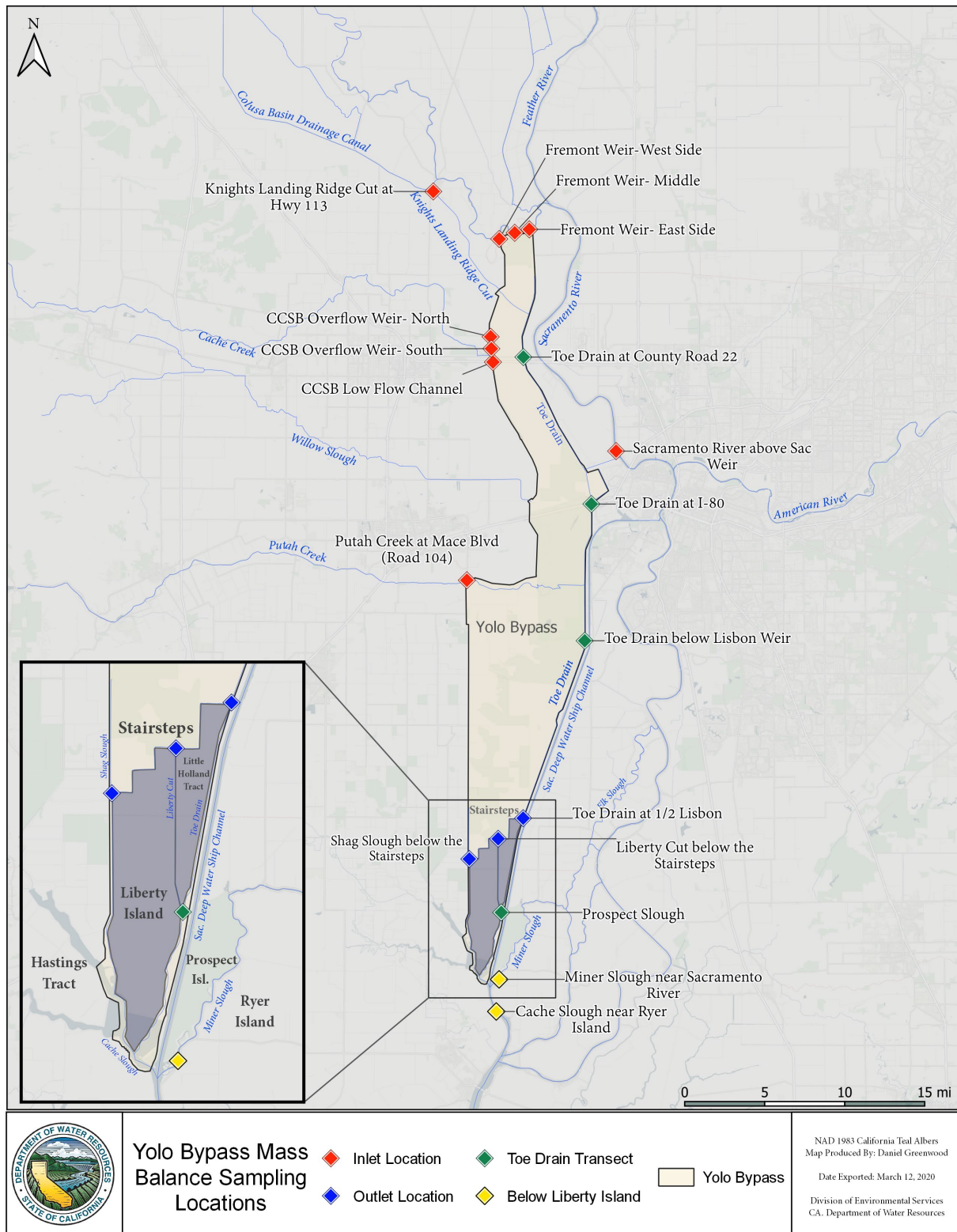
Mercury and Water Quality Parameters

Water samples were collected at the inlet and outlet locations and analyzed for several constituents, including uHg, fHg, uMeHg, fMeH, TSS, and organic carbon (TOC, DOC). The Environmental Protection Agency's (EPA) Method 1669 "clean hands-dirty hands" was used when collecting samples and while processing and filtering samples in the laboratory (EPA, 1995). Particulate Hg (pHg) and particulate MeHg (pMeHg), as well as particulate organic carbon (POC), were determined as the difference between their respective unfiltered and filtered values. All inlet locations, except for Putah Creek had nearby flow monitoring gages. Outlet sites on the Stairsteps lack flow gaging stations, therefore, after evaluating a modeling approach, outlet flows were estimated as the sum of the inlet flows.

Tributary Input Sources and Export of Methyl Mercury to the Delta

Water Balances

Over the course of the study, the state of California experienced a severe drought in Water Years (WYs) 2013-2016 classified as either dry, critical, or below normal (CDEC, http://cdec.water.ca.gov/reportapp/javareports?name=WSIHIST, accessed September 2019) and the Governor of California declared a drought state of emergency in 2014. The lack of flooding events resulted in the sampling of only one mini-flood event in 2014 and one flooding event in 2016. In contrast, WY 2017 was the second wettest year in a 122-year record and mass balance sampling occurred on nine occasions from January 2017 through April 2017 covering the full extent of the flooding season. Based on weather constraints, collection efforts were unable to collect enough samples to meaningfully compare mass balance differences between mini-flood and major flooding events. Therefore, mass balance insights summarized in this chapter are confined to the nine sampling events associated with WY 2017 (October 1, 2016-Sept. 30, 2017).

Intensive sampling of one of the wettest years on record provided the opportunity to evaluate a sustained flooding season when most of the uMeHg from the Yolo Bypass is transported to the Delta (Foe and others, 2008). Inputs consisted of the sum of Fremont Weir, Sacramento Weir, CCSB, KLRC and Putah Creek. Outputs consisted of the sum of the stations at the Stairsteps. Water balance calculations indicated that most of the water volume entering and leaving the Yolo Bypass was accounted for. The balance between inlet and outlet volumes was close to 100% for the overall 2017 flood event (see Technical Appendix B).

When spilling, the Fremont weir was the largest contributor of water to the Yolo Bypass accounting for an average of 75% of tributary inflows, followed by the Sacramento weir at 14%. The CCSB was a relatively small contributor to the overall water balance, providing on average 5% of the water volume entering the Yolo Bypass. Water balances were nearly identical between the nine-sampling events and the entire flood season (Figure 3-4). Other tributaries were also minor contributors to the total inflow. It is important to note that the sampling was designed to target periods of peak flow at the Fremont weir, which meant that samples collected at other inlets did not always correspond to peak flow periods. For example, Figure 3-5 shows the hydrographs for the Fremont Weir and CCSB and the point in the hydrograph when samples were collected. For flashier systems, like the CCSB, their load contributions may have been underestimated with this sampling scheme. On the one occasion when the Fremont weir was not overtopping (March 15, 2017), the CCSB became the dominant source (55%) of water into the Yolo Bypass (Figure 3-6), but this event was the smallest event overall.

Figure 3-4 Average Input Water Balances in Percent for the A) 2017 Sampling Events and B) Season Total from 1/9/17 to 5/4/17
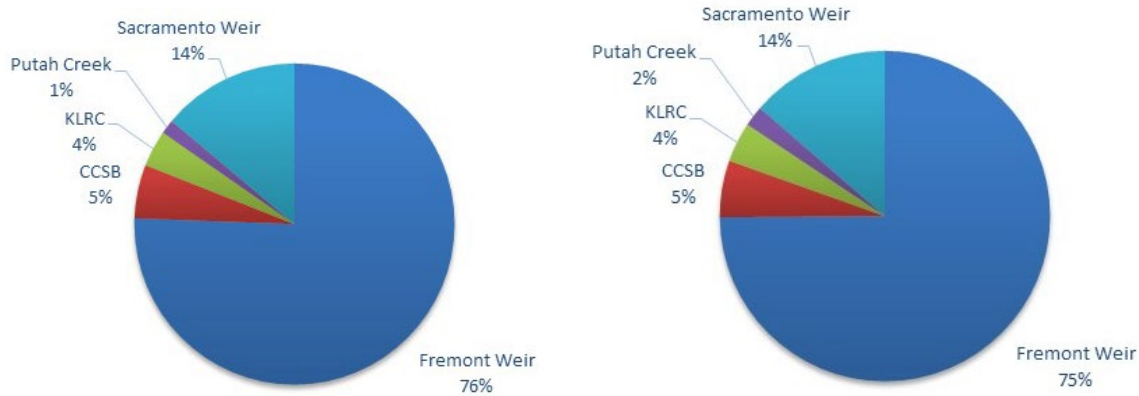
Figure Note: KLRC = Knights Landing Ridge Cut; CCSB = Cache Creek Settling

Figure 3-5 Daily Average Flow from the Cache Creek Settling Basin and the Fremont Weir January 2017 to April 2017
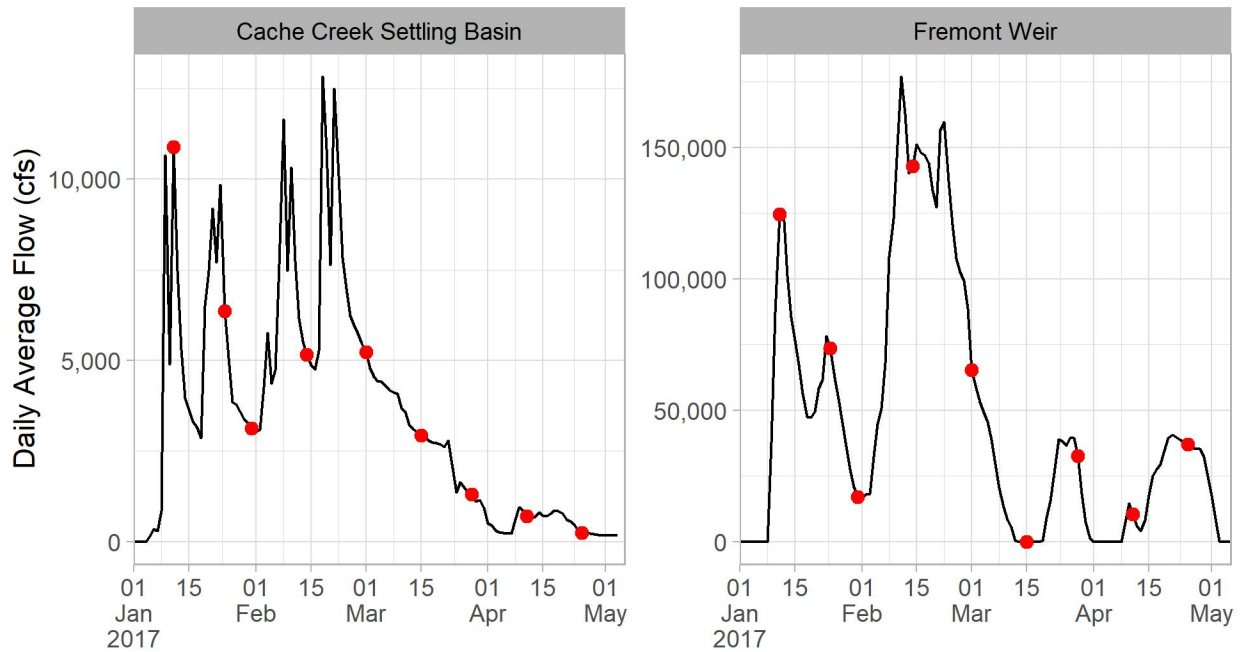
Figure Note: Sampling events shown in red

Figure 3-6 Proportion of Water Inputs to Total Inflow by Tributary and Date
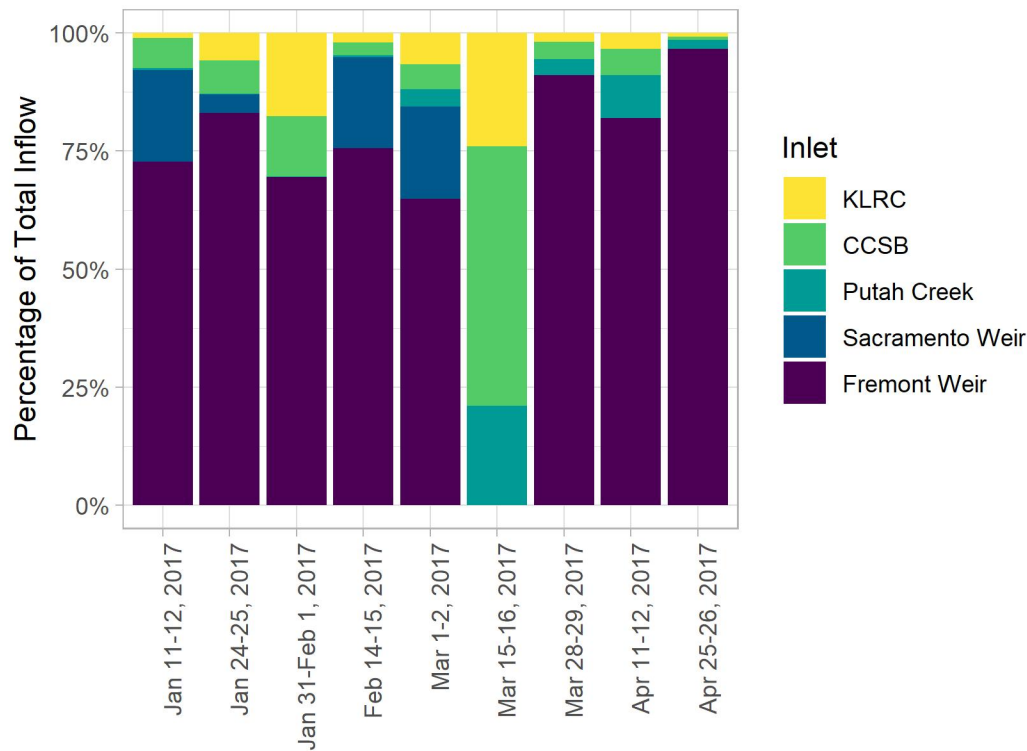
Methylmercury Concentrations in the Upper Yolo Bypass

Tributary concentrations of uMeHg varied spatially and across a broad range of tributary inflows. Concentrations of uMeHg in inlet tributaries ranged over almost an order of magnitude, from a low of 0.058 ± 0.008 ng/L at the Fremont Weir sites to a high of 0.515 ng/L at CCSB, both occurring on the last sampling event on 4/25/2017 (Table 3-2). The Cache Creek Settling Basin (CCSB) and the Knights Landing Ridge Cut (KLRC) exhibited the highest average concentrations of uMeHg (0.23 ± 0.12 and 0.242 ± 0.122 ng/L, respectively), and the Fremont Weir site had the lowest average uMeHg concentration (0.090 ± 0.028 ng/L) for the nine sampling events in 2017. In general, uMeHg values varied the least across all sampling events at the Fremont Weir and Sacramento Weir sites (Coefficient of Variation = 31% and 24%, respectively) and varied the most at the CCSB and KLRC, both of which had a coefficient of variation of 50%. Concentrations of tributary fMeHg and pMeHg each varied by an order of magnitude. The highest average fMeHg concentration occurred at KLRC, while the lowest average occurred at Fremont Weir (Table 3-3). For pMeHg, the highest average pMeHg was from the CCSB, while the lowest was from the Fremont Weir (Table 3-4). In terms of partitioning of uMeHg into particulate and filter passing fractions, partitioning occurred over a narrow range amongst the tributaries. CCSB had the highest percentage of pMeHg (65 ± 4.6 %) and KLRC had the lowest percentage of pMeHg (49 ± 16%) (data not shown, see Technical Appendix B).

Table 3-2. Summary of Tributary Inputs of uMeHg Concentrations (ng/L) for Nine Sampling Events to the Upper Yolo Bypass for Water Year 2017

Sampling Date	Fremont Weir	CCSB	Putah Creek	Sacramento Weir	KLRC
1/11/2017	0.146 ± 0.033	0.217	0.316	0.159	0.124
1/24/2017	0.098 ± 0.007	0.168	0.105	0.114	0.188
1/31/2017	0.065 ± 0.003	0.12	0.115		0.211
2/14/2017	0.11 ± 0.03	0.222	0.131	0.094	0.399
3/1/2017	0.083	0.162	0.158	0.156	0.276
3/15/2017		0.179	0.162		0.477
3/28/2017	0.081	0.210	0.161		0.189
4/11/2017	0.082 ± 0.002	0.318	0.137		0.119
4/25/2017	0.058 ± 0.008	0.515	0.127		0.198
Average (all dates)	*0.090 ± 0.028*	*0.23 ± 0.12*	*0.157 ± 0.063*	*0.13 ± 0.03*	*0.242 ± 0.122*
CV (all dates)	*31%*	*50%*	*40.2%*	*24%*	*50.4%*

Table Notes: CCSB = Cache Creek Settling Basin. KLRC = Knights Landing Ridge Cut. Fremont Weir concentration data represent the average of three collection sites: the east side, west side, and middle sampling stations. A standard deviation is given for the Fremont collections when all three sites were sampled. MeHg concentration data were excluded if the value of the filter-passing fraction was greater that the unfiltered value, which was the case for the Fremont Weir east location on 3/1/2017 and 3/28/2017. The CCSB data represent the average of two sampling sites, the north and south weirs, except for the 3/28/2017 and 4/11/2017 sampling dates which also include the low-flow channel, and the 4/25/2017 sampling date which is the average of the south weir and low-flow channel sampling sites. Particulate MeHg (pMeHg) concentrations were determined by difference (pMeHg = uMeHg – fMeHg).

First Flush Effect for Tributary Inflow Concentrations

A first flush effect with uMeHg is clearly evident during the first sampling event on January 11th for the Fremont Weir and Putah Creek sampling sites, driven primarily by an enhanced pMeHg concentration (Tables 3-2 through 3-4). The uMeHg concentration on the first sampling event at Fremont Weir (0.146 ± 0.033 ng/L) is higher than all the other sampling events, and 60% higher than the average concentration for all sampling events at the Fremont Weir (0.090 ± 0.028). Similarly, the uMeHg concentration on the first sampling event at Putah Creek (0.316 ng/L) is higher than all the other sampling events and was two-fold higher than the average for all 9 sampling events (0.157 ± 0.063 ng/L). The other sampling sites did not show a clear first flush effect with uMeHg or pMeHg. Interestingly, there was a reverse trend at CCSB, where uMeHg concentrations continually rose in the last three sampling events, cumulating in the highest uMeHg concentration being observed in the last sampling event (0.515 ng/L), which was double the average concentration for the entire flood event (0.23 ± 0.12 ng/L). The rise in uMeHg at the end of the flood event at CCSB were driven by increases in both fMeHg and pMeHg concentrations (Tables 3-3 and 3-4).

Table 3-3. **Summary of Tributary Inputs of fMeHg Concentrations (ng/L) for Nine Sampling Events to the Upper Yolo Bypass for Water Year 2017**

Sampling Date	Fremont Weir	CCSB	Putah Creek	Sacramento Weir	KLRC
1/11/2017	0.044 ± 0.009	0.082	0.042	0.042	0.054
1/24/2017	0.037 ± 0.003	0.058	0.044	0.057	0.102
1/31/2017	0.023 ± 0.002	0.040	0.049		0.130
2/14/2017	0.038 ± 0.003	0.074	0.058	0.029	0.246
3/1/2017	0.030	0.042	0.050	0.060	0.169
3/15/2017		0.060	0.060		0.172
3/28/2017	0.037	0.060	0.049		0.089
4/11/2017	0.037 ± 0.003	0.130	0.056		0.087
4/25/2017	0.023 ± 0.001	0.182	0.062		0.039
Average (all dates)	*0.034 ± 0.007*	*0.081 ± 0.047*	*0.052 ± 0.007*	*0.047 ± 0.014*	*0.12 ± 0.07*
CV (all dates)	*22%*	*57%*	*14%*	*31%*	*54%*

Table Notes: CCSB = Cache Creek Settling Basin. KLRC = Knights Landing Ridge Cut. Fremont Weir concentration data represent the average of three collection sites: the east side, west side, and middle sampling stations. A standard deviation is given for the Fremont collections when all three sites were sampled. MeHg concentration data were excluded if the value of the filter-passing fraction was greater that the unfiltered value, which was the case for the Fremont Weir east location on 3/1/2017 and 3/28/2017. The CCSB data represent the average of two sampling sites, the north and south weirs, except for the 3/28/2017 and 4/11/2017 sampling dates which also include the low-flow channel, and the 4/25/2017 sampling date which is the average of the south weir and low-flow channel sampling sites. Particulate MeHg (pMeHg) concentrations were determined by difference (pMeHg = uMeHg – fMeHg).

Table 3-4. **Summary of Tributary Inputs of pMeHg Concentrations (ng/L) for Nine Sampling Events to the Upper Yolo Bypass for Water Year 2017**

Sampling Date	Fremont Weir	CCSB	Putah Creek	Sacramento Weir	KLRC
1/11/2017	0.10 ± 0.03	0.135	0.274	0.117	0.070
1/24/2017	0.061 ± 0.008	0.11	0.061	0.057	0.086
1/31/2017	0.041 ± 0.003	0.085	0.066		0.081
2/14/2017	0.070 ± 0.029	0.15	0.073	0.065	0.153
3/1/2017	0.053	0.12	0.108	0.096	0.107
3/15/2017		0.12	0.102		0.305
3/28/2017	0.044	0.150	0.112		0.100
4/11/2017	0.045 ± 0.003	0.188	0.081		0.032
4/25/2017	0.035 ± 0.009	0.332	0.065		0.159
Average (all dates)	*0.056 ± 0.022*	*0.15 ± 0.07*	*0.10 ± 0.07*	*0.084 ± 0.028*	*0.12 ± 0.08*
CV (all dates)	*38%*	*47%*	*63%*	*33%*	*65%*

Table Notes: CCSB = Cache Creek Settling Basin. KLRC = Knights Landing Ridge Cut. Fremont Weir concentration data represent the average of three collection sites: the east side, west side, and middle sampling stations. A standard deviation is given for the Fremont collections when all three sites were sampled. MeHg concentration data were excluded if the value of the filter-passing fraction was greater that the unfiltered value, which was the case for the Fremont Weir east location on 3/1/2017 and 3/28/2017. The CCSB data represent the average of two sampling sites, the north and south weirs, except for the 3/28/2017 and 4/11/2017 sampling dates which also include the low-flow channel, and the 4/25/2017 sampling date which is the average of the south weir and low-flow channel sampling sites. Particulate MeHg (pMeHg) concentrations were determined by difference (pMeHg = uMeHg – fMeHg).

Variability in MeHg Concentrations with Inflow

Figure 3-7 shows how uMeHg, pMeHg, and fMeHg varied as a function of tributary flow for the Fremont Weir and the CCSB. For the Fremont Weir, all the forms of MeHg increased in concentration with increasing flow, while for the CCSB, the concentrations were much higher at very low tributary inflows. For the CCSB, there was no significant relationship between flow and concentration. Because the Fremont Weir accounts for approximately 75% of the hydrologic inflow (Figure 3-4), it has a dominant impact on MeHg concentrations in the Yolo Bypass. This increase in MeHg concentrations with flow in the Fremont Weir tributary input has important impacts on loads to the upper Yolo Bypass. It means that increases in load with hydrologic flow are driven not only by delivery of more water, but also by increases in MeHg concentrations as flow increases.

Figure 3-7 **Variation in MeHg Concentrations as a Function of Tributary Inflow for the Fremont Weir and Cache Creek Settling Basin**

Unfiltered MeHg   Filtered MeHg   Particulate MeHg
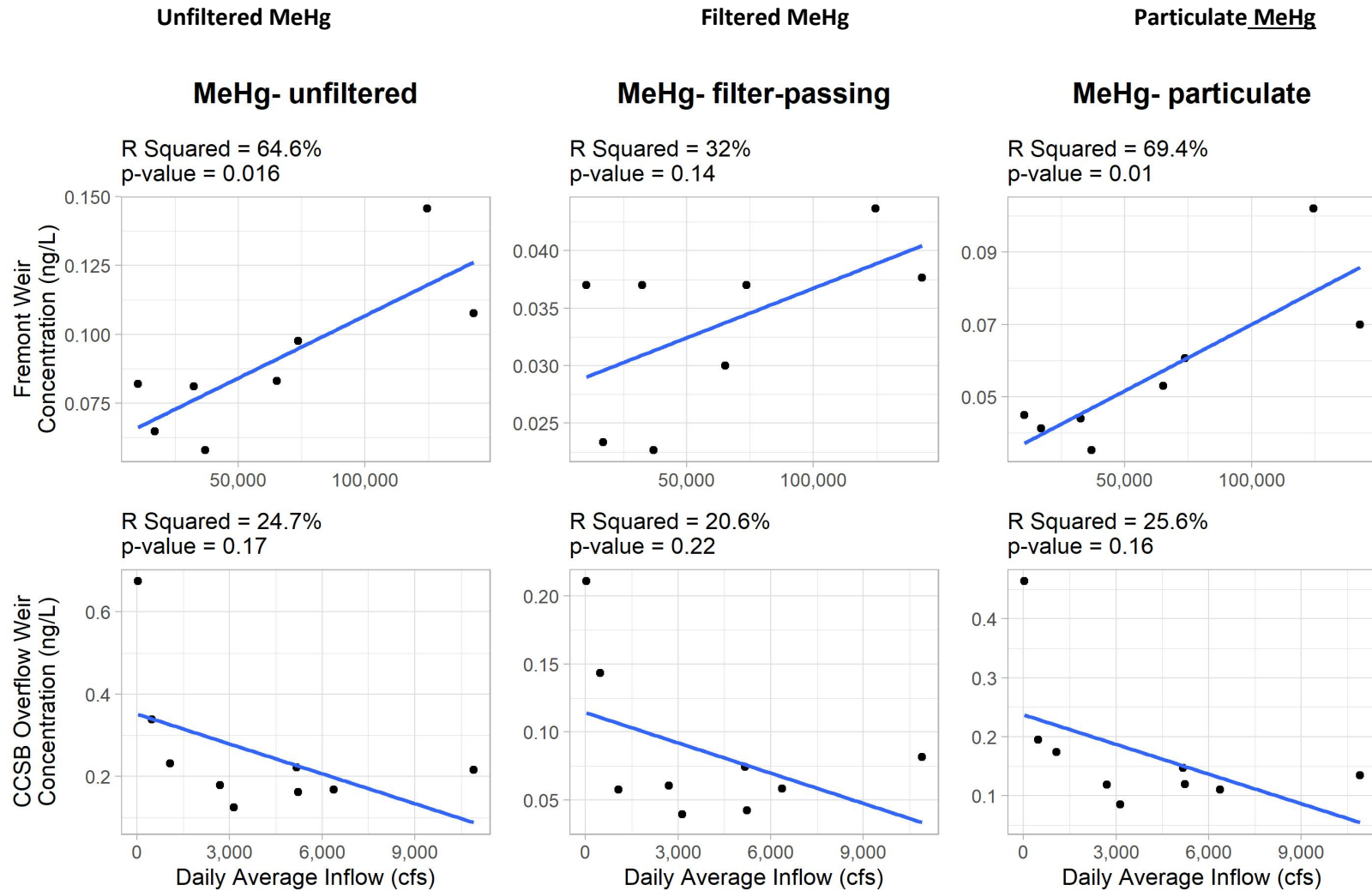
Internal Production or Loss of Mercury, Methylmercury and Several Biogeochemical Parameters in the Upper Yolo Bypass

Changes in concentrations of several parameters were evaluated as water traversed from north to south down the Yolo Bypass. Table 3-5 lists a comparison of the percentage increase of Hg and MeHg with several biogeochemical parameters between the tributary input at the Fremont Weir and an average of the Half-Lisbon and Liberty Cut export sites for the 2017 flood event. The data in Table 3-5 represent only those sampling events where the specific conductance at the export was within 15% of the specific conductance for the Fremont Weir input water. The average specific conductance for the west side tributaries (437 µS/cm) is considerably higher than the average for the Fremont Weir (123 µS/cm), allowing a clear distinction between east side from west side tributary sources at the export sites. The export site at Shag Slough was not used in this comparison because its specific conductance was similar to the specific conductance for west side water sources most of the time.

Table 3-5 Comparison of the Percentage Increase of Hg and MeHg with Several Biogoechemical Parameters between the Fremont Weir Tributary Input and Export at Liberty Island

Parameter (units)	Average Concentration at Fremont Weir	Average Export Concentration	% Increase in Export Concentration
Specific Conductance (µS/cm)	118	118	0.3%
Chloride (mg/L)	2.8	3.1	11%
uHg (ng/L)	13.2	14	5.9%
fHg (ng/L)	2.1	2.2	4.1%
pHg (ng/L)	11.1	11.8	6.3%
uMeHg (ng/L)	0.096	0.171	79%
fMeHg (ng/L)	0.035	0.066	91%
pMeHg (ng/L)	0.061	0.105	72%
TOC (mg/L)	2.3	2.3	-0.1%
DOC (mg/L)	1.8	1.9	9.3%
TSS (mg/L)	95	52	-45%
MeHg, solid phase (ng/g)	0.77	2.53	229%
TOC/TSS (proportion organic)	0.027	0.052	94%

Table Notes: TSS = Total Suspended Solids. TOC = Total Organic Carbon. DOC = Dissolved Organic Carbon. The average concentrations only include sampling events when the specific conductance value of the export was within 15% of the specific conductance observed at the Fremont Weir. The average export concentration was the average for collections obtained at Half-Lisbon and Liberty Cut, and the average concentration at Fremont Weir was the average of three collection sites: the east side, west side, and middle sampling stations.

This comparison suggests that there were significant increases in all forms of MeHg (uMeHg, fMeHg and pMeHg) during passage of flood waters through the upper Yolo Bypass, with only minor increases (4-6%) in the (inorganic) Hg forms (uHg, fHg, and pHg). The major MeHg form that showed increases was solid phase MeHg (i.e. MeHg on particles), which increased more than two-fold between the Fremont Weir input and export. The comparison also suggests that there is a substantial internal loss (45%) of Total Suspended Solids (TSS) and only minor or no changes in TOC or DOC. Note also that particles at the export site were far more organic rich (94%) than that for the Fremont Weir input, as evidenced by the

TOC/TSS ratio which describes the proportion of the solids that were organic in nature. This analysis strongly supports the contention that there is a substantial internal production of MeHg in the upper Yolo Bypass which enhances MeHg concentrations in overlying flood waters as it progresses from input to exit through the upper Yolo Bypass. As discussed in the Vegetation Senescence section of this report, one potential source for this enhancement is pastureland vegetation which releases its MeHg content both in dissolved and particulate phases.

Mass Balances - Mercury, Total Suspended Solids, and Organic Carbon

Tributary Input Loads

Tributary loads exhibited a first flush pattern for all forms of Hg, MeHg, and organic carbon, as well as TSS (Figure 3-8). The first sampling event occurred a few days after the Yolo Bypass first began flooding. In subsequent sampling events, loads generally fell by half or more for all parameters except MeHg, lending support to the first flush idea. MeHg loads were equally high on the February 14th sampling event which had the highest sample event flows. As discussed previously, there was a strong positive relationship between flow and uMeHg concentrations at the Fremont Weir.

Fremont Weir was the largest contributor of water to the Yolo Bypass and, on average, of the eight sampling events when the Fremont Weir was spilling it was the largest contributor of uHg (73%), uMeHg (68%), and TSS (80%) to the Yolo Bypass (Figure 3-9). Similarly, when the Sacramento Weir was spilling, it was the second largest water volume contributor to the Yolo Bypass, and was generally the second largest contributor of uMeHg loads. When open, the Sacramento Weir provided averages of 19% of the total inflow to the Bypass, and 28, 21, and 18% of the total input load of uHg, uMeHg, and TSS, respectively. While the gates of the Sacramento Weir are rarely open, this emphasizes that it can be an important source.

When compared to the Fremont Weir, the CCSB and KLRC were relatively small inputs of MeHg to the Yolo Bypass. Both the CCSB and KLRC contributed an average of 10% of the uMeHg input load when the Fremont Weir was spilling in 2017. However, when the Fremont Weir was not spilling, the CCSB generally became the second largest contributor of uHg. Overall, the CCSB contributed an average of 570 g/day of uHg during the 2017 flood. Excluding the one sampling event when the Fremont weir was not overtopping, the largest Hg and TSS loads from the CCSB were on the first two sampling events of the 2017 flood, which may be due to a first-flush effect. The CCSB contributed about 25% of the uHg and pHg input loads while it was about 7% of the total inflow during these first two sampling events. The CCSB contributed a much smaller percentage of the Hg input load to the Yolo Bypass after about 5 weeks into the 2017 flood which continued throughout the duration of the flood (except for when the Fremont Weir was not spilling on March 15th). Interestingly, the KLRC had a consistently higher percentage of the total mercury in the methylmercury fraction (MeHg/Hg ratios) than the other inputs (see Technical Appendix B). These higher ratios at KLRC suggest that the land use management and or habitat type associated with this site was more effective at converting inorganic Hg to MeHg.

Figure 3-8 Total Input Loads by Event for Hg, MeHg, Organic Carbon and TSS
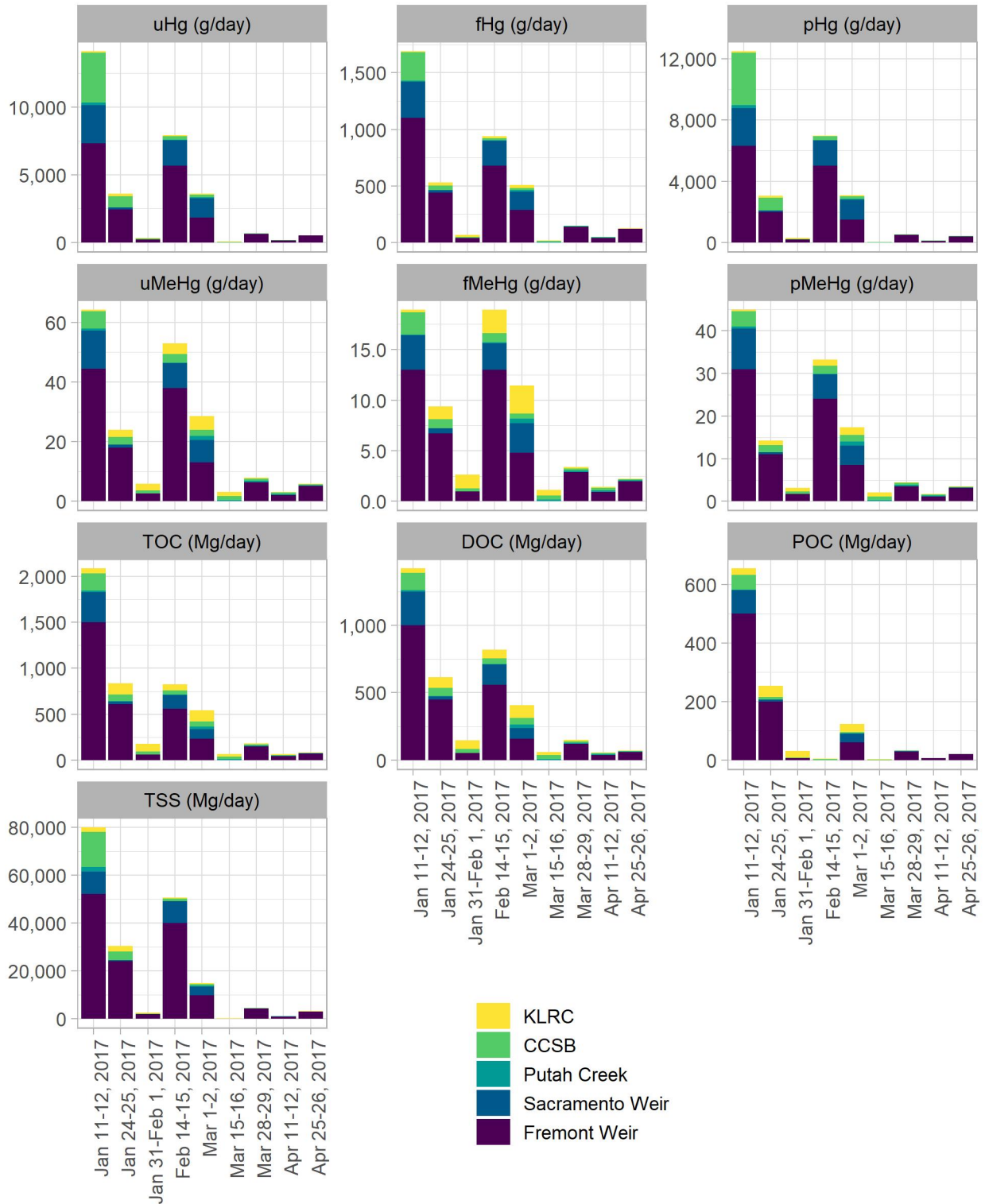
Figure 3-9 Proportion of Individual Tributary Loads to the Total Input Load

Regardless of the sampling event or the tributary, the pHg fraction strongly dominated all input Hg loads while input loads for MeHg, tended to be more evenly distributed between the particulate and filtered fractions (Figures 3-10 and 3-11). This relationship held regardless of the sampling event. KLRC generally showed the highest fraction of fMeHg and CCSB the highest fraction of pMeHg. Overall, 87% and 64% of the total inlet loads of Hg and MeHg, respectively, were in the particulate fraction during the 2017 flood.

Figure 3-10 Percentage of Filtered and Particulate uHg Fractions by Sampling Event for Inlet Tributaries into the Yolo Bypass
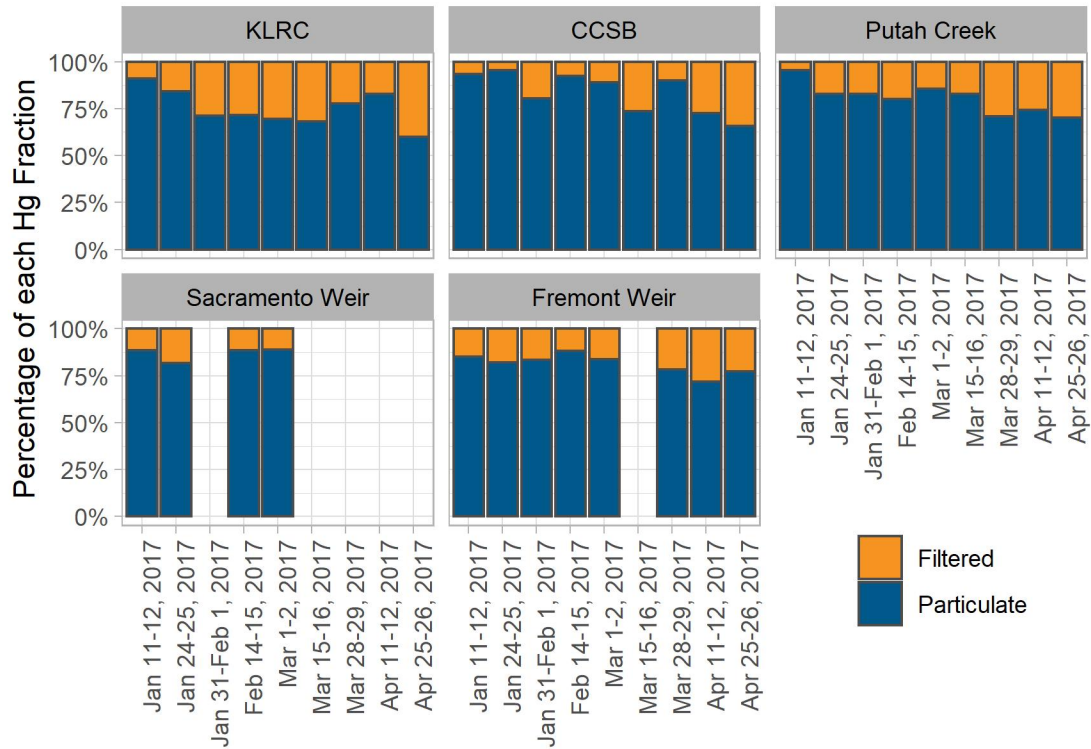
Figure 3-11 Percentage of Filtered and Particulate uMeHg Fractions by Sampling Event for Inlet Tributaries into the Yolo Bypass
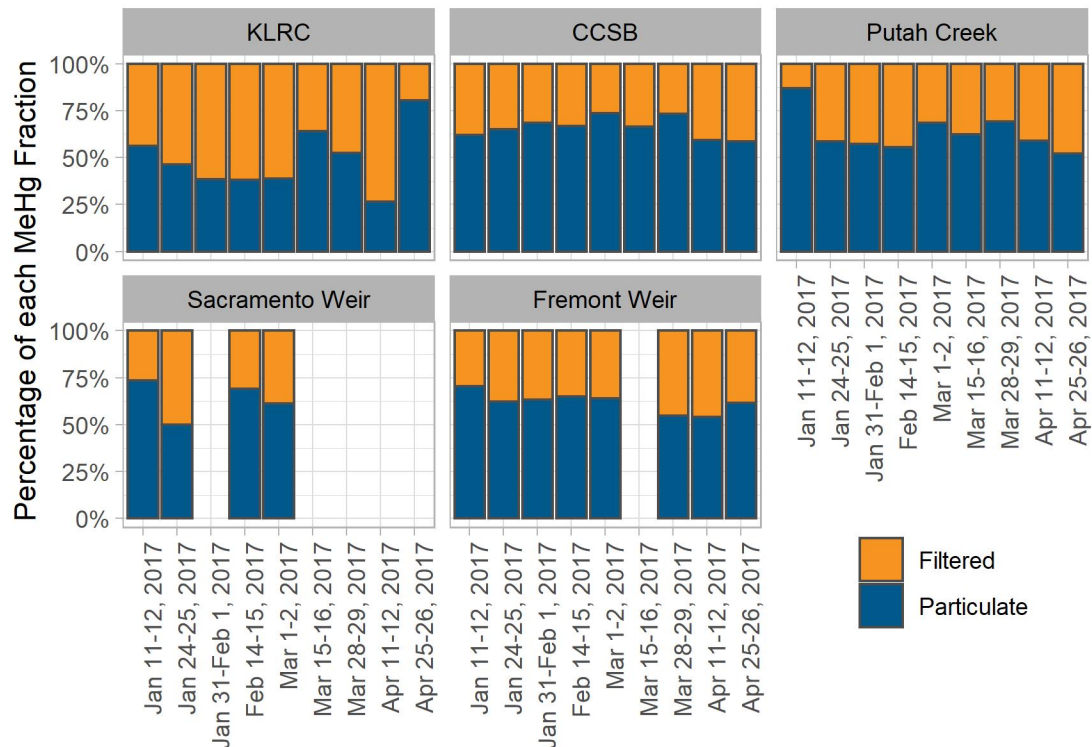
Average seasonal loads for uHg and uMeHg for tributaries into the Yolo Bypass for water year 2017 are shown below in Table 3-6. Detailed flows, and load associated with these calculations are presented in Technical Appendix B. The particulate fraction again strongly dominated uHg inflows while pMeHg, generally made up a little more than half of the uMeHg fraction. Note that the high level of uncertainty associated with these averages is due to the large changes in flows across the 9 sampling events and not the concentrations (see for example Tables 3-2 through 3-4). As illustrated in Figure 3-5, tributary input flows could vary by several orders of magnitude. For example, across the nine sampling events, total input flows varied between 5,338 cfs (March 15, 2017) to 188,700 cfs (February 14, 2017). These large variations translated to large variations in total input flows. Large changes in flow between sampling events resulted in large changes in loads. Thus, the uncertainty calculations associated with average loads for all sampling events in this document reflects the variation between large seasonal flow differences, and not uncertainties associated with individual sampling event estimates of loads.

Table 3-6 **Average uHg and uMeHg loads by tributary entering the Yolo Bypass**

Inlet location	uHg load (g/day)	uMeHg load (g/day)
Fremont Weir	2,100 ± 2,700 (81%)	14 ± 16 (62%)
Sacramento Weir	694 ± 1,070 (87%)	3.3 ± 4.9 (64%)
Cache Creek Settling Basin	570 ± 1,200 (84%)	1.9 ± 1.7 (66%)
Knight's Landing Ridge Cut	59 ± 65 (75%)	1.72 ± 1.61 (49%)
Putah Creek	40 ± 66 (81%)	0.421 ± 0.426 (63%)
Total	3,500 ± 4,800 (81%)	22 ± 23 (61%)

Table Note: Loads are the average calculated from nine sampling events collected from January 2017 through April 2017. Loads are in g/day ± 1 standard deviation. Numbers in parentheses are the percentage of the total load in the particulate form.

Net Export Loads

As discussed earlier, the sampling design allowed the division of the Yolo Bypass into an upper and lower reach. This approach provided a more accurate picture of the net exports to the Delta and was the first time that the influence of Liberty Island on total exports was examined. The upper reach encompasses the area receiving drainages from the inlets to the outlet at the Stairsteps drainage canals which covers about two-thirds of the length of the Yolo Bypass. The lower reach encompasses the area from the stairsteps to below Liberty Island which allowed us to isolate the effects of Liberty Island (see figure 3-3). Net loads associated with the upper reach were calculated by subtracting the sum of the tributary inlet loads from the stairstep outlet loads. Net loads associated with both reaches were calculated similarly by subtracting the sum of the tributary inlet loads from the loads below Liberty Island.

Upper Reach

Total exports from the upper reach showed a strong first flush phenomenon for uHg, all organic carbon fractions (DOC, POC and TOC), and to a lesser extent, TSS (Figure 3-12). Export loads of all forms of MeHg also showed a first flush phenomenon. Additionally, export loads associated with each form of MeHg were similar in both the first event and the February 14 event.

Figure 3-12 Export Loads by Date for the Upper Reach of the Yolo Bypass
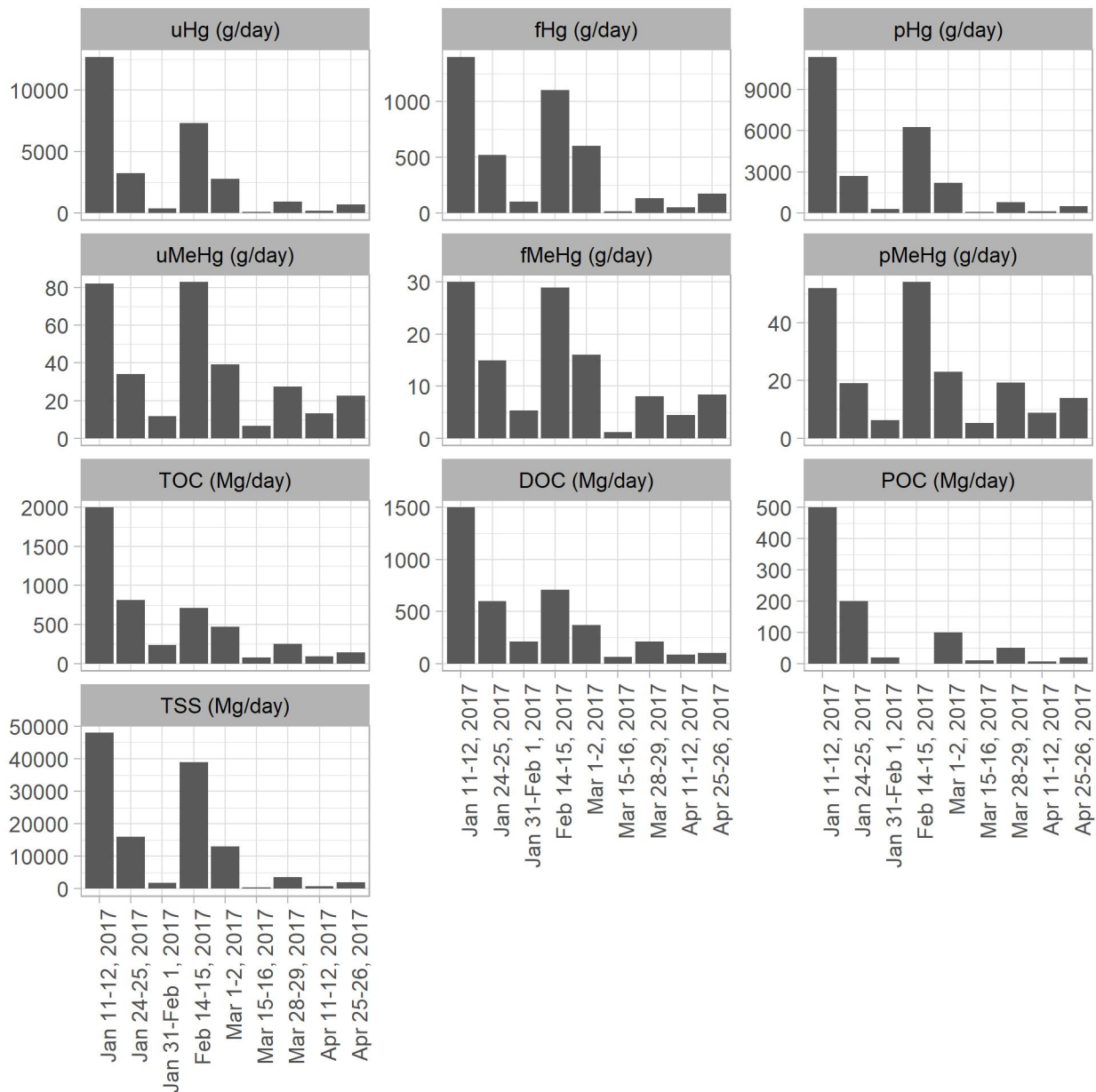
On average, the upper reach of the Yolo Bypass was a net sink for all fractions of Hg and a net source for all fractions of MeHg (Table 3-7). The net load of uHg deposited in the upper reach of the Yolo Bypass was predominately in the particulate form (~99%), while approximately 60% of the net uMeHg load was in the particulate form (Table 3-7). While the upper reach was a net sink for TSS and TOC, it was a net source of DOC.

Internal MeHg production in the upper reach of the Yolo Bypass resulted in a substantial increase in uMeHg loads exiting the Stairsteps. On average, 36 ± 29 g/day was exported from the upper reach of the Yolo Bypass. Of this, on average, 22 ± 23 g/day or 61% came from tributary inputs while, on average, internal production added an additional 14 ± 8.1 or 39%.

As with input loads, high levels of uncertainty reflect the large changes in flow used to calculate loads and are not indicative of the variability associated with the sampling of a single location or event. Calculations of the uncertainty associated with load measurements provides a means to evaluate the strength of mass balance calculations that indicate a reach is a net source or sink for a parameter. It should be noted that the net loads of all fractions of Hg within the entire Bypass had percent differences less than their measurement uncertainty of 11% making them inconclusive (Table 3-7). The percent difference of a net load quantifies the proportion of the load produced or retained within the system in relation to the load entering the system. Percent differences should be greater than the measurement uncertainty of the load values for their associated net loads to be conclusive.

.

Table 3-7 **Average Loads ± 1 std. dev. and Percent Differences for Hg Species (g/day) and other Water Quality Parameters (Mg/day) Entering and Leaving the Yolo Bypass for 9 Sampling Events in WY 2017**

Parameter	Input Load	Output Load (at Stairsteps)	Output Load (Below Liberty Island	Net Load- Upper Reach (Stairsteps - Input)	Percent Difference Upper Reach	Net Load Lower Reach (Below Liberty Island - Stairsteps)	Percent Difference Lower Reach	Net Load- Entire Bypass	Percent Difference Entire Yolo Bypass
uHg	3,500 ± 4,800	3,100 ± 4,300	3,700 ± 5,200	-320 ± 530	-9.2%	190 ± 810	5.5%	-170 ± 550	-4.3%
fHg	500 ± 600	450 ± 490	520 ± 580	-8 ± 100	-1.7%	26 ± 110	5.2%	20 ± 100	3.3%
pHg	3,000 ± 4,200	2,700 ± 3,800	3,200 ± 4,600	-320 ± 480	-11%	160 ± 690	5.2%	-200 ± 490	-6.0%
uMeHg	22 ± 23	36 ± 29	42 ± 41	14 ± 8.1	63%	3.7 ± 12	10%	18 ± 19	75%
fMeHg	7.7 ± 7.3	13 ± 10	17 ± 13	5.4 ± 3.4	70%	2.9 ± 4.1	21%	8.6 ± 6.9	101%
pMeHg	14 ± 16	22 ± 19	25 ± 29	8.6 ± 6.0	62%	0.49 ± 12	2.0%	9.3 ± 14	60%
TOC	500 ± 700	540 ± 620	670 ± 780	-4 ± 60	-0.7%	83 ± 160	14%	70 ± 100	12%
DOC	400 ± 500	400 ± 400	500 ± 500	10 ± 60	2.3%	30 ± 70	6.7%	40 ± 40	8.3%
POC	100 ± 200	100 ± 200	200 ± 300	-20 ± 50	-17%	40 ± 100	33%	10 ± 70	10%
TSS	20,000 ± 30,000	14,000 ± 18,000	20,000 ± 28,000	-7,000 ± 10,000	-34%	4,200 ± 10,000	27%	-3,600 ± 3,200	-15%

Table Note: Net loads at the Stairstep sampling sites plus the net loads below Liberty Island do not sum to the net loads exported from the Yolo Bypass because no samples were collected below Liberty Island on the April 11, 2017 sampling event.

All values are reported to appropriate significant digits. Average load calculations may not sum exactly based on individual event loads being either negative or positive and the use of significant figures.

Positive net load values represent net internal production and negative values represent loss within the segment. The percent differences of the net loads for the Upper Reach and Entire Yolo Bypass were calculated by dividing the average net loads by their associated average inlet loads. The percent differences of the net loads for the Liberty Island Reach were calculated by dividing the average net loads by their associated average outlet load measured at the Stairsteps location. Calculations for the Liberty Island Reach and the Entire Yolo Bypass exclude the April 11, 2017 sampling event because samples were not collected below Liberty Island during this event. Therefore, the net loads from the Upper and Liberty Island Reaches do not sum to the net loads exported from the Entire Yolo Bypass.

The partitioning between the filter-passing and particulate net MeHg loads from the upper reach changed through the course of the 2017 flood event. Net fMeHg loads were greater than the net pMeHg loads during the first two sampling events in 2017 (Figure 3-13, suggesting that diffusion of fMeHg from sediment porewater was the more influential source of MeHg at the start of the flood. The particulate fraction became the larger contributor to the net MeHg loads during the remaining seven sampling events in 2017 covering the last 3 months of the flood (Figure 3-13). Moreover, the MeHg concentration on solids, which provides an estimate of the amount of MeHg bound to the suspended sediment, increased at the three Stairsteps locations during the last four sampling events in 2017 (Figure 3-14). This hints that suspended organic and inorganic particles enriched with MeHg became the more important source of MeHg during the latter half of the flood. Additionally, as shown in Figure 3-15, the upper reach transitioned from a net sink to more of a net source of Volatile Suspended Solids (VSS) during the last three months of the flood. A measurement of VSS provides an estimate of the amount of organic material suspended in the water. Together, this suite of evidence points to an organic source for this end of season pMeHg.

Figure 3-13 **Net Internal Production of Filter-Passing and Particulate Methylmercury within the Upper Reach for Sampling Events in 2017**
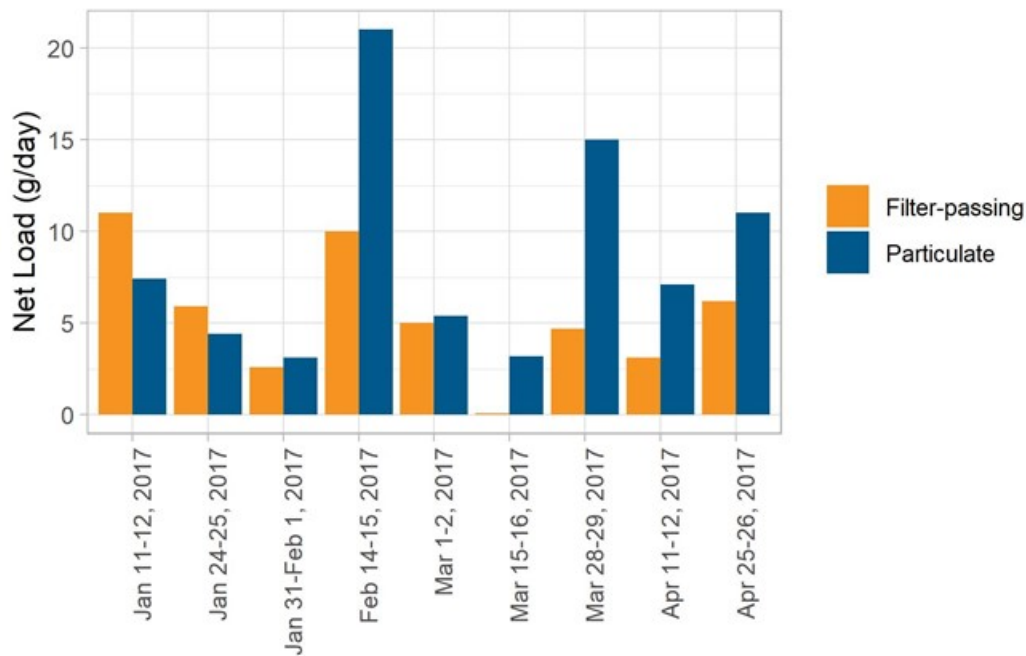
Figure 3-14 Methylmercury Concentrations on Solids at the Three Stairsteps Locations for Sampling Events in 2017
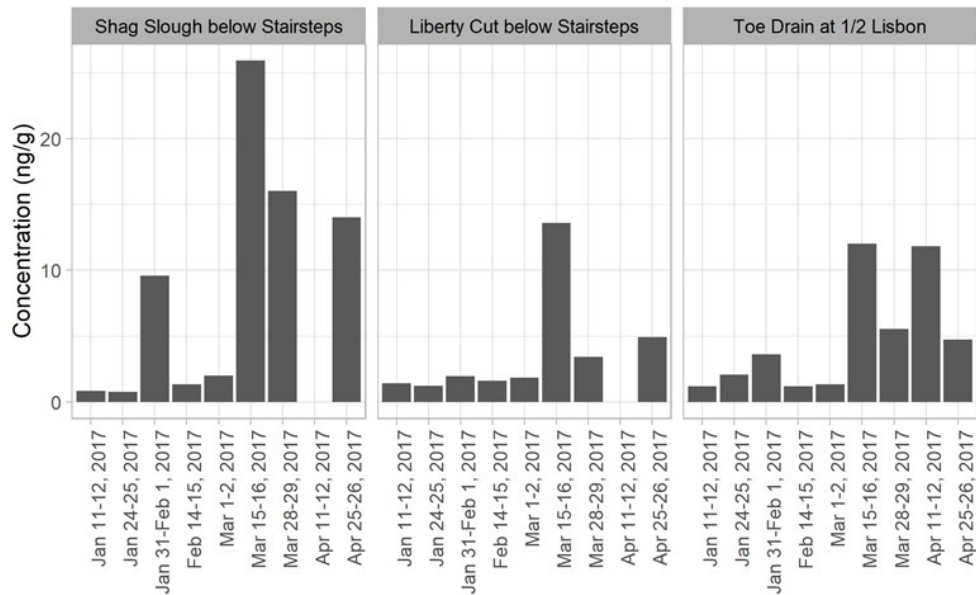
Figure 3-15 Net loads of Volatile Suspended Solids Within the Upper Reach for Sampling Events in 2017
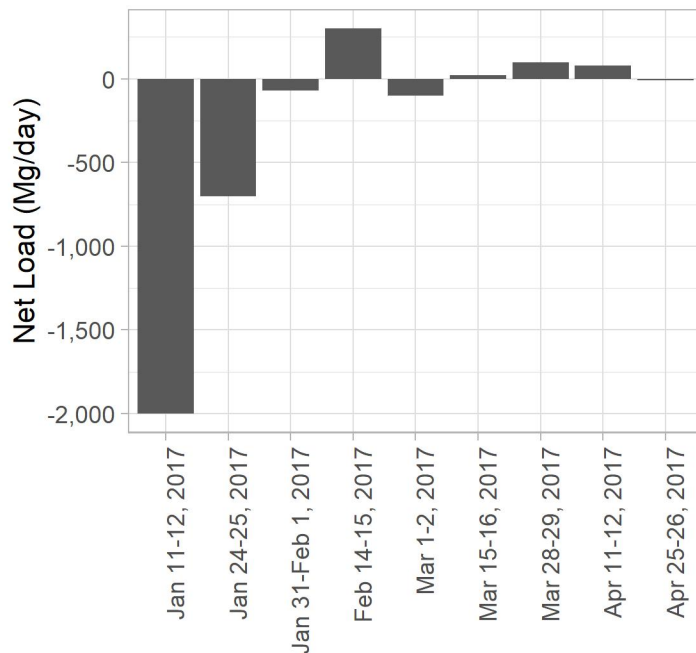
Figure Note: Negative values indicate a net sink. Positive values indicate a net source.

Net internal production of MeHg within the Yolo Bypass significantly increased as inflows increased particularly with fMeHg and uMeHg. The strongest positive correlation was observed with fMeHg within the upper reach where Yolo Bypass inflow explained 84% of the variation in the internal production of fMeHg (Figure 3-16). In contrast, total inflow to the Bypass did not have a significant effect on the internal production of pMeHg within the upper reach ($R^2 = 24\%$, p = 0.18). The strong positive relationship between inflow and the net internal production of fMeHg suggests that diffusion of fMeHg from sediment porewater is the process most affected by increasing inflow and inundated land.

Foe and others (2008) also documented a significant increase in net uMeHg production in the upper reach of the Yolo Bypass, however, the net internal MeHg relationship developed from our mass balance study was lower than that developed by Foe and others (2008) (Figure 3-17). Several lines of evidence suggest that the relationship developed by the two studies cannot be compared directly, and that similarities as well as differences exist. First, the four highest flows in WY 2017 occurred when the gates to the Sacramento Weir were open. Sacramento weir gates were not open in the Foe and others (2008) study. Second, in this study, the entire winter flood event, from January to April, was sampled, however, Foe and others (2008), collected samples exclusively in the spring from the beginning of March to the end of May. This difference in the timing of sample collection could be important since the spring months tend to have warmer water temperatures, which can increase mercury methylation rates. Third, the 2006 and 2017 sampling events had very different hydrographs. The Yolo Bypass flooded extensively twice during the 2006 wet season: from the end of December 2005 to the middle of February 2006, and from the beginning of March to the beginning of May 2006. In contrast, the 2017 flood consisted of one extended flood event from the beginning of January to the beginning of May 2017. These differences may have impacted Mg cycling. The two studies showed similar relationships between net internal MeHg production with flow once the four data points associated with the highest flows of the Sacramento Weir contributions are removed. Similarly, the two sampling events from WYs 2014 and 2016 of this study fall along the originally developed regression line calculated by Foe and others (2008).

Based on information provided in Table 3-7 Figure 3-18 provides a conceptual mass balance model for uMeHg loads for the Upper Reach of the Yolo Bypass for the nine sampling events in WY 2017.

Figure 3-16 Relationship between Net Internal Loads (Source or Sink) of Mercury (Filtered, Particulate and Total), Methyl Mercury (Filtered, Particulate and Total), and Total Suspended Solids to Total Water Inflow for the Upper Reach in the Yolo Bypass for Sampling Events in 2017
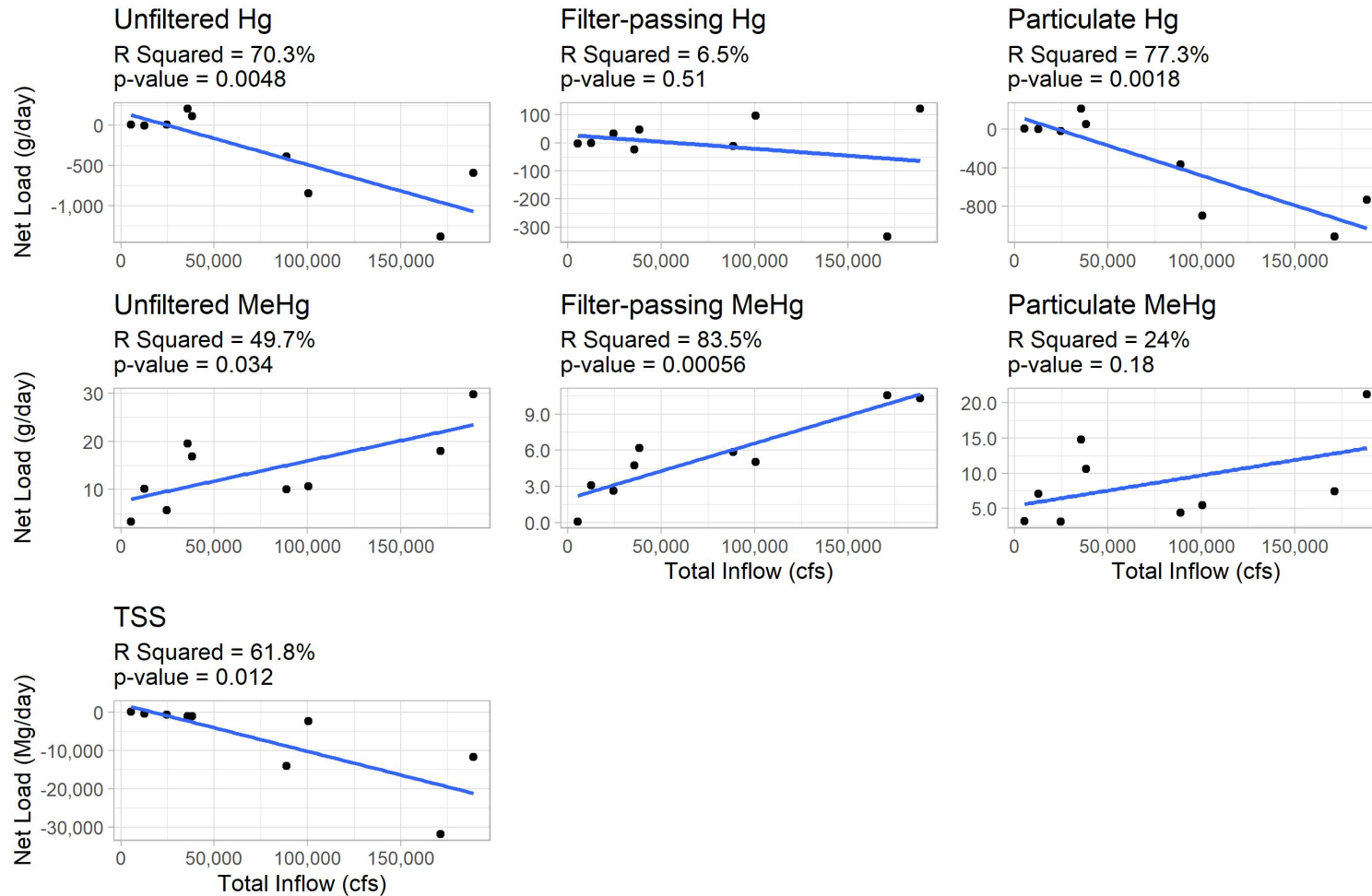
Figure 3-17 Comparison between Total Tributary Inflow and MeHg Loads Exported for Samples Collected in 2006 by Foe and others, (2008) and this Study (Water Years 2014, 2016 and 2017)
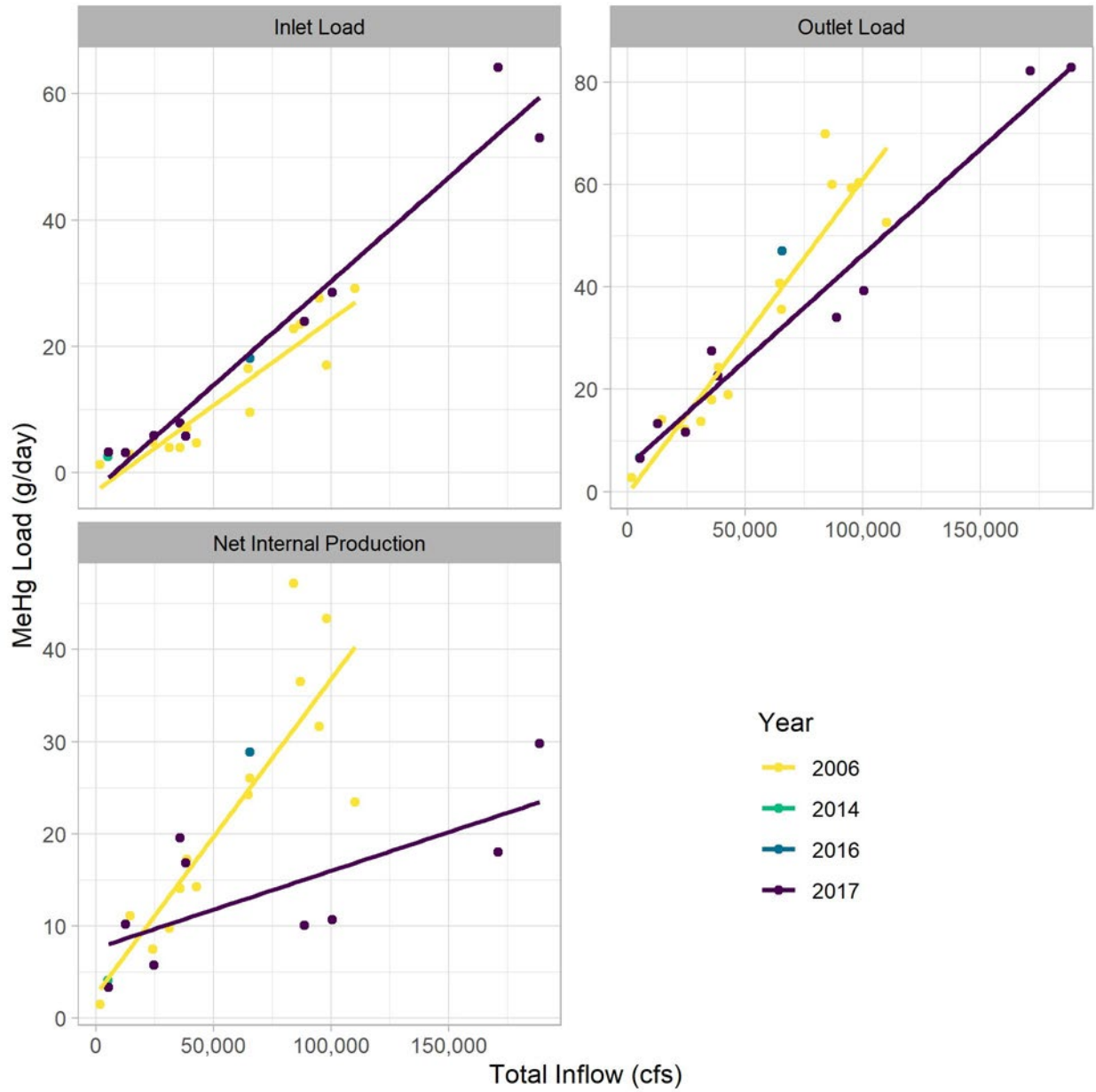
Figure 3-18 Mass Balance of Average Net uMeHg loads (in g/day ± 1 std. dev.) for Tributary Inputs and Loads Leaving the Yolo Bypass at the Stairsteps for WY 2017
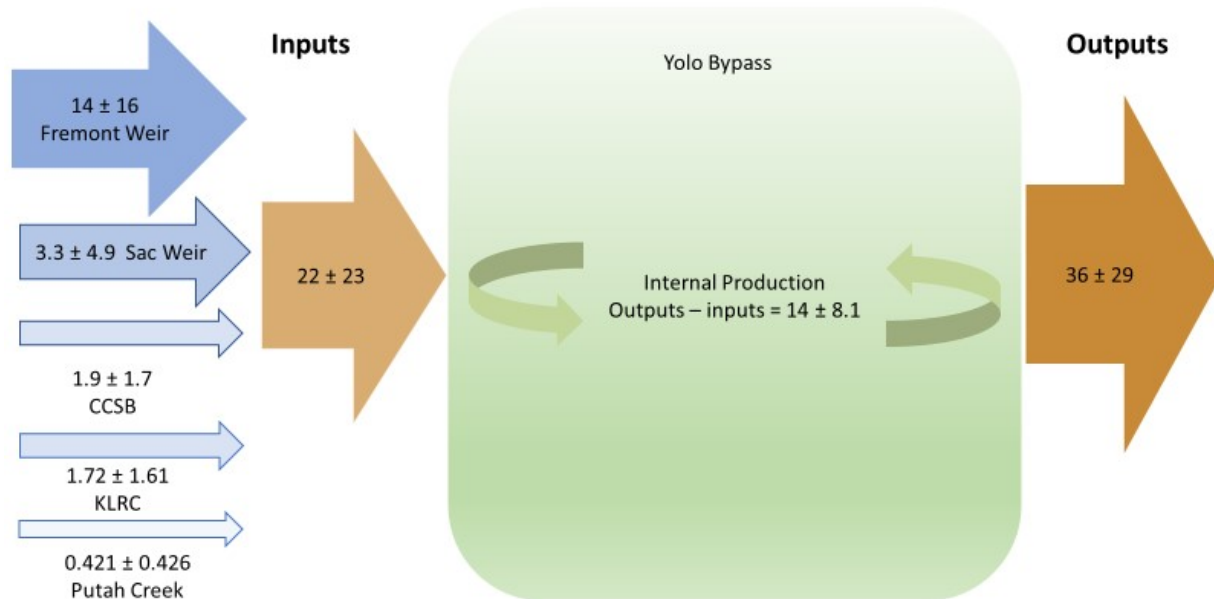
Figure Note: Input calculations included zero flows for Fremont and Sacramento Weirs. Outputs are the sum of discharges from the Toe Drain at Half Lisbon, Liberty Cut and Shag Slough below the stairsteps. High levels of uncertainty reflect the large variability in flows across the sampling events and not the uncertainty associated with load determination for a single location and event.

Upper + Lower Reach

Sampling below Liberty Island provided an overall picture of the loads exiting the full Yolo Bypass and an evaluation of Liberty Island contributions. Of the analytes listed in Table 3-7, Liberty Island, on average was always a net source. This contrasted with net production in the upper reach, which depending on the analyte, could, on average, be either a source or a sink. On average, Liberty Island contributed 16 percent to the uHg loads exported from the full Yolo Bypass and 14 percent of the export load of uMeHg leaving the full Yolo Bypass (Table 3-7). The lack of wetting and drying cycles may help explain the lower levels of uMeHg. Overall, 86% of the MeHg produced in this reach in 2017 was in the filter-passing fraction, which is much different than what occurred in the upper reach and the entire Yolo Bypass. It should be noted that the net loads of all fractions of Hg as well as uMeHg and pMeHg within the Upper Reach had percent differences less than their measurement uncertainty

As shown in Figure 3-19, the Liberty Island reach was consistently a source of fMeHg in all but two sampling events in 2017 (January 31st and March 15th), which were two events with some of the lowest inflows. The largest MeHg contributions from Liberty Island occurred during the large flow events associated with the first flush and mid-February with increased mobilization of particulates enriched with Hg and MeHg (data not shown, see Technical Appendix B). These results imply that the magnitude of the flood event in terms of flow may influence whether the Liberty Island reach is a source or sink of fMeHg and pMeHg with possibly different thresholds for each fraction.

Figure 3-19 Net Loads for the Entire Yolo Bypass Subdivided by Reach for Each Sampling Event
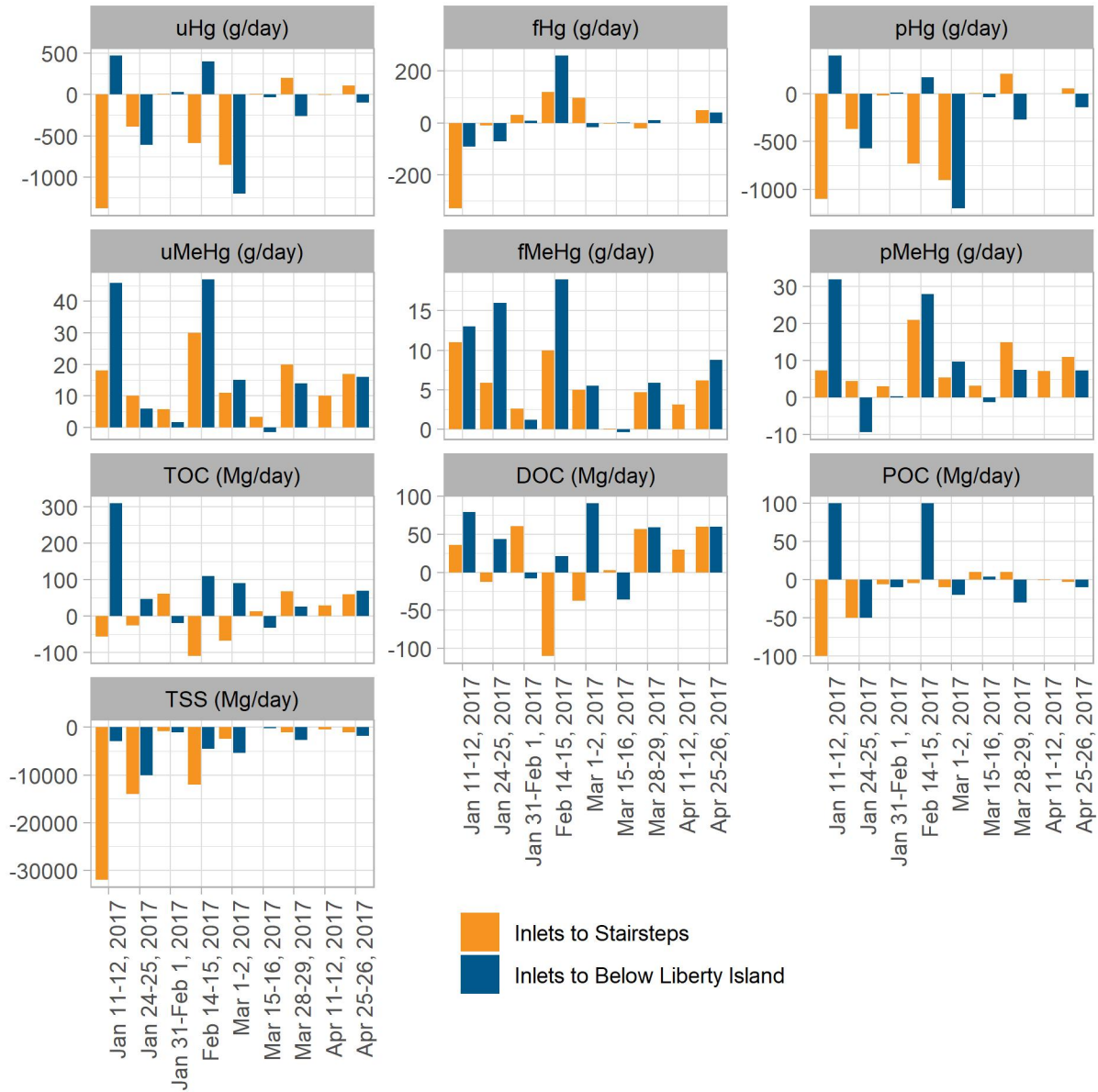
The conceptual model illustrated in Figure 3-20 extends the mass balance model for uMeHg loads to include the lower reach for nine events. There were eight sampling events in WY 2017 which were sampled both below Liberty Island and at the Fremont Weir. Most of this net internal production of uMeHg occurred in the Upper Reach between the inlets and the Stairsteps which supplied 79% of the total amount produced within the Bypass.

Figure 3-20 Mass Balance Model of Average Net uMeHg Loads Entering and Leaving the Entire Yolo Bypass Showing Net Internal Production at the Stairsteps and Liberty Island for Water Year 2017

Tributary Inputs

Export from Upper Yolo Bypass

Export from Liberty Island

Upper Yolo Bypass

Liberty Is.

Delta

pMeHg = 14 ± 16
fMeHg = 7.7 ± 7.3
uMeHg = 22 ± 23

Internal Production
pMeHg = 8.6 ± 6.0
fMeHg = 5.4 ± 3.4
uMeHg = 14 ± 8.1

pMeHg = 22 ± 19
fMeHg = 13 ± 10
uMeHg = 36 ± 29

Internal Production
pMeHg = 0.49 ± 12
fMeHg = 2.9 ± 4.1
uMeHg = 3.7 ± 12

pMeHg = 25 ± 29
fMeHg = 17 ± 13
uMeHg = 42 ± 41

Units = g/day
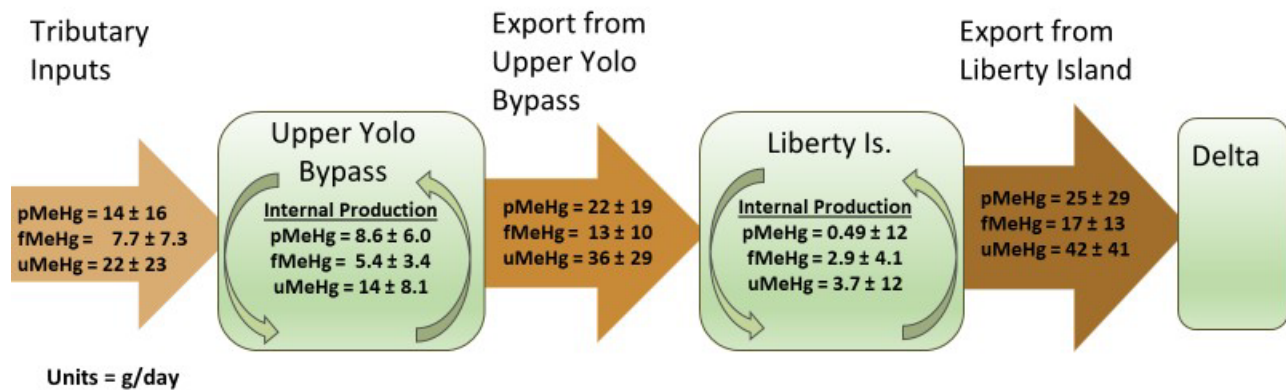
Figure Note: Inputs to the upper Yolo Bypass are the sum of averaged tributary inputs entering the upper reach of the Yolo Bypass. Export from the upper Yolo Bypass (at the Stairsteps) are the sum of average loads from the Toe Drain at Half Lisbon and Liberty Cut and Shag Slough below the Stairsteps. The difference between exports of the upper reach from the lower reach do not equal the calculated net production for Liberty Island for two reasons (1) the upper reach export loads are based on nine sampling events. Export loads exiting below Liberty Island are based on eight sampling events, and (2) there were both positive and negative net uMeHg loads determined for Liberty Island sampling events (see Figure 3-19).

Internal Methylmercury Production in the Upper Reach of the Yolo Bypass

As documented by our mass balance study and by Foe and others (2008), the upper reach of the Yolo Bypass is a net producer of MeHg. Identifying the drivers associated with this internal production is an essential step towards a BMP. To the extent possible, we used our field and laboratory studies to evaluate this data gap. These studies were: (1) the sediment-water exchange flux; (2) the sediment erosion studies (using Gust erosion chamber deployments); and (3) the laboratory and field-based mesocosm vegetation studies. The work focused primarily on the upper reach of the Yolo Bypass.

Sediment as a Source of Mercury

The DMCP defines sediment-water flux to flood water as the source of MeHg in open waters (CVRWQCB, 2011). Previous investigations have also shown this flux to be important (Choe and others, 2004; Heim and others, 2007). The importance of this source was investigated by conducting laboratory studies of sediment-water flux using intact cores to determine the diffusive flux of fMeHg and fHg from several different land use types. The objectives of the sediment-water flux study were to: 1) provide flux rates, for fMeHg for land use types found within the Yolo Bypass; 2) estimate loads of fHg and fMeHg from sediments by land use type and for total area of the Yolo Bypass; 3) estimate the importance of the sediment water exchange in controlling water column concentrations for fHg and fMeHg relative to other process; and 4) provide data useful to setting up and calibrating the D-MCM. Photos showing details of part of the experiment are shown in Figure 3-21. The location of core sample collection to evaluate the sediment-water flux associated with different land uses is shown in Figure 3-22. Details on sample collection, sample processing and data analysis can be found in Technical Appendix C.

Figure 3-21 Photos of A) Intact Sediment Cores Collected from Wild Rice Field in the Yolo Bypass. B) Pore Water Extraction from Sectional Cores Conducted in Glove Box Under Nitrogen
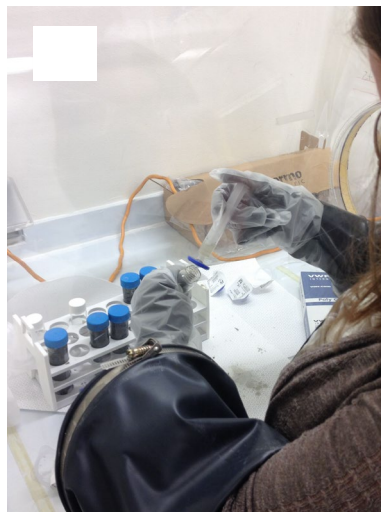
Figure 3-22 Location of Sample Collection Sites for Laboratory Sediment-Water Flux Experiments.
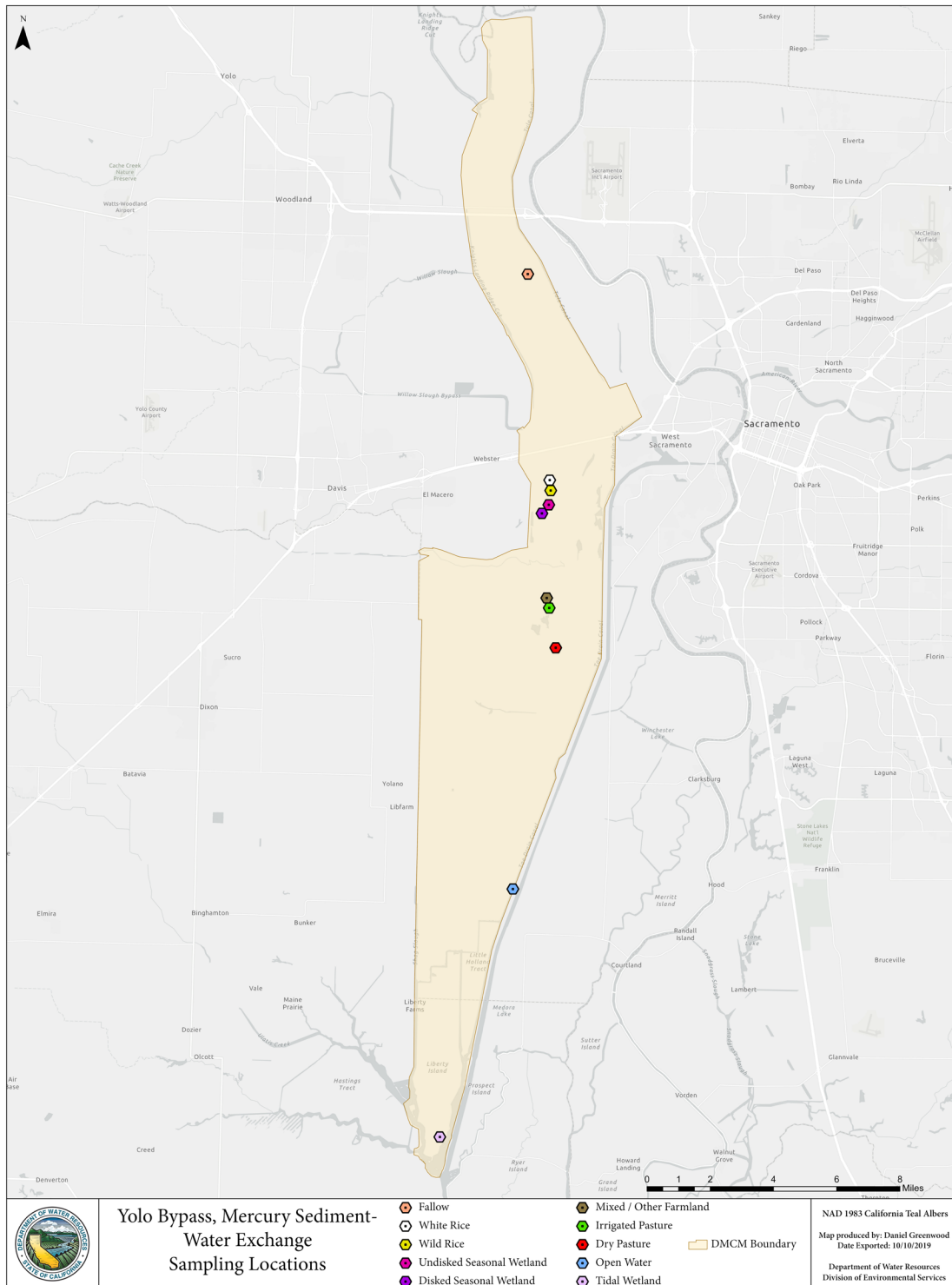
Sediment-water Hg and MeHg Flux

Sediment-water fluxes were determined using two approaches - direct measures of the concentration with time of fHg and fMeHg in overlying water from intact sediment cores and diffusional fluxes estimated from interstitial pore water and overlying water gradients. Results shown in this section reflect direct measurements from incubated cores as this approach captured both advective and diffusional components of Hg sediment-water fluxes thus represented the maximum for introduction of Hg and MeHg from sediments into the Yolo Bypass. Results from both approaches can be found in Technical Appendix C.

Results for fHg and fMeHg were highly variable between land use types (Table 3-8). The largest negative (into sediments) fluxes of fHg and fMeHg were observed in the permanently wetted land uses: -open water and tidal wetland sites. There was generally good agreement in the direction of fHg and fMeHg flux for all land use types with the exception being agricultural land used for white rice cultivation which showed flux into the sediment for fHg and flux out of the sediment for fMeHg. The largest fMeHg fluxes out of the sediments (>20 ng m^{-2} d^{-1}) were observed in seasonal wetland, fallow, and irrigated pasture lands. The range of fMeHg and fHg fluxes observed in this study are similar to those previously reported for open water and wetlands during late winter and spring in the Sacramento Bay-Delta, the Yolo Bypass, and other locations previously studied (see for example Choe and others, 2004, Mason and others, 2006 and Covelli and others 1999).

Table 3-8 **Sediment-Water Exchange Fluxes for fMeHg and fHg Determined Using Intact Core Incubations Collected from the Yolo Bypass with Overlying Water from the Sacramento River.**

Land Use	fMeHg Flux (ng m^{-2} d^{-1})[1]	fHg Flux (ng m^{-2} d^{-1})[1]
Irrigated Pasture	55.3 ± 20.3	114 ± 51.3
Fallow	28.6 ± 13.8	352 ± 140
Undisked Seasonal Wetland	25.8 ± 6.33	159 ± 25.7
Disked Seasonal Wetland	25.7 ± 8.93	156 ± 44.9
Non-irrigated Pasture	12.1 ± 3.9	150 ± 22.1
White Rice	8.91 ± 4.85	-97.4 ± 44.1
Mixed/Other Farmland	3.57 ± 6.76	203 ± 75.8
Wild Rice	2.97 ± 3.50	58.1 ± 29.7
Tidal Wetland	-3.65 ± 2.48	-621 ± 295
Open Water	-10.9 ± 8.95	-218 ± 132

Table Notes: Negative values indicate flux into the sediment. Values are the average ± 1 standard deviation of 4 cores.

Mercury and MeHg in Interstitial Pore Water

Interstitial pore water concentrations of fHg and fMeHg in surficial (0-2 cm) sediment by land use types are shown in Figures 3-23 and 3-24. Surficial pore water concentrations of fHg was highly variable and ranged from 6.53 to 125 ± 41 ng/L. Mean Sacramento River water uHg concentration was 1.75 ± 1.02 ng/L and porewater fHg concentrations were a factor of 3-71 times higher, indicating that there was a positive diffusive flux out of the sediments at all sites. Mean surficial pore water fMeHg concentrations ranged from 0.109 ± 0.037 to 20.3 ± 5.36 ng/L. The lowest fMeHg concentrations were observed in tidal wetlands, fallow, agriculture lands (the exception is wild rice fields) and open water. The highest pore water fMeHg concentrations were observed in seasonal wetlands, wild rice fields, and pasture land.

Porewater fMeHg concentrations were positively correlated with porewater DOC concentrations (data not shown, see Technical Appendix C).

Figure 3-23 Mean Interstitial Pore Water fHg Concentrations in Surficial (0-2 cm) Sediment from Several Land Use Types in the Yolo Bypass
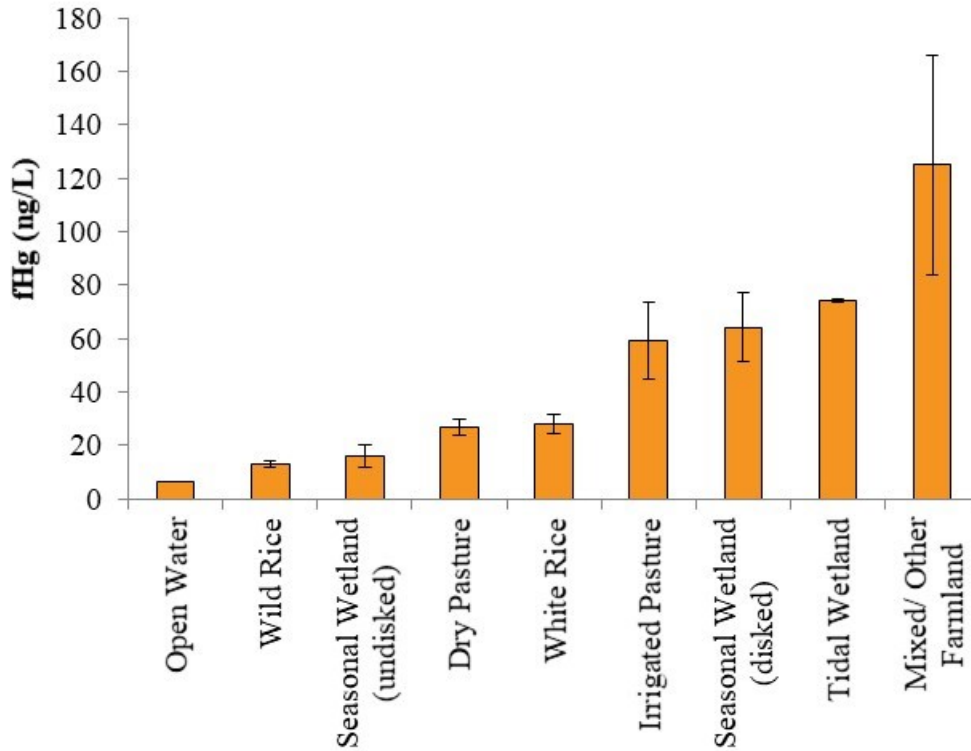
Figure Note: Pore water was isolated from intact sectioned cores under anoxic conditions. Error bars represent the standard deviation of triplicate field replicates

Figure 3-24 Mean Interstitial Pore Water fMeHg Concentrations in Surficial (0-2 cm) Sediment from Several Land Use Types in the Yolo Bypass
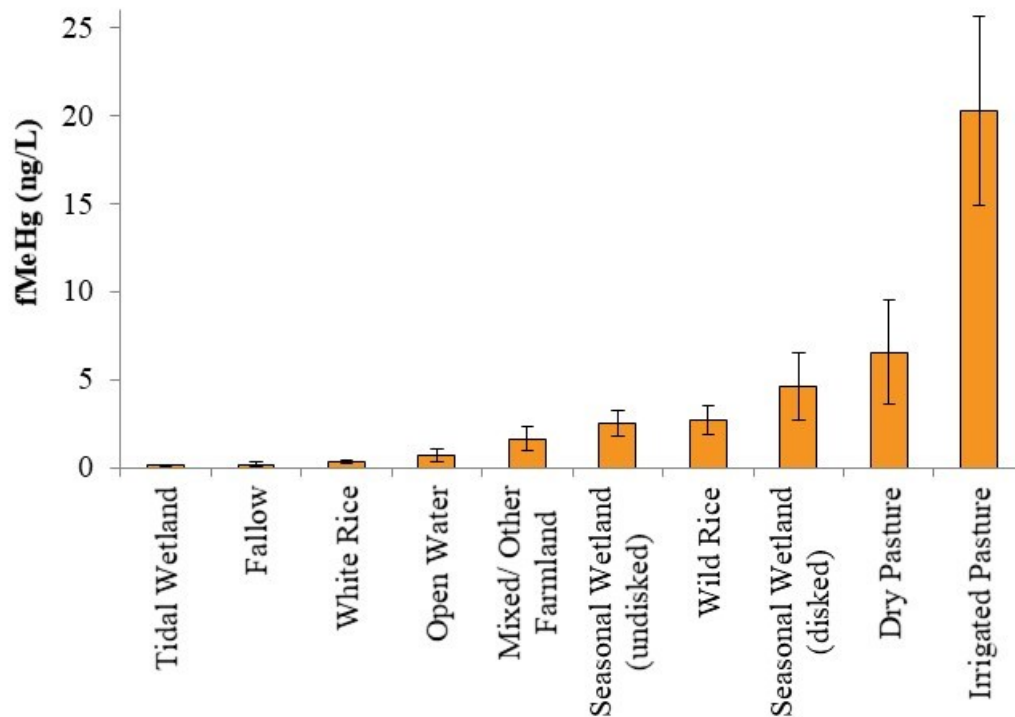
Figure Note: Pore water was isolated from intact sectioned cores under anoxic conditions. Error bars represent the standard deviation of triplicate field replicates

Sediment-water Exchange Loads to the Yolo Bypass

Estimation of fHg and fMeHg loads to the Yolo Bypass from sediment-water exchange for several land use types are given in Figure 3-25. The sediment-water exchange fluxes for the various land use types was scaled up to the land uses in the Yolo Bypass using the acreages in the D-MCM model. There are a number of uncertainties associated with this extrapolation, however, if the land use areas are correct and if the measured sediment water exchanges are representative of field conditions, then the fMeHg sediment-water exchange load to the Yolo Bypass is estimated at 5.04 ± 1.56 g/day. The greatest loading occurred from the two largest land uses in the upper reach of the Yolo Bypass—irrigated pasture and seasonal wetlands. This sediment-water exchange loading agrees remarkably well with the average fMeHg net load of 5.4 g/day determined from our Yolo Bypass mass balance study for the upper reach of the Yolo Bypass (Table 3-7).

Figure 3-25 **Estimation of fHg and fMeHg Loads to the Yolo Bypass from Sediment-Water Exchange for Several Land Use Types**
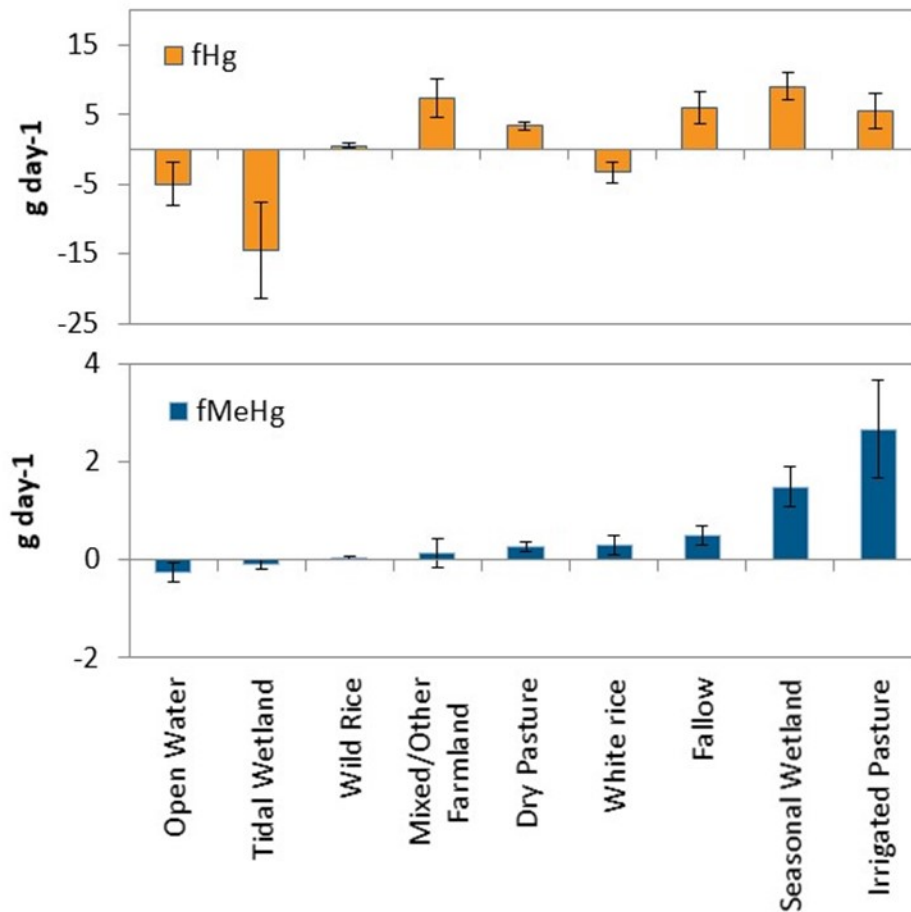
A conceptual model of the contribution of the filter-passing fraction of the sediment-water exchange load to the overall mass balance of uMeHg in the upper reach of the Yolo Bypass is depicted in Figure 3-26. If this sediment-water exchange flux for open water areas of the Yolo Bypass is representative of contributions from inundated Yolo Bypass sediments, then approximately 36% of the net internal production in the upper Yolo Bypass is accounted for via a sediment-water exchange flux of fMeHg. This leaves approximately 9 g/day of internal production of uMeHg unaccounted for. Two potential sources which have not yet been reliably quantified are erosion and resuspension of particles (see next section of this report). Quantification of these sources remain a gap in our knowledge of Hg transport and behavior in the Yolo Bypass. Another interpretation of this modelling effort is that there are other unidentified sources that contribute to the internal production of MeHg in the Yolo Bypass.

Figure 3-26 Contribution of fMeHg from Sediment-water Exchange in Open Water to the Mass Balance of Average uMeHg loads Entering and Leaving the Upper Yolo Bypass (WY 2017) and Unaccounted Masses
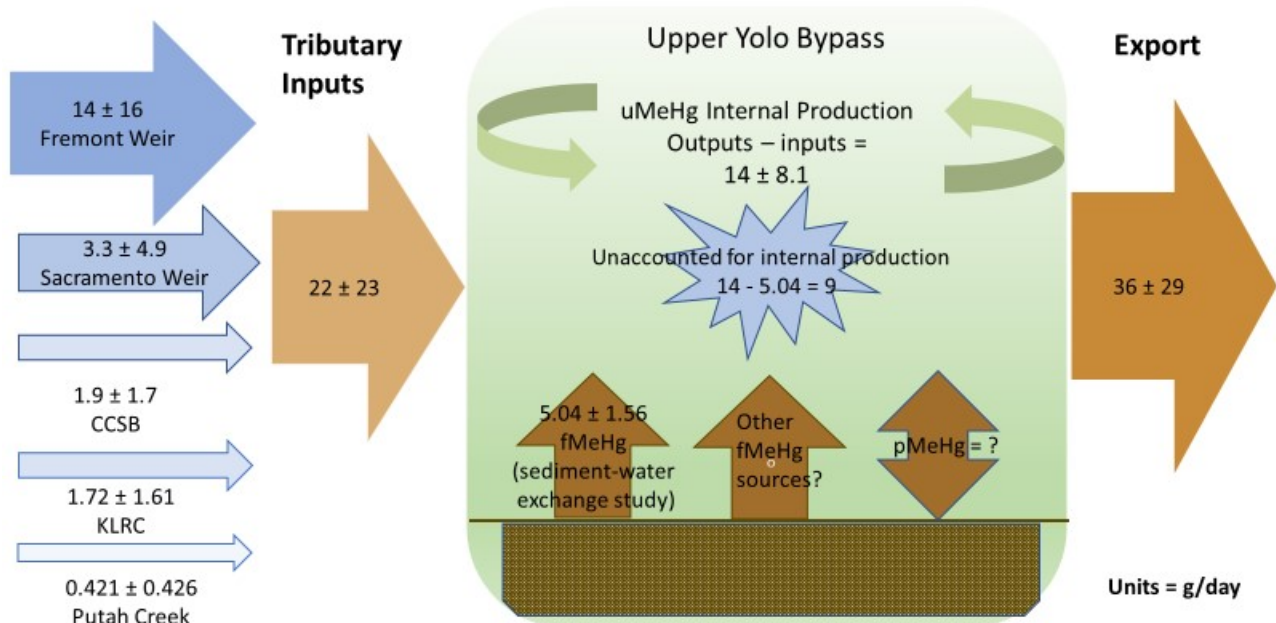
Figure Note: Outputs are the sum of average loads from the Toe Drain at Half Lisbon, Liberty Cut and Shag Slough below the stairsteps. Units are g/day ± 1 standard deviation.

It is important to point out that there are significant uncertainties associated with upscaling the sediment-water flux experiment results to determine MeHg loads for the Yolo Bypass. Uncertainties associated with this upscaling include, 1) accuracy of the base layer GIS map used to scale up for land use types, 2) assumptions that laboratory-based sediment-water exchange measurements with intact cores are representative of field conditions, 3) that short term (~24 hr) laboratory flux measurements are representative of inundation periods of days to weeks, 4) uncertainty in the experimental values, and 5) there is a paucity of sediment-water exchange measurements with which to make the load prediction. Additionally, sediment-water flux was measured over a short time-period whereas this figure assumes that the sediment-water flux remains constant over time. This assumption may not be correct and requires further laboratory experiments. Nevertheless, as a rough screening tool, these extrapolations provide a starting point to quantify sediment water exchange loads as well as useful relative comparisons to identify which land use types are most important in fluxes from the sediment and help to point to where refinement is needed.

Sediment Erosion

Erodibility of surface soils associated with different land use types in the Yolo Bypass was determined using a Gust erosion chamber. The Gust chamber subjects a core of sediment, extracted from the field, to controlled flow speeds arising from rotating flow inside a circular cylinder. The test erodes a very small

layer of surface sediment, typically less than a millimeter thick. The strength of the soil within this layer typically increases with depth and the soil strength versus depth is measured. The two primary results of the test are: 1) critical shear stress required to initiate motion, and 2) a relationship between excess shear stress (actual minus critical) and erosion rate. Gust erosion chamber results were used along with hydrodynamic modeling to predict erosion from different land use types in the D-MCM model. Evaluating erosion by land use type provides insight into the relative contribution of particulates, however, it doesn't provide information on deposition and resuspension of particles. Note that one limitation of the approach taken is that redeposition of the eroded sediments is not simulated. Another limitation is that only two cores were tested per land use. Results from one pair sometimes differed significantly, and there can also be large spatial gradients in erodibility within a given region or land use type.

Each of the major land use types in the D-MCM model were targeted for investigation of sediment erodibility using intact cores (Figure 3-27). Testing was performed in the field immediately after sample collection in the field (Figure 3-28). Erosion from irrigated pasture was tested with both intact vegetation and with the vegetation cropped closely to the soil level. Details associated with operation of the Gust Chamber and experimental results are given in Work and Schoellhamer, (2018) and in Technical Appendix D.

Erosion results for each land use type tested are presented as the initial critical shear stress at which erosion began (τ_{c0}) and the rate at which erosion increases as shear stress increases (Table 3-9). For the land use types sampled, irrigated pasture had the lowest critical shear stress, meaning that it required the smallest flow speed to initiate erosion. But in this case, the rate of increase of the resulting erosion, given higher flow speeds, was small suggesting that the thick vegetation in the unmodified irrigated pasture core resisted erosion. Similarly, the closely cropped core also featured miniscule erosion, likely because the roots helped protect the bed sediment from erosion (See Technical Appendix D). These results led to the recommendation that heavily vegetated areas be treated as unerodable in the D-MCM. The wild rice field sampled exhibited a higher critical shear stress, but also a much higher erosion rate, once the critical shear stress was exceeded. The erosion rate for wild rice was roughly three times greater than that for white rice. Of the land uses tested, the sediment tested from the Toe Drain was the most easily eroded.

Figure 3-27 Location of Sample Collections for the Gust Erosion Chamber Study
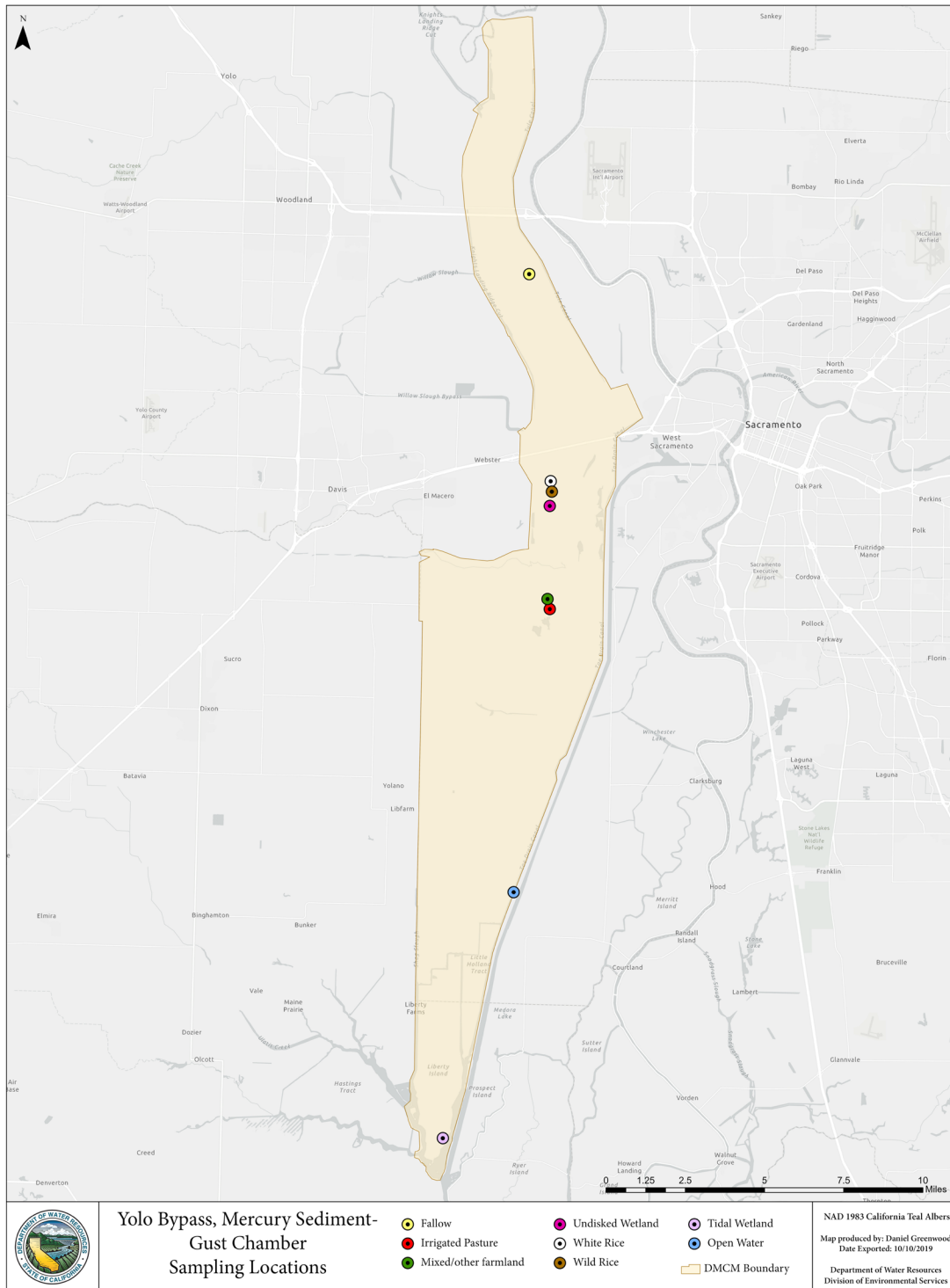
Figure 3-28 Photo of Sediment Erosion Study Experimental Setup in the Field Using Twin Gust Chambers (cylinders suspended above blue tub, lower right)

Table 3-9 Gust Chamber Measurements of Initial Critical Shear Stress (τ_{c0}) and the Rate of Erosion Increase with Shear Stress (dm/dτ_c) for Several Land Use Types in the Yolo Bypass

Land use	Initial critical shear stress τ_{c0} (Pascal, Pa)	dm/dτ_c, (kg/m²/Pa)
Toe Drain	0.075	1.27
Wild rice	0.25	0.429
Disked wetland	0.25	0.321
Liberty Island	0.25	0.276
Row crop	0.125	0.207
Undisked wetland	0.1625	0.194
White rice	0.25	0.142
Fallow	0.175	0.0832
Irrigated pasture	0.03	0.0084

Table Note: Land use soils are listed in order of erodibility (highest first).

The Gust erosion chamber studies showed that erosion increased rapidly at the beginning of each shear stress step applied, and then decreased until the next increase in shear stress. This observation indicated depth limited erosion, with little erosion occurring after the initial erosion at each shear stress increase. These results suggest that unless the shear stresses of subsequent floodwaters are higher than antecedent floodwater shear stresses, little erosion occurs until a higher shear stress is encountered. This suggests that

erosion may have the most impact during first flush events, and events where the velocities exceed the velocities of the first flush event. Note that since erosion studies could not quantify deposition or resuspension of particles, these shear stress results do not apply to those situations. Th results of the Gust chamber study support the mass balance study in the Yolo Bypass, which showed a first flush event for a number of analytes, including uHg,

It is reasonable to assume that pMeHg contributions from erosion and resuspension would contribute to the remaining unaccounted production of 9 g/day uMeHg (Figure3-26), however, we lacked a robust approach to translate Gust chamber erosion results into pMeHg values as loads (as documented in DWR, 2015, efforts to use a Bale Chamber to translate Gust Chamber erosion values to pMeHg values were unsuccessful). Therefore, we were unable to add Gust Chamber results to continue to balance the mass in Figure 3-26.

The Role of Vegetation in the Production of Methylmercury in the Yolo Bypass

The lack of mass balance for the internal production of MeHg from sediment-water exchange and the inability to quantify sediment erosion and resuspension (see Figure 3-26) led the technical team to explore other possible internal sources. The role of standing winter vegetation as an internal source was identified as a potential source and a study was initiated to quantify this potential source.

Several lines of evidence suggested that organic matter might be an unaccounted MeHg source contributing to the internal production of MeHg in the upper Yolo Bypass. First, the mass balance study determined that fMeHg loads were the greatest at the start of the flood season, but during the remaining sampling events the particulate fraction became the largest contributor to net MeHg loads (Figure 3-13). As shown in Table 3-5 concentrations of filtered and particulate MeHg increased within the Upper Reach of the Yolo Bypass. Also, the concentration of MeHg per gram of solid rose 229% between the inlet and outlet sampling sites (Table 3-5). These lines of evidence suggest that particulate fractions increased over space and time and filtered fractions increased spatially from north to south. Second, the upper reach transitioned from a net sink to more of a net source of Volatile Suspended Solids (VSS) during the last three months of the flood (Figure 3-15). VSS provides an estimate of the amount of organic material suspended in the water. This would likely result from decomposing plant matter as the flood event progresses. Third, as flood water transited from the Fremont Weir to its exit from the upper Yolo Bypass at the Stairsteps, TSS becomes enriched in organic content as evidenced by the TOC/TSS ratio (Table 3-5). One explanation for this increase in the organic content of the TSS is that the vegetation in the Yolo Bypass is contributing organic particles to the flood waters as it decays over prolonged inundation. Additionally, our Mass Balance study showed that our lowest flow rates occurred in the last third of the extended flood season, therefore, erosion was potentially not a large influence on increases of MeHg on particles. This suggests that as organic material increased, erosion potentially decreased, suggesting that the logical source for this increase in MeHg is decaying plant material.

Due to the large extent of managed vegetated cover present on the Yolo Bypass in the winter, we examined the hypothesis that internal production of MeHg could occur through the inundation and subsequent decay of submerged vegetation. In addition to the data collected in the mass balance study, this hypothesis is supported by previous work in the Yolo Bypass which showed that agricultural rice straw is a labile carbon source that stimulates MeHg production (Marvin-DiPasquale and others, 2014)

and a number of literature studies that support the role vegetation plays in the generation of MeHg (see for example, Hecky and others, 1991, Kelley and others, 1997, Trembley and others 1998, for the role of vegetation in newly inundated reservoirs, Branfireun, 2000, for the role of decomposing plant litter effects on MeHg production, and Lambertsson and Nilsson (2006) who argued that organic matter is the primary driver of MeHg production).

One managed land use that remains vegetated in the winter is pasture, the largest areal land use as quantified in the Yolo Bypass D-MCM land use grid. Unlike rice fields and seasonal wetlands, pasture lands are fully vegetated when the Yolo Bypass floods. Therefore, these vegetated lands may potentially serve as another source of internal MeHg production in the Yolo Bypass. This hypothesis is supported by the significant loss of pasture vegetation after prolonged flooding in the Yolo Bypass (Figure 3-29). (Chris Rocco, Yolo Wildlife Area, Water Manager personal communication).

Figure 3-29 Photos of Sequence of Vegetation Loss in the Yolo Wildlife Area Due to Seasonal Flooding

Figure Note: (A) Non-irrigated Pasture in May 2016 Prior to the Large Flooding Events in the Winter of 2017 (B) Non-irrigated Pasture Prior to Winter Flooding (Fall 2017) (C) Non-irrigated Pasture in March 2017 After Flood Event

In the Yolo Bypass there are two approaches to management of pasture lands—irrigated and non-irrigated. Irrigated pasture is periodically irrigated throughout the spring, summer and fall until winter rains provide water. Depending on the mix of vegetation, these pastures generally have a live, standing crop of vegetative biomass year-round. In contrast, non-irrigated pastures rely on rainfall to provide irrigation water. With the lack of supplemental water throughout the summer and fall growing season, non-irrigated pasture vegetation dies back and remains on the ground until seeds germinate during the following winter rainy season. Our experiments primarily focused on vegetation collected from non-irrigated pasture as this was the dominant management approach in the Yolo Wildlife Area. However, south of the Yolo Wildlife Area, irrigated pastureland dominates (personal communication, Solono County Resource Conservation District).

Experimental Approach

Vegetation senescence experiments were designed to answer questions about the role that dying and decaying vegetation plays in internal MeHg production in the Yolo Bypass during a flood event. The investigations helped to fill data gaps for the Yolo Bypass modelling effort, and to develop information that could be used to help develop Best Management Practices (BMPs) to reduce the production of MeHg and export loads from the upper reach of the Yolo Bypass. A series of studies were initiated to quantify MeHg releases from plants and sediments in pastures. Two pilot studies were first conducted to test and

validate methodologies prior to initiating three larger scale vegetation senescence (hereafter referred to as the VegSens studies) investigations. Two of the larger scale investigations were field-based mesocosm studies (VegSens 2017 and 2019) and the other was a detailed laboratory study (VegSens 2018). Sample locations for all VegSens experiments are shown in Figure 3-30. Photos of mesocosm and laboratory experimental setups are shown in Figures 3-31 to 3-33. Details on sample collection and methodology are given in Technical Appendix E.

Hypotheses

In contrast to the other investigations for this report, which were primarily characterization efforts to provide critical information for the D-MCM, the vegetation senescence experiments were hypothesis driven. As noted above, the pilot studies were designed to demonstrate that vegetation was potentially a source of MeHg during a flood event, and to help validate and determine experimental parameters for the larger scale mesocosm and laboratory studies. Several hypotheses were investigated in the pilot studies:

- Plants are a more significant contributor to methylmercury production (release to overlying water) than sediments alone (without plants).
- Irrigated and non-irrigated pastures release different amounts of MeHg to overlying water
- The duration of the senescence period is important to understanding the timing of the release or production of MeHg from the plant material. A lag period is likely to occur after a flood event before significant release or production is observed.
- Aeration of overlying water affects the release of MeHg to overlying water.

The major hypotheses tested in VegSens 2017, 2018 and 2019 were:

- Grazing the land will lower MeHg releases to overlying flood water
- Disking the land will lower MeHg releases to overlying flood water
- More vegetation results in more MeHg releases to overlying flood water

Figure 3-30 Sampling Locations for Vegetation Senescence Studies

Figure 3-31 VegSens 2017 Mesocosm Experiment. Photos of (A) Mesocosm Chambers with Feed Water and Aeration Lines shown. (B) Disked, Grazed and Ungrazed Treatments (left to right, respectively)

Figure 3-32 VegSens 2019 Mesocosm Experiment. Photos of (A) Ice Chests Serving as Individual Mescosms, (B) Disked, (C) Grazed and (D) Ungrazed Treatments

Figure 3-33 VegSens 2018 Laboratory Experiment
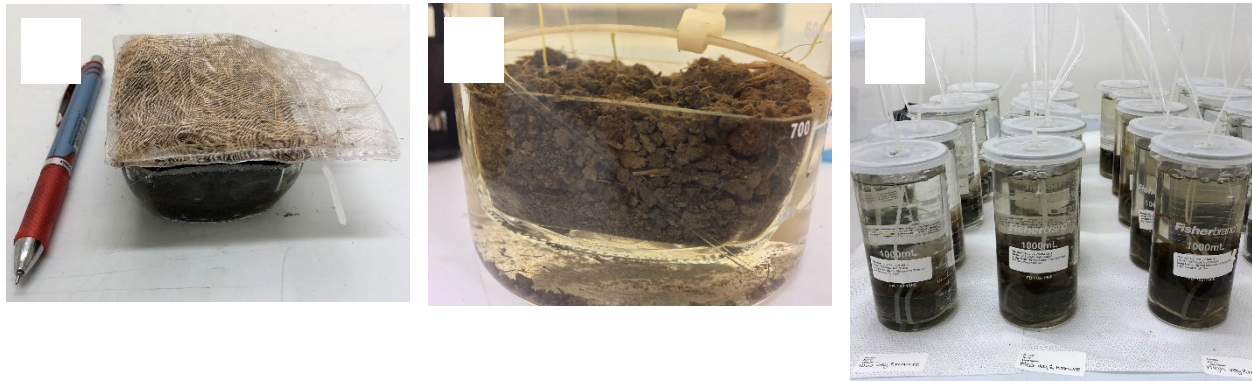
Figure Notes: Photos of: (A) Glass Dish with Test Sediment and Vegetation in Mesh Bag Prior to Experimental Set-up. (B) Close-up of Sediment Within Glass Dish Placed Within a 1 L Beaker. (C) Experimental set-up showing 1 L Beakers Containing Sediment With and Without Vegetation and Aeration Tubing

Pilot Studies

Two pilot studies were conducted in 2015 and in 2016 to provide proof of concept that vegetation was a major driver of MeHg production and to develop sampling and experimental methodology. Sampling techniques with 4-inch diameter core tubes were evaluated as well as the effect of several factors that could influence MeHg releases to the overlying water. These experiments helped to determine the importance of aeration of the overlying water, the optimal duration of an experiment, whether plants were a source of MeHg by comparing treatments with sediment only with treatments with sediment and plants and a comparison of irrigated and non-irrigated fields. Experiments were conducted by adding 1 L of Sacramento river water to treatments and following the change in fMeHg in the overlying water over a several-day incubation period. The increase in fMeHg mass (in ng) in the overlying water as a function of incubation time for the VegSens 2015 pilot study is shown in Figure 3-34. Results for VegSens 2016 can be found in Technical Appendix E.

Several critical observations resulted from the pilot studies which helped guide the development of the mesocosm and more detailed laboratory incubation studies. First, the 2015 pilot experiment showed that sediment with emergent vegetation had significantly higher production of fMeHg than sediments with the vegetation trimmed off ($p < 0.05$, ln transformed, Tukey HSD test). This demonstrated the proof of concept that inundated Yolo Bypass pasture vegetation could serve as a potential fMeHg source. Second, the 2015 pilot studies showed that oxic/anoxic conditions could markedly impact fMeHg production; anoxic conditions produced significantly more fMeHg ($p < 0.05$, ln transformed, Tukey HSD test), however, decomposing vegetation under oxic conditions also produced fMeHg. Because our mass balance study showed that flood waters are mostly oxic, it was important that incubation studies remained oxic to simulate realistic oxygen levels during flood events. Third, the 2016 pilot experiment showed that if water is not exchanged in incubated cores, then DOC levels can increase dramatically after a few days (data not shown). In our Yolo Bypass mass balance study, the DOC levels never exceeded 10 mg/L, therefore, like oxygen, incubation experiments required keeping DOC to levels observed in the flooded Yolo Bypass. Finally, the pilot experiments suggested that an experimental duration between 8-14 days or more should be sufficient to obtain significant changes in MeHg concentrations between treatments.

Figure 3-34 VegSens 2015 Pilot Study. Illustrated is the Increase in fMeHg Mass (ng) in Overlying Water as a Function of Incubation Time for Several Treatments
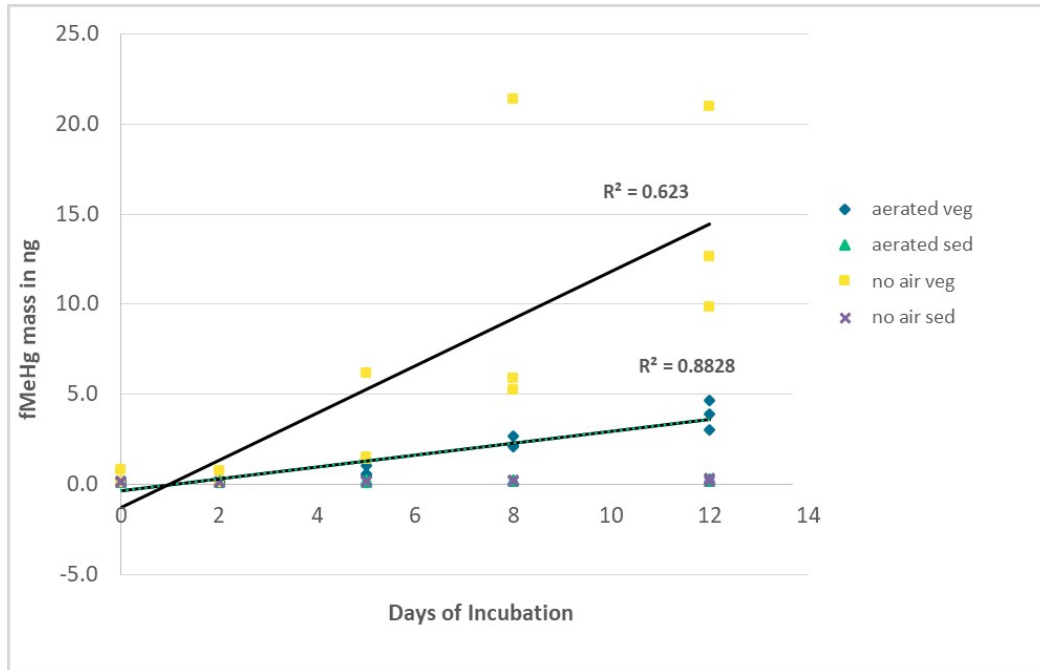
Mesocosm Studies – VegSens 2017 and VegSens 2019

Two field-based mesocosm studies were conducted– VegSens 2017 and VegSens 2019. Surface areas were increased significantly over the pilot experiments by placing soil and vegetation in ice chests resulting in surface areas that were 7 (VegSens 2017) to 43 (VegSens 2019) times greater than that of the pilot experiments. Two new types of sample treatments were added to these investigations, "disked" and "grazed" treatments. Disked samples represent a land use practice used in the Yolo Bypass. Land is mechanically disked to prepare the soil for planting or to turn-under undesirable vegetation. Grazed samples were collected in actively grazed, non-irrigated pasture areas in the Yolo Wildlife area. Ungrazed samples were created by fencing cattle out of the grazed area. Vegetation in the ungrazed and grazed areas were nearly a monoculture of rye grass (Lolium sp.). Specifically, the new hypothesis being tested was:

● The reduced vegetative biomass from disking of pastureland and grazing of cattle on pastureland (two common land management practices in the Yolo Bypass) will reduce MeHg production and lower the fMeHg introduction to overlying water during flood events by removing emergent vegetation available for methylation.

Methods and Experimental Design

Samples for VegSens 2017 were collected at site 3, and soil and plants for the VegSens 2019 study were collected at sites 3 and 4 (Figure 3-30). Biomass estimates at the time of sampling were determined by removing vegetation from three samples of ¼ or ½ m^2 surface areas, drying the vegetation in the laboratory at room temperature, and weighing when dry. VegSens 2017 and 2019 studies were conducted in November 2017 through January 2018 and February through March 2019, respectively. The ungrazed

site in VegSens 2017 (site 4) was constructed by fencing out cattle, whereas the grazed site was immediately adjacent and had cattle grazing on it. Vegetation consisted of a monoculture of dead rye grass. The same ungrazed location was used to collect samples for the VegSens 2019 study. A different location was used for the grazed site and unlike previous samples consisted of living rye grass and other plant species. The VegSens 2019 experiment was designed to improve upon the protocols used in the VegSens 2017 mesocosm experiment. The number of replicates was increased from 3 to 5 and the surface area of the mesocosms was increased 6-fold to more accurately represent and characterize ungrazed conditions.

Four treatments were prepared for VegSens 2017 and VegSens 2019: ungrazed, grazed, disked, and a water only control. The grazed and ungrazed treatments consisted of intact sod with no additional alterations. The disked treatment was meant to simulate disking of a vegetated field and was prepared by mixing the sod into the underlying soil to a depth of approximately 6 inches. The water only controls were ice chests with no sod. Overlying water was changed every 3 to 4 days to limit DOC build-up to < 10 mg/L and make the experiment more reflective of the conditions experienced during floods. fMeHg samples were collected once per week in VegSens 2017 and once every two weeks in VegSens 2019. Measurements were taken over a period of 4 weeks for VegSens 2019 and 5 weeks for VegSens 2017. Overlying water was changed twice a week, on days 3 and 7 of each sample week. The water from days 1 through 3 was discarded to eliminate excessive DOC buildup. The water from days 4 through 7 was used for measurements. Additional details are given in Technical Appendix E. In VegSens 2017, the time interval when MeHg was measured was: 1 Week (12/3/17 to 12/6/17); 2 Weeks (12/10/17 to 12/13/17); 3 Weeks (12/17/17 to 12/20/17); 5 Weeks (12/31/17 to 1/3/18). For VegSens 2019 water was only collected 2/15/2019 to 2/19/2019 and from 3/1/2019 to 3/5/2019.

Results - VegSens 2017

As shown in Figure 3-35 and Table 3-10 disking pasture vegetation into the soil consistently led to lower fMeHg levels than other treatments. By week 5, the grazed and ungrazed treatments both had significantly higher fMeHg concentrations than the disked treatment ($p < 0.025$, $p < 0.001$; respectively, post-hoc Tukey HSD, ln transformed data following significant 2-way ANOVA on ln transformed data). However, there was no significant difference in fMeHg production between grazed and ungrazed treatments ($p = 0.24$, post-hoc Tukey HSD, ln transformed data following significant 2-way ANOVA on ln transformed data).

Particulate methyl mercury (pMeHg) concentrations were determined in all treatments in Week 5. Results shown in Table 3-10 indicated that sediments as well as vegetation contributed to the pMeHg fraction, but that disked treatments produced less pMeHg than the vegetated treatments, however, in this experiment since the overlying water was only gently stirred, it did not represent the larger shear stresses encountered during large storms with current speed up to 5 ft/sec. Therefore, in this experiment, erosion and resuspended sediments was not accounted for.

Figure 3-35 VegSens 2017 Average fMeHg Concentrations for Disked, Grazed and Ungrazed Treatments at 2, 3 and 5 Weeks of Incubation
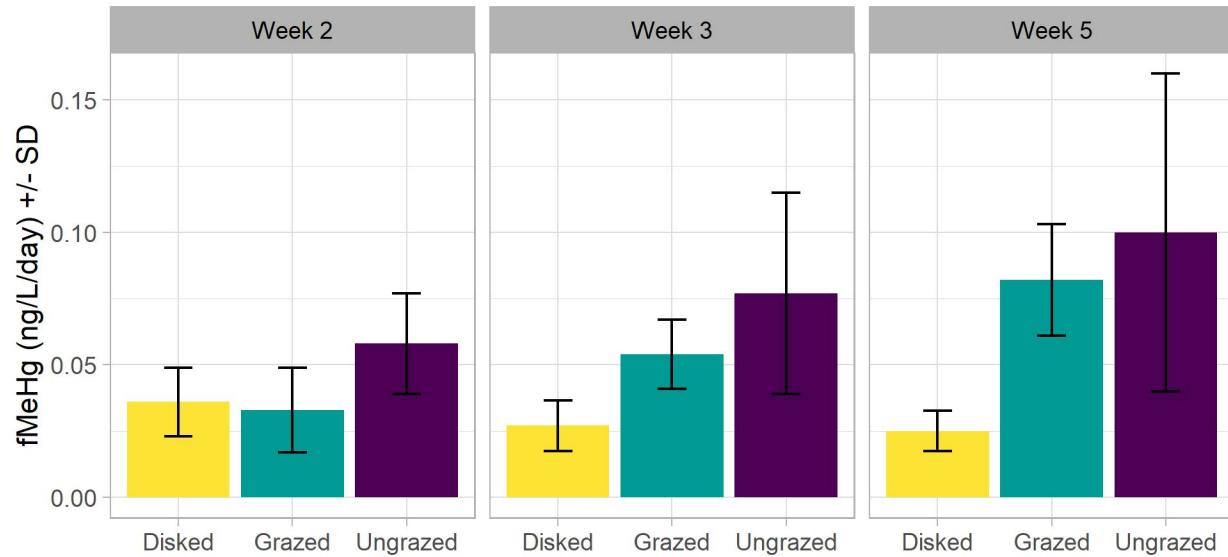
Figure Note: Units = ng/L/day ± 1 standard deviation

Table 3-10 VegSens 2017. Average Flux of fMeHg and pMeHg into Overlying Waters at 5 weeks of Incubation for Three Treatments (Disked, Ungrazed, and Grazed)

	Week 5 Average Flux[1] (ng/L/day)		
	Disked	**Grazed**	**Ungrazed**
fMeHg	0.024 ± 0.008	0.081 ± 0.021	0.101 ± 0.060
pMeHg	0.036 ± 0.022	0.057 ± 0.019	0.050 ± 0.002

[1] The average flux represents the mean ± (1) standard deviation of three replicates collected from a four-day incubation period at the end of the week. Raw data provided in appendix E1-2. pMeHg calculated as the difference between filtered and unfiltered MeHg

Results - VegSens 2019

Like the first mesocosm experiment, the VegSens 2019 mesocosm experiment examined differences in fMeHg production between disked, grazed, and ungrazed treatments, however the number of replicates was increased from 3 to 5 to increase the power to observe differences among treatments. The goal was to verify the disked results observed in the VegSens 2017 experiment and determine if there were also differences between the grazed and ungrazed treatments. Boxplots of fMeHg fluxes for weeks 2 and 4 are shown in Figure 3-36. The control waters (not shown, 5 total) were all below the detection limit of 0.013 ng/L.

Figure 3-36 VegSens 2019. Average fMeHg Concentrations for Disked, Grazed and Ungrazed Treatments at 2 and 4 Weeks of Incubation
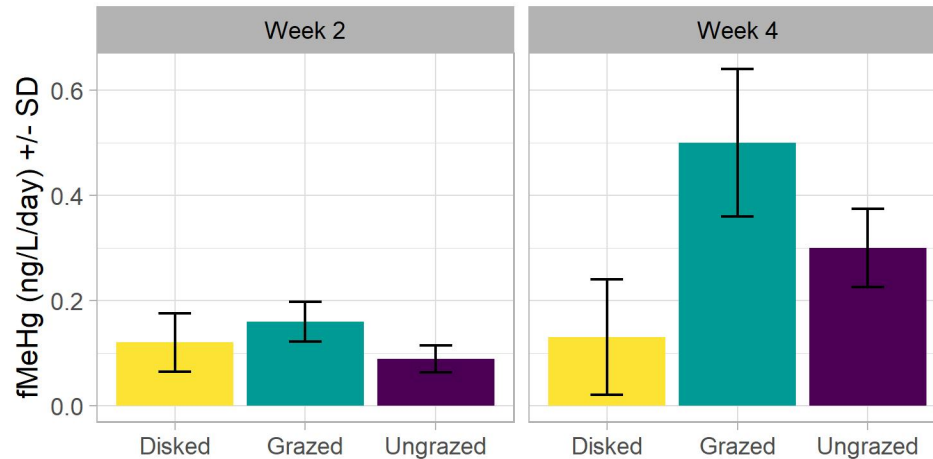
Figure note: Units are ng/L/day ± 1 standard deviation

Increasing the number of replicates did not change the conclusions reached in the VegSens 2017 mesocosm experiment. A 2-way ANOVA analysis on the natural log transformed data indicated a significant interaction effect between sampling events and land management practices (p < 0.01); therefore, multiple 1-way ANOVA analyses on natural log transformed data were used. When separated by sampling event, no significant differences were detected in week 2 between treatments. Like the VegSens 2017 results, week 4 fMeHg fluxes in the grazed and ungrazed treatments were both significantly higher than the disked treatment (p < 0.001, p < 0.025; grazed and ungrazed treatments, respectively). However, like the 2017 experiment, there was no significant difference in fMeHg production between the grazed and ungrazed treatments (p=0.23).

One confounding and important finding of the VegSens 2019 mesocosm experiment was the unexpected amount of fMeHg produced from the grazed treatment. The mass of the grazed treatment was approximately 40% of the ungrazed treatment, however, unlike the VegSens 2017 experiment and previous pilot studies, the flux of fMeHg, while not statistically significant, exceeded that observed in the ungrazed treatment. We hypothesize that these results were due to the different vegetation life stages used in the VegSens 2019 experiment. In the VegSens 2017 and pilot experiments, the plant material used was at the same point in its life-cycle, i.e. dead rye grass. However, for the VegSens 2019 experiment a new grazed treatment was used consisting of newly sprouted grass from recent rains. Thus, the grazed treatment consisted of freshly sprouted rye grass, while the ungrazed treatment consisted of dead rye grass. Because the new vegetation produced more fMeHg than old vegetation/biomass of vegetation, it is possible that fresh vegetation enhanced the production of MeHg. This has important land management consequences for the Yolo Bypass. Prior to winter floods, successive rainstorm events can trigger new biomass growth throughout pasture lands and other land uses. Therefore, fMeHg production driven by plant material may be a complicated function between the quantity of standing biomass of successive years of growth and the quantity of new growth prior to inundation by floodwaters.

VegSens 2018 Laboratory Experiment

The VegSens 2018 laboratory experiment was conducted to tightly control the variables associated with pasture lands. The main hypotheses tested in this study were:

- Disking the land will lower fMeHg releases to overlying water
- Grazing the land will lower fMeHg releases to overlying water
- More vegetation results in more fMeHg releases to overlying water

To evaluate the effects of grazing pressure and biomass, different levels of vegetation were added to 1-liter beakers within a given vegetated treatment. Vegetation used in the experiment was a monoculture of rye grass (Lolium sp.) initially collected from a non-irrigated and ungrazed pasture. Manure was included in grazed treatments and as its own isolated treatment to determine if it promoted methylation. A description of the seven treatments (with five replicates/treatment) is given in Table 3-11. Overlying water was changed at pre-determined intervals to ensure that DOC levels did not exceed levels measured in the field. The reader is directed to the Technical Appendix E for greater experimental details.

Table 3-11 **Treatments Tested in the VegSens 2018 Laboratory Study**

Treatment	Description
Control (Water Only)	Municipal tap water containing MeHg below the detection limit was used for all treatments
Sediment Only	Sieved through a 2 mm sized sieve to remove roots and larger organic matter
Ungrazed	Low, medium, and high biomass with vegetative biomasses adjusted to simulate different, a priori, non-irrigated pasture, summer biomass accumulations. Vegetation placed in mesh bags on top of sediment.
Disked Sediment	Low, medium, and high vegetative biomass disked into the sediment. Disked levels of vegetation based on biomass weights measured in ungrazed pasture
Grazed	Low, medium, and high biomass with vegetation and manure levels adjusted to simulate different, a priori, grazing pressures. Vegetation and manure placed in mesh bags on top of sediment
Manure Only	Low, medium, and high manure levels added at the same weight used in the grazed treatments. Manure placed in mesh bags on top of sediment.
Vegetation Only (no sediment)	Low, medium, and high biomass levels added at the same weights used in the ungrazed treatment.

Disking Effects

Disking pasture vegetation into the sediment was a highly effective approach to reduce fMeHg production. Disked treatments undergoing simulated inundation for either 4 or 8 weeks, all had significantly less fluxes in ng/L/day of fMeHg than either the grazed or the ungrazed treatments (Tukey multiple comparison test $p < 0.05$, ln transformed data) (Table 3-12, Figure 3-37). These results clearly demonstrate, that disking of pastureland is very effective at reducing fMeHg releases to overlying water during a flood event.

Table 3-12 VegSens 2018 Laboratory Study. Results of Tukey Pairwise Multiple Comparisons Tests between Fluxes of fMeHg in ng/L/day of Ungrazed, Grazed and Disked Treatments (ln transformed data)

Treatment Comparison	Incubation Period	p values for Tukey pairwise multiple comparisons of fMeHg fluxes in ng/L/day		
		High Biomass	Medium Biomass	Low Biomass
Ungrazed vs Disked	4 Weeks	0.0002	0.0001	0.0001
Ungrazed vs Disked	8 Weeks	0.0000	0.0002	0.0002
Ungrazed vs Grazed	4 Weeks	0.2312	0.0266	0.0266
Ungrazed vs Grazed	8 Weeks	0.0877	0.0908	0.0908
Grazed vs Disked	4 Weeks	0.0043	0.0248	0.0248
Grazed vs Disked	8 Weeks	0.0002	0.0107	0.0107

Table Note: Dark green cells show treatments significant at the $p < 0.05$ level. Light green shows treatments significant at the $p < 0.1$ level. Cells with no color are not significant at the $p < 0.1$ level.

Figure 3-37 VegSens 2018. Flux of fMeHg at 2, 4 and 8 Weeks of Incubation for Ungrazed Treatments with Low, Medium and High Biomass and Disked Sediment with Low, Medium, and High Levels of Vegetation Disked into the Sediment.
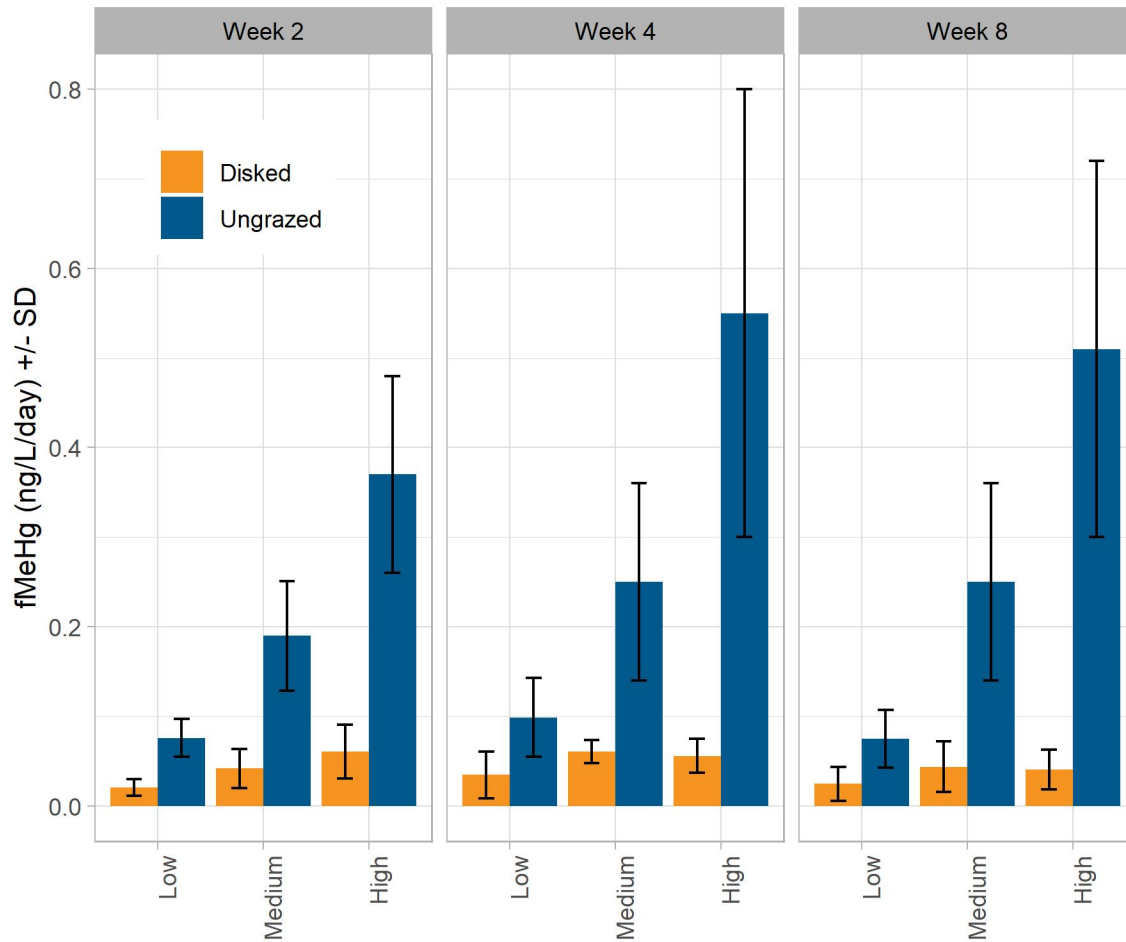
Figure note: units are ng/L/day ± 1 standard deviation; n=5 for each treatment.

Grazing Effects

In several cases, but not all, the grazed treatment had slightly lower rates of release of fMeHg to overlying water compared to the ungrazed treatment (Table 3-12). After 4-weeks of simulated inundation, there were significant differences at $p < 0.05$ in the treatments, with low and medium levels of biomasses (Tukey multiple comparisons, $p < 0.05$, ln transformed data). Comparing the 8-week incubation data, there were no significant differences at $p < 0.05$, but the treatments were significantly different at $p < 0.10$ between grazed and ungrazed treatments at all levels of biomass (Tukey multiple comparison, ln transformed data). These results partially support the hypothesis that grazed pastureland will have lower fMeHg releases to overlying water relative to ungrazed pastureland during a flood event.

Biomass Abundance Effects

The VegSens 2018 laboratory experiment provided several lines of evidence supporting the hypothesis that the greater the mass of vegetation in direct contact with overlying water, the greater the production and release of fMeHg to the overlying water. Biomass quantities added to experimental treatments were

ordered from low to high as disked < grazed< ungrazed. Patterns of MeHg flux were consistent with this treatment order (Table 3-13). Another way of assessing the relationship can be shown by comparing the flux of fMeHg released to overlying water with the mass of vegetation in four treatments: sediment-only, disked, grazed and ungrazed. This relationship is shown in Figure 3-38 for the 8-week incubation data using all three biomass addition levels. In this formulation, the different levels of biomass additions for each treatment can be independently accounted for. A very strong correlation was observed ($r^2 = 0.79$; $p < 0.01$); the higher the mass of vegetation present, the greater the flux of fMeHg, providing clear evidence that the amount of vegetation is very important in influencing the flux of fMeHg into overlying waters during a flood event.

Table 3-13 **VegSens 2018 Laboratory Study**

Treatment	2 Weeks Incubation (ng/L/day)[1]			4 Weeks Incubation (ng/L/day)[1]			8 Weeks Incubation (ng/L/day)[1]		
Biomass Level[2]	Low	Medium	High	Low	Medium	High	Low	Medium	High
Disked	0.021 ± 0.009	0.042 ± 0.022	0.061 ± 0.031	0.035 ± 0.026	0.061 ± 0.013	0.056 ± 0.019	0.024 ± 0.020	0.043 ± 0.028	0.041 ± 0.022
Grazed	0.059 ± 0.014	0.136 ± 0.067	0.122 ± 0.041	0.073 ± 0.025	0.126 ± 0.050	0.364 ± 0.400	0.055 ± 0.018	0.123 ± 0.057	0.230 ± 0.070
Ungrazed	0.076 ± 0.021	0.194 ± 0.061	0.367 ± 0.112	0.100 ± 0.044	0.252 ± 0.113	0.546 ± 0.256	0.076 ± 0.032	0.253 ± 0.107	0.510 ± 0.211
Manure plus sediment	0.014 ± 0.004	0.013 ± 0.003	0.024 ± 0.008	0.036 ± 0.020	0.039 ± 0.015	0.041 ± 0.009	0.027 ± 0.009	0.036 ± 0.015	0.048 ± 0.011
Vegetation Only	0.004 ± 0.001	0.083 ± 0.079	0.149 ± 0.037	0.005 ± 0.002	0.125 ± 0.124	0.223 ± 0.274	0.003 ± 0.009	0.143 ± 0.088	0.372 ± 0.183
Sediment Only[3]	0.007 ± 0.003			0.024 ± 0.016			0.023 ± 0.011		
Control Water[3]	0.008 ± 0.003			0.007 ± 0.006			0.006 ± 0.006		

Table Note: Given are the Mean and Standard Deviation for 5 Replicates of the Flux of fMeHg Into the Water in the Beaker for Seven Treatments at 2, 4 and 8 Weeks of Incubation

[1] Because of water changes twice each week, the fluxes given are based on the increases in concentration observed for a 4-day period at the end of each incubation period. Original data was divided by 4 to provide a concentration on a per day basis. Raw data is provided in Technical Appendix E1, Table E1-6

[2] See Technical Appendix Table E-8 for biomass levels added for the low, medium, and high treatments.

[3] There was no vegetation in the control water and sediment only treatments

.

Figure 3-38 VegSens 2018 Laboratory Study. Relationship Between Mass of Rye Grass Added to Disked, Grazed and Ungrazed Treatments and the Flux of fMeHg into Overlying Water at 8 Weeks of Incubation
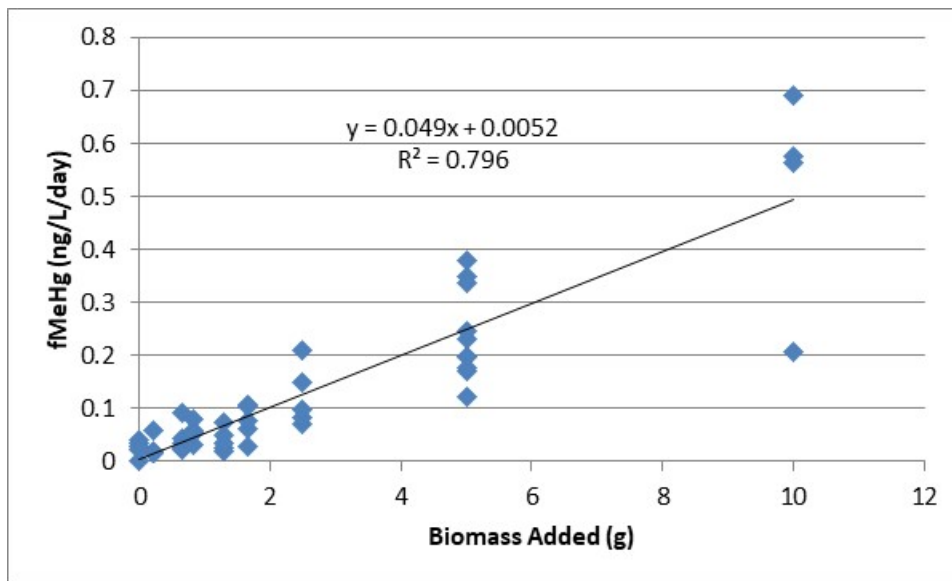
Finally, comparisons between treatments with and without vegetation provides another line of evidence supporting the influence of vegetation on fMeHg production. As shown in Table 3-13, except for control water, the sediment only treatment (with no added biomass) had the lowest fMeHg fluxes of all the treatments. The disked treatment, which had added vegetation mixed into the sediment (but with minimal emergent vegetation), produced slightly higher fMeHg fluxes (max ~2.5 times) than the sediment-only treatment for all incubation periods and biomass loading levels--with one exception, the low biomass diked treatment at 8 weeks of incubation had the same fMeHg flux as the sediment-only treatment. Similarly, comparisons between vegetation alone (with more vegetation added than the disked treatment) and disked showed that fMeHg fluxes in vegetation alone treatments were higher than disked treatments (max ~9 times) and even higher for sediment with no vegetation (max ~21 times), again with one exception--low vegetation alone biomass levels continued to show similar (or lower) fMeHg fluxes as disked and sediment alone treatments. This suite of evidence suggests that the quantity and presence of vegetation plays an important role in determining levels of fMeHg flux.

Investigation of Drivers of fMeHg Release to Overlying Water During a Flood Event

Using the experimental data from the VegSens 2018 laboratory experiments it is possible to assess whether certain land management practices or conditions are drivers of fMeHg production and release to overlying waters during a flood event. Two cases are worth examining: (1) the importance of vegetation relative to sediments as producers of fMeHg; and (2) the importance of manure as a component of a grazed pastureland.

Importance of Vegetation Relative to Sediment as a MeHg Source

Comparing ratios of fMeHg fluxes and statistical evaluations provided additional evidence that pasture vegetation stimulates fMeHg fluxes over sediment. Comparing the fMeHg fluxes between pasture vegetation and sediment alone provides information on the relative importance of vegetation as a driver of fMeHg flux. At weeks 4 and 8, the fMeHg flux increased as vegetation biomass levels increased and with the duration of the incubation. In contrast, sediment fMeHg flux was minor compared to the medium and high biomass levels (Table 3-14). Tukey pairwise statistical tests also support the hypothesis that the vegetation is the primary driver of MeHg production, not sediments (Table 3-15). The ungrazed/disked fMeHg flux ratio is also an indicator of the relative importance of vegetation compared to sediment since in the disked treatment, most of the vegetation is buried within the sediment and relatively little is on top of the sediment. The ungrazed/disked fMeHg flux ratio ranged from 2.9 to 10 across all biomass levels. There was a general trend of increasing ungrazed/disked fMeHg flux ratio with increasing biomass additions and with increasing incubation time. Tukey pairwise statistical tests of ln transformed data also support the hypothesis that the vegetation is the primary driver of MeHg production, not sediments (Table 3-15)

Table 3-14. **VegSens 2018 Laboratory Study. Selected fMeHg Flux Ratios for Different Biomass Levels**

MeHg Flux Ratios	4 Weeks Incubation (ng/L/day)			8 Weeks Incubation (ng/L/day)		
	Biomass Level[1]			Biomass Level[1]		
	Low	Medium	High	Low	Medium	High
Vegetation Only/Sediment Only	0.20	5.2	9.3	0.13	6.3	17
Ungrazed/ Disked	2.9	4.1	9.8	3.2	5.8	10

Table Note: Ratios calculated from MeHg flux listed in Table 3-10.

[1] See Technical Appendix Table E-8 for biomass levels added for each treatment.

Table 3-15 **VegSens 2018 Laboratory Study. Tukey Pairwise Statistical Tests Comparing the Vegetation Alone and Sediment Alone Treatments and Ungrazed and Disked Treatments at 4 and 8 Weeks of Incubation for Three Levels of Biomass.**

Treatment	Incubation Period	Low Biomass Level[1] (p-value)	Medium Biomass Level[1] (p-value)	High Biomass Level[1] (p-value)
Vegetation Alone vs. Sediment Alone	4 Weeks	0.003	0.015	0.505
Vegetation Alone vs. Sediment Alone	8 Weeks	0.003	0.000	0.000
Ungrazed vs. Disked	4 Weeks	0.0001	0.0001	0.0002
Ungrazed vs. Disked	8 Weeks	0.0002	0.0002	0.0000

[1] See Table E-8 for biomass levels added for each treatment

These results also raise the question of the role of sediment-water flux over extended periods of inundation. These experiments suggest that, over time, the contribution of sediment-water flux may be eclipsed by fMeHg flux from pasture vegetation. Vegetation Senescence and sediment-water flux experiments were not designed to evaluate this question, so this remains an area for further investigation.

Importance of Manure in the Generation of MeHg
At 4 and 8 weeks of incubation there was no significant differences between sediment only treatments with manure added and treatments consisting only of sediment (ln transformed data, Tukey multiple comparisons, $p > 0.05$, weeks 4 or 8) (Table 3-16). These results suggest that the presence of manure has no or minimal effect on MeHg production.

Table 3-16 **VegSens 2018 Laboratory Study. Summary of Tukey Pairwise Statistical Test Comparing Sediment Alone and Sediment Plus Manure Treatments at 4 and 8 Weeks of Incubation for Three Biomass Levels**

	Low Biomass[1] (p-value)	Medium Biomass[1] (p-value)	High Biomass[1] (p-value)
4 Weeks Incubation	0.677	0.596	0.882
8 Weeks Incubation	0.933	0.583	0.126

[1] See Technical Appendix Table E-8 for biomass levels added for each treatment

Pasture Vegetation as an Internal Source of MeHg to Flood Waters in the Yolo Bypass
Changes in rye grass MeHg mass were examined in situ and in VegSens 2018 and 2019 using non-irrigated pasture vegetation placed in mesh bags. For the 2018 laboratory study, dead rye grass, collected in the fall of WY 2017, provided the initial MeHg concentrations for pre-flood in-situ vegetation and for initial vegetative concentrations of bagged vegetation used in the VegSens 2018 laboratory study. Vegetation for VegSens 2019 mass calculations was collected at the same time and location as the sod samples collected for the VegSens 2019 experiment.

Concentrations and mass of MeHg of inundated rye grass increased in the laboratory over time. As shown in Table 3-17, MeHg concentrations in the vegetation increased 7 to 16-fold. The mass of MeHg associated with plant material increased between 5.7 and 12-fold. In parallel, vegetation decay was observed. Weight loss was 22 and 26 % for VegSens 2018 and 2019 experiments, respectively. This is consistent with visual observations. Before and after photos of a rye grass field, following the 4-month flood of WY 2017, showed most of the rye grass had either decomposed or been physically removed by floodwaters (Figure 3-29). These results clearly indicate that MeHg is produced in vegetation during a flood event, and that MeHg is slowly released as the plant decomposes when submerged.

Table 3-17 Concentrations and Masses of MeHg In Bagged Rye Grass Suspended in the VegSens 2018 And 2019 Mesocosms

Study	Initial MeHg Conc. (ng/g)	Final MeHg Conc. (ng/g)	Final/Initial Conc.	Initial MeHg Mass (ng)	Final MeHg Mass (ng)	Final/Initial Mass	% Weight loss (1-2 months)
VegSens 2019 (@ 4 weeks)	3.4 ± 0.3	56.8 ± 11.9	16.7	6.8 ± 0.7	83.4 ± 15.4	12.3	26.3 ± 4.11
VegSens 2018 (@ 8 weeks)	3.4 ± 0.3	25.1 ± 2.0	7.3	34.1 ± 3.3	194 ± 14.9	5.7	22.6 ± 5.1

Table notes: (1) 2.0 g of vegetation was used in VegSens 2019 (n=3), 10 g of vegetation was used in VegSens 2018 (n=5). The samples for determining starting concentrations for both experiments had n=5) The starting mass of MeHg in the plants was calculated by multiplying the concentration of MeHg in the plant material (n=5) by the biomass of the plant in the experiment (either 2 or 10g of tissue depending on the experiment). The final mass of MeHg in the tissue was determined by multiplying the weight remaining in the mesh bag after decomposition by the concentration of MeHg in the tissue. See Technical Appendix E for details.

The significance of this internal MeHg vegetation source from pastures into flood waters of the Yolo Bypass can be demonstrated by comparing it with the average net internal increase in the mass of uMeHg found in the Yolo Bypass Mass Balance studies and with the level of MeHg reduction required by the DMCP for the Yolo Bypass.

Based on pasture land biomass estimates (data not shown, see Technical Appendix E), concentrations of MeHg in decaying rye grass were scaled up to the areal coverage of pastureland in the Yolo Bypass (Table 3-18). As delineated in the land-use base map used by the Yolo Bypass D-MCM, pastureland covers an area of 70.6 km2. Using this approach, on average, the mass of MeHg associated with rye grass pasture over the course of a 120-day flood event was 1710 ± 560 g or 14.3 ± 4.6 g/day. This compares favorably with the uMeHg internal load values calculated in the Mass Balance study of 14 ± 8.1 g/day. Note that the Mass Balance study integrates all uMeHg contributions, not just pasture vegetation and that comparisons of field estimates of loads to those from a small number of laboratory experimental studies should be used with caution. There are a number of assumptions and inherent biases associated with scaling up these experimental studies, however, as a proof of concept, this exercise suggests a new and plausible source of internal Yolo Bypass MeHg production, not originally considered in the DMCP, requiring further investigation.

Table 3-18 Estimate of Total MeHg Mass in 70.6 km^2 of Pastureland and its Flux to Overlying Water During the Flood Event of 2017

Study	Initial MeHg Conc. (ng/g)	Final MeHg Conc. (ng/g)	Initial MeHg mass in 70.6 km^2 of pasture (g)	Final MeHg Mass in 70.6 km^2 of pasture (g)	Initial MeHg Flux for 120 days g/day	Final MeHg Flux for 120 days g/day
VegSens 2019 (@4 weeks)	3.4 ± 0.3	56.8 ± 11.9	188	2360	1.56	19.7
VegSens 2018 (@ 8 weeks)	3.4 ± 0.3	25.1 ± 2.0	187	1040	1.56	8.68
Field Collections after 2017 Flood (dry pasture)	1.9 ± 2.2	37.4 ± 3.6	105	1560	0.87	13.0
Field Collections after 2017 Flood (irrigated pasture)	1.9 ± 2.2	45.4 ± 36.2		1890		15.7
Average	2.9 ± 0.9	41.2 ± 5.9	160 ± 48	1710 ± 560	1.3 ± 0.4	14.3 ± 4.6

Table note: The determination of the production of MeHg in pastureland vegetation in the Yolo Bypass and its flux to overlying water during the flood event of 2017 is based on the VegSense 2018 and 2019 mesocosm experiments as well as post-flood field collections. The mass of MeHg in the pastures was calculated by multiplying the concentration of MeHg in the plants by the biomass of plants in all the pastures (see Technical Appendix E for biomass values). The flux was calculated by dividing the mass of MeHg in the pastures by 120 days (the approximate length of the 2017 flood).

The DMCP requires Yolo Bypass MeHg load reductions of 88 g/year from open water sources and 833 g/year collectively from all sources (CVRWQCB. 2011). Our estimate of 1710 ± 560 g of MeHg produced from senescing vegetation suggests there is enough MeHg in vegetation in pasturelands, that if its release from vegetation during a flood event could be mitigated (through land management practices), it would result in a major reduction, if not all of the DMCP goal of 833 g/year.

Conclusions

Mass Balance of MeHg in the Yolo Bypass

Depicted in Figure 3-39 is the mass balance of MeHg in the Yolo Bypass for WY 2017 determined from the Yolo Bypass mass balance study (Technical Appendix B). The internal production includes input fluxes for sediment-water exchange and vegetation senescence. Introduction of MeHg from erosion was difficult to estimate. We lacked a robust approach to translate Gust chamber erosion results into pMeHg values as loads. Therefore, we were unable to add Gust Chamber results to continue to balance the mass in Figure 3-39. It is reasonable to assume that pMeHg contributions from erosion and resuspension would contribute to the remaining unaccounted production, however, in terms of the largest land use in the Yolo Bypass D_MCM model, pasture erosion associated with Gust Chamber studies appeared negligible.

The average export flux of uMeHg from the upper Yolo Bypass (36 ± 29 g/day) exceed average tributary input fluxes (22 ± 23 g/day), indicating that there is an internal production within the upper Yolo Bypass of 14 ± 8.1 g/day, increasing the export concentration of uMeHg from the tributaries by 61%.
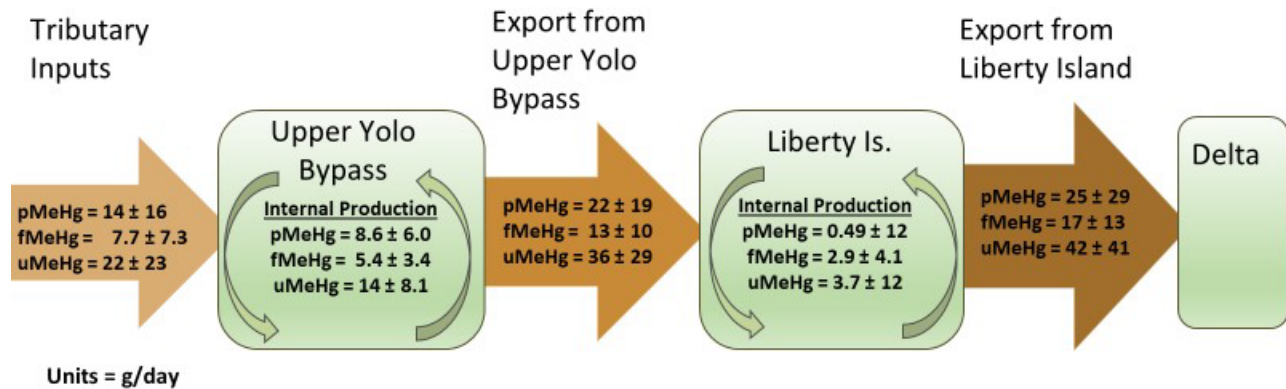
Figure 3-39 Mass Balance of MeHg in the Yolo Bypass for WY 2017

Figure Notes: (1) Given are average loads in g/day ± 1 standard deviation, (2) Internal production fluxes were determined by averaging the net difference (output –input) determined for each individual sampling event. Thus, the average flux for the internal production does not simply represent the difference between the average output flux minus the average input flux. In the case of Liberty Island, the difference between exports of the upper reach from the lower reach do not equal the calculated net production for two reasons a) the upper reach export loads are based on nine sampling events. Export loads exiting below Liberty Island are based on eight sampling events, and b) based on the sampling event, net uMeHg loads for Liberty Island were both positive and negative (see Figure 3-19), (4) The Liberty Island contribution to the total export is based on the difference between loads isolated at Ryer Island and Yolo Bypass output loads as calculated above the stairsteps.

The observation that the upper Yolo Bypass is a net internal source of uMeHg and that net loads of uMeHg increased with increasing inflow confirms previous observations made by Foe and others (2008) during an extended Yolo Bypass flooding event during the winter of 2005-06. The 2005-2006 study also covered the reach between the inlets and the Stairsteps and focused solely on uMeHg. One major difference between the current work and the 2005-2006 study was the magnitude of the load increase with increase in flow. The upper Yolo Bypass appeared to produce more uMeHg during the 2005-2006 study than during the 2017 flood event at comparable flows. This disparity in load observations in different flood events may be related to differences in the sampling programs (see Technical Appendix B for details), but it also strongly suggests that mercury behavior, fate and transport can differ markedly between years in which the Bypass floods.

A major advancement in the mass balance for MeHg in this current study over the previous mass balance study by Foe and others (2008) was to investigate the contribution of Liberty Island as a source/sink of MeHg entering the Delta. The total uMeHg export flux to the Delta, with the Liberty Island contribution, is 42 ± 41 g/day. The average internal production of uMeHg for Liberty Island, determined from individual sampling events was 3.7 ± 12 g/day, which adds approximately 10% to the uMeHg flux from the upper Yolo Bypass. This estimate of internal production is lower than one would predict from the net flux difference between the average export flux minus the average import flux (42 g/day – 36 g/day = 6 g/day; which corresponds to an increase of 14% to the uMeHg load from the upper Yolo Bypass). One possible explanation for the high uncertainty associated with the average internal production not agreeing more precisely with the net difference between the import and export at Liberty Island is that on several sampling events, Liberty Island was a net sink for uMeHg. Estimates of the internal production of uMeHg within Liberty Island suggest that on average Liberty island may be a small contributor of uMeHg (3.7 ± 12 g/day), although the uncertainty, as represented by the standard deviation, in establishing the Liberty Island average internal production flux is three times the estimated average.

Another major advancement in the mass balance for MeHg in this current study over the previous mass balance study by Foe and others (2008) was the partitioning of the uMeHg into particulate and filter-passing fractions (Figure 3-39). In general, pMeHg made up most of the uMeHg, ranging between 60 and 64% of the average uMeHg for all load determinations, with the exception of Liberty Island, where the average internal production of pMeHg made up only 13% of the uMeHg fraction.

It is important to highlight that this Yolo Bypass mass balance for MeHg has significant uncertainty associated with the load estimates for the three MeHg fractions determined (i.e. uMeHg, fMeHg, and pMeHg), but that the uncertainty associated with these <u>averages</u> is due to the large changes in flows across the 9 sampling events. As shown by r^2 values, there were highly significant relationships between load and flow (Figure 3-16 and Technical Appendix B). Flow explained ~ 50% and 83% of the net uMeHg loads for the upper reach and entire Yolo Bypass respectively. These results illustrate the influence of flow on load calculations and explains the high variability associated with average loads. This uncertainty, as a result of large changes in flow, impedes our ability to close with certainty the mass balance. The closure can be no better than the uncertainty associated with the individual loads estimated for the individual MeHg fractions. Nevertheless, given this caveat, the mass balance shows reasonable closure, suggesting that the major loads have been identified. It is entirely possible that other smaller loads have not been identified.

In addition, other sources potentially contributed to uncertainty, including; 1) the paucity of data (there were only 9 grab sample events); 2) the difficulty of collecting samples across the entire hydrograph; 3) the ability to scale up laboratory and field-based mesocosm and sediment-water exchange studies to the entire Yolo Bypass; 4) the heterogeneity of land use types in the Yolo Bypass; 5) the ability to monitor a process over the time scale of a flood event; and 6) the inherently large variability of MeHg as well as Hg and TSS loads during a flood event of this magnitude and duration with extremely large fluctuations in flow. Additional and more detailed discussions of why there is so much uncertainty is given in the next section on Data Gaps and Next Steps and in the individual chapters in the technical appendices.

First Flush Event Mass Balance

Depicted in Figure 3-40 is the mass balance of MeHg determined for the upper Yolo Bypass from the <u>initial</u> sampling event for WY 2017 (1/11-12/2017), which we are characterizing as a "first flush" event. The first flush event showed significant load enhancements over the average loads observed for the entire flood event. There was also another high flow event on February 14th, surpassing the hydrologic flow on January 11th, in which MeHg loads again rose up, suggesting that a "first flush" type event can occur more than once during a seasonal flood if hydrologic flow reaches elevated levels. The uMeHg tributary load into the upper Yolo Bypass during the first flush event (64 g/day) was about triple the average uMeHg load determined for all sampling events (22 ± 23 g/day). Similarly, the export uMeHg load from the upper Yolo Bypass during the first flush event (82 g/day) was about 2 times the average uMeHg export load determined for all sampling events (36 ± 29 g/day). The first flush event for Liberty Island was dominated by the pMeHg fraction, accounting for approximately 70% of the total load exported from the combined upper Yolo Bypass and Liberty Island areas.

The concentrations of MeHg during the first flush event in the upper Yolo Bypass were also elevated over the average concentration for all 9 events. For example, the concentrations of uMeHg, fMeHg and pMeHg during the first flush event from the Fremont Weir sampling site, which represented the majority

of the fresh water flow (73%), were 0.146, 0.044 and 0.10 ng/L, respectively and the average values for the 8 sampling events from the Fremont Weir sampling site (including the first flush event) were 0.090 ± 0.028, 0.034 ± 0.007 and 0.056 ± 0.022 ng/L, for uMeHg, fMeHg and pMeHg, respectively. The process driving the increase in concentration with increasing flow has not been elucidated. Because MeHg concentrations in the Fremont Weir site were also enhanced during the first flush event, it is clear that increasing MeHg loads with increasing flow reflect both the enhanced delivery of water and an increase in MeHg concentration associated with the increased hydrologic load. The exception perhaps being the internal production of MeHg.

Figure 3-40 **Methylmercury Mass Balance for the First Flush Event on January 11, 2017 in the Upper Yolo Bypass.**
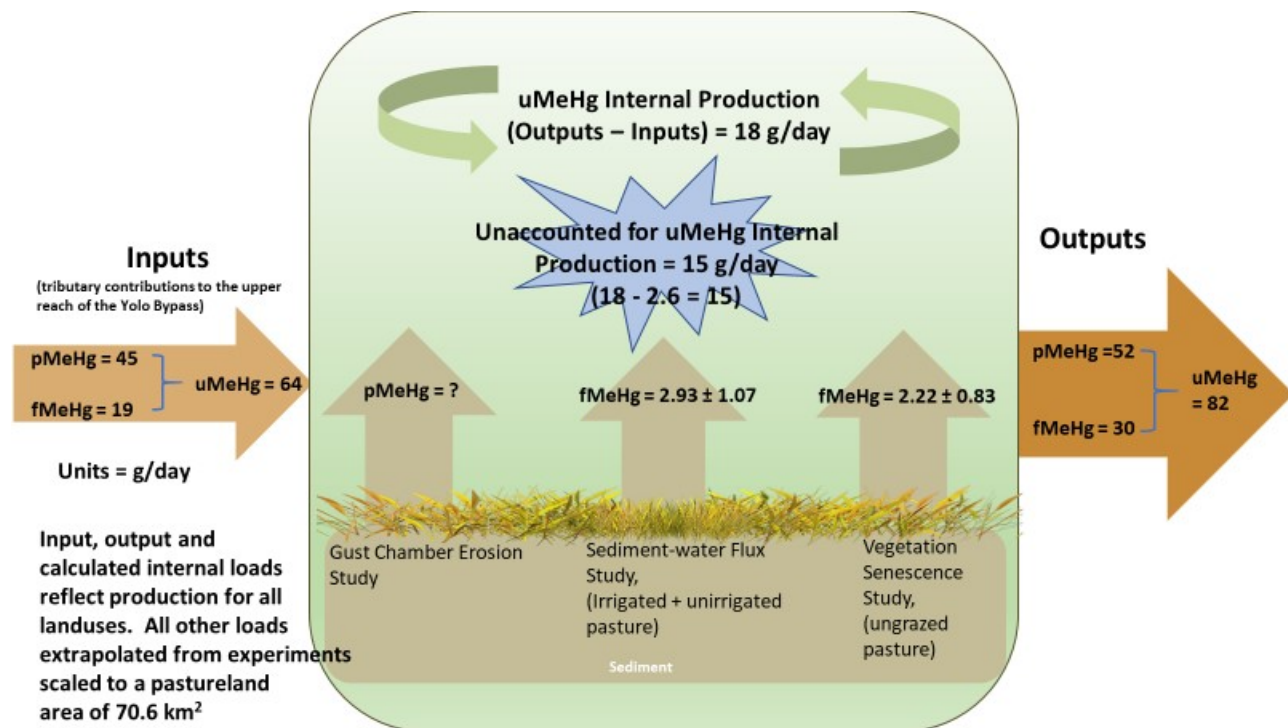
Figure Note: The data for the sediment-water exchange flux and the vegetation senescence flux were scaled to a pastureland area of 70.6 km². The flux of 2.6 g/day represents an average flux obtained from the sediment-water flux study and the Vegetation Senescence study. Inputs were calculated as the sum of tributary input loads collected on January 11, 2017. Output loads represent the sum of the loads calculated from the Toe Drain at Half-Lisbon, Liberty Cut and Shag Slough below the Stairsteps on January 12, 2017.

The net internal production of uMeHg in the upper Yolo Bypass during the first flush event, based on the export load minus the input load of 18 g/day, is similar to or perhaps slightly greater than the average net internal production determined for the entire flood event in 2017 (14 ± 8.1 g/day). The source of the internal production of MeHg during the first flush event is not clear. In pasture lands, sediment-water exchange and vegetation senescence studies both produced estimates of fMeHg fluxes to the overlying water of about 2.6 g/day, leaving about 15 g/day of internal production for the entire Yolo Bypass unaccounted for. As the vegetation was only recently flooded, it is assumed that the breakdown of the vegetation has not yet been significant and that release of MeHg contained within the plant tissue is minimal. It is possible that pMeHg from erosion accounts for a majority of the unaccounted-for internal

production. The Gust Chamber erosion studies conducted in pastureland land showed minimal erosion, but this was not necessarily the case for other landuses (see Table 3-9), however it was difficult to reliably convert Gust Chamber erosion values into definitive flux values for erosion contributions, therefore, in the conceptual model this term was not estimated. Additionally, there may be fMeHg processes that we did not capture in our laboratory work that would require further investigation.

The partitioning of the uMeHg into filter-passing and particulate fractions during the first flush event were similar to that observed for all sampled flood events in WY 2017. For example, the tributary input load during the first flush event was 70% in the particulate fraction, while the average pMeHg tributary input for the 2017 flood event was 64% pMeHg. Similarly, the export pMeHg during the first flush event was 63% of the uMeHg load, while the average pMeHg for the export from the upper Yolo Bypass during the 2017 flood event was 61% pMeHg.

Flooded Pastureland Vegetation as an Internal Source of MeHg to the Yolo Bypass

The mesocosm studies suggest that during periods of extended flooding, vegetation, and not sediment, may be the principal driver behind the net loads leaving the upper reach of the Yolo Bypass. Depicted in Figure 3-41 is a timeline of the increase in methylmercury in pasture vegetation during a seasonal cycle in the Yolo Bypass in which a flood event occurs. In the spring, the pastureland has new vegetation that is actively growing. By fall to early winter the pastures reach peak vegetation biomass. In the winter, a flood event covers the vegetation and it begins to slowly decompose. During the flood event, there is a significant conversion of the inorganic Hg to MeHg within the vegetation after 4 to 8 weeks of incubation, such that after several months of flooding, the levels of MeHg in plant tissues have increased more than 10-fold. By early to late spring, after the flood event has ended, the vegetation has almost completely decomposed, leaving mostly barren pastureland. Concomitantly, all the MeHg that was contained in the plant tissues has been released to the overlying water, both as dissolved and particulate MeHg. It is also recognized that some portion of the plant MeHg likely undergoes de-methylation during the decomposition process and that a significant portion is exported or removed to sediments as pMeHg.

Figure 3-41 Seasonal Cycle of Pastureland Biomass and Associated Methylmercury Content in the Yolo Bypass During a Season in Which a Flood Event Occurs

160 g MeHg   1710 g MeHg   Most MeHg Mass Exported

Spring (medium biomass)   Fall/Early Winter (high biomass)   Flood (decomposing biomass)   Post Flood (minimal or no biomass)
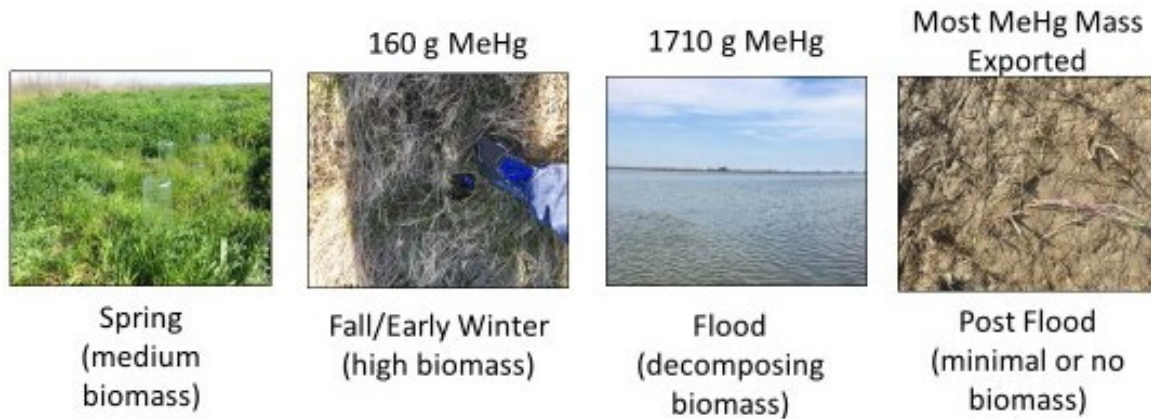
Figure Note: The site depicted is a non-irrigated pastureland which is where all the samples for the mesocosm studies were obtained. See Table 3-18 for calculations of MeHg mass.

A distinction should also be made between fresh and senescent vegetation in producing MeHg. The fresh vegetation in VegSens 2019 produced a higher flux of fMeHg to overlying water than the dry vegetation even though the fresh vegetation biomass was only 40% of the dried vegetation. This example illustrates the compounding difficulty of understanding the effects of grazing, disking, and vegetation age/condition on MeHg production and the flux of fMeHg to overlying waters. New vegetation starts growing as soon as the ground is wetted by rain, usually in October or November. If the biomass of the new vegetation is significant at the start of the flooding event there would ultimately be a larger mass of MeHg available for introduction into flood waters in the Yolo Bypass than if the vegetation that was flooded originated from older vegetation that was dead and dried out during the previous summer. Additionally, irrigated pasture remains green and alive throughout the winter.

The relative significance of decaying vegetation on flooded pastureland as an internal source of MeHg to flood waters in the upper Yolo Bypass is illustrated in a conceptual mass balance model in Figure 3-42. The 2017 and 2019 Vegetation Senescence studies determined a fMeHg flux of 1.4 ± 0.8 g/day and an estimated pMeHg flux of 2.2 ± 1.3 g/day (lower left portion of Figure 3-36; see Technical Appendix E for details) based on the disked mesocosm treatments. Combining these two fluxes provides a sediment-water exchange flux for uMeHg of 3.6 ± 2.1 g/day, which represents only 26% of the internal production. The emergent vegetation mesocosm treatment (lower right-hand portion of (Figure 3-42) includes both the fMeHg introduction from sediment-water exchange and the release of fMeHg from decaying vegetation, which combined introduce 4.4 ± 3.0 g/day of fMeHg to the overlying water (see Technical Appendix E for details). The estimated pMeHg contribution from this treatment (blue arrows and boxes) add another 7.0 ± 4.8 g/day, for an overall load of uMeHg to overlying water from flooded pastureland vegetation of 11.4 ± 7.8 g/day. By difference, the contribution of uMeHg to overlying flood water from senescent vegetation only (lower middle portion of Figure 3-42) is estimated at 7.8 ± 1.8 g/day; 3.0 ± 0.7 as fMeHg (orange arrows and boxes) and 4.8 ± 1.1 as pMeHg (blue arrows and boxes).

The emergent vegetation alone accounts for 56% of the internal production determined by the Yolo Bypass mass balance study. Adding in the sediment-water exchange to the vegetation senescence contribution and 83% of the internally produced MeHg in the Yolo Bypass can be accounted for by

introduction from flooded pastureland. Within the uncertainty of the load calculations, the internal production from sediment-water flux and vegetation senescence effectively balances the internal production of uMeHg determined from the mass balance study. Our work could not adequately quantify the pMeHg contributions of erosion, deposition and resuspension of solids, and only estimate the pMeHg contributions from sediment-water exchange and vegetation senescence. Therefore, in this conceptual model, the importance of pMeHg in the Yolo Bypass is not currently understood or constrained.

Figure 3-42 Conceptual Model of the Importance of Pastureland Vegetation in the Internal Production of MeHg in the Upper Yolo Bypass
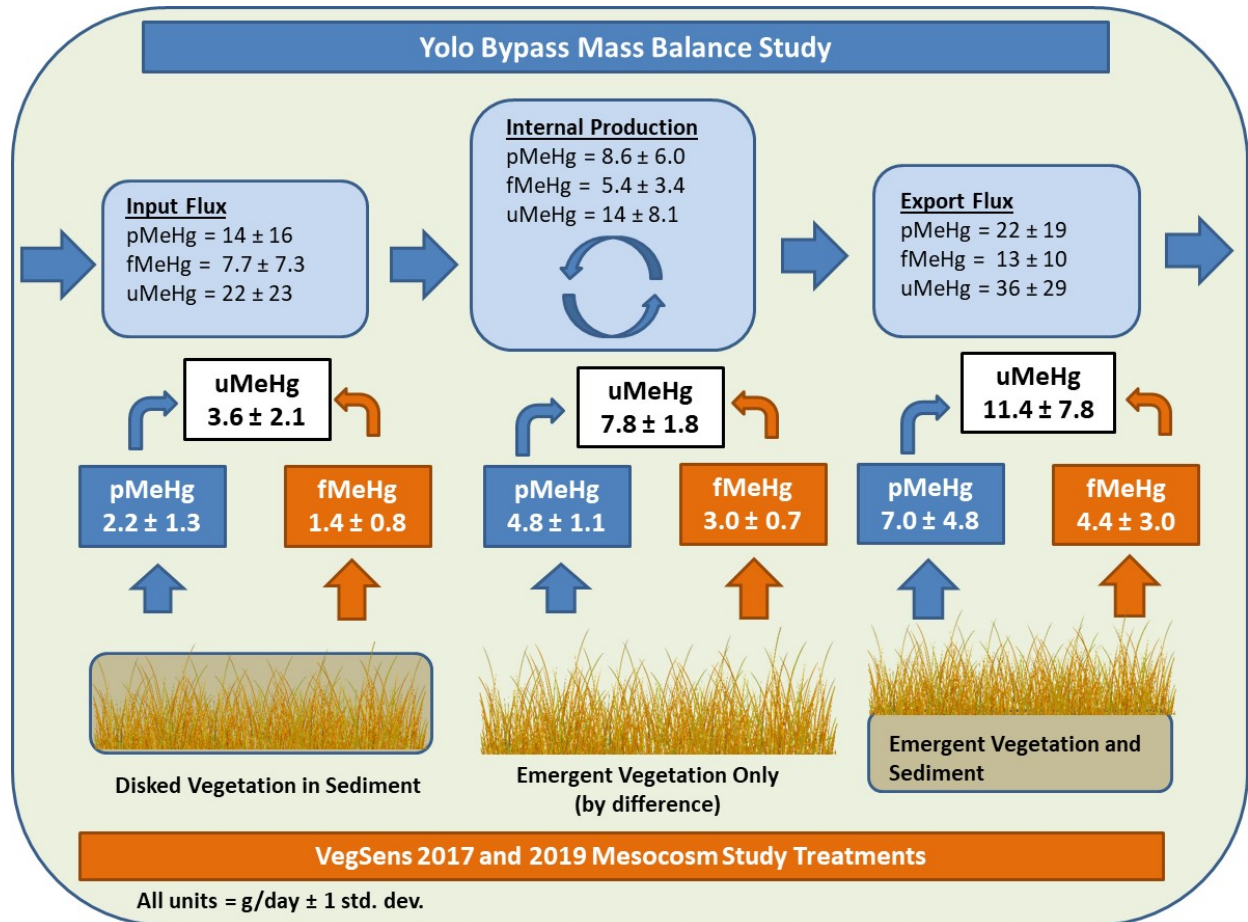
Figure note: The upper portion of Figure 3-42 repeats the mass balance of MeHg in the upper Yolo Bypass determined from the mass balance study described in Figure 3-39. The lower portion of Figure 3-42 shows the loads of MeHg introduced to overlying water determined during the VegSens 2017 and 2019 mesocosm studies. The introduction of fMeHg to overlying water from pastureland with emergent vegetation is shown in the lower right-hand portion of Figure 3-42 (orange arrows and boxes) and includes both the sediment-water exchange and introduction from decaying vegetation. The introduction of fMeHg to overlying water from sediment-water exchange processes (lower left portion of Figure 3-42; orange arrows and boxes) was estimated based on the disked vegetation mesocosm treatments. The introduction of fMeHg to overlying water from senescent emergent vegetation alone was estimated as the difference between the emergent vegetation and disked vegetation treatments (lower middle portion of Figure 3-42; orange arrows and boxes). An estimate of the pMeHg input to overlying water from the mesocosm treatments was estimated based on the ratio of pMeHg/fMeHg of 1.6 determined during the Yolo Bypass mass balance study (blue arrows and boxes)

Data Gaps and Next Steps-Field Studies

- The mass balance study for WY 2017 was based on just 9 manual sampling events. This paucity of data does not permit coverage of the hydrograph with the detail necessary to capture time dependent flux details. More high frequency sampling is needed, focusing on capturing peaks in the hydrograph as well as rising and falling flows. Use of automated sampling stations at key inlet and export points would fill this data gap and reduce uncertainty.

- Major biogeochemical processes often control the behavior, fate and transport of minor constituents, like mercury and methyl mercury in aquatic systems. Identifying clear linkages between mercury and methylmercury and a major biogeochemical process(es) will help with the development of best management practices to minimize the production of methylmercury within the Yolo Bypass and its export to the Delta. One investigation of particular relevance is the role that organic matter plays in methylmercury production and transport in the Yolo Bypass.

- Current sediment-water exchange flux measurements were conducted on short duration (1-2 days) investigations. We do not know how sediment-water exchange fluxes of mercury and methylmercury change over time, from initial flooding through month-long periods of inundation. Data are needed on the sediment-water flux throughout the flood event to more accurately capture this important flux.

- Given the areal size of the Yolo Bypass additional measurements of sediment-water exchange, pore water and solid phase concentrations for the land use types studied would decrease current uncertainties in mercury loads from the sediment. Studies should be conducted on vegetated and non-vegetated examples of each land use type.

- Gust Chamber erosion studies had limitations due to sample size and site heterogeneity. Future erosion research should increase sampling size, replication and spatial coverage to reduce uncertainty associated with the heterogeneity of the large geographical area of the Yolo Bypass.

- The Gust Chamber results describe only erosion processes, but deposition processes can be important in a floodway, both for its effect on subsequent erosional events and for mercury budgets.

- It is not known what the primary source(s) are for the (inorganic) mercury that accumulates in pasture vegetation. A likely source is the large mercury burden that currently exists in pastureland sediments. What role current exogenous sources of mercury from tributaries contribute to mercury levels in vegetation is not clear. Of particular interest is discharges from Cache Creek Settling Basin and whether the form of mercury released is readily available for uptake by vegetation and methylation. In addition, there are other possible sources as well, including atmospheric mercury deposition. Identifying the most important sources may help to guide development of a BMP for reducing methylmercury production during a flood event.

- Previous work has shown incomplete mixing of Yolo Bypass tributary water masses during flooding events (Sommer and others, 2007), therefore, understanding the effects on methylation from source waters originating from the western and eastern side of the fully flooded Yolo Bypass may also be an important piece to understanding methylation dynamics in the Yolo Bypass

- Pasture vegetation showed significant increases in methylmercury content during simulated flood events in the upper Yolo Bypass. Current vegetation senescence studies, as sources for methylmercury production in the Yolo Bypass, focused primarily on rye grass contributions. This work should be expanded to include quantification of methylmercury production during a flood event from other types of vegetation, irrigated and non-irrigated pastures, fresh and old vegetation, and

more accurate measurements of vegetation biomass in the Yolo Bypass. This will help reduce the uncertainty associated with the determination of the flux for this process and help identify the drivers to focus BMPs.

- Vegetation senescence studies primarily focused on methylmercury in the filter-passing fraction. Further studies are needed to understand vegetation contributions to particulate methylmercury introduction during a flood event.

- Vegetation senescence studies showed the importance of vegetation quality (i.e. whether the organic matter is readily metabolizable) and biomass quantity as possible drivers of mercury methylation in vegetation. A major question to resolve is whether vegetation quality or simply the biomass of vegetation present limits methylmercury production. Answering this question will help to develop targeted BMP's for limiting methylmercury production.

- The field and mesocosm studies all showed that disking of fields significantly reduces the input of methylmercury to overlying water during a flood event. What is not clear is whether disking pasture areas is a viable alternative for pasture management in the Yolo Bypass. A first step toward answering this question is to explore the feasibility of using disking in pasture lands through discussions with land-owners and the Resource Conservation Districts, followed by verifying disking results through field experiments.

- While not conclusive, it appears that grazing of cattle reduces vegetation biomass and the introduction of methylmercury to overlying waters during a flood event. Additional small-scale grazing studies need to be conducted to confirm the significance of its potential reduction. If grazing can be shown to significantly reduce methylmercury reduction during a flood event, then it should be evaluated as a viable alternative for pasture management in the Yolo Bypass.

- Approaches to reduce vegetative biomass in pasturelands by means other than disking and grazing should be explored. For example, evaluating the reduction of vegetative biomass using fall flood-up practices, like those already used in rice fields and seasonal wetlands.

- The Liberty Island reach, like the upper Yolo Bypass, was also a net producer and exporter of methylmercury to the Delta. Therefore, it is important to include the Liberty Island reach in any future studies involving determinations of loads of mercury or methylmercury to the Delta.

Limitations and Complications to Conducting Large-Scale Field Studies in the Yolo Bypass

In our workplan/technical memo, larger field trials were originally proposed to examine the questions ultimately pursued through laboratory and mesocosm experiments. The roadblocks necessitating a return to a mesocosm and laboratory experimental approach remain, and any future field studies seeking to evaluate control mechanisms will need to spend resources to overcome them. For example, we had proposed using the experimental ponds in the Yolo Wildlife Area to conduct large-scale experiments, to overcome limitations often associated with heterogeneity issues often encountered in small-scale field experiments. However, any work in the experimental ponds would have required the expense of rehabilitating the ponds back to their original state as a useable system. This will include dredging the ponds of fill and grading the sites to allow the head pressures created by the system to flow at velocities observed in the flooded Yolo Bypass. To evaluate grazing pressure, this will require the cooperation of

ranchers to closely control cow's movement onto only designated experimental sites. Re-creating vegetative biomass observed in the Yolo Bypass within the experimental ponds will require successive seasons of agricultural management to build up biomass to ambient conditions before experiments can be conducted.

One significant and unavoidable issue to conducting large-scale field manipulations in the Yolo Bypass is the water source. The water source for the experimental ponds is the Toe Drain which consists of ground water and recirculated agricultural drain water which intermittently has high MeHg concentrations (Moss Landing Marine Laboratory, unpublished data). Toe Drain water quality is very different from the low MeHg concentrations found in the dominant flood waters in the Yolo Bypass. Pilot tests may be needed to see how a land use reacts under inundation from different source waters. This approach has value beyond the use of the experimental ponds as Cache Creek Settling Basin waters have much higher concentrations of Hg and MeHg than flood waters originating from overtopping of the Fremont Weir.

Finally, there are site access limitations, and moreover safety concerns, with sample collections in the Yolo Bypass during full flood periods.   Tuning the Yolo Bypass Dynamic Mercury Cycling Model (D-MCM) could have benefitted from data in areas within the fully flooded Yolo Bypass, rather than its peripheries.

References

Branfireun M. 2000. *The Role of Decomposing Plant Litter in Methylmercury Cycling in A Boreal Poor Fen.* Department of Geography. Master of Science. McGill University, Montreal, 2000.

Choe K-Y, Gill GA, Lehman RD, Seunghee H, Heim WA, and Coale KH. 2004. "Sediment-Water Exchange of Total Mercury and Monomethyl Mercury in the San Francisco Bay-Delta." Limnology and Oceanography, Volume 49, Issue 5, Pages 1512-1527. https://doi.org/10.4319/lo.2004.49.5.1512.

Covelli S, Faganeli J, Horvat M, Brambati A. 1999. "Porewater Distribution and Benthic Flux Measurements of Mercury and Methylmercury in the Gulf of Trieste (Northern Adriatic Sea)." Estuarine, Coastal and Shelf Science. Volume 48, Issue 4, Pages 415-428.

CVRWQCB. 2011. Amendments to the Water Quality Control Plan for the Sacramento River and San-Joaquin Basins for the Control of Methylmercury and Total Mercury in the Sacrament-San Joaquin River Delta Estuary (Attachment 1 to Resolution NO. R5-2010-0043. Viewed online at: https://www.waterboards.ca.gov/centralvalley/water_issues/tmdl/central_valley_projects/delta_hg/2011_1020_deltahg_bpa.pdf. Accessed: Aug. 22, 2019. Last updated: June 13, 2019.

Department of Water Resources 2015. Open Water Workgroup Progress Report. Delta Mercury Control Program. Prepared by the Open Water Workgroup and the Open Water Technical Group. Submitted to the Central Valley Regional Water Quality Control Board, Region 5, October 20, 2015. 203 pages. Available at: https://www.waterboards.ca.gov/centralvalley/water_issues/tmdl/central_valley_projects/delta_hg/control_studies/deltahg_oct2015pr_openwater.pdf. Accessed January 20, 2020.

EPA. 1995. Method 1669: Sampling Ambient Water for Trace Metal as EPA Water Quality Criteria Levels. United States Environmental Protection Agency. Office of Water (4303). EPA 821-R-034, April 1995. 42 pages.

Foe C, Louie S, and Bosworth D. Task 2. Methyl Mercury Concentrations and Loads in the Central Valley and Freshwater Delta, August 2008. In Transport, Cycling, and Fate of Mercury and Monomethyl Mercury in the San Francisco Delta and Tributaries: An Integrated Mass Balance Assessment Approach. CALFED Mercury Project Final Report, September 15, 2008. Available at: http://islandora.mlml.calstate.edu/islandora/object/islandora%3A08af4458-e767-4484-9bae-b0608b47852b. Accessed July 24, 2020.

Hecky RE, Ramsey DJ, Bodaly RA, Strange NE. 1991. Increased Methylmercury Contamination in Fish in Newly Formed Freshwater Reservoirs. In: Suzuki T, Imura N, Clarkson TW (Eds.). Advances in Mercury Toxicology. Plenum, New York, Pages 33-52.

Heim W A, Coale KH, Stephenson M, Choe Key-Young, Gill, GA, and Foe C. 2007. "Spatial and Habitat-Based Variations in Total and Methyl Mercury Concentrations in Surficial Sediments in the San Francisco Bay-Delta." Environmental Science and Technology Volume 41, Issue 10, pages 3501-3507. https://doi.org/10.1021/es0626483.

Kelly CA, Rudd JWM, Bodaly RA, Roulet NP, St.Louis V, Heyes A. 1997. "Increases in Fluxes of Greenhouse Gases and Methyl Mercury Following Flooding of an Experimental Reservoir." Environmental Science and Technology, Volume 3, Pages 1334-1344.

Lambertsson L, Nilsson M. 2006. "Organic material: The Primary Control on Mercury Methylation and Ambient Methylmercury Concentrations in Estuarine Sediments." Environmental Science and. Technology, Volume 38, Pages 1487–1495.

Mason RP, Kim E-H, Cornwell J, Heyes D. 2006. "An Examination of the Factors Influencing the Flux of Mercury, Methylmercury and Other Constituents from Estuarine Sediment." Marine Chemistry, Volume 102, Issues 1–2, Pages 96-110.

Marvin-DiPasquale, M, Windham-Myers L, Agee J, Kakouros E, Kieu LH, Fleck JA, Alpers CN, Stricker CA. 2014. "Methylmercury Production in Sediment from Agricultural and Non-Agricultural Wetlands in the Yolo Bypass, California, USA." Science of the Total Environment. Volume 484, Pages 300–307.

Sommer TR, Harrell WC, Swift TJ. 2007. "Extreme Hydrologic Banding in a Large-River Floodplain, California, USA." Hydrobiologia, Volume 598, Pages 409-415

Suddeth Grimm R, Lund JR. 2016. "Multi-Purpose Optimization for Reconciliation Ecology on an Engineered Floodplain: Yolo Bypass, CA." San Francisco Estuary and Watershed Science, Volume 14, Issue 1, Article 5, 23 Pages

Tremblay A, Cloutier L, Lucotte M. 1998. "Total Mercury and Methylmercury Fluxes Via Emerging Insects in Recently Flooded Hydroelectric Reservoirs and a Natural Lake." Science of the Total Environment, Volume 219, Pages 209-221.

Mercury Open Water Final Report for Compliance with the Delta Mercury Control Program

Chapter 4.-Yolo Bypass - Mercury and Methylmercury Modeling Studies

Submitted by the Open Water Mercury Modeling Work Team

Aug 31, 2020

The Open Water Mercury Modeling Workgroup

California Department of Water Resources — Division of Environmental Sciences

Carol DiGiorgio
David Bosworth

California Department of Water Resources — Bay Delta Office

Prabhjot Sandhu
Ali Abrishamchi
Jamie Anderson
Hans Kim
Kevin He
En-Ching Hsu
Kijin Nam
Hari Rajbhandari
Min-Yen Yu
Tara Smith
Eli Ateljevich

Reed Harris Environmental Ltd.

Reed Harris
David Hutchinson.
Matt Gove
Cody Beals
Don Beals

U.S. Geological Survey — Upper Midwest Science Center

Randy Hunt

Acknowledgements

Contents

List of Figures

List of Tables

List of Acronyms and Abbreviations

CVRWQCB	Central Valley Regional Water Quality Control Board
CCSB	Cache Creek Settling Basin
cfs	Cubic Feet per Second
Delta	Sacramento-San Joaquin Delta
D-MCM	Dynamic Mercury Cycling Model
DOC	Dissolved Organic Carbon
DMCP	Delta Mercury Control Program (DMCP)
DWR	(California) Department of Water Resources
fHg	filtered Hg
fMeHg	filtered MeHg
GIS	Geographic Information System
Hg	Mercury
Hg(II)	Inorganic Hg in oxidized state (+2)
Hg(0)	Elemental Mercury
Inorganic Hg	Sum of Hg(II) and Hg(0)
KLRC	Knights Landing Ridge Cut
MeHg	Methylmercury
PEST ++	Parameter Estimation Software
THg	Total Mercury-sum of all forms of inorganic Hg and MeHg
TSS	Total Suspended Solids
uHg	An unfiltered (aqueous) mercury (sample)
uMeHg	An unfiltered (aqueous) methylmercury (sample)
WY	Water Year(s)

Introduction-Yolo Bypass Mercury and Methylmercury Modeling

The Delta Mercury Control Program (DMCP) requires the (California) Department of Water Resources (DWR) to reduce methylmercury (MeHg) open water sediment flux from areas out of compliance in the Sacramento-San Joaquin Delta (Delta) and the Yolo Bypass (See Chapter 1). Application of a mercury (Hg) mass balance mechanistic model, complemented by field data and laboratory approaches, was approved by the Central Valley Regional Water Quality Control Board (Regional Board) to pursue and evaluate options to reduce MeHg supply from open water sediments via operational changes. Chapter 3 summarized the scientific studies conducted as part of the approved Workplan. The objective of Chapter 4 is to summarize and provide key findings of interest associated with model development and model findings to management and policy makers for the Yolo Bypass, based on the application of the Dynamic Mercury Cycling Model (D-MCM). While D-MCM is a proprietary model (EPRI, 2013) the approach to Hg cycling in D-MCM has been published (Harris and others, 2012, Hudson and others, 1994). In addition to the Technical Appendix, any model input and output information is available on request.

Site Description

The Yolo Bypass

The Yolo Bypass is a 3-mile wide, 40 mile-long, 59,000-acre flood conveyance system that diverts flood waters from the Sacramento River around the City of Sacramento (Figure 4-1). The Yolo Bypass floods in roughly 7 out of 10 years with inundation occurring typically between October and April. When completely flooded, the Yolo Bypass approximately doubles the wetted area of the Delta (Schmitt, 2011) and can carry up to four times the flow of the Sacramento River's main channel during large floods (Suddeth Grimm and Lund, 2016). The project design capacity is 343,000 cfs (DWR, 2010).

The primary source of water to the Yolo Bypass is the 2-mile wide Fremont Weir where water passively flows into the Yolo Bypass when the Sacramento river reaches 32 feet stage height (NAVD88 datum) or approximately 60,000 cfs. Additional tributaries into the Yolo Bypass include the Knight's Landing Ridge Cut (KLRC), the Cache Creek Overflow weir and low flow channel for the Cache Creek Settling Basin (CCSB), Willow Slough and Putah Creek (Figure 4-1). Depending on flood flows, the flood gates of the Sacramento Weir can also be opened. The dominant hydrological feature at the southern end of the Yolo Bypass is Liberty Island, a 5,300-acre parcel of open water and wetland habitat that is tidally influenced except during large floods in the Yolo Bypass. Just north of Liberty Island is the feature referred to as the Stairsteps drainage canals (Figure 4-1).

Figure 4-1. **Yolo Bypass Schematic Map**
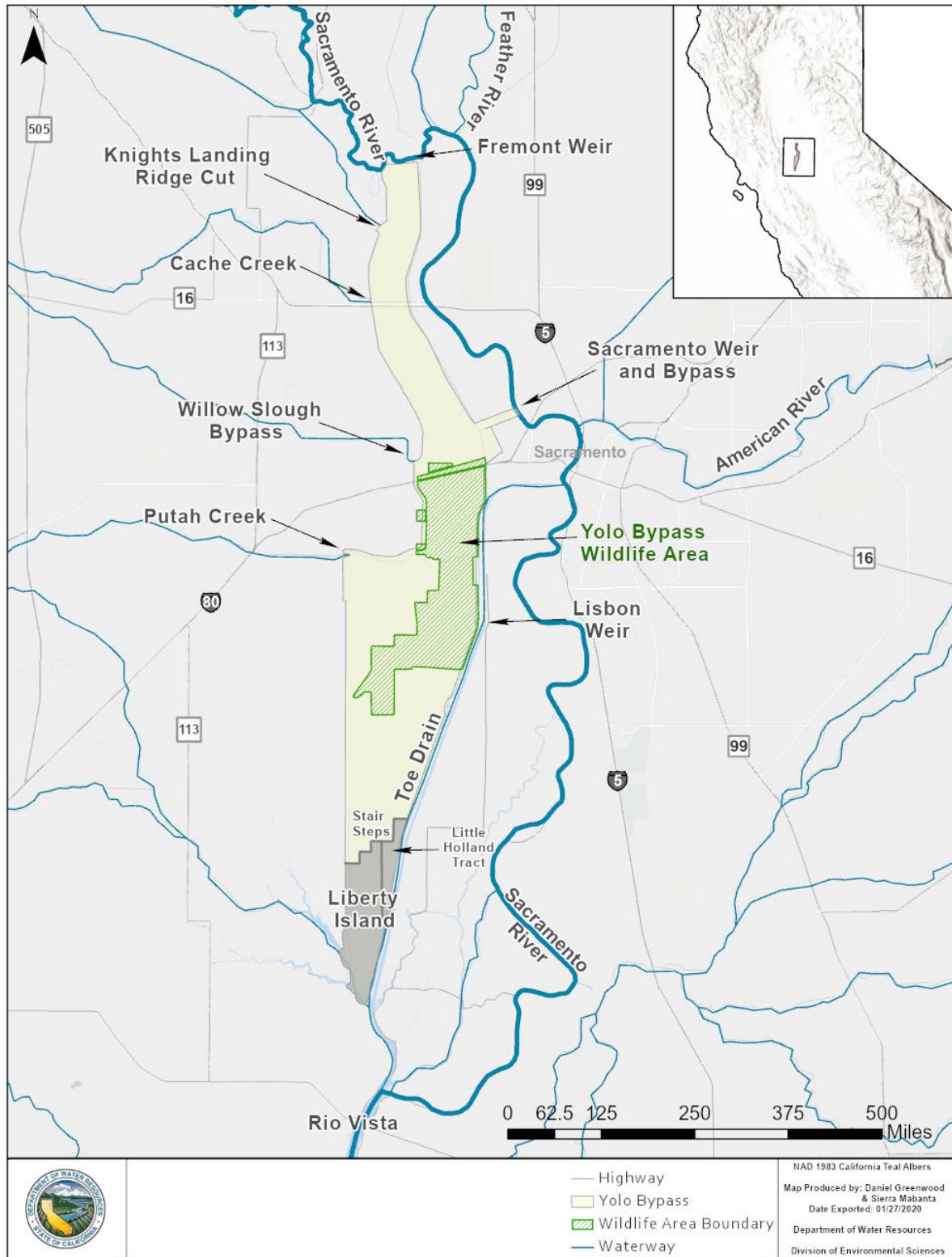
Study Objectives and Approach

Objectives

The primary objectives associated with developing a biogeochemical Hg cycling model to the Yolo Bypass were to:

- Create a model that can simulate concentrations, fluxes, transport and fate of inorganic Hg and MeHg in water and surface sediments in the Yolo Bypass.
- Use the model to evaluate processes governing MeHg supply to the Yolo Bypass.
- Use the model to help evaluate whether there are operational changes or other strategies that can be implemented to reduce ambient MeHg concentrations in Yolo Bypass floodwaters.

Model Integration with other Project Studies

The overall project included studies based on mechanistic modelling, field and laboratory data (Figure 4-2, Table 4-1). The model analysis was designed to primarily use existing models and data. Supplemental additional studies were carried out to provide information needed to better characterize conditions affecting Hg, and specifically MeHg loads, in the Yolo Bypass. Summary results for the studies in Figure 4-2 other than modeling can be found in Chapter 3, as well as detailed information in the Technical Appendices.

Figure 4-2 **Yolo Bypass Modeling, Field and Experimental Study Components**
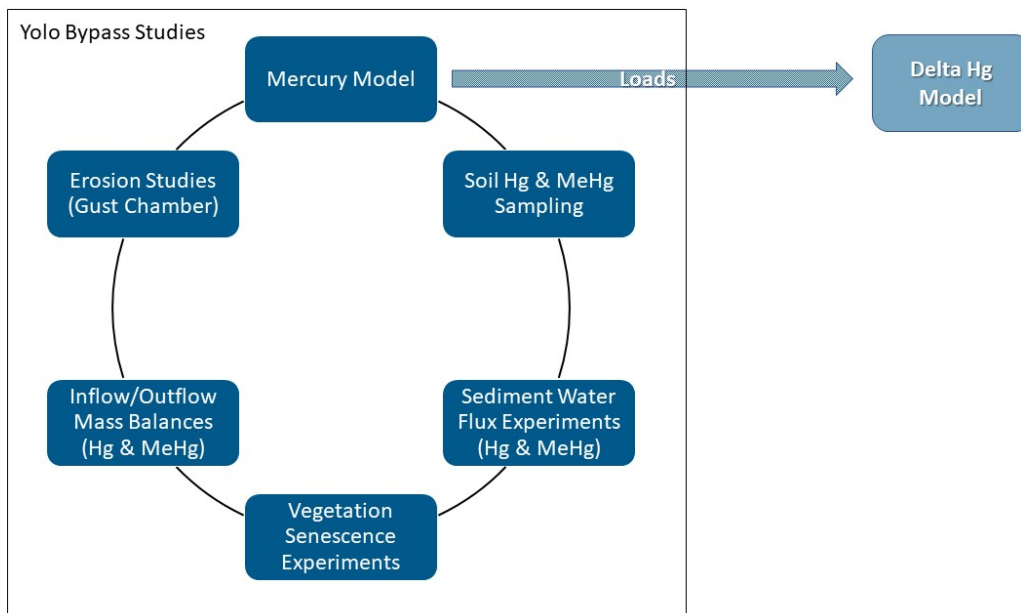
Table 4-1 Studies Carried Out to Support Modelling

Information Source	Information Provided	How was the Information Used?
2017 Yolo Bypass Mass Balance Study	Hg, MeHg, TSS, and other water chemistry concentrations and fluxes at inlet, outlet and intermediate locations in the Yolo Bypass.	Development of boundary tributary fluxes for suspended sediment, Hg and MeHg Used to help calibrate Hg and MeHg partitioning between solids and dissolved phase in model. Comparison with model results for other years, whether the Yolo Bypass is a source or sink for sediments, Hg and MeHg
Sediment-water Flux Study	THg and MeHg concentrations in pore water and sediment solids. Pore-water chemistry (DOC, pH, etc.)	Combined with other data to help calibrate Hg concentrations in surface sediments in model. Used to help calibrate dissolved fluxes of Hg and MeHg from sediments to overlying water in model.
Soil Hg concentration study	Soil concentrations of Hg and MeHg in different land uses and locations in the Yolo Bypass	Contributed to data used to estimate Hg and MeHg concentrations in surface soils in the Yolo Bypass Used to help calibrate surface sediment concentrations of Hg and MeHg in model. Used to help calibrate model resuspension fluxes of Hg and MeHg from sediments to water in model.
Gust Chamber Erosion Study	Sediment resuspension rates for different flow velocities and shear stresses, in different land uses in the Yolo Bypass	Assisted to estimate sediment resuspension rates in the Yolo Bypass as a function of flow.
Vegetation Senescence Studies	Effects of vegetation on MeHg production.	Contributed to model calibration of effects of vegetation Provided information to compare with results of model simulations of effects of removing vegetation

Model Selection

At the time of Workplan approval, no single model existed to adequately simulate hydrology, sediment transport and Hg cycling in the Delta and/or Yolo Bypass. For the Yolo Bypass, two existing models were used in combination, one simulated hydrology and the other simulated sediment transport and Hg in water and sediments. Both models were capable of 2D simulations needed for the Yolo Bypass. Hg simulations explicitly followed MeHg and two forms of inorganic Hg (Hg(II) and Hg(0)). The Yolo Bypass was simulated first, and results were then passed to the Delta Model (see Chapter 5). The modeling domain for the two models is shown in Figure 4-3. The model analysis did not simulate MeHg in the food web, as the key end point was MeHg loads from sediments to open waters.

Figure 4-3. Modeling Domains for Yolo Bypass D-MCM and the DSM2-Hg Models
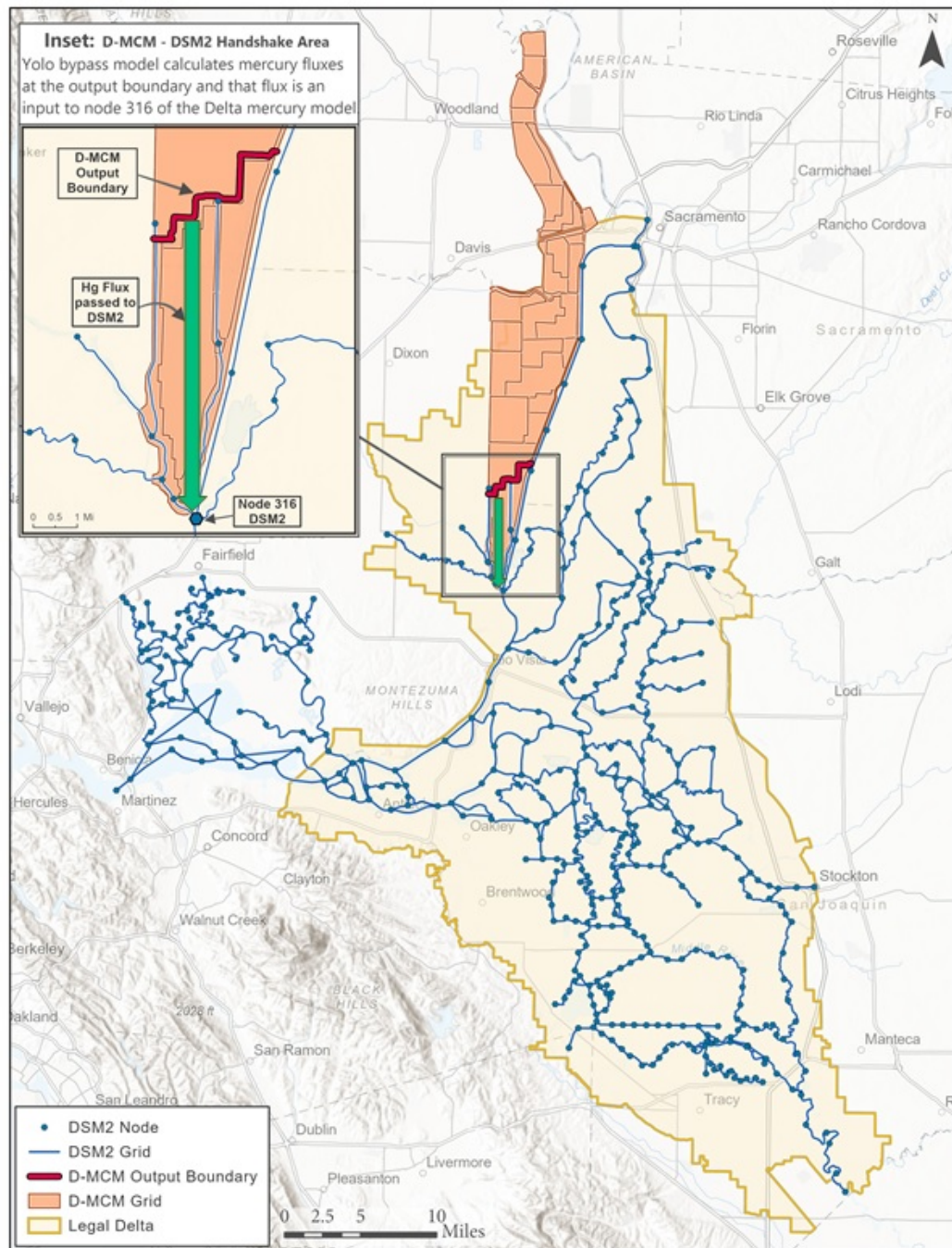
From the Hg perspective, the Yolo Bypass is especially challenging to simulate because conditions affecting Hg cycling, including MeHg supply, are highly variable and change quickly. Most of the Yolo Bypass is intermittently wet and dry, a situation known to affect MeHg production, but difficult to quantify. There have also been many human activities in the Yolo Bypass beyond flood control, including rice agriculture, and management of seasonal wetland and pasture habitats. These land uses affect site conditions that influence MeHg supply, for example hydrology and the supply of organic matter.

The Dynamic Mercury Cycling Model (v4.0, EPRI, 2013) was chosen to model Hg and MeHg in the water column and sediment bed in the Yolo Bypass. The D-MCM is a Windows-based simulation model for personal computers. A summary of the approach used in D-MCM to represent Hg cycling in aquatic systems is presented in a later section. Previous versions of D-MCM have been used in large multidisciplinary research projects in the Gulf of Mexico (Harris and others, 2012a), Florida Everglades (Harris and others, 2003a), METAALICUS (Harris and others, 2007), and Wisconsin Lakes (Hudson and others, 1994). It has also been used in pilot TMDL studies in Florida (Atkeson and others, 2003) and Wisconsin (Harris and others, 2003b) and a model analysis of the effects of climate change on Hg cycling and bioaccumulation in the Great Lakes Basin, funded by the US EPA (Harris and others, 2015, 2012b).

Major Components of Model Analysis – Yolo Bypass
Application of D-MCM to the Yolo Bypass included the following steps:

1. Development of model grid
2. Estimates of hydrology
3. Estimates of suspended sediment loads (other than vegetation)
4. Incorporation of vegetation
5. Calibration of the model to available data for suspended sediments and Hg
6. Sensitivity/uncertainty analysis, and
7. Simulations of sensitivity runs agreed to with Regional Board

Model Grid Development
D-MCM was set up for the Yolo Bypass using a coarse spatial resolution with 47 cells, each assumed to have uniform characteristics internally. D-MCM is not a high spatial resolution model, and a finer spatial scale analysis would also not have been adequately supported with the level of data available and the uncertainties regarding some aspects of Hg cycling within the Yolo Bypass (e.g. effects of vegetation and wetting/drying). The model grid reflected 5 GIS layers that considered the following features:

- Land use
- Hg and MeHg concentrations in sediments
- Agricultural disking (the model calibration did not distinguish disked/undisked areas)
- Hydrology - Fraction of time wet
- Hydrology - wet/dry cycling frequency

Multiple land uses within the Yolo Bypass were grouped as follows to develop the model grid: pasture, fallow, white rice, wild rice, seasonal wetlands, tidal marshes, mixed other, and water conveyance channels. Individual parcels of land in the Yolo Bypass used for various purposes were too small to be represented individually in the model analysis. Therefore, model cells were set up, to the extent possible, to include a single dominant land use within each cell, while maintaining the same overall fractions of land used for different purposes in the Yolo Bypass. Information on land used for crops was drawn primarily from a 2005-2009 survey conducted by Howitt and others (2013). Land use data in the Yolo Wildlife Area were obtained from the Yolo Wildlife Area manager. In addition, wetland GIS data developed by Duck's Unlimited for the Delta Methylmercury TMDL TMDL Nonpoint Source

Workgroup (NPS Workgroup, 2012) and the National Wetlands Inventory were also examined (U.S. Fish and Wildlife Service, 2020).

Surface sediment concentrations of Hg and MeHg vary within the Yolo Bypass. Characterization of the spatial variability of surface sediment Hg and MeHg concentrations was carried out using data from 1999-2016 (see additional discussion later in Chapter).

Frequency of land wetting and frequency of wet/dry cycling have the potential to stimulate Hg methylation. These factors were characterized using outputs from previous hydrodynamic simulations carried out for 1997-2012 using a model called TUFLOW (additional information is provided later in the Chapter). Frequency of wetting was calculated as the percentage of wet days in TUFLOW simulations in a given TUFLOW cell. Wet/dry cycling was defined as the average number of wet/dry cycles per year in TUFLOW simulations. GIS layers were created for each factor, and both displayed a slight east to west gradient across the Yolo Bypass.

The final model grid is shown in Figure 4-4. It features 17 permanently wet cells (classified as water) and 30 land (seasonally wet) cells classified under different land use types. Additional details on the development of the model grid are available in the 2015 Progress Report (DWR, 2015).

Outputs from the Yolo Bypass model were passed to the Delta model at the stairsteps. This location was chosen rather than the bottom of Liberty Island because flows at the stairsteps are primarily in one direction (downstream). Conditions below the stairsteps do not have a large effect on Hg above the stairsteps.

Figure 4-4 Model Grid Used for the Yolo Bypass Dynamic Mercury Cycling Model

Cell #	Land use
1	Fallow
2	Mixed/other
3	Water
4	Water
5	Water
6	Water
7	Water
8	Water
9	Water
10	Water
11	Water
12	Water
13	Water
14	White rice
15	Fallow
16	Mixed/other
17	Fallow
18	White rice
19	Wild rice
20	Wetland
21	Mixed/other
22	Fallow
23	White rice
24	Wild rice
25	Wetland
26	Wetland
27	Mixed/other
28	Wetland
29	Pasture
30	Pasture
31	Wetland
32	White rice
33	Wetland
34	Pasture
35	Tidal marsh
36	Tidal marsh
37	Mixed/other
38	Mixed/other
39	Pasture
40	Tidal marsh
41	Pasture
42	Water
43	Water
44	Water
45	Water
46	Water
47	Water

D-MCM Grid

- Pasture
- Fallow
- White rice (disked)
- Wild rice (disked)
- Mixed/other
- Mixed/other (disked)
- Seasonal wetland
- Seasonal wetland (disked)
- Tidal marsh
- Water conveyance

0   5   10 km

Model Approach

Approach to Hydrology

Hydrology for D-MCM simulations must be estimated externally to the model and then provided as input information. For this study, hydrology was available from a hydrodynamic model called TUFLOW (www.tuflow.com), previously developed for DWR as part of an EIS/EIR for the Yolo Bypass Salmonid Habitat Restoration and Fish Passage Project (DOI/DWR, 2019). TUFLOW outputs were available for Water Years (WY) 1997-2012 (October 1996 - May 2012). Because this was the period that realistic hydrology could be represented in Yolo Bypass simulations, this was also the period that D-MCM was applied to simulate Hg. As shown in Table 4-2 this time period captured a wide range of flow conditions, including some of the wettest years on record with sustained flooding in the Yolo Bypass, and drought years when little or no overtopping of the Fremont weir occurred.

Table 4-2 Index of Sacramento Valley Water Year Classification.

Water Year	Index
1997	W
1998	W
1999	W
2000	AN
2001	D
2002	D
2003	AN
2004	BN
2005	AN
2006	W
2007	D
2008	C
2009	D
2010	BN
2011	W
2012	BN

Water Year classifications from wettest to driest are: W=Wet, AN=Above Normal, BN=Below Normal, D=Dry, C=Critical (CDEC 2020).

TUFLOW simulations used a grid with much higher spatial resolution (approximately 25' x 25') than the D-MCM Hg analysis. TUFLOW outputs were aggregated spatially to match the Hg model grid consisting of 47 cells. TUFLOW outputs were also aggregated in time from hourly to daily average estimates.

Hydrology in the Yolo Bypass is complex, with a high degree of human intervention:

a. <u>Flood control</u>: TUFLOW simulations considered natural flows and the management of water for flood control during the wet season from October through May each year but did not simulate summer flows and did not consider other water uses in the Yolo Bypass.

b. <u>Agriculture and wetland management</u>: Rice cultivation occurs in the Yolo Bypass, as well as management of wetland areas where water is added seasonally to enhance waterfowl habitat. Both

of these uses involve water additions and removals. Estimates of water usage for these purposes were calculated in a coarse manner (information available upon request)

To allow a single simulation from October 1996-May 2012, rather than simulate 16 wet seasons separately, summer flows from June-September were generated each year to hydrologically link TUFLOW results for different wet seasons. This was done by calculating summer flows for each model cell that would transition from the water volume at the end of a TUFLOW simulation in May to match the volume of water in October, used to start the next wet season simulation with TUFLOW.

Approach to Represent Suspended and Bed Sediments

D-MCM was set up for the Yolo Bypass with four particle types:

a. Organic matter other than vegetation
b. Vegetation solids.
c. Fine inorganics (e.g. silt and clay)
d. Coarse inorganics (e.g. sand)

Each particle type had unique properties in terms of particle densities, settling velocities, resuspension rates, and Hg partitioning (ratio of solids:dissolved concentrations).

Tributary loads for suspended sediments were estimated using empirical approaches that varied among tributaries. For example, Fremont Weir is an important source of suspended sediments to the Yolo Bypass. Measurements of suspended sediment at Fremont Weir were limited (n=13 in 2006, n=9 in 2016/2017). Daily suspended sediment estimates were available however for the simulation period at Freeport, approximately 36 river miles downstream in the Sacramento River (Sacramento River Forum, 2020). A relationship between suspended sediment concentrations between Fremont Weir and Freeport was developed to estimate daily suspended sediment concentrations at Fremont Weir (see comparison of observed and estimated SSC at Fremont Weir in Figure 4-5). For other tributary inflows to the Yolo Bypass, daily flow estimates were available (from TUFLOW), but daily measurements of other constituents, e.g. suspended sediments, were not. Regressions were developed between suspended sediments and flow for these inflows using limited tributary-specific observations. Daily flow estimates for tributaries from the TUFLOW model were then used to estimate daily suspended sediment concentrations in these inflows to the Yolo Bypass.

Figure 4-5 Regression-Estimated and Field-Measured Concentrations of Suspended Sediments at Fremont Weir in 2006 and 2017
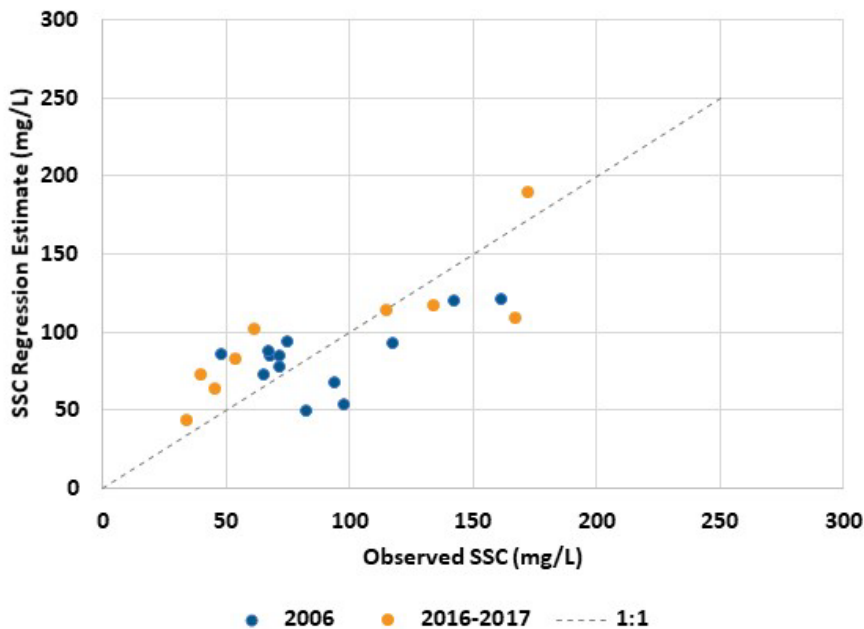
Figure Note: 2006 observations from Foe and others, 2008. 2017 observations from DWR Mass Balance Study.

Once loaded into Yolo Bypass waters, suspended sediments could settle to the sediment bed or remain in suspension. Resuspension of sediments from the sediment bed to overlying water was also included. TUFLOW velocity estimates were used to estimate shear stress and sediment resuspension in the Yolo Bypass at high resolution. These resuspension estimates were summed within each of the 47 Hg model cells and used as inputs to Hg simulations. Terrain-specific erosion experiments were carried out using a Gust chamber to support the model analysis (Technical Appendix D). In the sediment bed, the active surface layer was assigned a thickness of 2 cm and a mass balance was maintained for sediment mass. The difference between inputs (settling) and losses (resuspension and decomposition) determined if there was net accumulation or erosion of the surface sediment layer.

Vegetation also supplied solids to the system during die-off periods each year. Approximately 3/4 of the surface area of the Yolo Bypass upstream of the stairsteps was assigned as pasture, white rice, wild rice or seasonal wetland terrain. When compared to the overall external supply of sediments to the Yolo Bypass, vegetation solids loads were secondary (17%). In terms of the supply of organic matter however, vegetation supplied more than half (63%) and was an important source of carbon supporting wet season MeHg production in simulations.

As shown in Figure 4-6, different seasonal patterns for growth and die-off, and peak biomasses were developed for pasture, wetlands, white rice and wild rice vegetation (Figure 4-6).

Vegetation solids were quickly delivered through the water column to sediments following senescence and were instantly mixed into the surface sediment layer with other sediments. In reality, vegetation solids may remain as a separate compartment from surface sediments, but the current construct of D-MCM did not allow this configuration. Vegetation was assumed to decompose within the sediment bed more easily than other sediments. Overall, the timing, magnitude and fate of vegetation in D-MCM simulations of the Yolo Bypass was viewed as a preliminary treatment that could be refined if future modeling is carried out.

Figure 4-6 **Model Inputs for Vegetation Biomass**
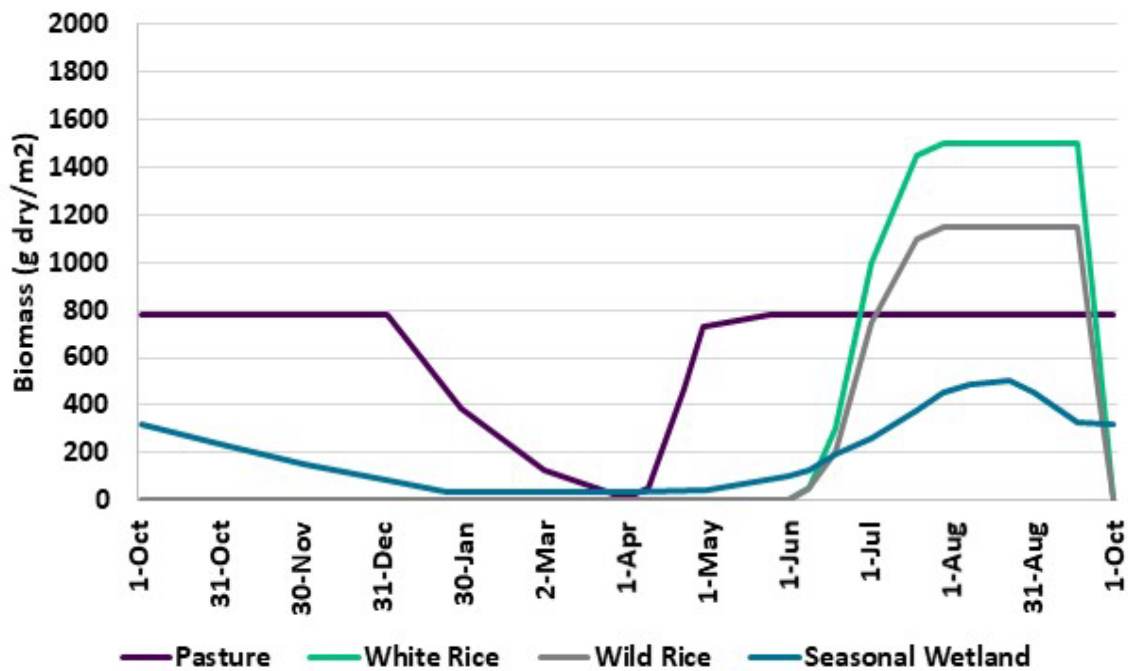
Figure Note: Seasonality of growth and die off was based on Stephenson (2019). Peak biomass values: pasture from Stephenson (2020), white rice and wild rice based on Wyndham-Myers and others (2014), seasonal wetland from Stephenson (2017).

Approach to Represent Hg Cycling

Hg cycling was simulated using the D-MCM model. D-MCM is a time dependent, mechanistic mass balance model for Hg cycling and bioaccumulation, modeling the cycling and fate of three major forms of Hg (MeHg, inorganic Hg (II), and elemental Hg) in aquatic systems. Model compartments include one or more layers in the water column and sediments and can include a food web (not done in this analysis). Key Hg processes in D-MCM are shown in Figure 4-7. D-MCM also includes vegetation, which is important in the Yolo Bypass, where land types include seasonal wetlands, rice agriculture and intermittently flooded pasture lands. Although the effects of vegetation on Hg cycling, and MeHg production in particular, could only be simulated coarsely in D-MCM, this first attempt still provided. insights into the role of vegetation on MeHg supply. The model is capable of simulating systems using a

1, 2 or 3D scheme. For the Yolo Bypass, the D-MCM was set up in a 2D configuration, where conditions varied in the direction of flow and horizontally perpendicular to flow but were well mixed vertically.

Figure 4-7 Schematic Representation of Processes Modeled by The Dynamic Mercury Cycling Model (Vegetation not Shown)
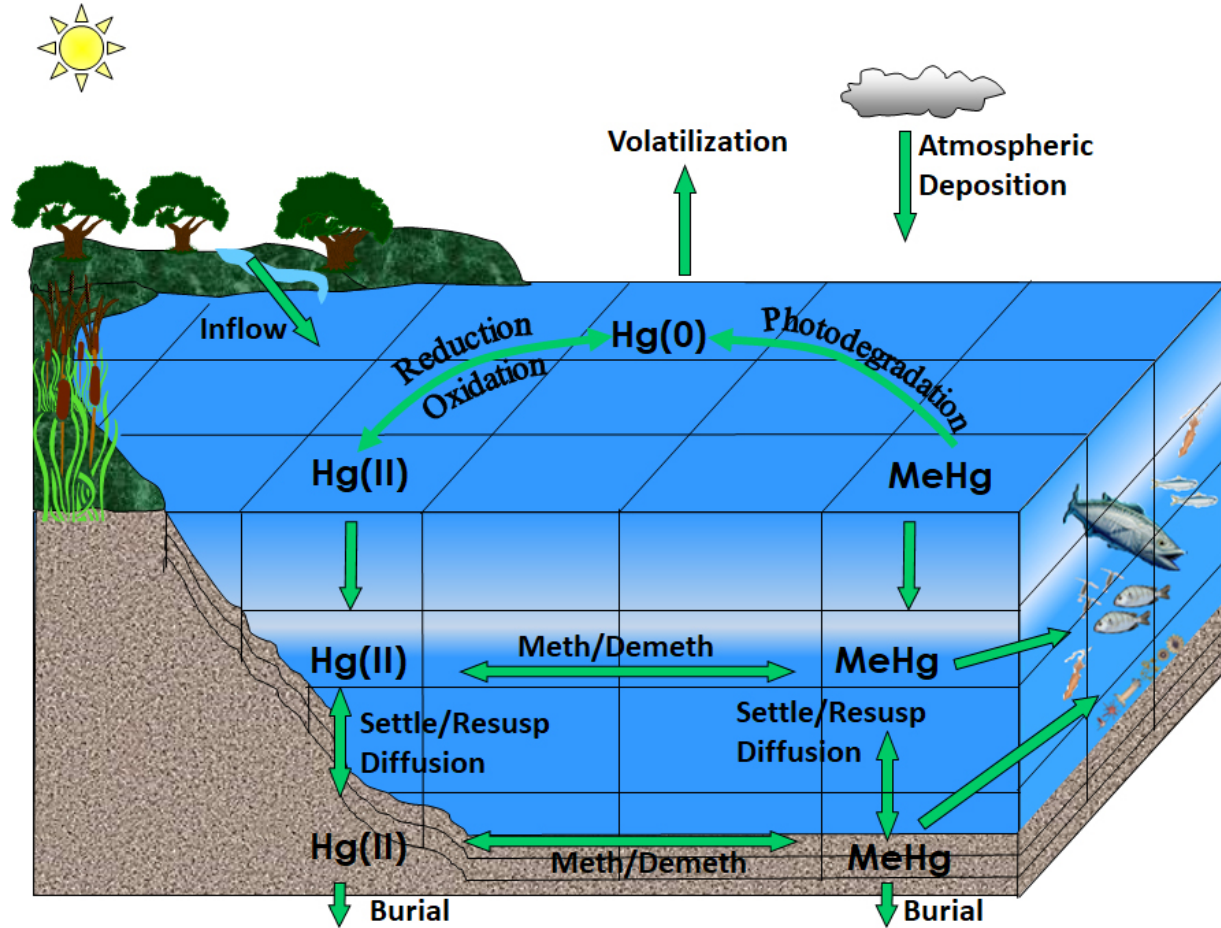
Atmospheric wet deposition of inorganic Hg was estimated using data from the nearest Mercury Deposition Network (MDN) site, CA72, near San Jose. The site was operated from January 11, 2000 through December 27, 2006. Weekly data were used to estimate overall monthly averages for the entire period of record, for use in the DSM2-Hg analysis. Dry Hg deposition was assigned a constant value of 19 ug/m2/yr, the mean value reported by Tsai and Hoenecke (2001) for the San Francisco Bay Estuary from August 1999 through November 2000.

Tributary loads of inorganic uHg and uMeHg were based on empirical relationships between concentrations and flow or TSS (which was subsequently estimated on the basis of flow). This was done using tributary-specific data to the extent possible. For example, comparisons of regression estimates and field-based estimates of uHg and uMeHg loads to the Yolo Bypass for Cache Creek Settling Basin are shown in Figure 4-8 and Figure 4-9.

Figure 4-8 Regression Model versus Field Estimates of uHg Loads to the Yolo Bypass from the Cache Creek Settling Basin
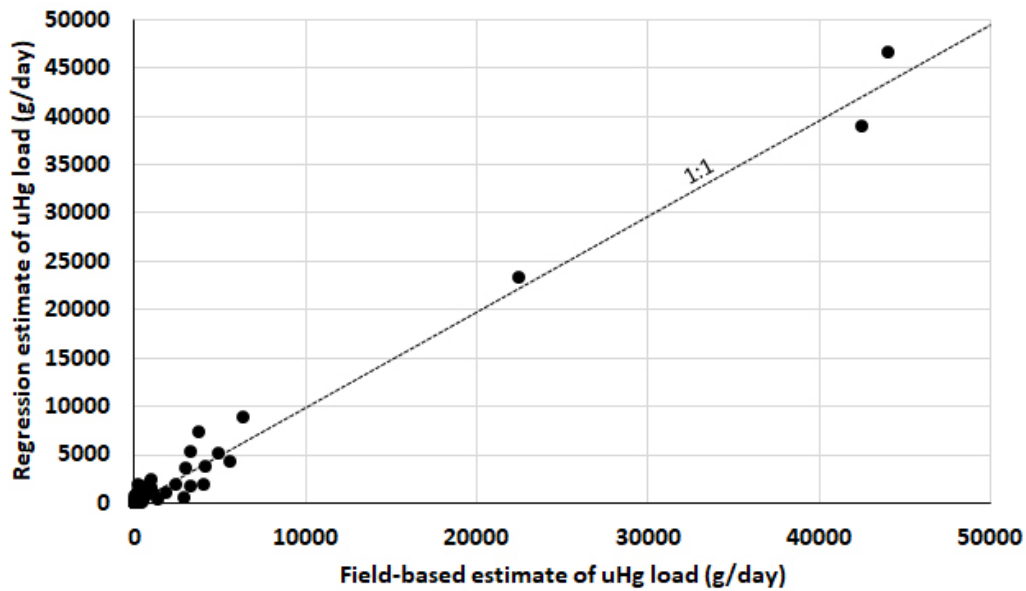
uHg concentrations were based on daily average flow estimates from TUFLOW model: $[uHg_{(ng/L)}] = 0.0193 * Flow_{(cfs)} + 10$ if Flow < 10,600 cfs, $[uHg_{(ng/L)}] = 0.0966 * Flow_{(cfs)} - 800.36$ if Flow > 10,600 cfs,. Data from USGS (2019)

Figure 4-9 Regression Model Estimates of MeHg Loads to the Yolo Bypass Versus Field-Based Estimates for the Cache Creek Settling Basin
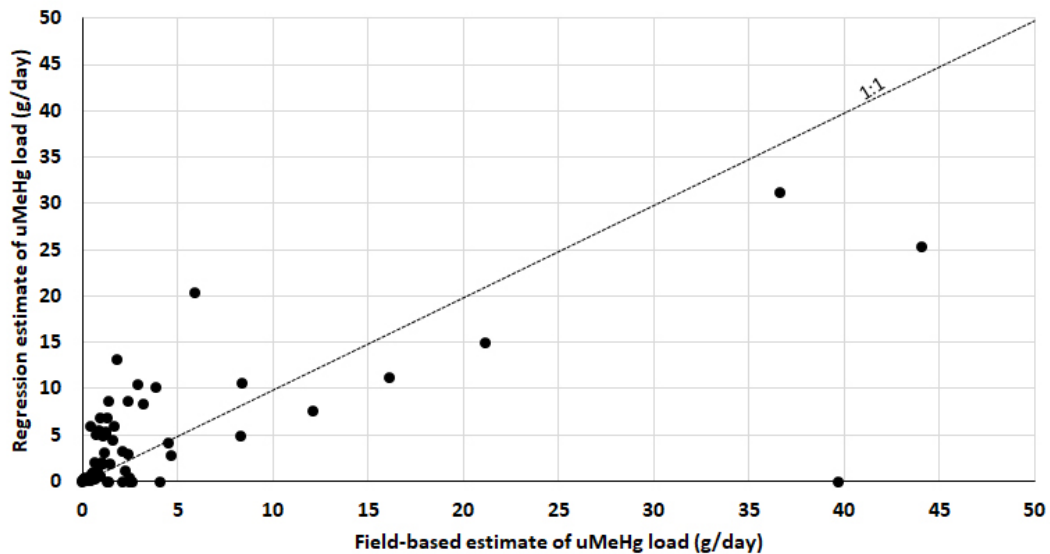
Figure Note: Data from USGS (2019)

Initial sediment bed concentrations of Hg and MeHg for each model cell (0-2 cm) were estimated using data from 2005-2016 (this study Technical Appendix F; Heim and others, 2010; Marvin-DiPasquale and others (2009). Observations from different years were combined due to limited data availability. Data were filtered to include only samples in the top 5 cm and for the months from October through May, above the stairsteps. The resulting dataset included 106 samples for Hg and 103 for MeHg. In both cases most samples (94%) were collected in 2015-2016.

Approach to Model Calibration

D-MCM was calibrated for the period from October 1996-May 2012, when necessary hydrologic information was available from the TUFLOW model (US DOI, 2019). TUFLOW hydrology used in simulations was not changed during the model calibration. It is often desirable to calibrate a model to one dataset and validate the model by applying it to a different dataset and comparing model results to observations. Due to the limited amount of available data, all observations were used to calibrate the model. It is also preferable to use data collected within the calibration period when comparing model results to observations. For this study, most of the available sediment Hg and MeHg data were collected in 2015-2016, outside the calibration period for water years 1999-2012.

Flows through Yolo Bypass are primarily unidirectional until the area known as the Stairsteps. Downstream of the Stairsteps in Liberty Island, tidal influences and two-way flows become more important. Given the limitations of TUFLOW model, and limited data for Hg, MeHg and SSC downstream of Liberty Island that become more important when there is tidal back flow, the model calibration focused on data upstream of the Stairsteps.

D-MCM results for suspended sediments and Hg were compared to field observations in the Yolo Bypass, upstream of the Stairsteps (Figure 4-1). Various model inputs ("parameters") were adjusted to improve the fit between the model and observations. This was done in two stages. First an initial manual calibration was performed, visually comparing model results to observations. This was done for suspended sediment concentrations, then Hg and finally MeHg in water and surface sediments. The manual calibration was carried out until results were subjectively deemed adequate to be used as a starting point for the final calibration using parameter estimation software (PEST ++) (See Technical Appendix H). PEST++ continued to systematically adjust selected model parameters (e.g. rate constants) to reduce the overall error between model results and observations for SSC, Hg and MeHg in water (filtered and unfiltered), and sediments (solids and porewater). Parameter estimation techniques have generally been applied previously to hydrologic models but are less commonly applied to geochemical contaminant models. Unlike the manual calibration, PEST ++ varied parameters related to suspended sediments, Hg and MeHg simultaneously in order to reduce the overall error for these three components combined. Because the number of observations available and some observation values can have order-of-magnitude differences, variable weighting was applied to allow PEST ++ to obtain a more balanced match across the different types of observations. PEST ++ software continued to adjust parameter values the best fit was obtained.

Uncertainty Analysis

The quantitative framework of the PEST++ simulations provided information used for assessing model uncertainty. For example, certainty associated with the value of the Hg(II) partitioning constant improved dramatically during the PEST analysis, while information contained in the observations provided was not

sufficient to improve certainty for the model input related to resuspension of coarse inorganic sediments (Figure 4-10). The improvement in certainty depends in part on the number and type of observations available for parameters. A related concept is identifiability (Doherty and Hunt 2009). Parameter identifiability extends traditional parameter sensitivity by accounting for confounding parameter correlation, as the both parameter sensitivity and correlation drive the performance of parameter estimation. A parameter that has higher identifiability is more constrained by information contained in the observations therefore has less room to vary. Model forecasts that depend on that parameter are therefore more certain. A parameter having low identifiability, on the other hand, is not highly constrained by observations. Parameters with low identifiability and a large influence on model results are candidates to focus future data collection \ to improve certainty associated with model results. That analysis is possible but was outside the scope of the current work.

Figure 4-10 **Uncertainty Associated with Two Model Input Parameters, Prior to and Following PEST++ Analysis**
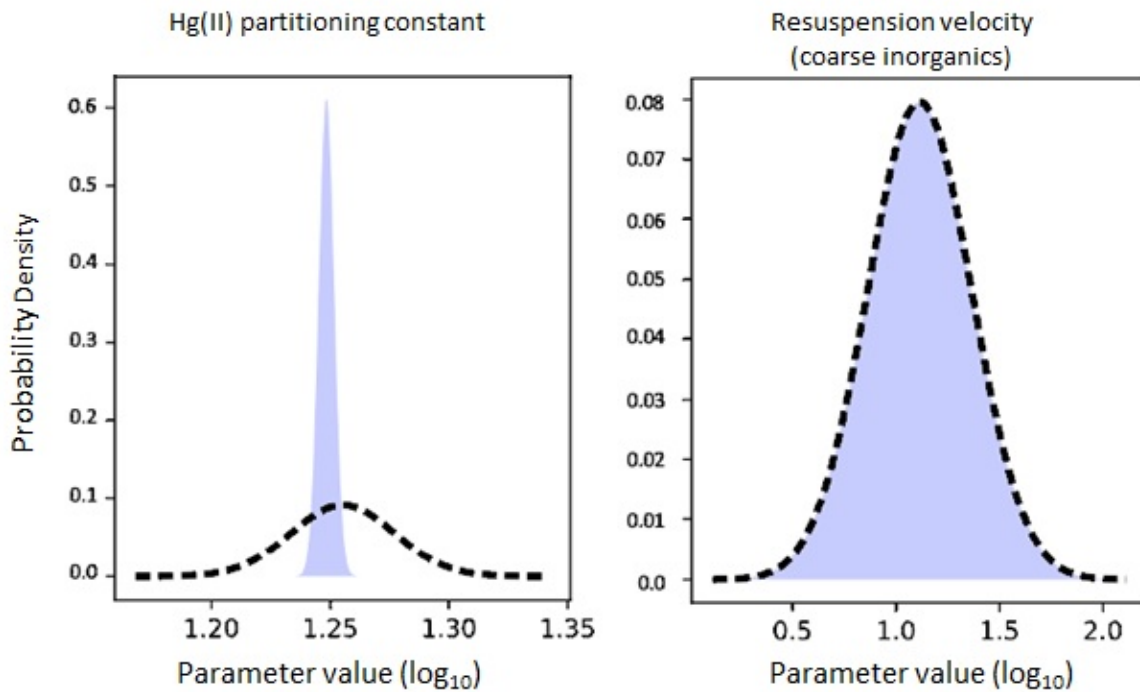
Figure Note: Dashed line = prior to PEST++ analysis. Blue area = after PEST++ analysis.

PEST++ also generated information that helped to estimate the uncertainty associated with model results. Uncertainties for two model forecasts, average annual loads averaged (1998-2012) for uHg and uMeHg, are shown in Figure 4-11. Both forecasted annual export fluxes (uHg and uMeHg) are appreciably more certain after the PEST++ calibration. An important limitation should be noted. The reported uncertainty only includes adjustable parameters included in the uncertainty analysis; all other model design and related inputs relating to process, structure and parameters are assumed to be perfectly known for the purposes of the uncertainty calculation (Hunt 2017). For example, the model assumed the pool of Hg(II) available for methylation was the dissolved concentration in sediment porewater, and that carbon turnover reflected the

activity of methylating microbes. This results in relatively smaller uncertainty ranges and should be taken as a reflection of the true uncertainty. In reality, there is significant uncertainty regarding both of these issues. In the absence of providing PEST with information to quantify these uncertainties in the conceptual model, it was effectively assuming the model approach was correct. Overall then PEST was given information allowing it to capture some but not all of the uncertainty involved in model forecasts. A second limitation is that the computationally efficient linear approach used can result in reported forecast uncertainties spanning unrealistic ranges. e.g. negative uHg export forecast in Figure 4-11 (shown in grey) prior to the PEST refinement of the calibration. More computationally intensive uncertainty approaches, such as Monte Carlo, do not exhibit this type of confounding artifact, but were not implemented in this work. Regardless, the uncertainty analysis performed conveys the primary findings regarding which model forecasts had relatively higher uncertainty, and which were most improved during calibration.

Figure 4-11 Forecasted Average Annual Export of (a) uHg and (b) uMeHg at the Stairsteps for October 1997 – May 2012
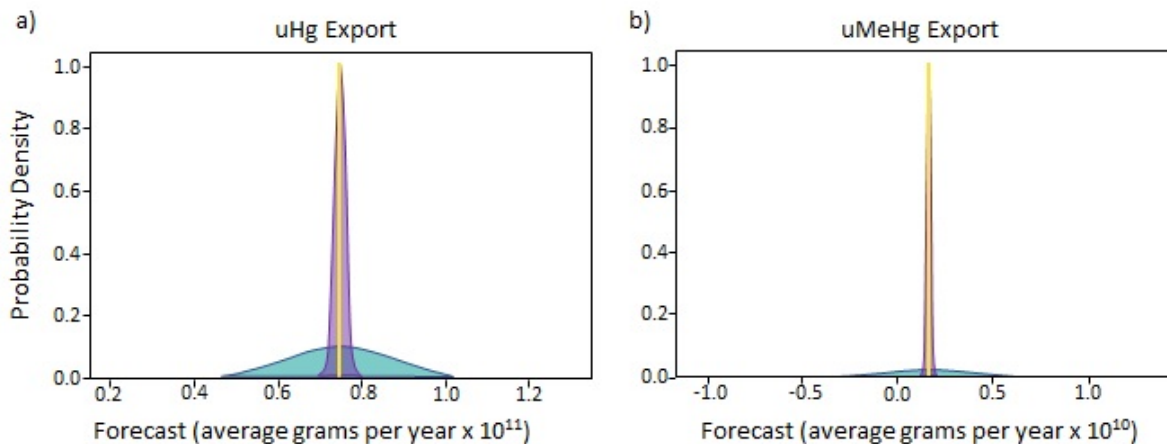
The gray bell curve is the forecast uncertainty prior to the PEST++ model calibration; the blue bell curve is the uncertainty after the PEST++ calibration. The red line is the forecasted value from the calibrated DMCM model. Note that prior uncertainty spanning a negative load forecast in (b) is a result of the approach used and does not reflect the actual probability of physically unrealistic negative loads.

Sensitivity Simulations

Following the calibration of the model to existing conditions, a series of simulations was carried out to examine the sensitivity of the model forecasts to changes in selected model inputs (Table 4-3). These simulations were developed in consultation with the Regional Board. 50% reductions were applied to the model inputs shown in Table 4-4. Simulations were carried out for the same period as the model calibration (October 1996-May 2012). The export of MeHg at the stairsteps was used as the key metric to assess the effect of each simulation.

Table 4-3 Sensitivity Analyses Agreed upon with Regional Board

Category	Goal
Particle Related	Investigate sensitivity of simulated MeHg to changes in suspended sediment inputs to the Yolo Bypass. Begin by varying suspended sediment concentrations from the Cache Creek Settling Basin (CCSB).
External Inorganic Hg Loads	Investigate sensitivity of simulated MeHg to changes in inorganic Hg inputs from tributaries to the Yolo Bypass. Begin by varying CCSB inorganic Hg concentrations to the Yolo Bypass. Investigate sensitivity of simulated MeHg to changes in atmospheric inputs.
External MeHg Loads	Investigate sensitivity of simulated MeHg to changes in MeHg inputs from tributaries to the Yolo Bypass. Begin by varying CCSB MeHg concentrations to the Yolo Bypass.
Internal MeHg Loads	Investigate sensitivity of simulated MeHg to the rate of MeHg supply generated within the Yolo Bypass.
Influence of Vegetation	Investigate sensitivity of simulated MeHg to vegetation effects in the Yolo Bypass. Begin by reducing pasture or seasonal wet-land vegetated areas in the model.

Table 4-4 Model Inputs Changed for Sensitivity Simulations

Category		Model Input Changed (50% reduction in all cases)
Particle related	1	Cache Creek Settling Basin outflow suspended sediment concentrations
	2	Fremont Weir suspended sediment concentrations
External inorganic Hg loads	3	Cache Creek Settling Basin outflow Hg(II) concentrations
	4	Fremont Weir Hg(II) concentrations
	5	Atmospheric wet Hg(II) deposition
External MeHg loads	6	Cache Creek Settling Basin outflow MeHg concentrations
	7	Fremont Weir MeHg concentrations
Internal MeHg loads	8	Methylation rate constants in all Yolo Bypass sediments
Vegetation	9	Vegetation biomass loads to Yolo Bypass sediments

Yolo Bypass D-MCM Calibration Results

Calibration Improvement with PEST++

During the calibration of the model to existing conditions from October 1996 - May 2012, the PEST++ analysis reduced the error between observations and model estimates by 51% relative to the initial manual calibration. (Technical Appendix H)

Hydrology Results

The largest source of water to the Yolo Bypass in simulations was Fremont Weir, representing 71% of inputs for the overall period from October 1996-May 2012 (Figure 4-12a). The total amount of flow and the relative contributions of different water sources varied widely among the simulated years (Figure 4-13a, Figure 4-14a). The relative importance of Fremont Weir as a source of water varied appreciably among years, from 0-86% and was greater in wet years (expected for a flood control structure). While Knights Landing Ridge Cut represented 10% of the tributary supply of water for the overall simulation period (Figure 4-12a), it represented up to 80% of tributary inputs in dry conditions (Figure 4-14a).

Suspended Sediment Calibration Results

The greatest source of suspended sediments to the Yolo Bypass in simulations was also the Fremont Weir, representing two thirds of freshwater input for the overall period from October 1996-May 2012 (Figure 4-12b). Similar to water loads to the Yolo Bypass, the annual sediment loads and the relative contributions of different tributaries varied widely among the simulated years (Figure 4-13b, Figure 4-14b). In wet years, Fremont Weir was the largest source of suspended sediments, followed by Cache Creek Settling Basin. Knights Landing Ridge Cut was a secondary overall source of suspended sediments for the simulation period (9%), but increased in importance in dry years, representing up to 90% of tributary sediment inputs (Figure 4-14b)

Within the simulation period, suspended sediment data were available in 5 model cells upstream of the stairsteps. An example of simulated and observed suspended sediment concentrations is shown in Figure 4-15 for cell 42, a section of the Toe Drain passing the Stairsteps (Figure 4-4). Additional plots for other sites with observations are provided in Technical Appendix G.

Overall, the Yolo Bypass (to the Stairsteps) was simulated to be a net sink for suspended sediments, with less sediment exported at the stairsteps each year than loaded externally from tributaries (Figure 4-16). Overall, between October 1996 through May 2012, the loads of suspended sediments exiting the Yolo Bypass at the Stairsteps were 30% less than the sediment load entering the Yolo Bypass from its tributaries. (18-69% range among years). Trapping efficiency tended to be greater in dry years.

Figure 4-12 Average Estimated Tributary Loads of Suspended Sediment, uHg(II) and uMeHg to the Yolo Bypass, October 1996- May 2012
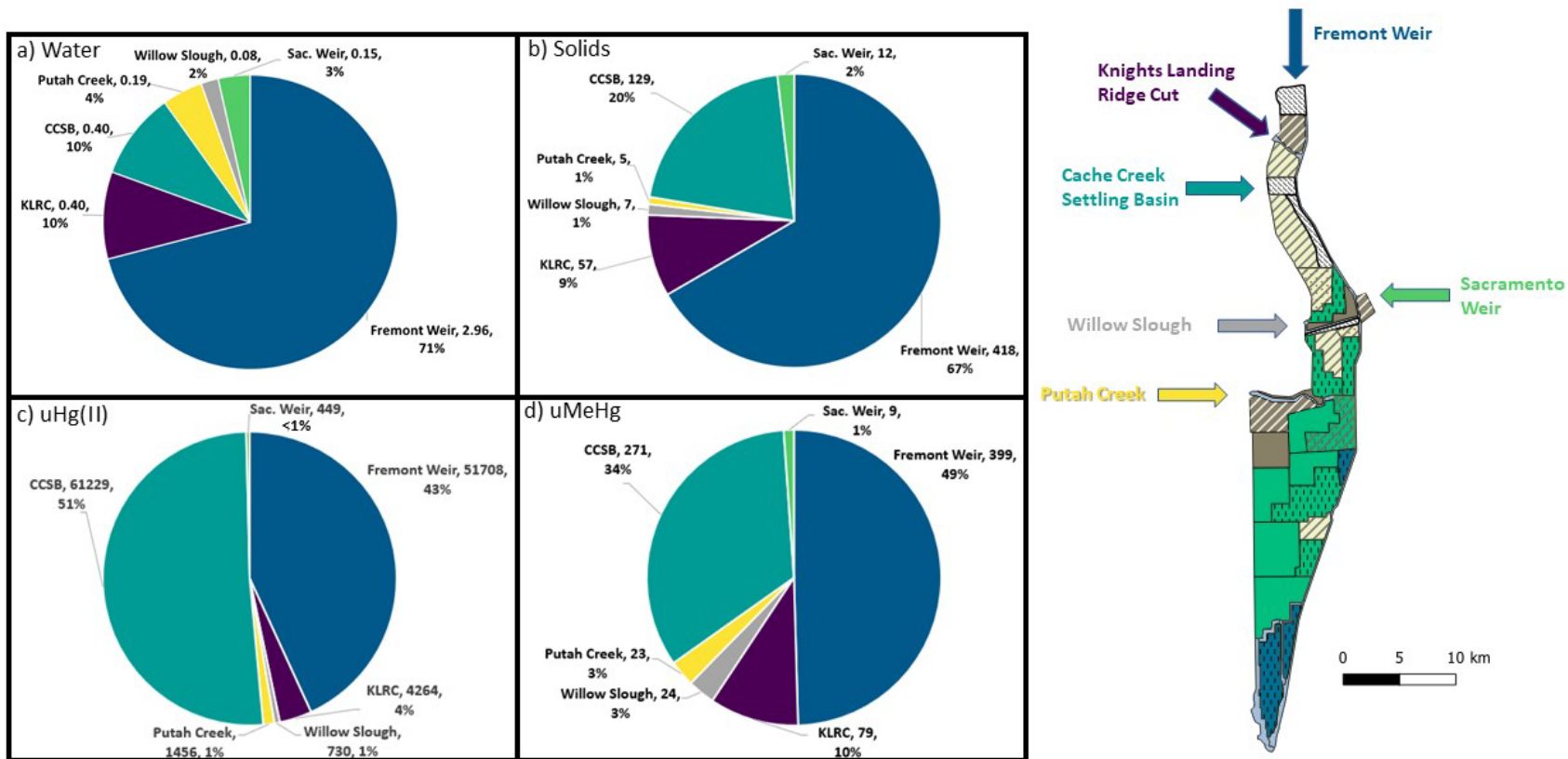
Figure Note: CCSB = Cache Creek Settling Basin, KLRC = Knights Landing Ridge Cut. Values in labels are loads and percentage of totals. Water load = km3/yr; Suspended sediment load = 1000's of tonnes/year; Hg and MeHg loads = g/yr

Figure 4-13 Estimated Tributary Loads of a) Water, b) Suspended Sediment, c) uHg(II) and d) uMeHg to the Yolo Bypass by Water Year
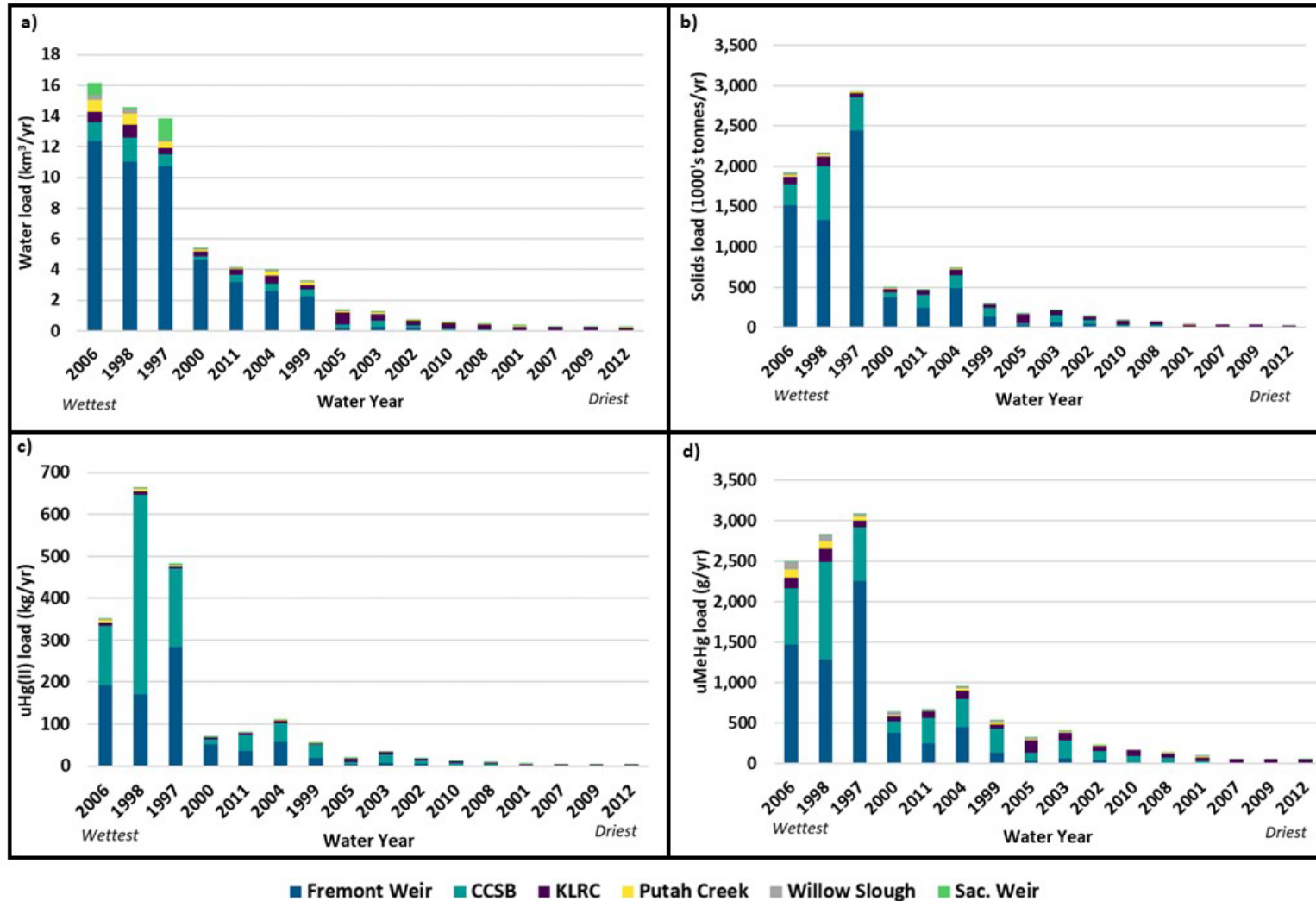
Figure Note: CCSB = Cache Creek Settling Basin, KLRC = Knights Landing Ridge Cut. Years are arranged from wettest (left) to driest (right)

Figure 4-14 Estimated Fractions of Tributary Loads of a) water, b) suspended sediment, c) uHg(II), and d) MeHg to the Yolo Bypass by water year
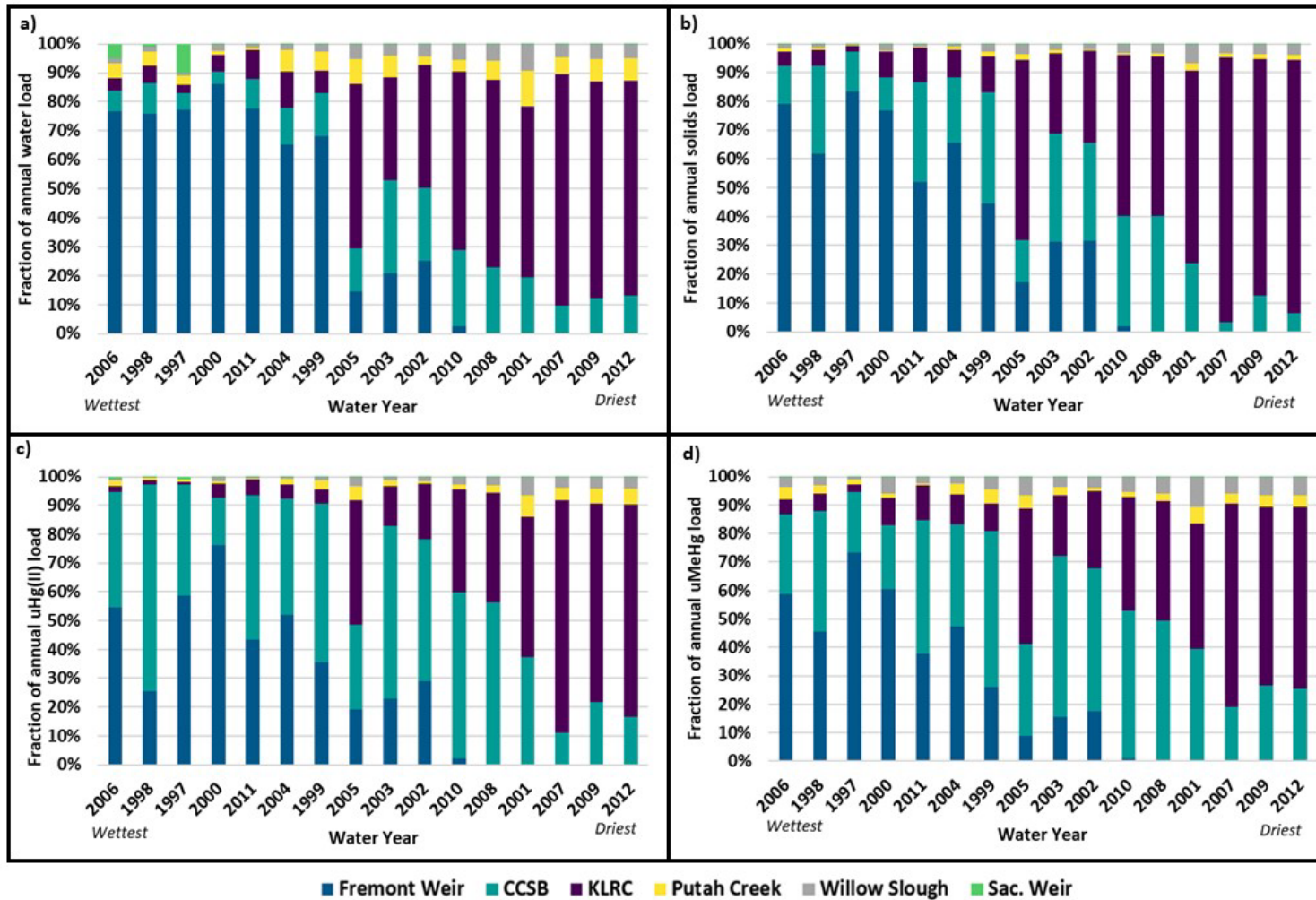
Figure Note: CCSB = Cache Creek Settling Basin, KLRC = Knights Landing Ridge Cut. Years are arranged from wettest (left) to driest (right)

Figure 4-15 Simulated and Observed Suspended Sediment Concentrations in Model Cell 42
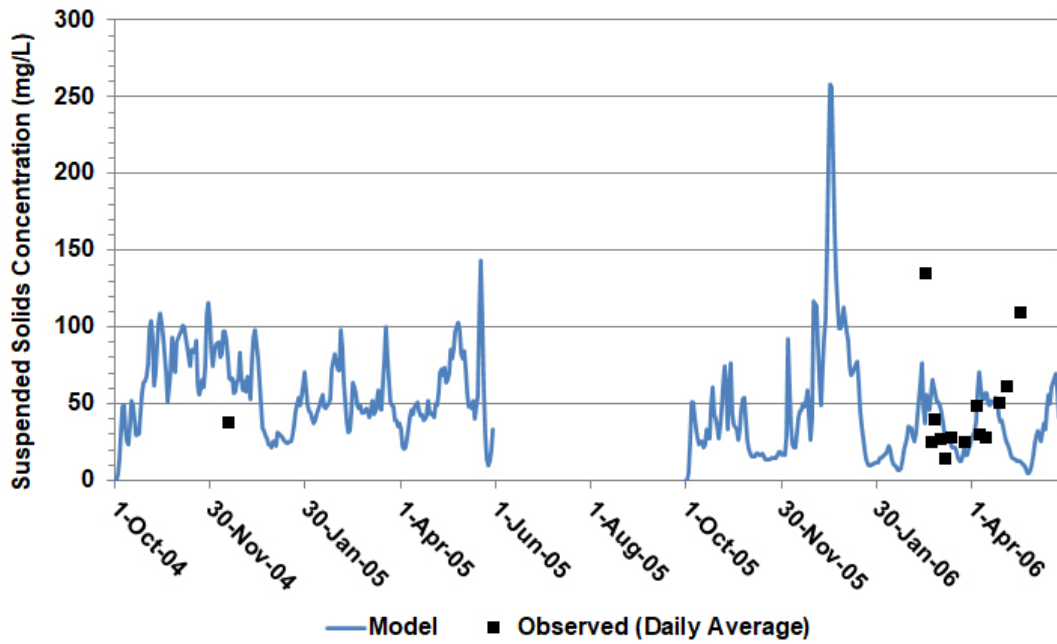
Figure Note: Cell 42 located in Toe Drain. See Figure 4-4 for location. Data from Louie and others (2008)

Figure 4-16 Simulated Yearly Ratios of Freshwater Export/Inflows for Suspended Sediments, Inorganic Hg and MeHg in the Yolo Bypass for Water Years 1997-2012
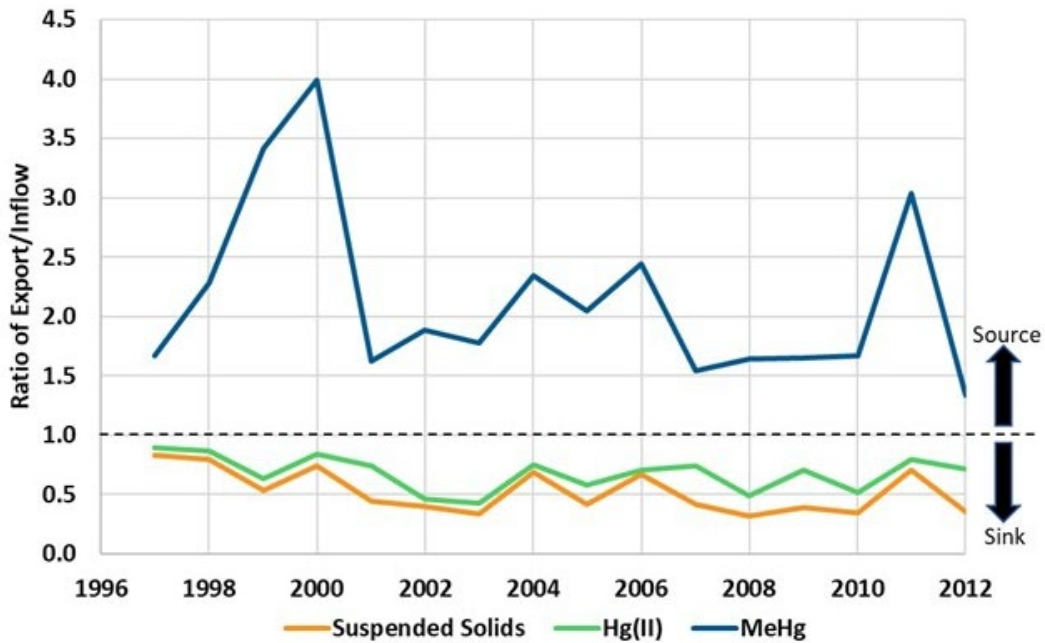
Figure Note : Values >1 = net source, Values < 1 = net sink.

Inorganic Hg Calibration

The largest estimated sources of inorganic Hg were from the Cache Creek Settling Basin and the Fremont Weir (Figure 4-12c), representing a combined 94% of the total tributary load for October 1996-May 2012. Among individual water years, Fremont Weir represented 0-76% of overall loading of inorganic Hg, while Cache Creek Settling Basin represented 11-72% (Figure 4-14d). These two sources had greater relative importance in wet years. In drier years, Knights Landing Ridge Cut was the largest estimated tributary source of inorganic Hg, up to ~80% of the annual total. Direct atmospheric loading of inorganic Hg was small, less than 3 percent of tributary loads for the simulation period. For the overall simulation period, the Yolo Bypass was a net trap for inorganic Hg (Figure 4-16), with 20 percent less exported at the stairsteps than was loaded from tributaries, (11-58% range among years). Trapping efficiency was generally greater in drier years.

For the simulation period, water column concentrations of uHg, upstream of the stairsteps, were available within the boundaries of 6 model cells upstream of the stairstep. An example of simulated and observed concentrations of uHg is shown in Figure 4-17 for a location in the Toe Drain (model cell 42). Additional plots for other sites with observations are provided in Technical Appendix G. Model simulations also reasonably reflected Hg concentrations in the surface of the sediment bed in the Yolo Bypass (Figure 4-18a), although porewater concentrations of inorganic Hg(II) were underestimated (Figure 4-18b).

Figure 4-17 **Simulated and Observed Concentrations of uHg(II) in Model Cell 42**
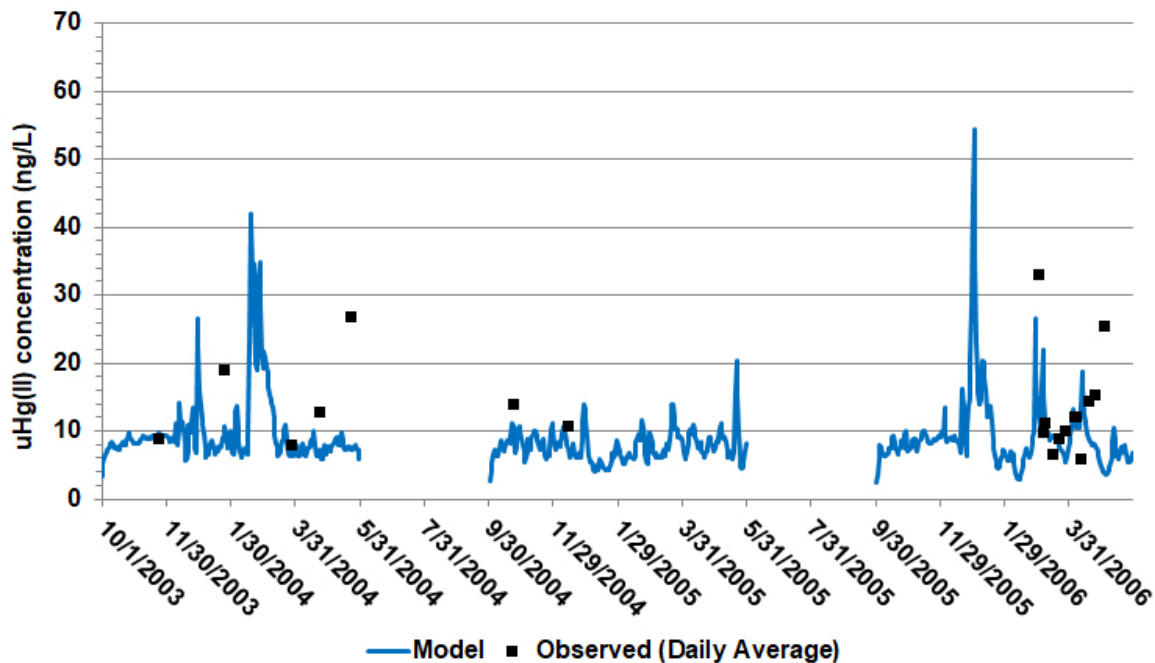
Figure Note: See Figure 4-4 for location. Data from Louie and others (2008), Larry Walker Associates (2005)

Figure 4-18 Simulated and Observed Concentrations of Hg and MeHg Surface Sediments, and Hg(II) and MeHg in Pore Waters in Yolo Bypass Model Cells
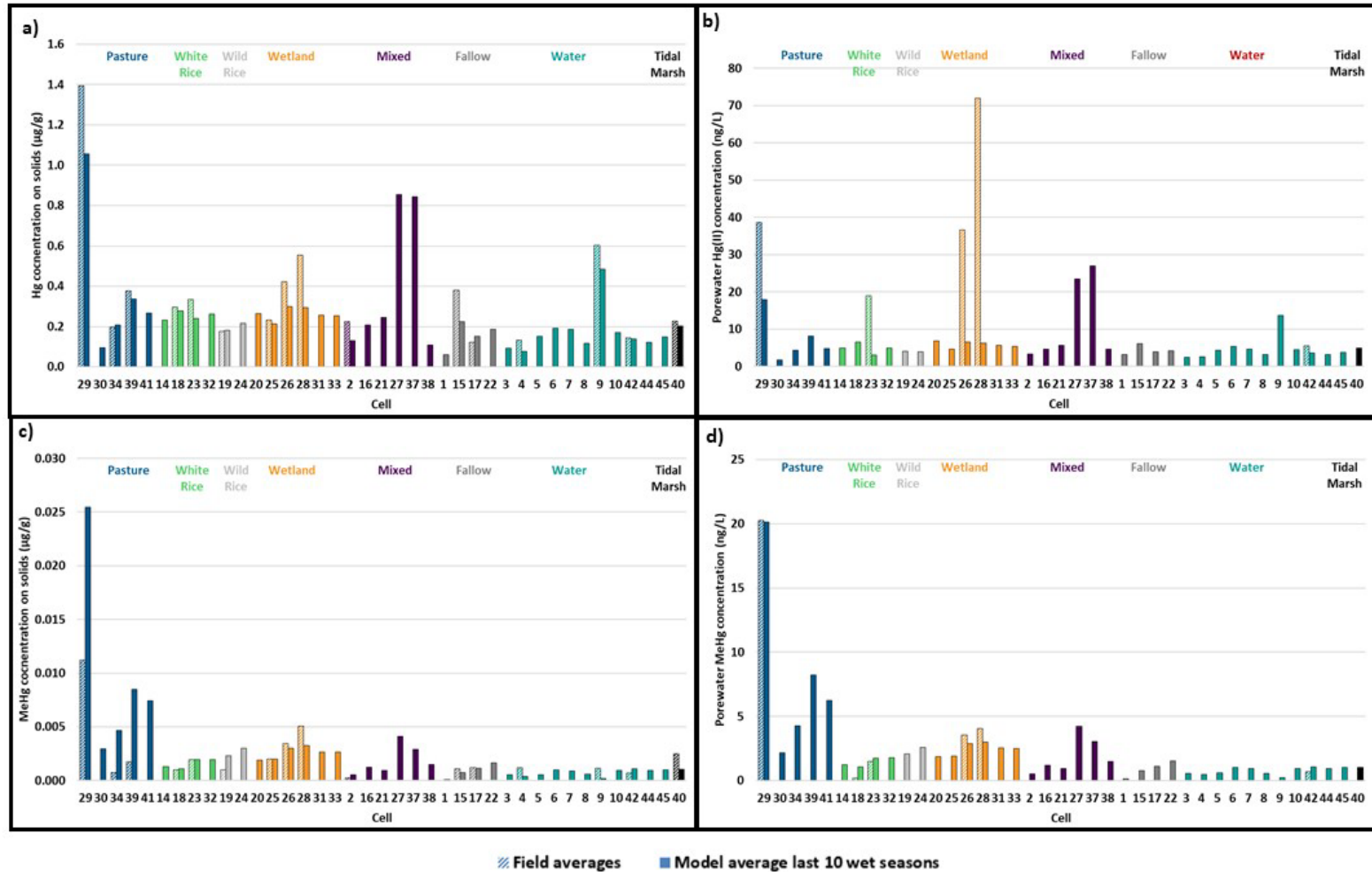
Figure Note: Model Values are averages for the last 10 wet seasons (Oct-May) of the simulation in the 2 cm thick surface layer. Observations are based on 2005-2016 (Oct-May only) data from DWR and Marvin-DiPasquale and others (2009). Cells are grouped by land use, indicated with colors. No observations were available for cells with no bars for field data.

MeHg Calibration Results

Overall, the Yolo Bypass (to the stairsteps) was simulated to be a net source for uMeHg, i.e. the export of MeHg exceeded tributary inputs. This occurred in simulations via sediment production and the associated flux to overlying waters. The average annual net load of MeHg as water passed through the Yolo Bypass (to the stairsteps) was roughly 1000 g/yr (Figure 4-19). The Yolo Bypass was a net source of uMeHg in every year simulated (export/tributary load >1.0 in all years (Figure 4-16). Atmospheric MeHg sources were small, less than 1% of the total supply. The largest tributary source of uMeHg for the overall simulation period was Fremont Weir (49% of the tributary supply) followed by Cache Creek Settling Basin (34%) (Figure 4-12d), representing a combined 83% of the total tributary uMeHg load for October 1996 - May 2012. Among individual water years, Fremont Weir represented 0-71% of tributary MeHg loading, while Cache Creek Settling Basin represented 19-57% (Figure 4-14d). Similar to tributary loading for sediments and inorganic Hg, the Fremont Weir and the Cache Creek Settling Basin had greater relative importance in wet years, while the Knights Landing Ridge Cut was more important in dry years, providing up to ~70% of the annual total MeHg supply from tributaries.

Figure 4-19 **Estimated Tributary and In-Situ uMeHg Loads to the Yolo Bypass**
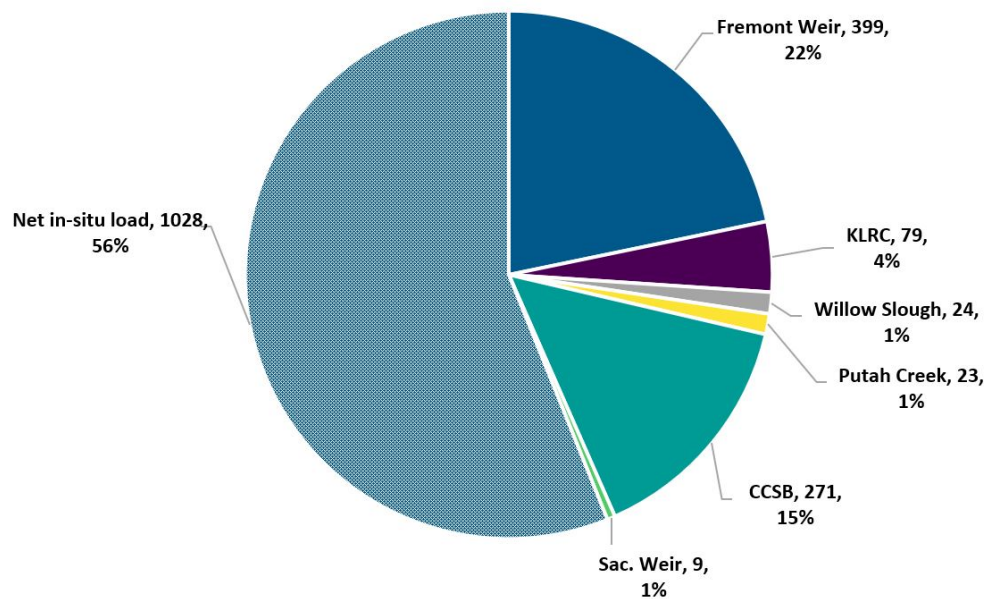
Figure Note: Values in labels are MeHg loads expressed as g/yr averages for October 1996-May 2012, and percentage of totals. KLRC = Knights Landing Ridge Cut, CCSB = Cache Creek Settling Basin, Sac. Weir = Sacramento Weir. Net in-situ load = outflows at the stairsteps minus tributary inflows.

Water column concentrations of uMeHg were available within the boundaries of 7 model cells upstream of the stairsteps for the simulation period. An example of simulated and observed concentrations of uHg is shown in Figure 4-20 for a cell in the Toe Drain (cell 42). Additional plots for other sites with observations of MeHg concentrations in water are provided in Technical Appendix G. Model simulations also reasonably reflected MeHg concentrations in surface sediments and porewater in the Yolo Bypass (Figure 4-18c and d).

Figure 4-20 Simulated and Observed uMeHg Concentrations in Model Cell 42
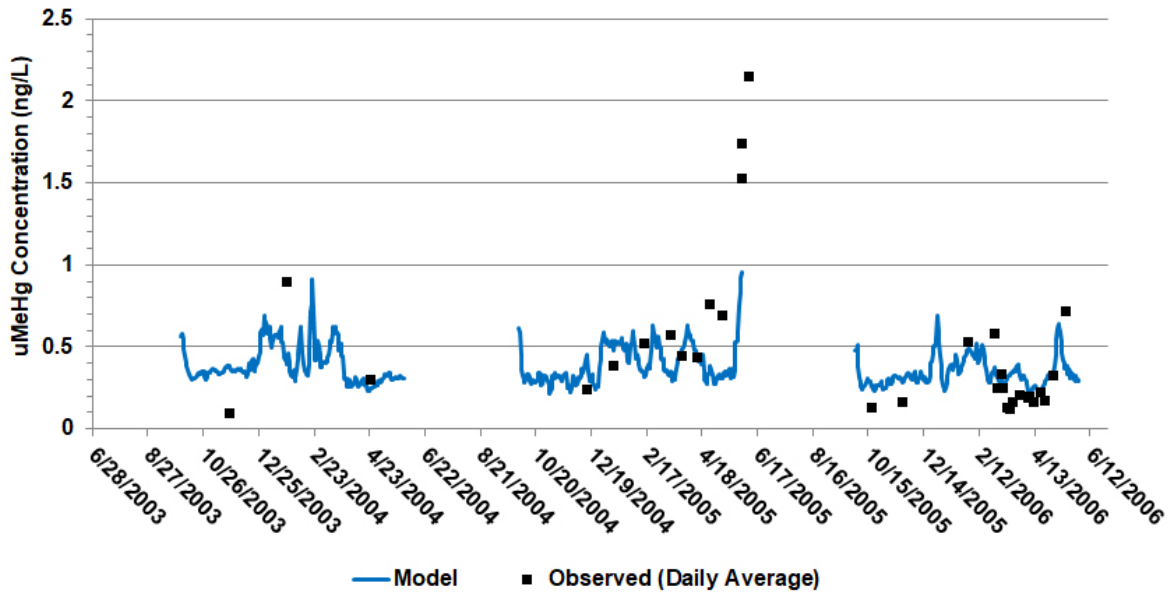
Figure Note: See Figure 4-4 for location. Data from Foe and others (2008) and Larry Walker Associates (2005).

Comparisons to Previous Studies

As a check on the performance of the model, calibration results were compared to other studies where possible. Given that different studies have different purposes and usually involve different time periods and methods, it was not expected that results would be directly comparable or identical. The purpose of the comparison was to compare in terms of general magnitudes and trends (e.g. relative importance). Examples are provided below for suspended sediment inflows and outflows (Figure 4-21), uHg tributary loads (Figure 4-22) and uMeHg tributary loads (Figure 4-23).

Figure 4-21 Comparison of Estimated Tributary Suspended Sediment Loads and Export for the Yolo Bypass, from Springborn and others (2011) and this study
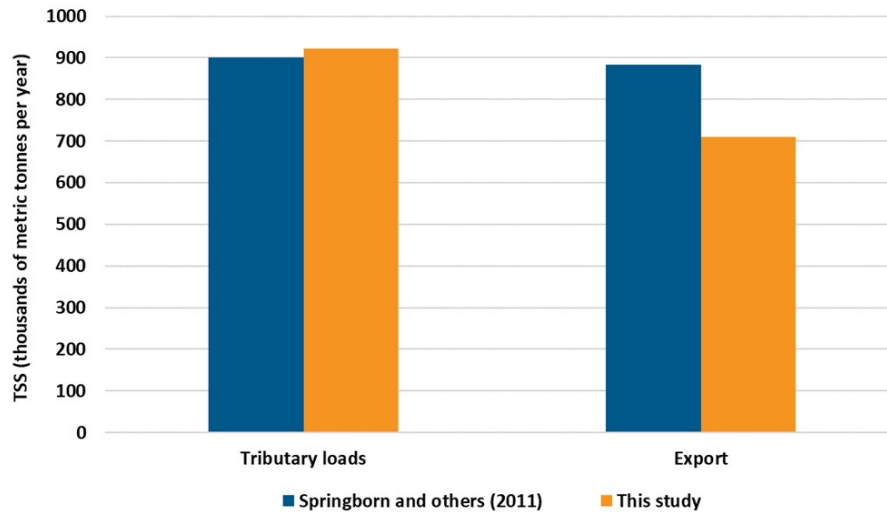
Figure Note: Tributary loads represent the sum of the Fremont Weir, the Sacramento Weir, Knight's Landing Ridge Cut, Cache Creek Settling Basin (low flow channel and overflow weir), Willow Slough, and Putah Creek. Export for this study was at stairsteps.

Figure 4-22 Comparison of Estimated Tributary uHg loads to the Yolo Bypass (1997-2003) from Springborn and others (2011) and this study
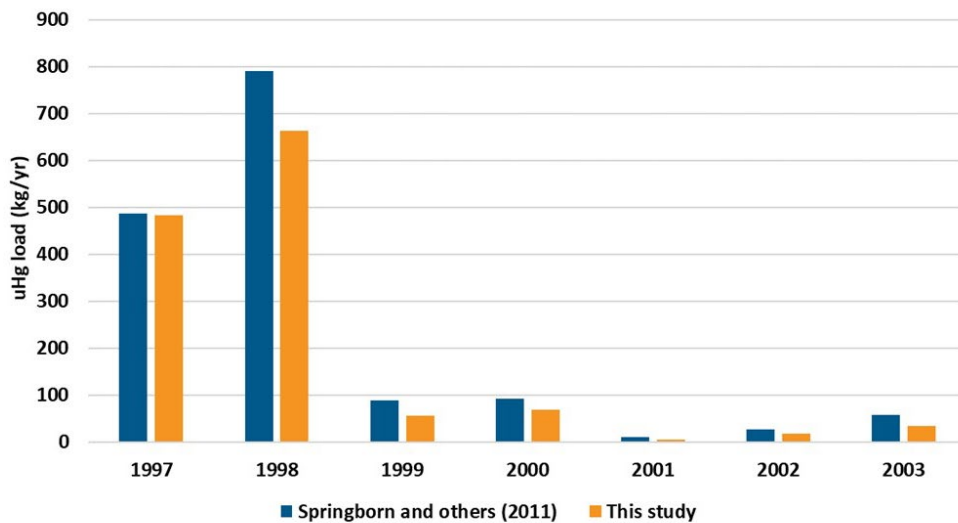
Figure Note: Tributary loads represent the sum of the Fremont Weir, the Sacramento Weir, Knight's Landing Ridge Cut, Cache Creek Settling Basin (low flow channel and overflow weir), Willow Slough, and Putah Creek.

Figure 4-23 Comparison of Estimated Tributary MeHg Loads to the Yolo Bypass for Water Years 2000-2003, from Wood and others (2011) and this study
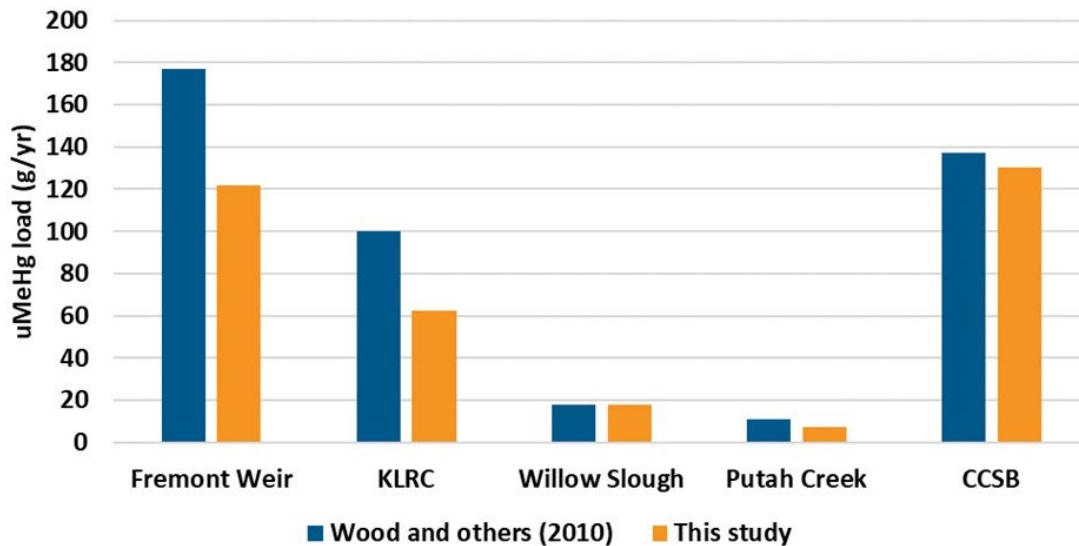
Sensitivity Scenario Results

Results for the nine scenario simulations developed by DWR and Regional Board staff (Table 4-4) are summarized in Table 4-5, in terms of the effect on the downstream export of MeHg at the stairsteps, averaged for water years 1998-2012. In some cases, the results were unexpected, and it became apparent that interpreting the simulations simply based on the modeled percent change in uMeHg export could be misleading. Overall, the simulations reduced the predicted export of uMeHg at the stairstep from less than 5% up to roughly 20%. The largest benefit was associated with the simulation reducing the efficiency of converting Hg(II) in Yolo Bypass sediments into MeHg by 50% (Simulation #8). This simulation reduced the gross production of MeHg in Yolo Bypass sediments by ~50%. The average annual net flux of MeHg from sediments to water declined by about 1/3 for water years 1998-2012. Given that the portion of the overall MeHg supply to the Yolo Bypass from tributaries was unaltered during this simulation, MeHg export at the stairsteps declined less for this simulation, roughly 20%, than the MeHg load from sediments to water.

Simulations #6 and #7, which reduced uMeHg concentrations in inflows from the CCSB and the Fremont Weir respectively, reduced MeHg export by 5-10%. Results from some of these simulations had less effect than anticipated. For example, reducing the load of suspended sediments from the CCSB (and associated Hg(II) and MeHg) had a small effect on MeHg concentrations and export in the Yolo Bypass, despite CCSB being an important source of Hg(II) in the Yolo Bypass budget. A closer examination of the simulation indicated that the 16-year simulation may not have allowed sufficient time for the effects of this simulation to be fully realized.

A simulation (#9) that reduced the supply of vegetation solids to the sediment bed after die-off by 50% produced less than a 5% decline in MeHg export. This was surprising given the results of a complementary simulation that removed all vegetation from, leading to a predicted decline of roughly 60% in net MeHg production in Yolo Bypass sediments (Figure 4-24).

Table 4-5 Summary of Simulated Effects of Sensitivity Analyses for MeHg Export from the Yolo Bypass at Stairsteps.

Category	Change to Model Inputs	Change in MeHg Export	Interpretation
Particle related	1 Reduce CCSB TSS concentrations 50%	Very small decline (<5%) ⬇	The modeled decline in MeHg export from the Yolo Bypass was less than expected. This may have been related to the time required for effects to be fully evident, which may have been longer than the 16-year simulation. The decline in sediment loading slowed sedimentation rates which affected how quickly Yolo Bypass sediments responded to changes in Hg loading. It is expected that a greater decline would have occurred if the simulation could be extended for a longer simulation period.
	2 Reduce Fremont Weir TSS concentrations 50%	Minimal change ↔	Hg concentrations entering the Yolo Bypass via the Fremont Weir were lower than the average for all tributaries in simulations. Fremont Weir suspended sediments tended to "dilute" the average Hg concentrations of sediments entering the Bypass from all tributaries. Less supply of sediments over Fremont weir therefore had competing influences: (1) reduced load of Hg associated with particles, versus (2) less "dilution" of other particles entering the Bypass from other tributaries with higher Hg concentrations. The net result in the simulation was almost no change in sediment Hg concentrations and MeHg export.
External inorganic Hg loads	3 Reduce CCSB inorganic Hg concentration 50%	Very small decline (<5%) ⬇	The response was less than expected. Reasons had not been clearly identified at the time of publication of this report.
	4 Reduce Fremont Weir inorganic Hg concentrations 50%	Very small decline (<5%) ⬇	The response was less than expected. Reasons had not been clearly identified at the time of publication of this report.
	5 Reduce atmospheric wet Hg(II) deposition 50%	Minimal change ↔	Atmospheric Hg deposition represented less than 3% of the overall external load of inorganic Hg.
External MeHg loads	6 Reduce CCSB MeHg concentrations 50%	Modest decline (5-10%) ⬇	CCSB supplied about 15% of the overall MeHg load to the Yolo Bypass in simulations (external plus internal loads). Reducing this load by 50% had a moderate effect on MeHg export at the downstream end of the system.
	7 Reduce Fremont Weir MeHg concentrations 50%	Modest decline (5-10%) ⬇	Fremont Weir supplied about 20% of the overall MeHg load to the Yolo Bypass in simulations (external plus internal loads). Reducing this load by 50% had a moderate effect on MeHg export at the downstream end of the system.
Internal MeHg loads	8 Reduce methylation rate constants in all Yolo Bypass cells 50%	Moderate decline (~20%) ⬇	Yolo Bypass sediments supplied about half of the overall MeHg load in simulations (external + internal). This simulation reduced MeHg production in Bypass sediments by roughly half, reducing the overall load of MeHg to the Yolo Bypass (internal + external sources) by about 20%

Category	Change to Model Inputs	Change in MeHg Export	Interpretation
Vegetation	9　Reduce vegetation biomass load to sediments 50%	Very small declne (<5%) ⬇	This simulation reduced the supply of organic matter to Yolo Bypass sediments. Gross methylation declined about 20%, but microbial demethylation also declined. Net methylation declined about 10%. Reduced upward flux of MeHg from sediments to water was partly offset by reduced settling of MeHg from water to sediments, because of less settling sediments. Reduced vegetation inputs could reduce MeHg loads and export from the Yolo Bypass more than suggested by this simulation. See discussion of results.

Figure 4-24 Simulated Effect of Removing all Vegetation on Simulated Net MeHg Production in the Yolo Bypass
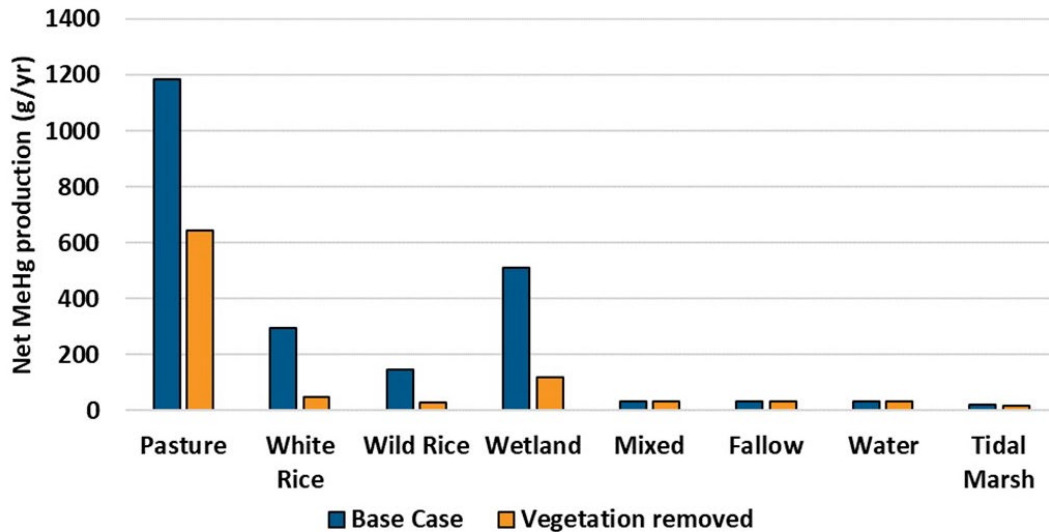
Figure Note: Net MeHg production = Sediment methylation minus sediment demethylation. Fluxes are averages above stairsteps for October 1997 – May 2012. Overall reduction in net methylation for Yolo Bypass sediments was nearly 60%. Little change occurred for net methylation in model cells without vegetation (Water channels, mixed, fallow).

Discussion

A model analysis was carried out to simulate Hg cycling in water and sediments in the Yolo Bypass, with an emphasis on sources of MeHg. It was clear prior to the model analysis that flow and sediment transport would be important processes. The model framework therefore included components for hydrology, sediment transport, inorganic Hg and MeHg in water and surface sediments. The modeling was carried out at a relatively coarse spatial resolution, representing Yolo Bypass with 47 cells (Figure 4-4). This reflected a combination of the model capabilities, data limitations and uncertainties regarding Hg cycling, such as the influence of different land use types and effects of soil wetting and drying. Increased data and knowledge of Hg cycling would be needed to warrant a higher special resolution analysis in the Yolo Bypass. Additional information is provided below.

Model Fit to Observations

Data were limited but sufficient to carry out a model calibration for suspended sediments, uHg and uMeHg for the period October 1996-2012. Data for fHg and fMeHg were included in the model calibration but were only available for 2 cells during the model calibration period (n=14 for fHg, n=9 for fMeHg) and were insufficient for calibration purposes. PEST++ significantly improved the preliminary manual calibration, reducing the overall misfit between observations and the simulation by about half. The final model calibration reasonably captured the magnitude and variability of observations in the water column (e.g.Figure 4-16, Figure 4-17, Figure 4-18). In the surface layer of the sediment bed (0-2 cm), the model also reasonable matched observed average concentrations of Hg and MeHg on solids, and pore

water MeHg concentrations (Figure 4-20). Observed pore water Hg(II) concentrations were underestimated with the model. As mentioned earlier, sediment observations were combined from 2005-2016 for Hg and MeHg due to limited data availability. This assumed no systematic change in Hg concentrations during this period. It also does not address seasonal variability that may occur for MeHg concentrations.

Simulated Hg and MeHg Fluxes

The largest estimated source of water to Yolo Bypass for the calibration period from October 1996-May 2012 was Fremont Weir (71%, Figure 4-12a). The largest external sources of suspended sediment, Hg(II) and MeHg were Fremont Weir and CCSB (Figure 4-12b,c,d). Cache Creek Settling Basin was the single largest estimated source of Hg(II) to the Yolo Bypass (51% for the overall simulation). A detailed examination the model results raised the possibility however that the Hg(II) load from the Cache Creek Settling Basin could be overestimated under high flow conditions. There were flow events during the simulation period that exceeded the flows encountered during actual field sampling programs. This meant that the regression used to estimate inorganic Hg concentrations on the basis of flow had to be applied on some occasions to conditions outside the observed range. This issue is not interpreted to put into question whether Cache Creek Settling Basin is an important source of inorganic Hg, rather it is a question of how important, and under what circumstances.

The 16-year simulation period spanned a wide range of hydrologic conditions ranging from wet to critically dry years (Table 4-2). Estimated flows from October - May ranged 65X among simulated years, based on TUFLOW modeling. In wet years, most of the freshwater load to Yolo Bypass was from Fremont Weir, while Knights Landing Ridge Cut was more important in dry years (Figure 4-13a, Figure 4-14a). Estimated tributary loads of suspended sediments, Hg(II) and MeHg also varied by more than an order of magnitude among years, strongly influenced by hydrology. Fremont Weir and the Cache Creek Settling Basin were the largest tributary sources of Hg(II) and MeHg in wet years (Figure 4-13c,d, Figure 4-14c,d). Knights Landing Ridge Cut was a secondary source of suspended sediment, Hg(II) and MeHg in wet years but became more important (in relative terms) in dry years, representing the largest individual tributary source of water, suspended sediment, Hg(II) and MeHg in some dry years.

The Yolo Bypass (to the stairsteps) was simulated to be a net trap for suspended sediments and uHg, with roughly 30% less outflow of suspended sediments, and 20% less outflow of Hg(II) at the stairsteps than loaded from tributaries. These model results are averages for the calibration period from October 1996-May 2012. For the same period, the Yolo Bypass (to the stairsteps) was simulated to be a net source for uMeHg, via sediment production and the associated flux to overlying waters. The export of MeHg at the stairsteps was roughly twice the tributary load. The net load of MeHg to water passing through the Yolo Bypass, i.e. the difference between outflow and inflow fluxes, was approximately 1000 g/yr (Figure 4-19). Most of this net load occurred during the wet season, when more of the Yolo Bypass was flooded, and flows were greater. This loading rate is comparable to net MeHg loads based on field estimates of flows and concentrations at major inflow and outflow locations in the Yolo Bypass, carried out by DWR from January 11, 2017 to April 25, 2017 (Chapter 3). The average net MeHg load from the 2017 study was 14.1 g/day (difference between outflow and inflow). The Yolo Bypass model simulations in this study did not include 2017, so direct comparisons cannot be made. However, the model average for the same date range (January 11 – April 25), for years classified as wet in Table 4-2 (2017 was a wet year), was 18 g/day (range 11-32 g/day among these wet years).

The model estimates of MeHg loading in the Yolo Bypass also compared well with the The Delta Mercury Control Program (DMCP) estimate for water years 2000-2003. Wood and others (2010) estimated a total MeHg load of 1068 g/yr to the Yolo Bypass for this period. This included 604 g/yr of loading as water passed through the Yolo Bypass, from open waters, wetlands, agricultural drainage, atmospheric deposition and NPDES facilities. The model difference between outflow and inflow fluxes for the same period was 618 g/yr. The model flux from sediments to water would be slightly greater (some of the flux from surface sediments would be photodegraded rather than exported downstream). Foe and others (2008), also estimated the Yolo Bypass to be a net source of MeHg using inflow and outflow data from water year 2006 (a wet year).

The net load of MeHg to water passing through the Yolo Bypass was influenced in simulations primarily by the net flux from sediments to overlying water, and photodegradation which removed MeHg. As a result, the flux of MeHg from sediments to water was larger than the difference between inflowing and outflowing fluxes, and is estimated to be on the order of 1200 g/yr.

Key Processes

The model analysis confirmed the key roles of hydrodynamics on Hg cycling and MeHg supply in the Delta. Increased flow led to increased tributary loads (Figure 4-13). The supply of water, suspended sediment, Hg(II) and MeHg all varied by an order of magnitude or more among the years simulated. The relative importance of tributaries also varied widely among years, depending on the hydrology, as discussed above. Flow events also led to a high degree of short term variability in simulated fluxes and concentrations of suspended sediment, Hg(II) and MeHg. The high temporal variability at different time scales, e.g. events and annual averages, has important implications when using available data to set targets for MeHg loading, and when monitoring for compliance.

The Yolo Bypass also has several other features with the potential to affect MeHg supply, including vegetation, agriculture, wetlands, excess inorganic Hg from historical mining upstream, and large tracts of land experiencing wetting and drying periods. Vegetation was an important factor affecting MeHg production in simulations. The treatment of vegetation in D-MCM is considered coarse and conceptually could be revisited. For example, after vegetation senesces in the model, vegetation solids are first delivered to the water column, where exchange can occur with surface waters. The vegetation solids then settle quickly and mix into the surface layer of the sediment bed. Effectively the vegetation supplies carbon and stimulates methylation in surface sediments. In reality, vegetation may remain sufficiently intact initially after senescence to be a distinct compartment that rests on the sediment surface where decomposition occurs. This could lead to differences in the effects of vegetation on methylation and MeHg supply to the water column, relative to the current model construct. Overall though, the model analysis suggest that vegetation has a strong influence on MeHg production in the Yolo Bypass. In simulations this effect was primarily via the additional supply of organic matter in simulations, consistent with experimental work described in Chapter 3 and studies by the US Geological Survey (e.g. Marvin-DiPasquale and others, 2014)

The D-MCM model is also constructed on the basis that higher concentrations of dissolved Hg(II) available for methylation lead to higher MeHg production. Thus areas with vegetation and higher Hg(II) concentrations in surface sediments tended to have higher MeHg concentrations (e.g. cell 29, a pasture cell in Figure 4-18). Other pasture cells with lower Hg(II) concentrations also had vegetation but lower

MeHg concentrations in surface sediments (e.g. cells 34 and 39), supporting the assumption that Hg(II) concentrations affect MeHg production, in addition to the presence of vegetation.

While wetting and drying cycles have been shown to affect MeHg production in other settings (e.g. Gilmour and others, 2004), insufficient data were available to assess this issue for the Yolo Bypass. Finally, it is important to note that large tributary sources of uHg and uMeHg do not necessarily lead to higher concentrations within the Yolo Bypass. The combination of a high flow and low concentration for a tributary could lead to a source being large relative to other tributary inputs but acting to dilute concentrations in receiving waters. If, for example, measures were taken that reduced the flow of a source with lower than the average MeHg concentration for tributaries (Fremont Weir), it might not lead to lower concentrations in Bypass waters. Additional simulations would be needed to explore this concept, but the key point is that it is important to consider concentrations as well as loads for tributaries when evaluating remedial options.

Sensitivity Scenarios

The nine sensitivity scenarios developed by DWR and Regional Board staff (Table 4-4, Table 4-5) reduced the predicted export of uMeHg at the stairsteps from less than 5% up to roughly 20%. Given that all simulations vary a specific input (e.g. tributary concentration or reaction rate constant) by 50%, the results reflect a system with multiple sources of MeHg. The simulation that reduced the gross production in Yolo Bypass sediments by half, and the net load of MeHg from surface sediments to water by 1/3, reduced MeHg export by less, about 20%, because other sources of MeHg were not changed. Regarding options to reduce the supply of MeHg from sediments to water within Yolo Bypass, the sensitivity analysis suggests that measures reducing the production of MeHg in Bypass surface sediments could be beneficial, but the challenge is identifying options that are practical in a system with a surface area exceeding 200 km^2. The model analysis, experimental studies described in Chapter 3, and previous work by the US Geological Survey collectively indicate that vegetation promotes MeHg production, at least partly by supplying labile carbon.

The net flux of MeHg from surface sediments to water included three components in the simulation: diffusion, resuspension, and settling. Diffusion and resuspension of MeHg tend to move MeHg from surface sediments to overlying water, while settling at least partially offsets the upward fluxes. Some sensitivity scenarios affected the relative balance of these three terms affecting the net load to water. For example, removing vegetation affected not just the production of MeHg, but also settling and sedimentation in simulations. Reducing tributary loads of suspended sediments reduced not just the sediment load, but also the supply of Hg(II) and MeHg, and affected sedimentation rates in the Yolo Bypass. Sedimentation rates in turn affect how quickly the surface sediment layer responds to changes in conditions, e.g. how quickly will Hg(II) and MeHg concentrations decline if loading declines? The model analysis carried out was capable of providing some initial insights into the response of the system to perturbations but in situations involving changes to the balance of multiple competing influences on MeHg supply, reliable quantification of these changes would require a better understanding and more realistic model representation of some key processes. Additional discussion is provided below.

Conclusions

An existing model of Hg cycling was combined with outputs from a hydrodynamic model and applied to Yolo Bypass waters and surface sediments. The model calibration reasonably reflected observations for

suspended sediments, Hg and MeHg concentrations in the water column and surface sediments and compared reasonably with some load estimates from other published studies. The use of parameter estimation software (PEST++) significantly improved the model fit to observations, reducing the error in the preliminary manual calibration by half. The largest external sources of sediment, Hg and MeHg for the overall 16-year simulation were Fremont Weir and CCSB, especially in wet years. KLRC was more important in dry years. Sediment production of MeHg in the Yolo Bypass and supply to overlying waters was important. The simulated export of MeHg at the stairsteps was roughly twice the inflowing tributary supply. In contrast to MeHg, less suspended and sediments and Hg(II) were exported than loaded from tributaries for the 16 year simulation period, i.e. the Yolo Bypass (to the stairsteps) was a net trap for these constituents. Vegetation and inorganic Hg concentrations both affected MeHg production in simulations. The vegetation effect was primarily via the additional supply of organic matter. Fluxes of inorganic Hg and MeHg varied by an order of magnitude or more among the years simulated, which spanned a wide range of hydrologic conditions. This has implications in terms of developing TMDL target MeHg loads and associated monitoring programs designed to determine if TMDL targets are met. A multi-year perspective is needed as well as the ability to capture short term dynamics.

Data/Knowledge Gaps and Next Steps

Data gaps: Available field data were limited in terms of characterizing boundary inflow loads, and concentrations within the Yolo Bypass, for suspended sediments, Hg and MeHg. This issue was magnified by the dynamic nature of hydrology in the Bypass, leading to a high degree of temporal and spatial variability that could not be captured with limited sampling. This constrains the current ability to quantify mercury cycling in the Yolo Bypass to a coarser perspective rather than a tightly quantified analysis. Additional data are needed to better characterize inflow loads and within-Bypass conditions for a range of hydrologic conditions and a range of years. A multi-year perspective is needed as well as the ability to capture short term dynamics. These data include measurements of inorganic Hg and MeHg in filtered, unfiltered and particulate phases in the water column and sediments, as well as ancillary data such as water chemistry and sediment characterization. Manual sampling and analysis for suspended sediments and Hg can be labor intensive and costly. Alternative options to obtain higher-frequency data should be considered, e.g. surrogates that can be sampled continuously (e.g. turbidity for suspended solids) and the use of automatic samplers for Hg.

Knowledge gaps: There are scientific gaps that also contributed to uncertainty in the model analysis, including:

- How does vegetation influence MeHg cycling and production? Better information is needed regarding the magnitude and timing of the supply of carbon and subsequent decomposition that supports MeHg production, for different land uses.
- Is the availability (for methylation) of Hg(II) contamination from legacy upstream mining similar to the availability of other sources of Hg(II)?
- Is mercury on suspended and bed sediments readily exchangeable or are some sources of inorganic Hg more important that others, in terms of supplying MeHg production? The analysis carried out in this study assumed that Hg on solids is readily exchangeable with the dissolved phase. Closely related to this question is the need for more data on filtered and particulate concentrations of inorganic Hg and MeHg in tributaries and Yolo Bypass waters.
- What is the influence of wetting and drying cycles? Wetting and drying is known to affect MeHg production. Existing data were insufficient to examine this issue in the Yolo Bypass. Field data in

surface sediments and surface waters in areas with different wetting and drying patterns would be useful, along with ancillary water chemistry (e.g. DOC, pH, redox, temperature).

Modeling Scope:

- ○ <u>MeHg in fish</u>: Given that fish and shellfish MeHg levels are the ultimate end point of interest, the model analysis could be extended to include a food web and bioaccumulation component.
- ○ <u>Management Scenarios</u>: Further testing of model scenarios would be beneficial. Discussions of results to-date and potential scenarios that could help identify practical solutions to reduce MeHg supply should continue.
- ○ <u>Climate change</u> is altering conditions in the Delta that have the potential to affect Hg cycling and bioaccumulation (see for example, Dettinger and others, 2016 and Chapter 6). This issue should be incorporated into future assessments.
- ○ <u>Uncertainty:</u> The continued used of PEST++ would be beneficial to help quantify uncertainty and identify the types of data that would most effectively reduce uncertainty in model predictions is recommended.

- **Model Development:**
  - ○ D-MCM was an appropriate tool to use for the study reported here, given the level of data available and the state of knowledge of Hg cycling. A more realistic model analysis could be carried out using a single model that represents hydrodynamics, sediment transport, water quality and Hg cycling, capable of high spatial resolution in 2D. This is beyond the capabilities of D-MCM (or any other 2D or 3D model currently). D-MCM is not constructed in a manner amenable to such enhancements. Consider integrating Hg into an existing high-resolution model that already simulates hydrodynamics, sediment transport and water quality. This could involve using one model for the Yolo Bypass and another (DSM2-Hg) for the Delta, or a single model for the Delta and the Yolo Bypass. Preferably the software would be publicly available software.
  - ○ The representation of vegetation in D-MCM was coarse in terms of capturing the effects of vegetation on methylation via carbon supply and decomposition. A more realistic representation of vegetation would allow better simulations of remedial options involving vegetation.
  - ○ A supporting field program (see comments above) would be needed to take advantage of the increased model capability.

References

Atkeson, T.D., D.M. Axelrad, C.D. Pollman, and G.J. Keeler (2003) Integrating Atmospheric mercury Deposition with Aquatic Cycling in the Florida Everglades: An Approach for Conducting a Total Maximum Daily Load Analysis for an Atmospherically Derived Pollutant. Integrated Summary, Final Report.

CDEC (2020) http://cdec.water.ca.gov/reportapp/javareports?name=WSIHIST, Accessed July 20, 2020.

Department of Water Resources 2010. Fact Sheet, Sacramento River Flood Control Project Weirs and Flood Relief Structures. December 2010. Available at https://www.waterboards.ca.gov/waterrights/water_issues/programs/bay_delta/california_waterfix/exhibits/docs/STCDA%20et%20al/scda_54.pdf, Accessed: November 25, 2019.

Department of Water Resources 2015. Open Water Workgroup Progress Report. Delta Mercury Control Program. Prepared by the Open Water Workgroup and the Open Water Technical Group. Submitted to the Central Valley Regional Water Quality Control Board, Region 5, October 20, 2015. 203 pages. Avalable at: https://www.waterboards.ca.gov/centralvalley/water_issues/tmdl/central_valley_projects/delta_hg/control_studies/deltahg_oct2015pr_openwater.pdf. Accessed January 20, 2020.

Department of Water Resources (2020) Statewide Crop Mapping. Available at: https://data.cnra.ca.gov/dataset/statewide-crop-mapping). Accessed August 17, 2020.

Doherty, J., and Hunt, R.J., 2009, Two statistics for evaluating parameter identifiability and error reduction. Journal of Hydrology 366: 119-127, doi:10.1016/j.jhydrol.2008.12.018

EPRI (2013) Dynamic mercury Cycling Model for Windows 7/Vista/XP. D-MCM Version 4.0. User's Guide and Technical Reference. December 2013. Product ID 3002002518

Foe C, Louie S, and Bosworth D. (2008) Task 2. Methyl Mercury Concentrations and Loads in the Central Valley and Freshwater Delta, August 2008. In Transport, Cycling, and Fate of Mercury and Monomethyl Mercury in the San Francisco Delta and Tributaries: An Integrated Mass Balance Assessment Approach. CALFED Mercury Project Final Report, September 15, 2008.

Gilmour, C., D. Krabbenhoft, W. Orem and G. Aiken. Appendix 2B-1: Influence of Drying and Rewetting on Mercury and Sulfur Cycling in Everglades and STA Soils. Aquatic Cycling of Mercury in the Everglades (ACME) Group Preliminary Drew/Rewet Experiments (2/02 – 1/03). 2004 Everglades Consolidated Report.

Harris RC, Pollman C, Beals D, Hutchinson D. 2003a. *Modeling Mercury Cycling and Bioaccumulation in Everglades Marshes with the Everglades Mercury Cycling Model (E-MCM)*. Final Report. Prepared for the Florida Department of Environmental Protection and South Florida Water Management District. June 2003

Harris RC, Pollman C, Hutchinson D. 2003b. Wisconsin Pilot Mercury Total Maximum Daily Load (TMDL) Study: Application of the Dynamic Mercury Cycling Model (D-MCM) to Devil's Lake, Wisconsin. Submitted to the United States Environmental Protection Agency Office of Wetlands Oceans and Watersheds. December 2003

Harris RC, Rudd JWM, Amyot M, Babiarz C, Beaty KG, Blanchfield PJ, Bodaly RA, Branfireun BA, Gilmour CC, Graydon JA, Heyes A, Hintelmann H, Hurley JP, Kelly CA, Krabbenhoft DP, Lindberg SE, Mason RP, Paterson MJ, Podemski CL, Robinson A, Sandilands KA, Southworth GR, St. Louis VL, Tate MT. 2007. "Whole-ecosystem study shows rapid fish-mercury response to changes in mercury deposition." Proceedings of the National Academy of Sciences of the United States of America. Volume 104, Issue 42, Pages 16586–16591

Harris RC, Pollman C, Hutchinson D, Landing W, Axelrad D, Morey S L, Dukhovskoy D, and Vijayaraghavan K. 2012a. A Screening Model Analysis of Mercury Sources, Fate and Bioaccumulation in the Gulf of Mexico. Environmental Research, Volume 119, Pages 53-63

Harris RC, Gilmour CC, Beals C. 2012b. Effects of Climate Change on Mercury Cycling and Bioaccumulation in the Great Lakes Region. Great Lakes Atmospheric Deposition (GLAD) Program 2009 GLAD Program Contract 09-05. Prepared for the U.S. Environmental Protection Agency. October 2012

Harris RC, Hutchinson D, Beals C, Beals D, Engstrom D. 2015. Great Lakes Restoration Effects on Fish Mercury Levels. Great Lakes Restoration Initiative (GLRI). Report for Grant Agreement No. GL-00E00691-0. June 2015. Prepared for the U.S. Environmental Protection Agency

Hudson RJM, Gherini, SA, Watras CJ, Porcella, DB. 1994. Modeling the Biogeochemical Cycle of Mercury in Lakes: The Mercury Cycling Model (MCM) and Its Application to the MTL Study Lakes. In Mercury Pollution - Integration and Synthesis. C.J. Watras and J.W. Huckabee (Eds.). CRC Press Inc. Lewis Publishers

Heim, WA, Newman A, Byington A, Hughes B, Stephenson M. 2010. Spatial Distribution of Total Mercury in the Yolo Bypass: Implications for Land Use Management of Mercury Contaminated Floodplains. May 2010. Final report submitted to Chris Foe and the Central Valley Regional Water Quality Control Board.

Howitt, R., MacEwan, D., Garnache, C., Azuara, J.M., Marchand, P., Brown, D., Six, J., Lee, J. 2013. Final Report. Agricultural and Economic Impacts of Yolo Bypass Fish Habitat Proposals. Prepared for Yolo County. April 2013.

Hudson FJM, Gherini SA, Watras CJ, Porcella DB, 1994. Modeling the Biogeochemical Cycle of Mercury in Lakes; The Mercury Cycling Model (MCM) and its Application to the MTL Study Lakes. In: Watras, C.J., Huckabee, J.W. (Eds.) Mercury Pollution-Integration and Synthesis CCRC Press Inc. Lewis Publishers.

Larry Walker Associates (2005) Yolo Bypass Water Quality Management Plan Report. Prepared under CALFED Watershed Grant, Agreement # 4600001691 for the City of Woodland. May 2005

Louie, S., C. Foe, D. Bosworth (2008). Mercury and Suspended Sediment Concentrations and Loads in the Central Valley and Freshwater Delta (Task 2). Central Valley Regional Water Quality Control Board.

Marvin-DiPasquale M., C.N. Alpers, and J.A. Fleck (2009) Mercury, Methylmercury, and Other Constituents in Sediment and Water from Seasonal and Permanent Wetlands in the Cache Creek Settling Basin and Yolo Bypass, Yolo County, California, 2005−06. Open File Report 2009-1182

Marvin-DiPasquale M., L. Windham-Myers, J.L. Agee, E. Kakouros, L.H. Kieu, J.A. Fleck, C.N. Alpers, and C.A. Stricker (2014) Methylmercury production in sediment from agricultural and non-agricultural wetlands in the Yolo Bypass, California, USA. Science of the Total Environment 484: 288–299

Non-Point Source Workgroup 2012. Memo to Diane Beaulaurier, Central Valley Regional Water Quality Control Board. Subject: Knowledge Base for Nonpoint Sources Methylmercury Control Study. Available at: http://delta-mercury-nps.org/documents/NPSWorkgroup_Memo_KnowledgeBase.pdf, Accessed: July 22, 2020.

Sacramento River Forum (2020) https://www.sacramentoriver.org/forum/index.php?id=gismy&rec_id=5 accessed 7/17//2020

Schmitt M, 2011. Natural Resources Defense Council. Building River: The Yolo Bypass-Hiding in Plain Sight https://www.nrdc.org/experts/monty-schmitt/building-rivers-yolo-bypass-hiding-plain-sightAccessed 7/2/2020

Springborn M, Singer MB, Dune T. 2011. "Sediment-adsorbed total mercury flux through Yolo Bypass, the primary floodway and wetland in the Sacramento Valley, California." Science of the Total Environment, Volumes 412-413. Pages 203-213.

Stephenson, M. (2020) Spreadsheet titled MeHg mass estimates Vegsens 3-17-20.xlsx

Stephenson, M. (2019) Information forwarded in email from C. DiGiorgio to R. Harris July 19, 2019

Stephenson, M. (2017) Spreadsheet titled Stephenson (2017) biomass of plants.xlsx

Suddeth Grimm R, Lund JR. 2016. "Multi-Purpose Optimization for Reconciliation Ecology on an Engineered Floodplain: Yolo Bypass, CA." San Francisco Estuary and Watershed Science, Volume 14, Issue 1, Article 5, 23 Pages

Tsai, P. and R. Hoenicke (2001) San Francisco Estuary Regional Monitoring Program for Trace Substances. San Francisco Bay Atmospheric Deposition Pilot Study Part 1: Mercury. SFEI Contribution 72. July 2001. San Francisco Estuary Institute

TUFLOW. Viewed online at: https://www.tuflow.com. Accessed: September 10, 2019.

US DOI, Bureau of Reclamation/DWR. 2019. Yolo Bypass Salmonid Habitat Restoration and Fish Passage, Final Environmental Impact Statement/Environmental Impact Report, Appendix D. May 2019. Available at: https://www.usbr.gov/mp/nepa/nepa_project_details.php?Project_ID=30484. Accessed July 20, 2020.

U.S. Fish and Wildlife Service. 2020. National Wetlands Inventory. Available at: https://www.fws.gov/wetlands/. Accessed. July 6, 2020.

US Geological Survey (2019) Spreadsheet titled "CCSB_DWR_NWIS.AQ_wy2010-19_SSC-Hg_to-Reed-Harris_8Nov2019.xlsx" emailed from C. Alpers to R. Harris, November 9, 2019.

Wood, ML, Foe CG, Cooke J, Louie SJ. 2010. Sacramento – San Joaquin Delta Estuary TMDL for Methylmercury. Staff Report – Regional Water Quality Control Board, Central Valley Region. Rancho Cordova, California. Viewed at: https://www.waterboards.ca.gov/centralvalley/water_issues/tmdl/central_valley_projects/delta_hg/archived_delta_hg_info/april_2010_hg_tmdl_hearing/apr2010_tmdl_staffrpt_final.pdf

Wyndham-Myers, L., M. Marvin-DiPasquale, E. Kakouros, J.L. Agee, L.H. Kieu, C.A. Stricker, J.A. Fleck, and J.T. Ackerman (2014). Mercury cycling in agricultural and managed wetlands of California, USA: Seasonal influences of vegetation on mercury methylation, storage, and transport

Mercury Open Water Final Report for Compliance with the Delta Mercury Control Program

Chapter 5. Delta-Mercury and Methylmercury Modeling Studies

Submitted by the Open Water Mercury Modeling Workgroup

Aug 31, 2020

The Open Water Mercury Modeling Workgroup

California Department of Water Resources — Division of Environmental Sciences

Carol DiGiorgio
David Bosworth

California Department of Water Resources — Bay Delta Office

Prabhjot Sandhu
Ali Abrishamchi
Jamie Anderson
Han Sang "Hans" Kim
Kevin He
En-Ching Hsu
Kijin Nam
Hari Rajbhandari
Min-Yen Yu
Tara Smith
Eli Ateljevich

Reed Harris Environmental Ltd.

Reed Harris
David Hutchinson.
Matt Gove

U.S. Geological Survey — Upper Midwest Science Center

Randy Hunt

Acknowledgements

Contents

List of Figures

List of Tables

List of Acronyms and Abbreviations

Bureau	Bureau of Reclamation
CalFed	CalFed Bay-Delta Program, former state and federal consortium focused on Delta issues
CVP	Central Valley Project
cfs	Cubic Feet per Second
Delta	Sacramento-San Joaquin Delta
D-MCM	Dynamic Mercury Cycling Model
DMCP	Delta Mercury Control Program (DMCP)
DSM2-Hg	Delta Simulation Model, version 2, Mercury Model
DWR	(California) Department of Water Resources
fHg	Filter-passing Mercury
fMeHg	Filter-passing Methylmercury
Hg	Mercury
Hg(II)	Inorganic mercury with an oxidation state of +2
Hg(0)	Elemental mercury
Inorganic Hg	Sum of inorganic Hg(II) and Hg (0)
MeHg	Methylmercury
PEST ++	Parameter Estimation Software
SSC	Suspended Sediment Concentration
SWP	State Water Project
SWRCB	State Water Resources Control Board
Hg	Total Mercury (sum of inorganic mercury and MeHg)
uHg	Unfiltered (aqueous) mercury
uMeHg	Unfiltered (aqueous) methylmercury
USGS	United States Geological Survey
WWTP	Waste Water Treatment Plant
WY	Water Year(s)

Introduction

The Delta Mercury Control Program (DMCP) requires the California Department of Water Resources (DWR) to reduce methylmercury (MeHg) open water sediment flux from areas out of compliance in the Delta and Yolo Bypass (See Chapter 1). An existing hydrodynamic and water quality model was extended to include features needed to simulate mercury (Hg) in the Delta. This included the addition of a compartment to represent surface sediments, the ability to simulate suspended sediments in the water column and sediment bed, and the ability to simulate inorganic Hg and MeHg in the water column and sediment bed. The updated model is called Delta Simulation Model, version 2, Mercury Model (DSM2-Hg). This effort was complemented by modeling, field, and laboratory studies in the Yolo Bypass. The approach was approved by the Central Valley Regional Water Quality Control Board (Regional Board) to evaluate the potential effects of operational changes on Hg cycling and MeHg supply.

The objective of Chapter 5 is to summarize and provide key findings of interest to management and policy makers associated with the application of DSM2-Hg. Details are provided in Technical Appendix I which focuses on the Hg module, and Technical Appendix J which focuses on the suspended and bed sediment modules. When packaged for public release, DWR will publish model source code, executable files, and other information on the DSM2 website (DWR, 2020a).

Site Description

The Delta

The Sacramento-San Joaquin Delta (Delta) is the largest freshwater tidal estuary on the west coast of the United States. It is formed by the confluence of the Sacramento and San Joaquin Rivers and lies just east of where the rivers enter Suisun Bay (Figure 5-1). The Delta is the hub of California's two largest surface water delivery projects, the State Water Project (SWP), operated by DWR, and the Central Valley Project (CVP), operated by the Federal Bureau of Reclamation (Bureau). The Delta provides a portion of the drinking water for 29 million Californians and irrigation water for agriculture. The Delta comprises a 700-mile maze of sloughs and waterways surrounding more than 60 leveed tracts and islands. The estuary provides habitat critical to the survival of many fish and wildlife species.

The operation of the Delta is subject to a complex array of water rights, flow criteria, and endangered species laws. In terms of water rights, the SWP and CVP are subject to several water right permits issued by the State Water Resources Control Board (SWRCB). In addition to setting water quality criteria that translate into operational standards within the Delta and the Delta watershed, the SWRCB also sets in-stream flow standards. DWR and the Bureau must obtain authorization for any taking of threatened or endangered species. Together this complex set of regulations impose strict constraints on how and when the SWP and CVP can move water.

The Yolo Bypass (Figure 5-1) provides flood control protection for Sacramento and other riverside communities. During high flows, water is diverted from the Sacramento River north of Sacramento into the Yolo Bypass. Water flows through the Bypass and back into the Delta just north of Rio Vista. These Yolo Bypass flows are a source of sediment and Hg in the Delta.

Figure 5-1 Boundaries of the Legal Delta
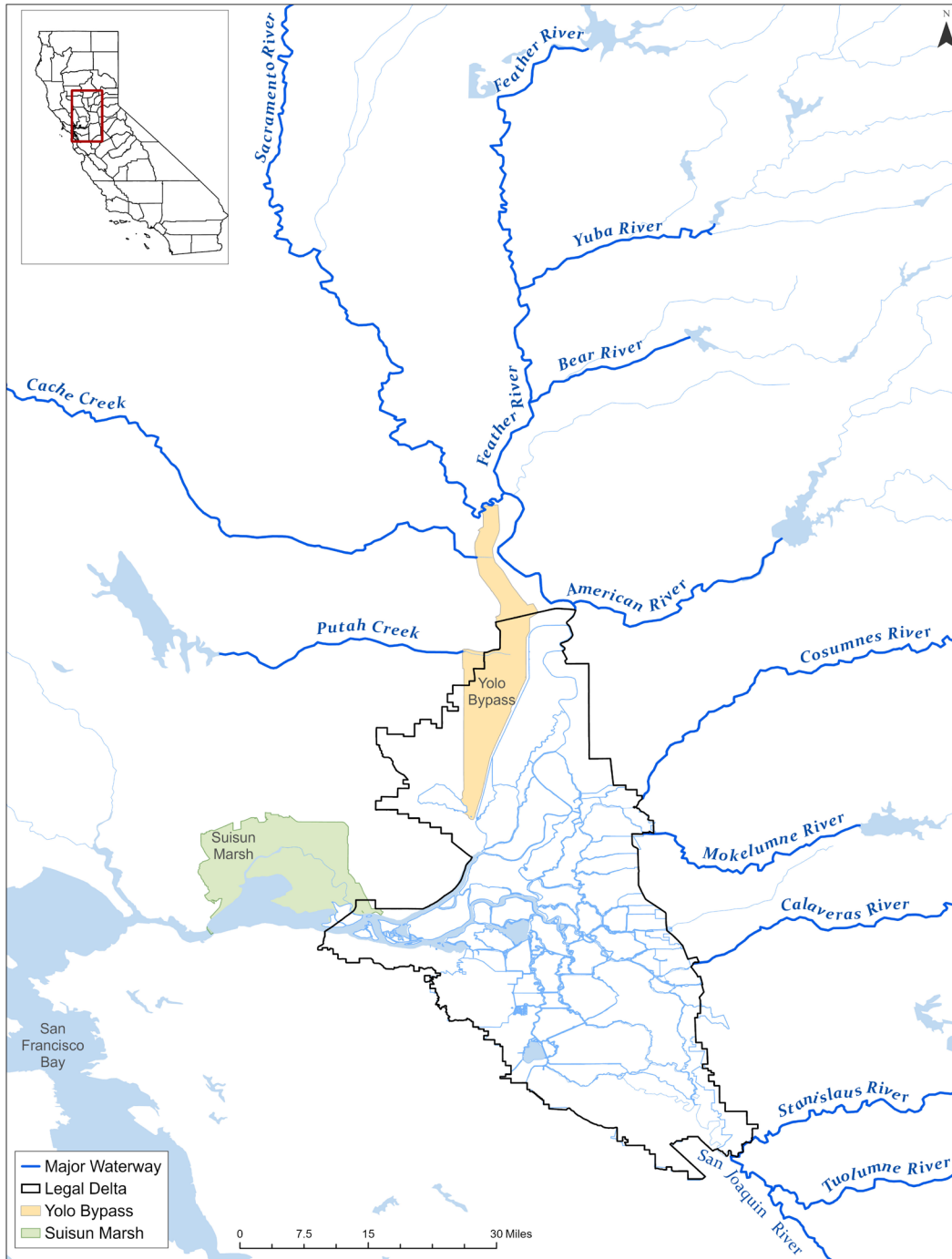
Sediment and Hg transport in the Delta are driven by the combination of tidal flows from San Francisco Bay and freshwater inflows from the Sacramento and San Joaquin Rivers, some minor tributaries and during flood events from the Yolo Bypass. Freshwater inflows into the Delta are highly variable but are modulated by upstream reservoir operations (Table 5-1). For the 2000-2006 study period, median flows for the Sacramento and San Joaquin Rivers are around 18,000 cfs and 2,200 cfs respectively. Median exports from the State Water Project and Central Valley Project were 4,800 cfs and 4,200 cfs

respectively. When operating, median Yolo Bypass flows were around 730 cfs with maximum flows in excess of 250,000 cfs. The Yolo Bypass and Delta Hg models described in this report provide tools for exploring how hydrologic variability, SWP and CVP operations, and other factors may affect Hg and sediment transport and fate, including MeHg loads, in the Delta.

Table 5-1 **Ranges of Major Delta Inflows and Exports Oct 1, 1999 to July 31, 2006**

	Inflows			Exports	
	Sacramento River (cfs)	San Joaquin River (cfs)	Yolo Bypass (cfs)	State Water Project (cfs)	Central Valley Project (cfs)
Maximum	92,790	34,767	256,214	(9,120)	(4,678)
Median	17,805	2,181	0 or 732**	(4,801)	(4,201)
Minimum	4,705	950	(40)*	0	0

Source: California Data Exchange Center *upstream tidal flows at toe drain during summer

**Flows from the Yolo Flood Control Bypass into the Delta are episodic. The median flow of the entire time period is zero. The median value for when the Yolo Bypass is flowing is 732 cfs.

Study Objectives and Approach

Objectives

The primary objectives associated with the development and application of DSM2-Hg were to:
- Create a numerical model that can simulate concentrations, fluxes, transport and fate of inorganic Hg and MeHg in water and surface sediments in the Delta.
- Use the model to evaluate processes governing MeHg supply to the Delta.
- Use the model to help evaluate whether there are operational changes or other strategies that can be implemented to reduce ambient MeHg concentrations in the Delta.

Development of the DSM2-Hg model also provides a tool to explore additional questions in the future, beyond the direct scope of the current analysis. As an open source model, interested stakeholders could also use and refine the model to include other desired inputs.

As discussed in Chapter 1, due to resource, time, and technical constraints, a manually calibrated Delta Hg model fulfills DWR's Delta open water portion of the DMCP. Additional Delta sensitivity and scenarios proposed in the workplan were not conducted[1]. All changes from the original Workplan were approved by the Central Valley Regional Water Quality Control Board (Technical Appendix A).

---

[1] After report submittal, Delta sensitivity runs were conducted and can be found in Technical Appendix K.

Model Selection

It was clear during the design phase of the project that Hg cycling in the Delta is strongly influenced by hydrodynamics and sediment transport. Furthermore, conditions can change rapidly in the Delta, and can vary spatially over relative short distances. A model framework was needed that could represent not just Hg, but also freshwater and tidal flows and sediment transport, including temporal and spatial variability. Another feature important for Hg simulations was to explicitly include a sediment bed compartment in the model framework. This is because MeHg production often occurs in the surface layer of the sediment bed, and because legacy inorganic Hg contamination in surface sediments can affect MeHg production and supply to overlying waters.

No single model existed at the outset of the study with all the features needed to simulate Hg cycling, and the primary influences on Hg cycling, in the Delta. An effort was therefore undertaken to extend an existing DWR hydrodynamic model for the Delta, the Delta Simulation Model version 2 (DSM2) (DWR, 2020a), to include a sediment bed module, suspended sediment transport and fate, and Hg cycling in water and the sediment bed. A separate effort unrelated to Hg replaced the water quality module in DSM2 with an updated General Transport Module (GTM) (Hsu and others, 2014) that is modular to allow additional constituents, such as Hg, to be added to the model. The resulting DSM2-Hg model simulates hydrodynamics, sediment transport, and the cycling and fate of three major forms of Hg (MeHg, Hg(II), and elemental Hg(0)) in the water column and surface sediments of the Delta (Figure 5-2).

DSM2 is a one-dimensional (1-D) model, suitable for applications where gradients occur in one direction (along the flowpath in this case) but are assumed to be the same (well-mixed) vertically and horizontally perpendicular to flow. This is a reasonable assumption for the Delta's open water channels but becomes a limitation once conditions have significant variability in two or three dimensions, such as downstream in San Francisco Bay which has conditions that also vary with depth and across the width of the bay. Thus, the downstream limit of DSM2 was set at Martinez (Figure 5-3) to keep the model domain primarily in the channelized part of the Delta. Martinez is also the location of a long-term tidal gage which provides data for modeling tidal flows into and out of the Delta. Since greater confidence in 1-D conditions occurs in areas upstream of Chipps Island (Figure 5-3) and since Chipps Island is closer to the downstream boundary of the legal Delta than the model's downstream boundary at Martinez, modeled exports of mercury and suspended sediment to San Francisco Bay presented in this report were calculated at Chipps Island.

Tributary inflows represented in DSM2 include the Sacramento, San Joaquin, Cosumnes, Mokulmne, and Calaveras Rivers and the Yolo Flood Control Bypass (Yolo Bypass). Water supply exports in DSM2 include the State Water Project (SWP), the federal Central Valley Project (CVP), and Contra Costa Water District. Consumptive use of water on the 142 Delta islands is also represented in DSM2 (DWR, 2020b). Ongoing development of DSM2 is documented in annual reports to the State Water Resources Control Board (CNRA, 2020).

An overview of DSM2-Hg follows. Additional information on the development of the Hg, suspended sediment, and sediment bed modules is provided in Appendix I and Appendix J, respectively.

Figure 5-2 Key Features of the Delta Mercury Model (DSM2-Hg)

Delta Mercury Model (DSM2-Hg)

Forms of Mercury Modeled
- Methylmercury (MeHg)
- Hg(II)
- Elemental Hg (Hg(0))

Model Domain and Study Period
- Open water channels in the Sacramento San Joaquin Delta between Sacramento, Venalis and Martinez. Emphasis on results upstream of Chipps Island.
- Mercury calibration period: October 1999 to July 2006
- Simulation time step 15-minutes

Connection to the Yolo Bypass
- Flows and constituent loads from the Yolo Bypass enter the DSM2-Hg model near Liberty Island
- Yolo Bypass flow and concentrations can be provided by the Yolo Bypass Hg model, field data if available, or synthetic data

Potential Future Model Applications
- Scenario testing (options to reduce MeHg supply). Scenarios may involve running other models and require other resources.
- Refined model analysis along with field program to address data and knowledge gaps
- Improved characteriziation of spatial and temporal patterns for Hg and MeHg cycling and supply in Delta
- Replicate historical conditions
- Sensitivity of Delta Hg/MeHg concentrations to changes in flows, etc-- (may involve running other models and require other resources).

Figure 5-3 Delta Mercury Model (DSM2-Hg) Domain, Inflow and Outflow Locations.
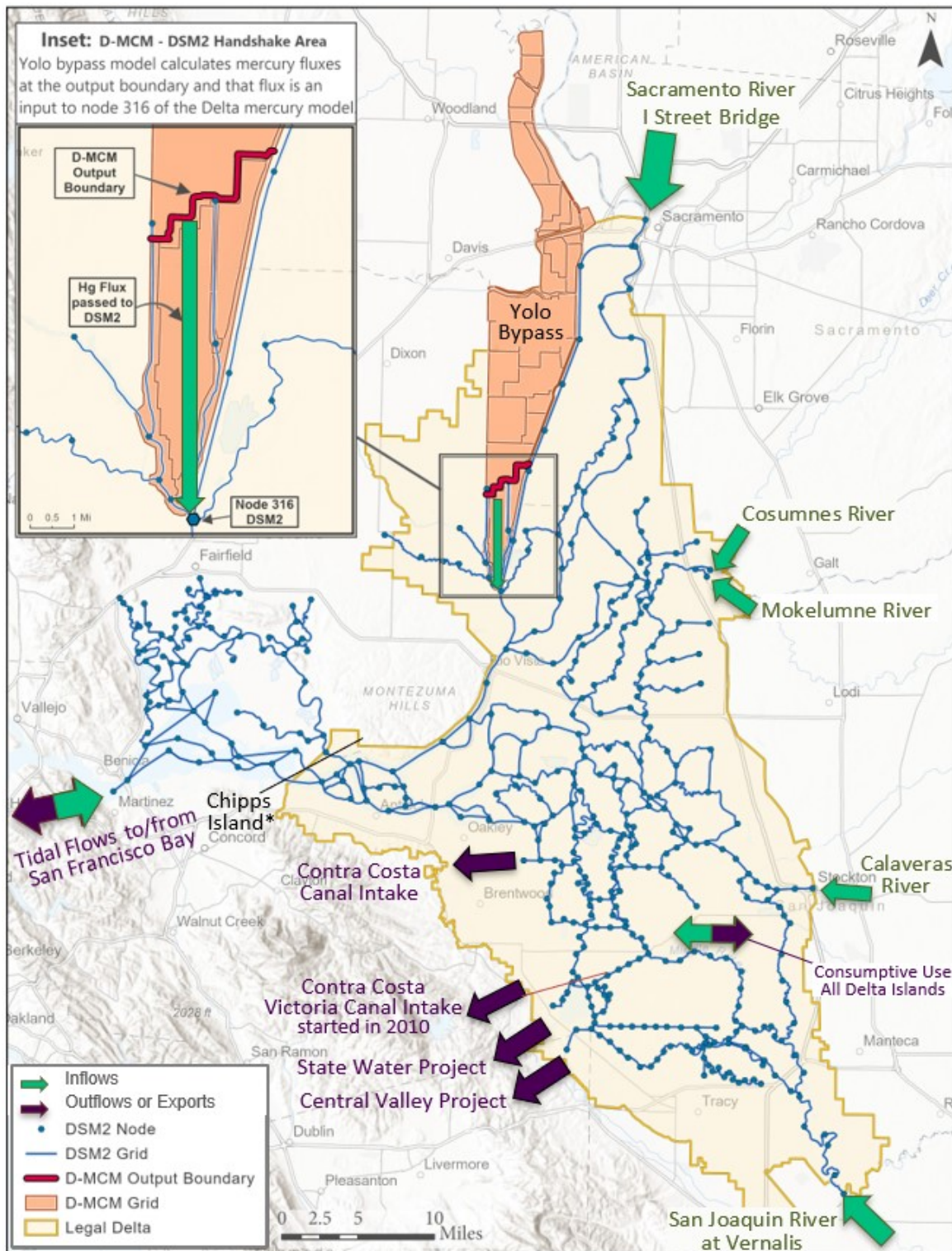
Figure Note: Separate Yolo Bypass model domain also shown in orange. Inset shows how outputs from Yolo Bypass model (D-MCM) were passed as loads to DSM2-Hg model.

*Flux calculations at Chipps Island are computed as the sum of three channels indicated by the black line.

Major Components of Delta Hg Model Analysis

Application of DSM2-Hg to the Delta included the following major steps

1. Data assembly and review
2. Identification of best data years for model calibration
3. Simulation of hydrology for calibration period October 1999- July 2006 (completed prior to this study)
4. Simulation and calibration of suspended sediment loads, transport and fate in open water channels and sediment bed of the Delta.
5. Manual calibration of DSM2-Hg for inorganic Hg and MeHg in the water column and bed sediments
6. Calibration refinement, sensitivity and uncertainty analysis with parameter estimation software (PEST++, future task)

The Delta model analysis was based on extending the capabilities of an existing model and using existing data. The Delta modeling effort was also supported by a separate model analysis of Hg in Yolo Bypass, described in Chapter 4. The Yolo Bypass model provided estimates of suspended sediment, inorganic Hg and MeHg loads to the Delta model.

Similar to the Yolo Bypass model analysis, the calibration goal was ultimately to refine the manual calibration and carry out a sensitivity/uncertainty analysis of the Delta Hg model using PEST++. Time constraints prevented including this approach in this report, however, it is anticipated that work will continue to calibrate the model using PEST++, with results available as a future addendum.

Figure 5-4 Components Associated with the Development of the DSM2-Hg Model
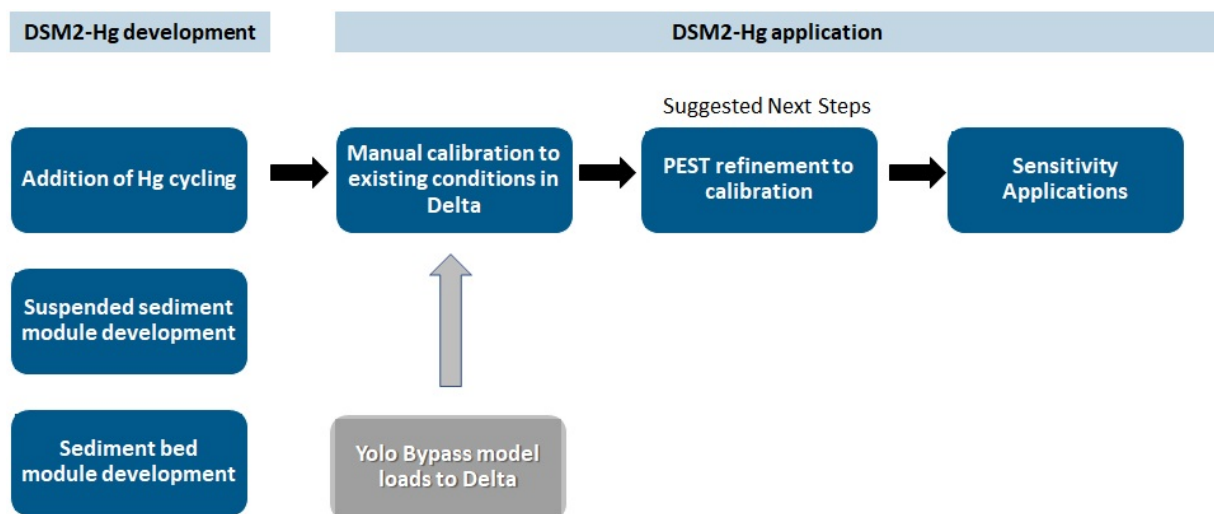
Approach to Hydrology

A review of data needed for simulations indicated that the best data years for Hg model calibration were during water years 2000-2006 (October 1999-July 2006). DSM2 had previously been applied and calibrated for water flow for this time period during other studies (Finch, 2014; Liu and Sandhu, 2012, Liang, 2018). As shown in Table 5-2 and Figure 5-5, the Hg calibration period captured a wide range of flow conditions, including some of the wettest years on record with sustained flooding in the Yolo Bypass and some drought years. The best data period for calibration of the suspended sediment component of the model analysis was 2010-2013. DSM2 had also previously been applied and calibrated to simulate water flows for this period. All simulations were carried out using short time steps (15 minutes) needed for estuarine conditions with tidal flows.

Table 5-2 Hydrologic Year Types for Hg and Suspended Sediment Simulation Periods

Water Year	Year Type	
	Sacramento Valley	San Joaquin Valley
Hg Calibration Period		
2000	Above Normal	Above Normal
2001	Dry	Dry
2002	Dry	Dry
2003	Above Normal	Below Normal
2004	Below Normal	Dry
2005	Above Normal	Wet
2006	Wet	Wet
Suspended Sediment Calibration Period		
2010	BN	Above Normal
2011	W	Wet
2012	BN	Dry
2013	D	Critical

Table Note: https://info.water.ca.gov/cgi-progs/iodir/WSIHIST

Figure 5-5 Delta Mercury Model (DSM2-Hg) Boundary Inflows and Exports Oct. 1999 to July 2006
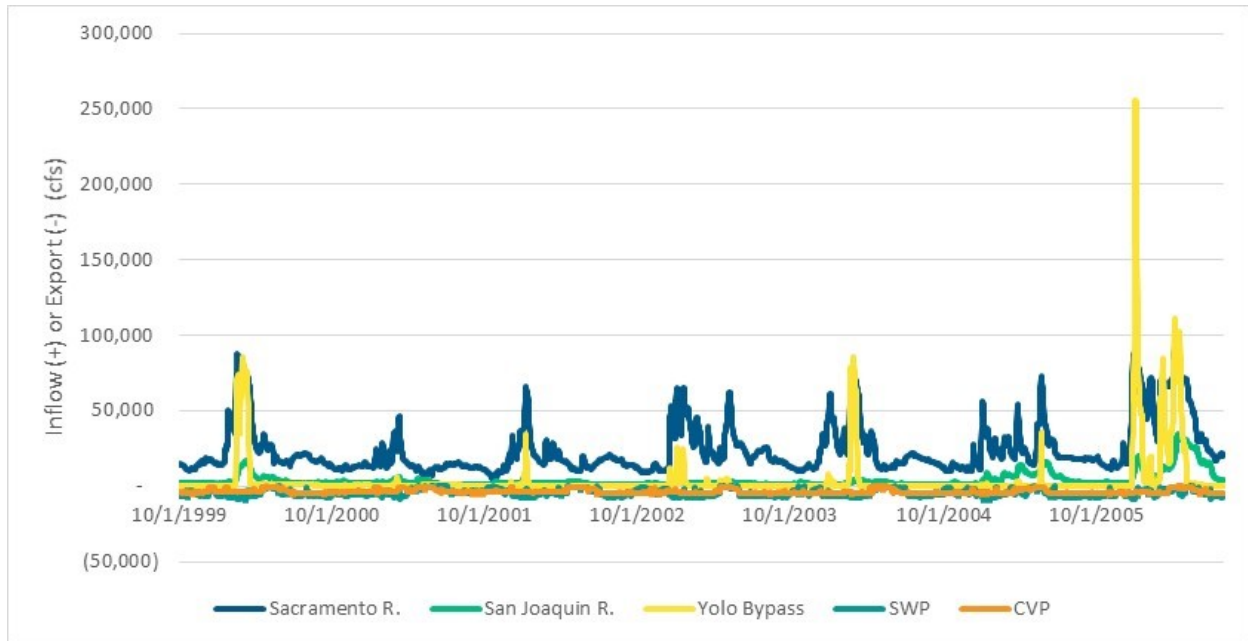
Approach to Represent Suspended and Bed Sediments

DSM2-Hg represents both suspended sediments in the water column and bed sediments using 3 particle types:

    a.   Coarse inorganics (e.g. sand)
    b.   Fine inorganics (e.g. silt and clay)
    c.   Organic matter

Each particle type has unique properties in terms of particle densities, settling velocities, resuspension rates, and Hg partitioning (ratio of solids:dissolved concentrations). The model has a 2-layer sediment bed to represent erosion and settling of sediments at the channel bed.

Tributary suspended sediment loads to the Delta for most locations shown in Table 5-4 were based on data collected by the United States Geological Survey (USGS). The exception was the Yolo Bypass where loads to the Delta were based on D-MCM simulations of Yolo Bypass. Specifically, Yolo Bypass sediment export was estimated at the stairsteps and passed to DSM2- Hg at node 316 below Liberty Island (see insert in Figure 5-3). Therefore, this modeling exercise did not fully capture the role of Liberty Island on Hg cycling and transport.

Approach to Represent Mercury Cycling

Hg cycling was added to DSM2, based on the approach used in the D-MCM model for the water column and sediment bed (Figure 5-6). Three major forms of Hg were simulated: MeHg, Hg(II), and elemental

mercury (Hg(0)). Given that Hg(0) is also inorganic, the sum of Hg(II) and Hg(0) is referred to in the report as inorganic Hg. MeHg production was assumed to occur primarily in the surface sediment bed.

Figure 5-6 **Representation of Mercury cycling in DSM2-Hg.** Based on D-MCM (EPRI, 2013)
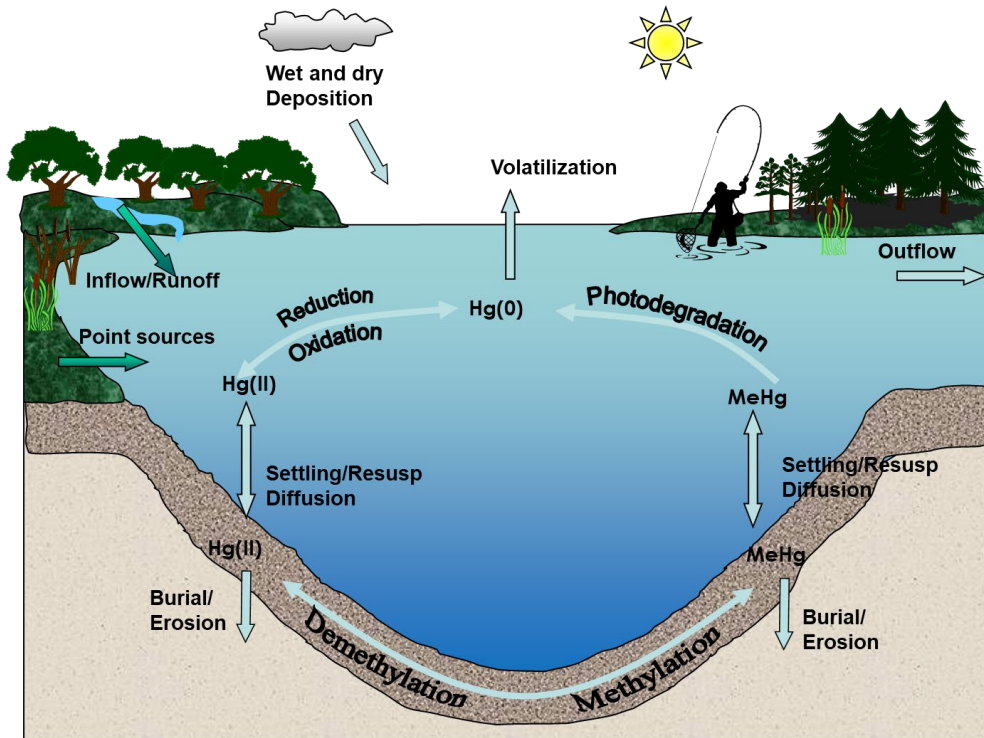
Atmospheric wet deposition of inorganic Hg was estimated using data from the nearest Mercury Deposition Network (MDN) site, CA72, near San Jose. The site was operated from January 11, 2000 through December 27, 2006. Weekly data were used to estimate overall monthly averages for the entire period of record, for use in the DSM2-Hg analysis. Dry Hg deposition was assigned a constant value of 19 ug/m2/yr, the mean value reported by Tsai & Hoeneike (2001) for the San Francisco Bay Estuary from August 1999 through November 2000.

Tributary loads of inorganic Hg and MeHg were based on empirical relationships between Hg concentrations and flow or SSC, for most locations shown in Table 5-4. This was done using tributary-specific data to the extent possible. Yolo Bypass loads to the Delta for inorganic Hg and MeHg were estimated with the D-MCM model (Chapter 4).

The DMCP identified numerous sources of MeHg to the Delta, including fluxes from sediments to open waters. DSM2-Hg included 3 fluxes at the sediment water interface: settling, resuspension of sediment and diffusion, that combined to produce the net flux out of or into sediments (Figure 5-7).

Figure 5-7 Sources and Sinks of MeHg in Delta Waters
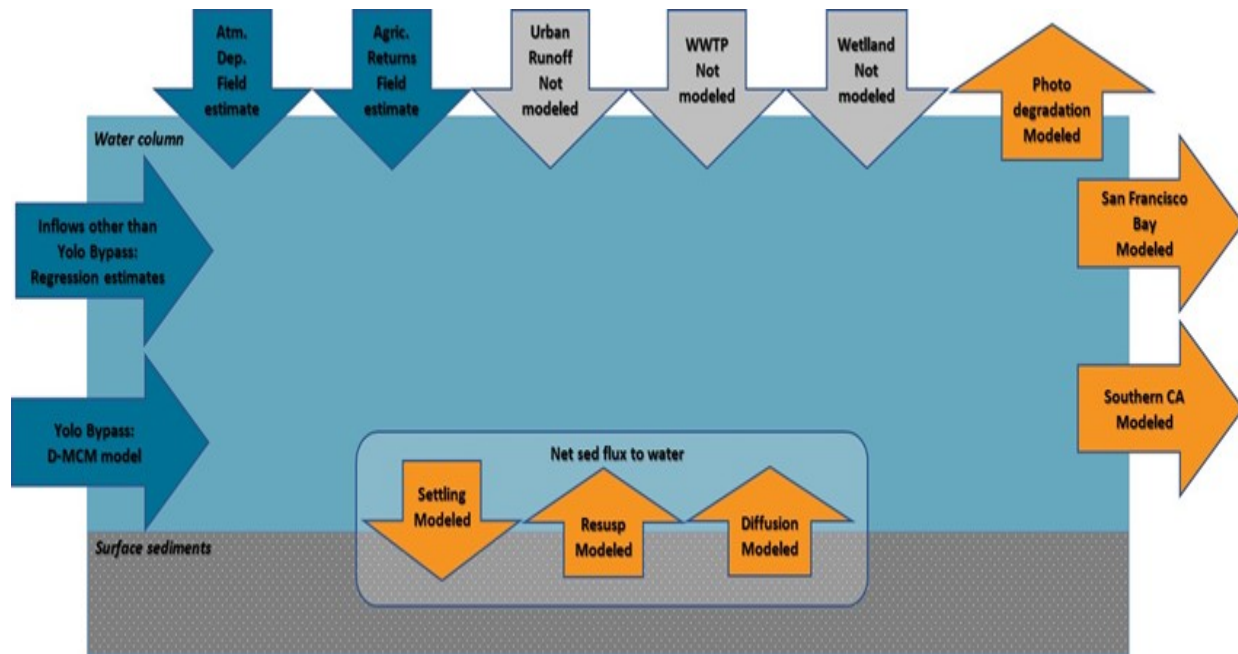
Figure Note: D-MCM = Dynamic Mercury Cycling Model, WWTP = Wastewater Treatment Plant. Modeled fluxes are shown in orange. Boundary fluxes were estimated externally (blue). Fluxes not included in the model analysis are shown in grey.

Approach to Model Calibration for Suspended Sediments and Mercury

Model calibration was required for suspended sediments, inorganic Hg and MeHg. The calibration for suspended sediments was carried out first, followed by inorganic Hg, then MeHg. Suspended sediments and Hg used separate calibration periods that corresponded with the best available field data for each constituent (Table 5-3). Most of the analysis presented in this chapter is for the Delta Hg model calibration period from October 1999 to July 2006.

Table 5-3 Calibration periods for suspended sediment and mercury

Constituent	Calibration Period
Suspended Sediment	Calibration Oct 2010-Sept 2013 Validation Oct 2013-Sept 2016
Mercury	October 1999 – July 2006

Table Note: CalFed = CalFed Bay-Delta Program, DMCP = Delta Mercury Control Program

The suspended sediment module was calibrated and validated using 15-minute suspended sediment concentrations provided by the U.S. Geological Survey based on field observations of turbidity and flow (Figure 5-8) (Morgan-King and Wright, 2013). The calibration period was from October 2010 to September 2013 (wet, below normal, and dry years) and the validation period was from October 2013 to September 2016 (critical, critical, and below normal years. The calibration variables were the erosion coefficient and the particle size for each sediment type. Additional information on the suspended sediment calibration and observed data can be found in Appendix J and Hsu and others, 2019.

The calibrations of inorganic Hg and MeHg concentrations were based on observations in surface waters at thirteen locations shown in Figure 5-8. Observations of uHg, fHg, uMeHg and fMeHg were available for comparisons. Due to the limited overall availability of Hg data, all observations within the Hg calibration period from October 1999-July 2006 were used to calibrate the model (as opposed to using some of the data for validation). Details on information used for calibration are provided in Technical Appendix I. The calibrations for inorganic Hg and MeHg were done manually, varying selected model inputs to improve the fit between the model and observations. Model calibration results were evaluated graphically. Ultimately the calibration will be refined using parameter estimation software (PEST++), similar to the approach used for the Hg model analysis for Yolo Bypass (Technical Appendix H). At the time of preparation of this report, only the manual DSM2-Hg calibration was available.

Figure 5-8 Stations used for DSM2-Hg Calibrations of SSC, Inorganic Hg and MeHg in Surface Waters
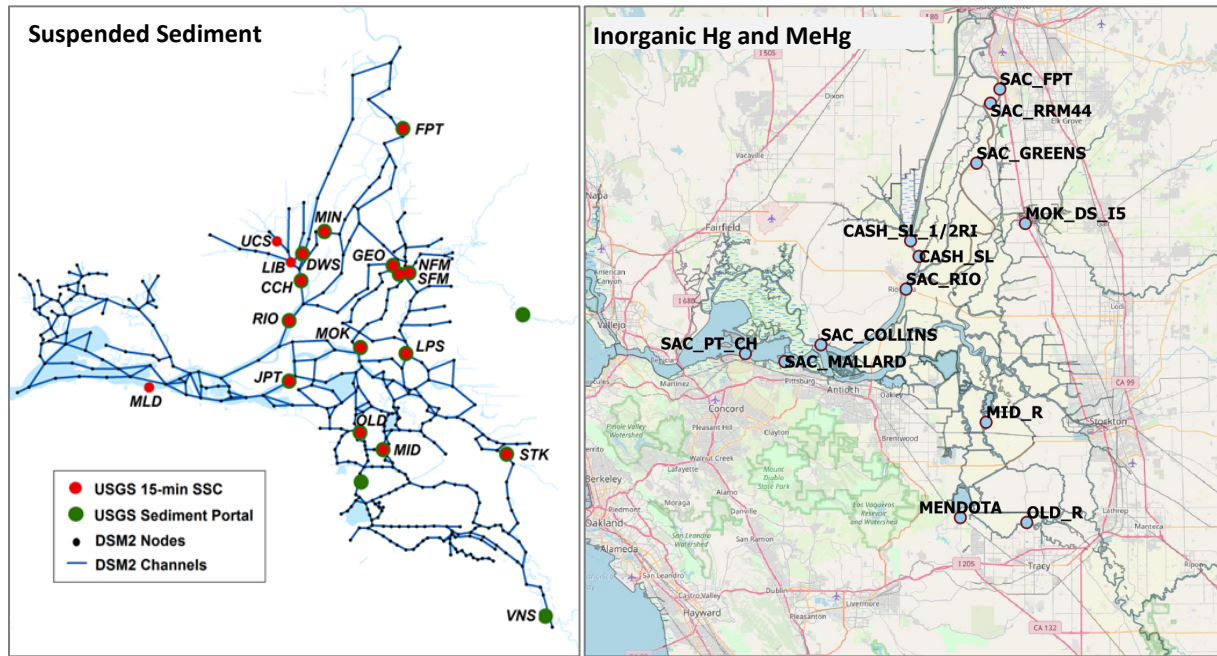
Figure Note: Suspended sediment locations are defined in Table 4-1 of Hsu and others 2019 included in Appendix J. Mercury monitoring locations are defined in Appendix I. Figures in this chapter that refer to these locations identify the locations in a figure note.

Table 5-4 Locations used for DSM2-Hg Inflow and Export Calculations

Location	Inflow or Export	DSM2 Node	Latitude/Longitude
Sacramento River at I Street	Inflow	330	38.5864, -121.5064
San Joaquin River at Vernalis	Inflow	17	37.6638, -121.2501
Yolo Bypass at Liberty Island	Inflow	316	38.2313, -121.6741
Cosumnes River at Michigan Bar	Inflow	446	38.2546, -121.4215
Mokelumne River at Woodbridge	Inflow	447	38.2483, -121.4255
Calaveras River at Stockton	Inflow	21	37.9667, -121.3697
State Water Project	Export	Clifton Court/Banks Pumping Plant	37.8019, -121.6202
Central Valley Project	Export	181/Jones Pumping Plant	37.7970, -121.5852n
Chipps Island	Tidal Flows	Channel 437 Channel 442 Channel 511	38.046494°, -121.888239° 38.046494°, -121.888239° 38.067735°, -121.853877°

Table Note: Combined flows through DSM2 channels 437, 442, and 511 near Chipps Island were used in tidal import and export calculations between the Delta and San Francisco Bay. These locations were selected to reduce the uncertainty associated with the concentrations assigned at the downstream boundary at Martinez. Note that latitude/longitude information is provided for reader reference but is not used in the Delta Hg model.

Delta Hg Model Simulation and Calibration Results

Hydrology Results

The largest tributary source of water to the Delta in simulations was the Sacramento River, representing 72% of inputs for the overall period from October 1999 – July 2006 (Figure 5-9). The largest simulated loss of water from the Delta for the same period was net export (adjusting for tidal flows) to San Francisco Bay (Figure 5-9). As noted earlier, the model analysis carried out here included a wide range of hydrologic conditions ranging from dry to wet years (Table 5-2).

The simulation period included a wide range of annual freshwater inflows, varying 4.3X from 17,956 cfs in water year 2001, to 77,930 cfs in water year 2006 (averages). The relative importance of different water sources also varied among years. The Yolo Bypass, for example, ranged from 1-25 % of the overall tributary supply of water among the years simulated.

Figure 5-9 **Estimated Average Water Inflows and Outflows for the Delta from October 1999 to July 2006**

Into the Delta

Leaving the Delta

Legend (Into the Delta):
- Sacramento (72%, 24160 cfs)
- San Joaquin (12%, 3964 cfs)
- Yolo Bypass (12%, 4117 cfs)
- Cosumnes (1%, 490 cfs)
- Mokelumne (2%, 506 cfs)
- Calaveras (< 1%, 191 cfs)

Legend (Leaving the Delta):
- CVP (11%, 3533 cfs)
- SWP (14%, 4445 cfs)
- Chipps Island (75%, 24216 cfs)
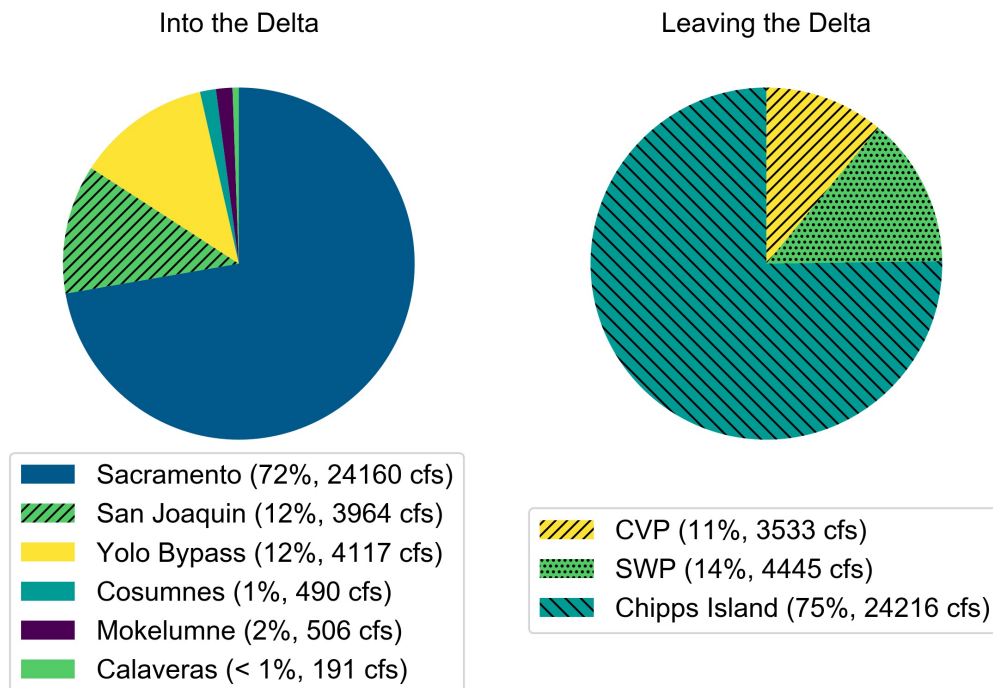
Suspended Sediment Calibration and Results

An example of simulated and observed suspended sediment concentrations (SSC) is shown Figure 5-10. Overall, the modeled results capture observed trends and extreme events for Delta suspended sediment concentrations. These results reflect the suspended sediment calibration and validation period from 2010-2013. The calibrated suspended sediment model was then used for the mercury study period of October 1999 to July 2006.

Figure 5-10 **Observed and Simulated Suspended Sediment Concentrations in Delta Waters.**
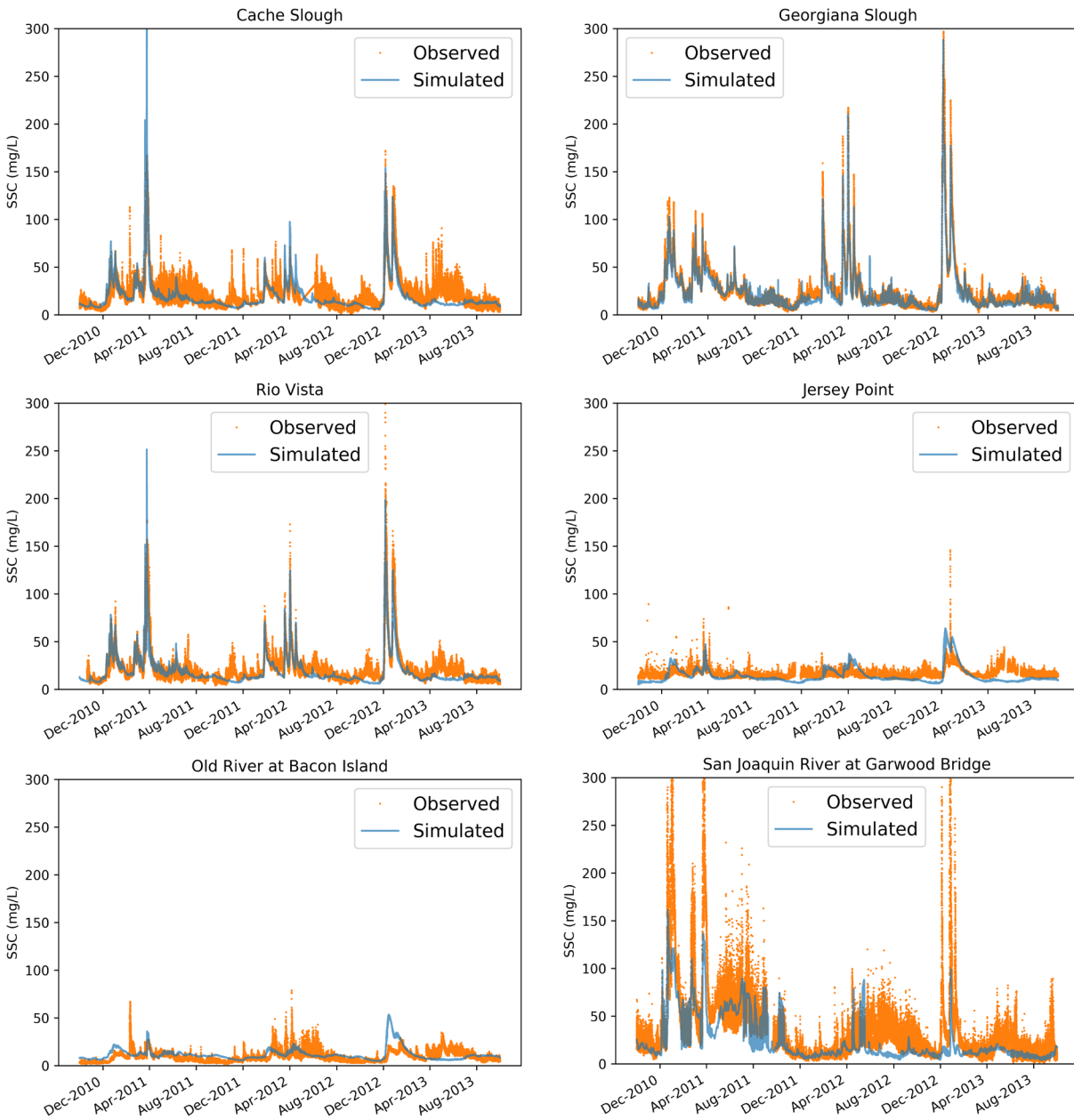
Figure Note: See Figure 5-8 for a map of the observation locations: Cache Slough at Ryer Island (CCH), Georgiana Slough(GEO), Rio Vista (RIO), Jersey Point (JPT), Old River at Bacon Island OOLD) and San Joaquin River at Garwood Bridge (/STK). Data from USGS (Morgan-King and Wright, 2013).

The largest estimated suspended sediment loads to the Delta from October 1999 to July 2006 were from the Sacramento River (72%) (Figure 5-11, Table 5-5). The Yolo Bypass and San Joaquin Rivers contributed 15% and 12% respectively. Nearly 90% of the suspended sediments that flowed out of the Delta, exited the Delta at Chipps Island and flowed into San Francisco Bay. The State Water Project and federal Central Valley Project exported 6% and 4% of the suspended sediment loads respectively in simulations. The relative proportions of the sediment loads from different sources are consistent with a 2003 Delta sediment budget (NHC, 2003).

Consistent with previous findings (Louie and others, 2008), DSM2-Hg model results simulated the Delta as a net sink for sediment. The export of suspended sediment at Chipps Island was roughly half of the inflowing supply for the overall simulation period (Table 5-5). The greatest suspended sediment loads occurred during the winter months (Figure 5-12). The Delta remained a net sink for suspended sediments for all months during the simulation (Figure 5-13).

Figure 5-11 **Estimated Average Delta Suspended Sediment Inflows and Outflows for October 1999 to July 2006**
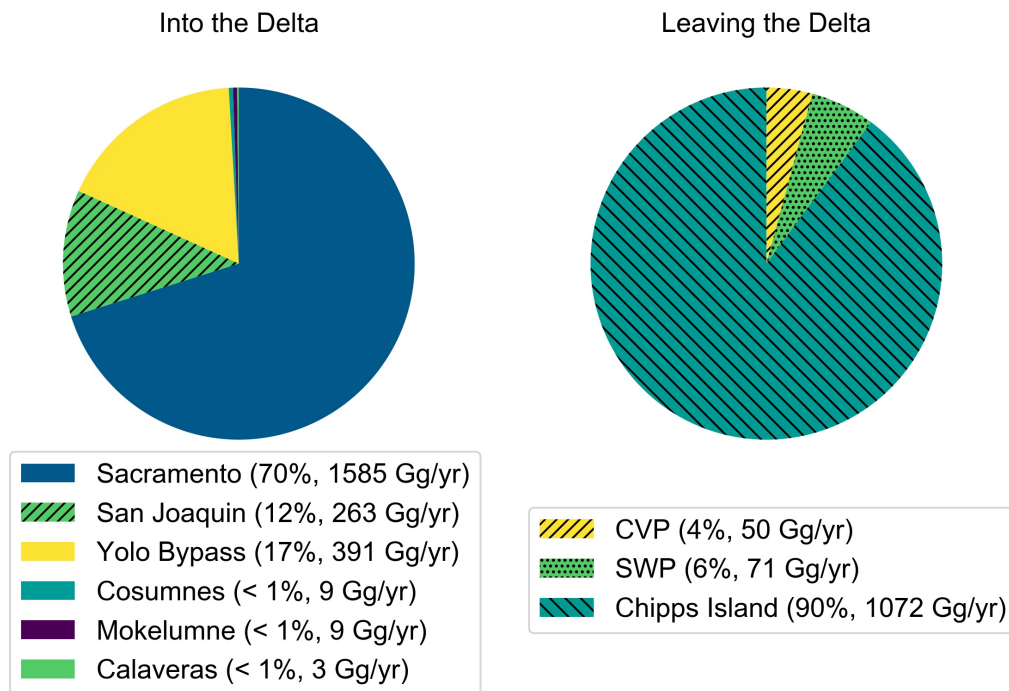
Figure Note: Inflow loads based on Outflow fluxes simulated with DSM2-Hg.

Data from USGS (Morgan-King and Wright, 2013).

Table 5-5 Estimated Average Inflows and Outflows of Suspended Sediment, uHg(II) and uMeHg for the Delta from October 1999 - July 2006

Location	Load					Average concentration		
	Flow	SSC	uHg(II)	uMeHg		SSC	uHg(II)	uMeHg
Inflows:	cfs	Gg/yr	kg/yr	g/yr		mg/L	ng/L	ng/L
Sacramento	24160	1548	270	2897		72	12.5	0.13
San Joaquin	3964	257	30	594		73	8.5	0.17
Yolo Bypass	4117	382	69	1908		104	18.7	0.52
Mokulumne	506	8	2	31		19	3.9	0.07
Calaveras	191	3	4	23		20	22.2	0.14
Cosumnes	490	9	4	143		20	8.5	0.33
All inflows	33428	2207	378	5597		74	12.7	0.19
Outflows:								
CVP	3533	49	12	305		16	3.9	0.10
SWP	4445	69	16	379		17	4.2	0.10
Chips Island	24216	1047	237	3785		48	10.9	0.18
All outflows	32194	1165	265	4469		41	9.2	0.16
Outflow/inflow		0.53	0.70	0.80				

Table Note: Loads are estimated using tributary-specific regressions of parameter concentrations as a function of flow or SSC, except for the Yolo Bypass, which was based on results from the D-MCM model. Outflows were based on DSM2-Hg results. Average concentrations are the constituent loads divided by the flows. Outflow/Inflow values are dimensionless ratios.

Figure 5-12 Monthly Modeled Suspended Sediment Loads in the Delta by Location from October 1999 through July 2006
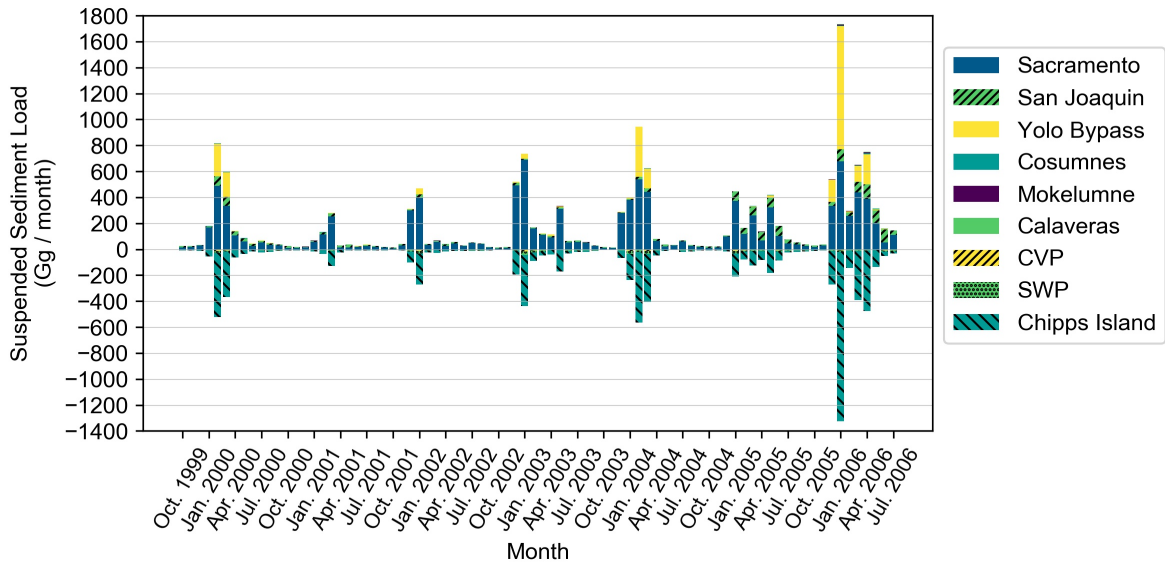
Figure Note: Positive values indicate inputs. Negative values are exports.

Figure 5-13 Monthly Modeled Net Suspended Sediment Loads in the Delta by Location from October 1999 through July 2006. Negative values indicate a net sink (outflows less than inflows)
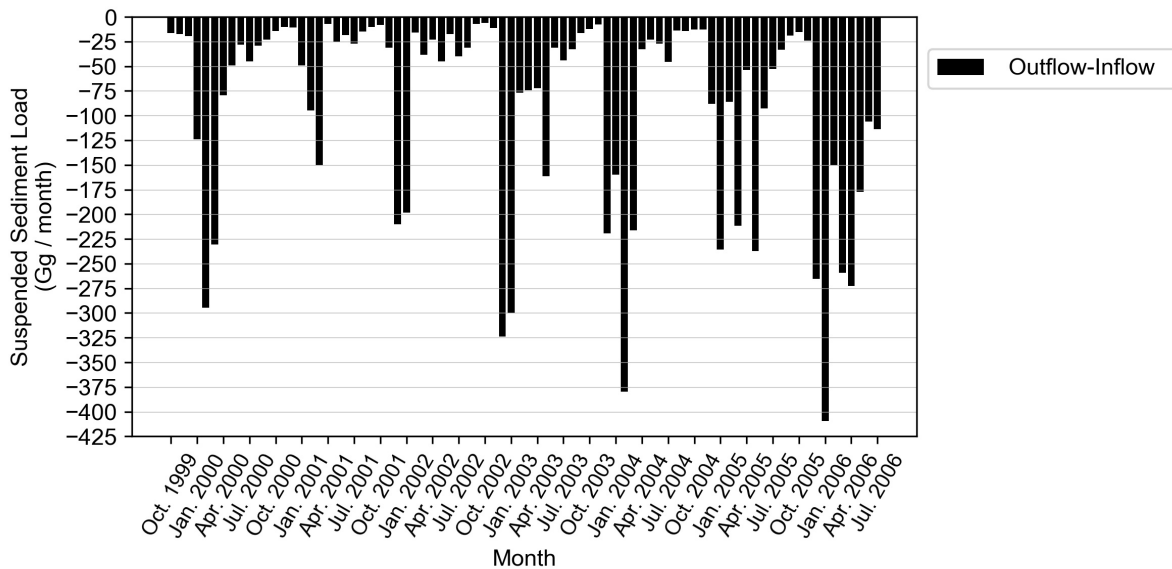
Mercury Calibration

Mercury Concentrations in Delta Surface Waters

Examples of observed and calibrated model results for uHg and uMeHg in surface waters on the west side of the Delta are shown in Figure 5-14 and Figure 5-15. The model calibration reasonably matched observations. The model simulation from October 1999-July 2006 was characterized by highly dynamic conditions and rapid simulated changes in water column concentrations of Hg and MeHg. Observations did not display the same variability, but this may have been partly related to short term events potentially not captured during sampling. Alternatively, the model may have overestimated temporal variability. Additional model results for the calibration of Hg and MeHg in surface waters are provided in Technical Appendix I.

Figure 5-14 Observed and Simulated uHg Concentrations in Delta Surface Waters (west side locations) 2000-2006
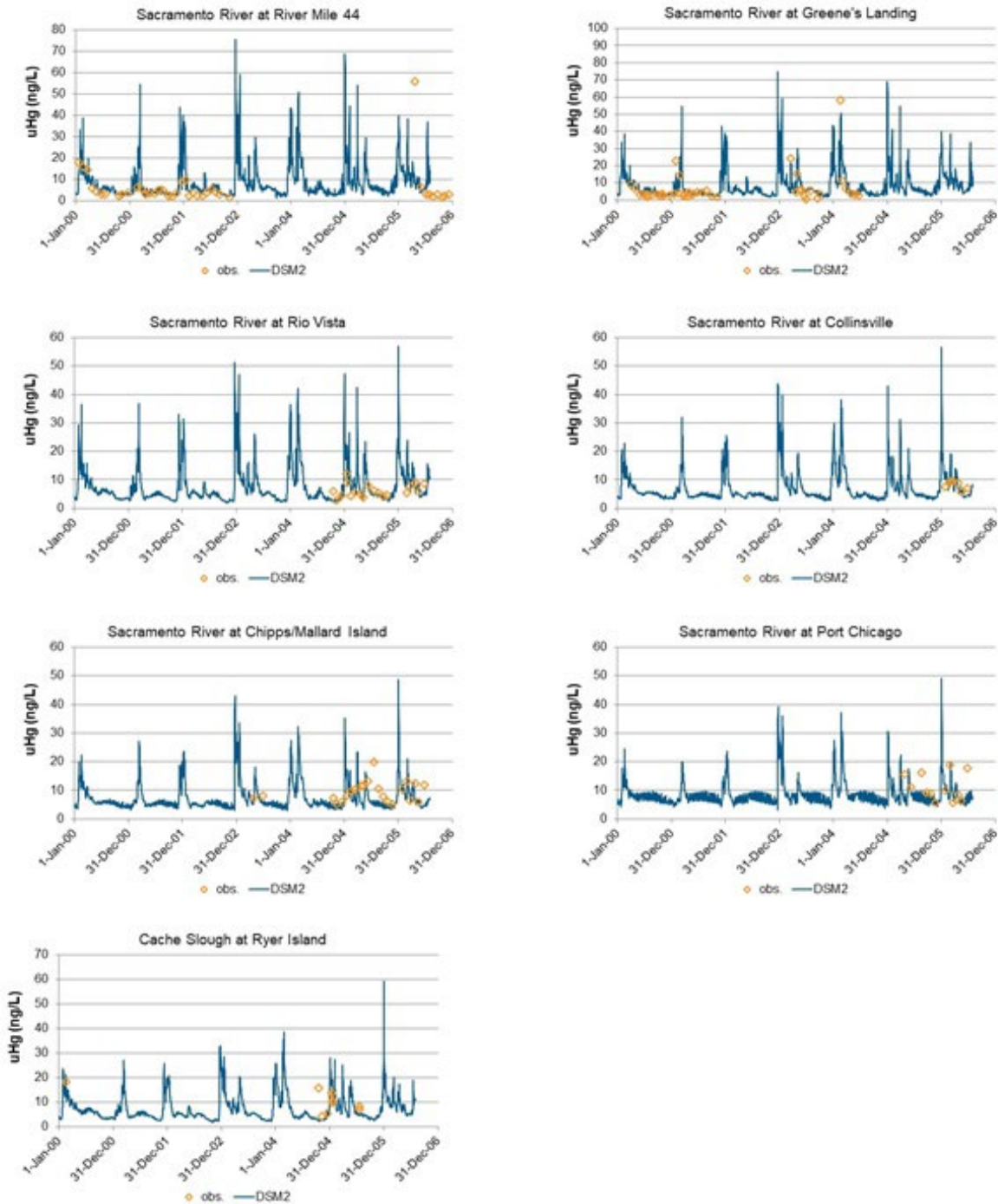
Figure Note: See Figure 5-8 for a map of the observation locations: Sacramento River at Greene's Landing (SAC_Green's), Rio Vista (SAC_RIO), Collinsville (SAC_COLLINS), Chipps/Mallard Island (SAC_MALLARD), and Port Chicago (SAC_PT_CH) and Cache Slough at Ryer Island (CASH_SL). Observed data from Louie and others, 2008, except Sacramento River at River Mile 44 from Coordinated Monitoring Program, 2004. Sacramento River at Greene's Landing from Foe, 2003 and SRWP, 2004.

Figure 5-15 Observed and Simulated uMeHg concentrations in Delta Surface Waters (west side) locations, 2000-2006
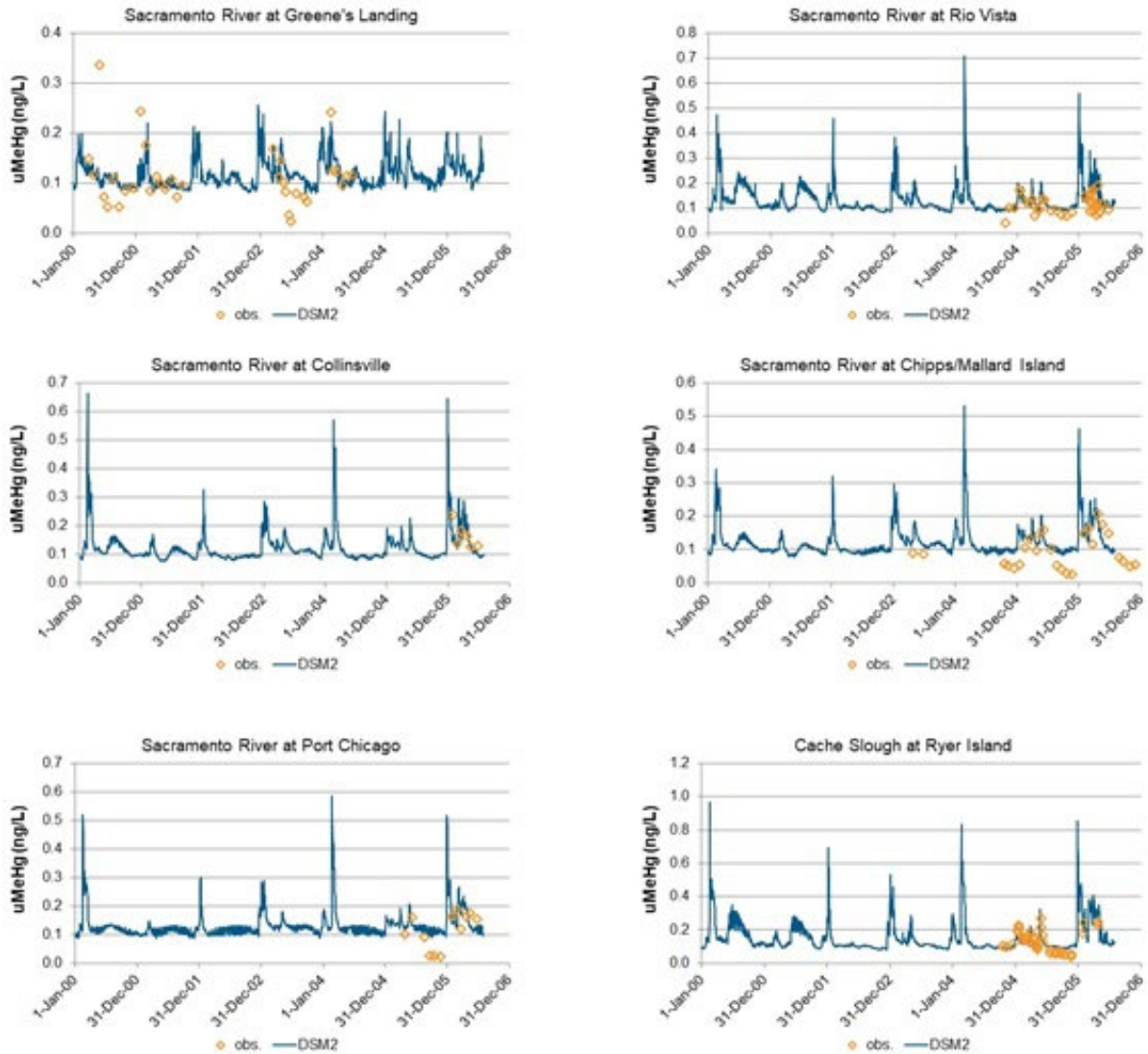
Figure Note: See Figure 5-8 for a map of the observation locations: Sacramento River at Greene's Landing (SAC_Green's), Rio Vista (SAC_RIO), Collinsville (SAC_COLLINS), Chipps/Mallard Island (SAC_MALLARD), and Port Chicago (SAC_PT_CH) and Cache Slough at Ryer Island (CASH_SL). All observed data from Foe and others, 2008. Additionally, data also used from Foe, 2003 for Sacramento River at Greene's Landing and SRWP, 2004.

Spatial Concentration Patterns

Water Column Spatial Concentration Patterns

Simulated spatial patterns for high, median and low flow conditions during the Hg calibration period (October 1999 to July 2006) are shown in Figure 5-16. Some spatial features of the simulation included the following:

- When the highest flow occurred in the Sacramento River, (~92,000 cfs), SSC and uHg(II) concentrations were higher on the periphery of the Delta and lower in the Central Delta. This pattern was not evident for uMeHg. Similar trends occurred when the highest flow occurred in Yolo Bypass (256,200 cfs), but concentrations of SSC, uHg(II) and uMeHg were generally higher than when the Sacramento River flow was highest.

- When the median flow for the simulation period occurred in the Sacramento River (17,850 cfs), simulated concentrations of SSC, uHg(II) and uMeHg were less variable and generally lower in magnitude than during the high flow dates presented. Concentrations in downstream areas (Suisun Bay) were simulated to be higher than upstream.

- For low Sacramento River inflows (~4,700cfs), concentrations of all three constituents are lower than in the high flow case, and contributions from the San Joaquin River appear to have more relative influence. These patterns are for the snapshots in time shown in Figure 5-16, and further investigation would be required to see if these patterns are consistent under similar flow conditions. Field data were insufficient to identify Delta-wide spatial trends to compare with model results.

Figure 5-16 Simulated Suspended Sediment, uHg(II) and uMeHg Concentrations for High, Median and Low Flow Conditions During Model Mercury Calibration Period Oct 1999 to July 2006.
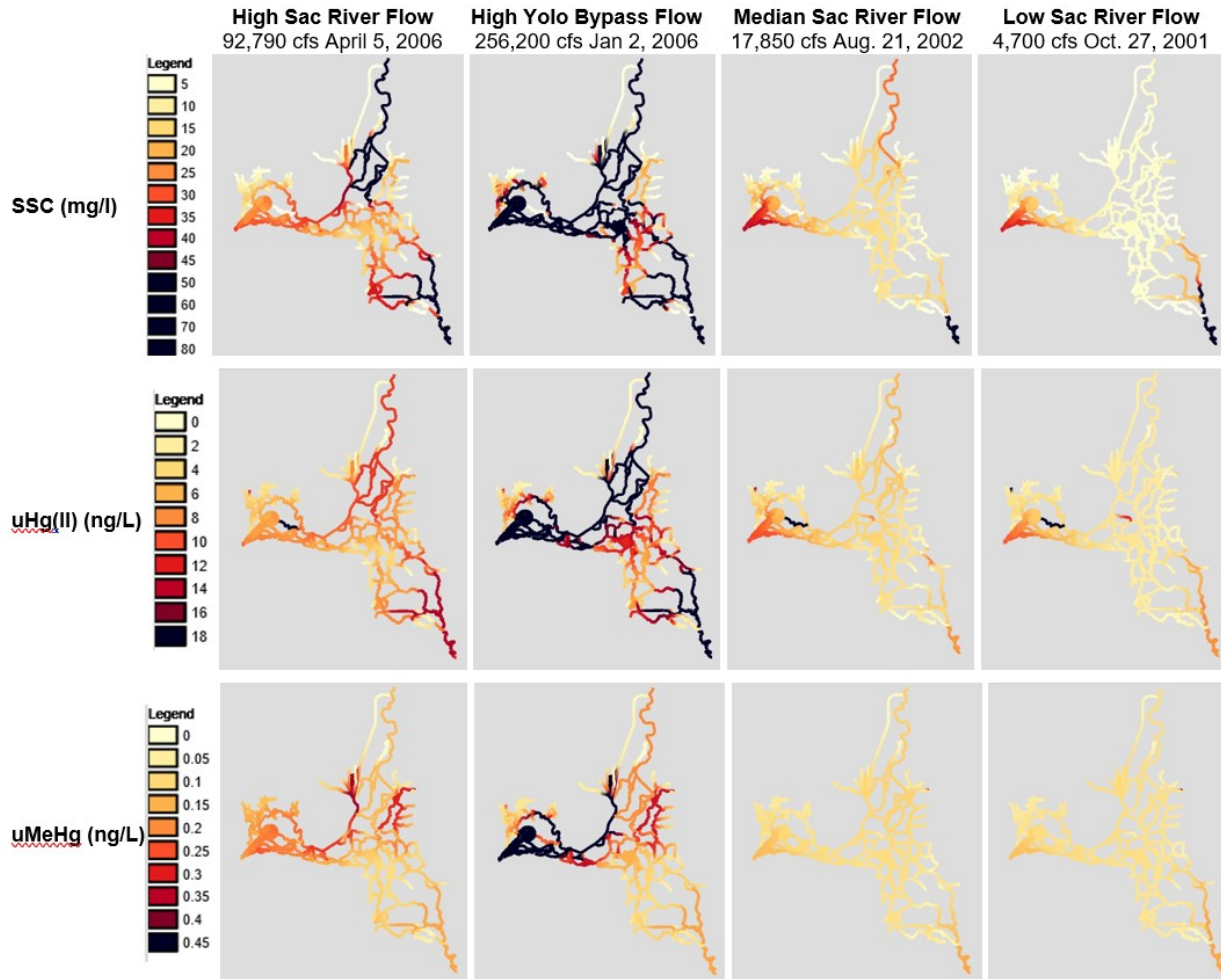
Bed Sediment Spatial Patterns

Observations and model results for Hg and MeHg concentrations in surface sediments are shown in Figure 5-17. Due to limited data all observations from 1999-2017 were included, and averages were calculated at locations with multiple samples. Model results are presented for the last day of the simulation period (August 2, 2006).

Observed Hg concentrations in surface sediments were highest in the Yolo Bypass, and were generally higher in downstream Delta areas modeled than the Central Delta. Observed MeHg concentrations in surface sediments were also highest in the Yolo Bypass. In contrast with Hg, MeHg concentrations in surface sediments were higher in the Central Delta than in Detlta areas downstream. It is important to note, especially for MeHg, that the data included in Figure 5-17 were collected during different studies, span multiple years and include samples from all months of the year. Because MeHg concentrations vary seasonally and among years, biases may exist when all data are included in plots. This could lead to the appearance of spatial patterns that are not real, or a lack of patterns where some exist. For these reasons, further analysis of existing data, and likely the collection of additional sediment data, would be needed to more reliably establish spatial patterns for MeHg concentrations in sediments and whether these change with time. The purpose of Figure 5-17 is therefore primarily to demonstrate that simulated concentrations of Hg and MeHg in the surface layer of the sediment bed are comparable in magnitude.

Figure 5-17 Observed and Simulated Sediment Bed Hg and MeHg Concentrations in the Delta
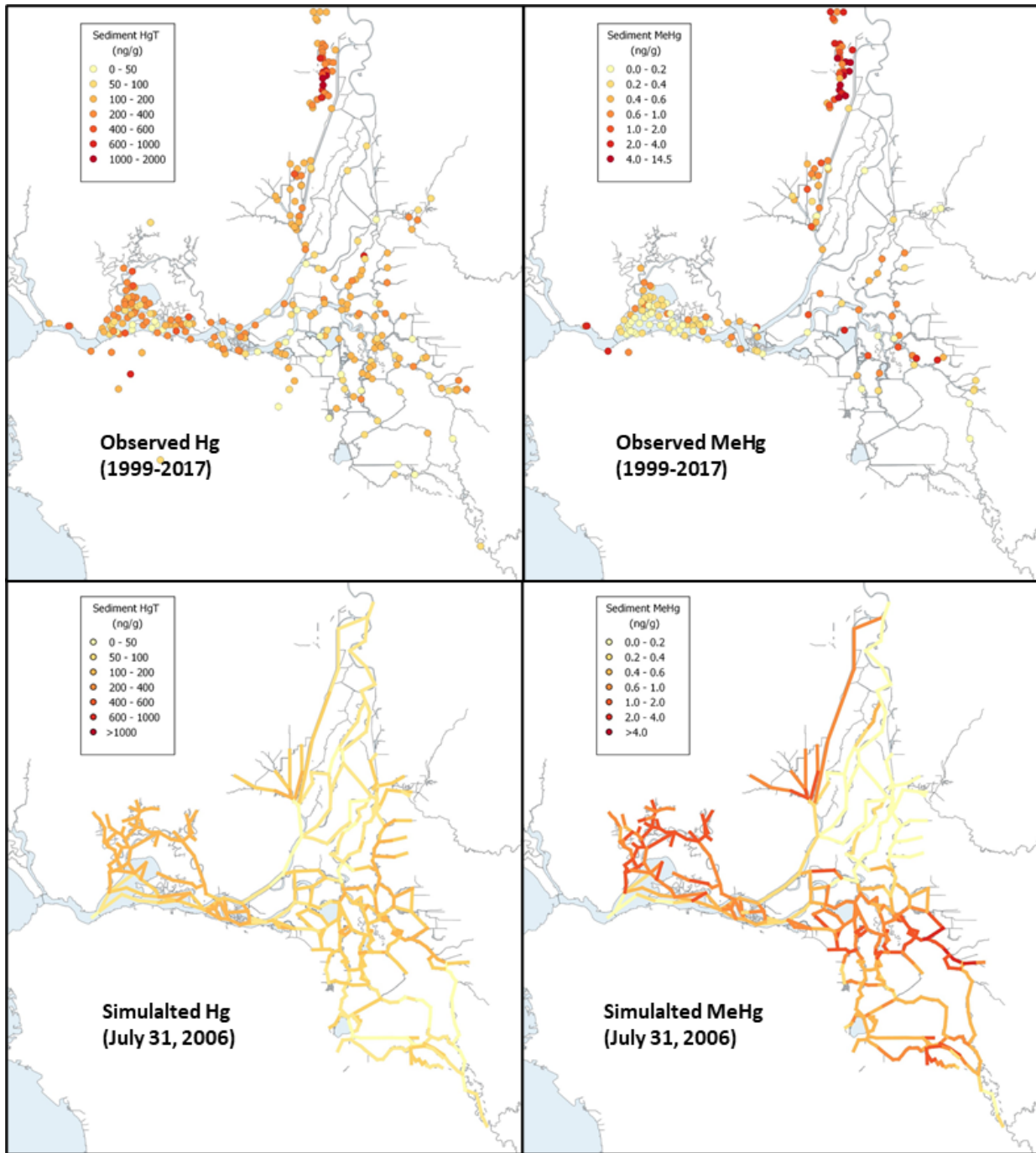
Figure Note: Observations are from 0-5 cm depth, span 1999- 2017 and include all months of the year. Where multiple samples were collected at the same location, values are averaged. Data from Bay and others, 2012; CEDEN, 2018; DiGiorgio, 2018 a,b; Heim and others 2007; Slotton and others; 2002.

Mercury Inflow and Outflow Fluxes

For the overall Hg calibration period October 1999 – July 2006, the Sacramento River was the largest estimated inflowing freshwater source of Hg(II) and MeHg to the Delta (71% and 52% respectively, Figure 5-18. Table 5-5). The magnitude and relative importance of Hg(II) and MeHg loads varied widely among years and months (Figure 5-19, Figure 5-20). Annual freshwater inputs of Hg(II) and MeHg each varied by approximately 6-fold for water years 2000-2006. The relative importance of tributaries as sources of Hg and MeHg also varied from year to year. Yolo Bypass represented about one third of the external supply of MeHg to the Delta for the overall simulation period (Figure 5-18), but this ranged from 3-50% among the years simulated (Figure 5-21). Under some high-flow months, Yolo Bypass was the largest external source of MeHg to the Delta (Figure 5-20).

The largest simulated outflows of inorganic Hg(II) and MeHg were exports at Chipps Island (89% and 85% respectively, see Figure 5-18). The Delta was simulated to be a net long-term sink for Hg and MeHg, exporting roughly half the inflowing load of Hg and 87% of the inflowing MeHg load.

Figure 5-18 Estimated Average Annual Delta uHg(II) and uMeHg Inflows and Outflows for Oct.1999-July 2006. Inflow loads are from regressions based on tributary field data. Outflows are modeled with DSM2-Hg.

Into the Delta

Leaving the Delta

uHg(II)
- Sacramento (71%, 277 kg)
- San Joaquin (8%, 31 kg)
- Yolo Bypass (18%, 70 kg)
- Cosumnes (< 1%, 4 kg)
- Mokelumne (< 1%, 2 kg)
- Calaveras (< 1%, 4 kg)

uHg(II)
- CVP (5%, 13 kg)
- SWP (6%, 17 kg)
- Chipps Island (89%, 242 kg)

uMeHg
- Sacramento (52%, 2966 g)
- San Joaquin (11%, 608 g)
- Yolo Bypass (34%, 1953 g)
- Cosumnes (3%, 146 g)
- Mokelumne (< 1%, 32 g)
- Calaveras (< 1%, 24 g)

uMeHg
- CVP (7%, 312 g)
- SWP (8%, 387 g)
- Chipps Island (85%, 3874 g)
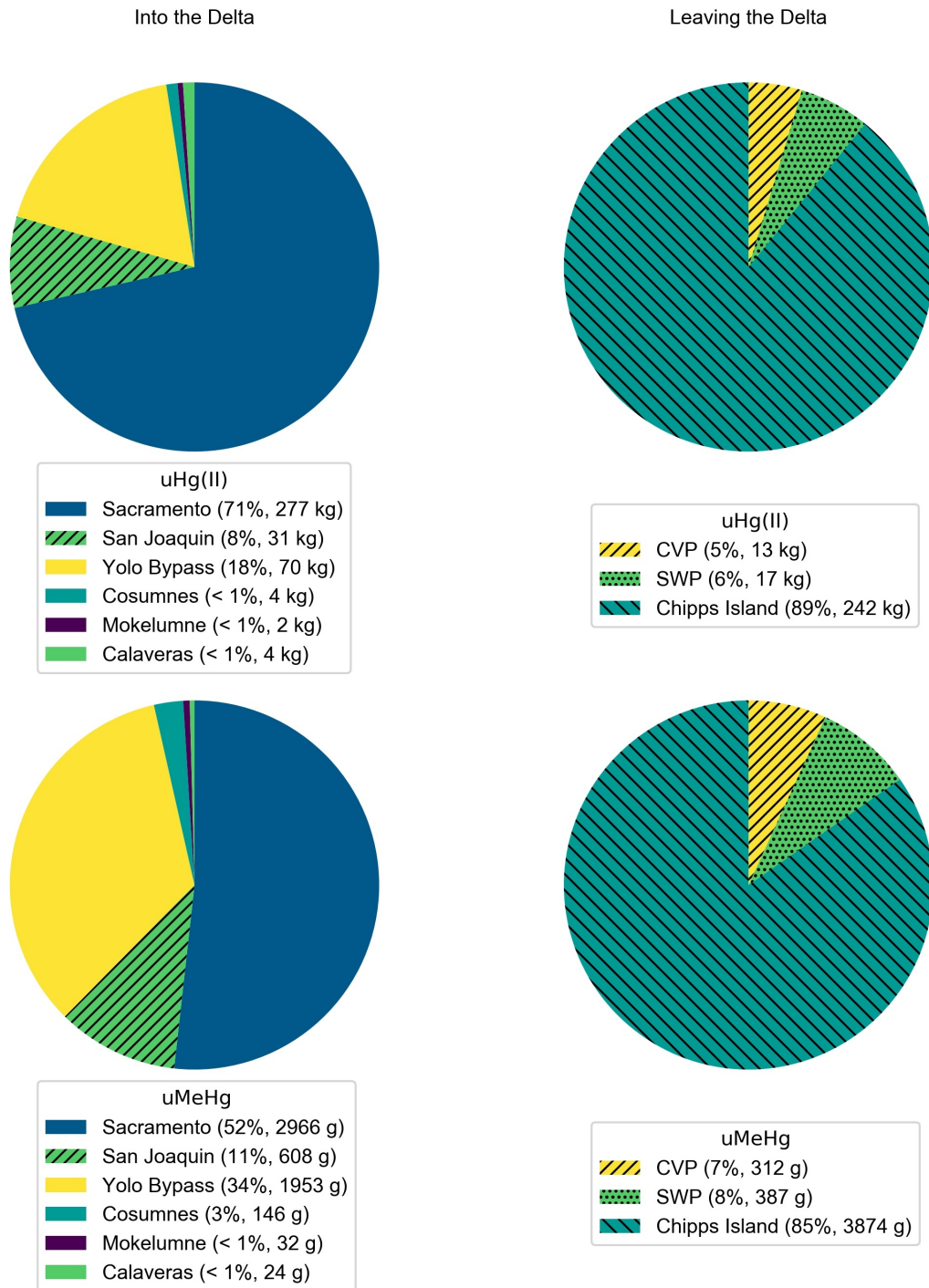
Figure Note: Inflow loads are from regressions based on tributary field data. Outflows are modeled with DSM2-Hg.

Figure 5-19 Estimated Annual Delta Inflows and Outflows for uHg(II) and uMeHg for Oct. 1999 to July 2006.
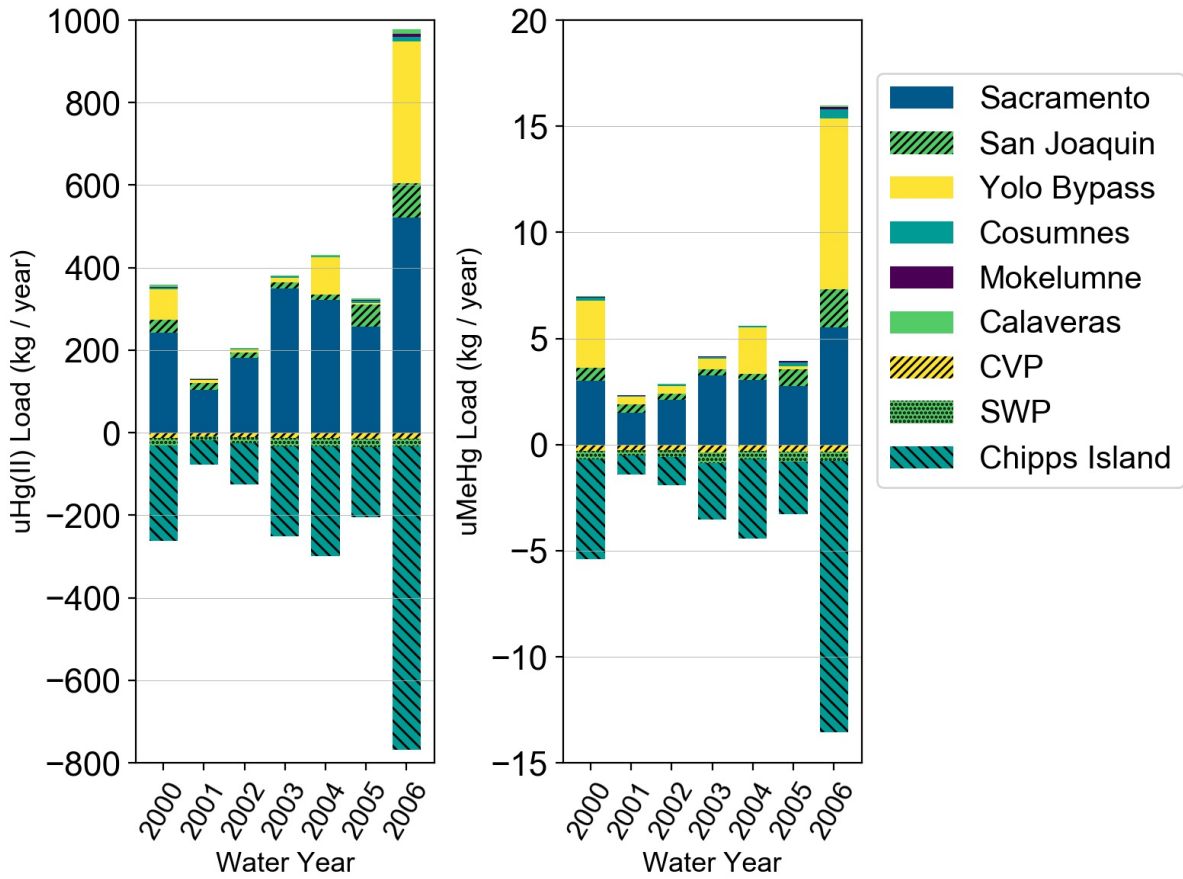
Figure Note: Inflow loads (positive) are from regressions based on field data. Outflows (negative) are modeled with DSM2-Hg.

Figure 5-20 Estimated Monthly Inflows and Outflows for Hg(II) (top panel) and MeHg (bottom panel) in the Delta for Oct. 1999 to July 2006
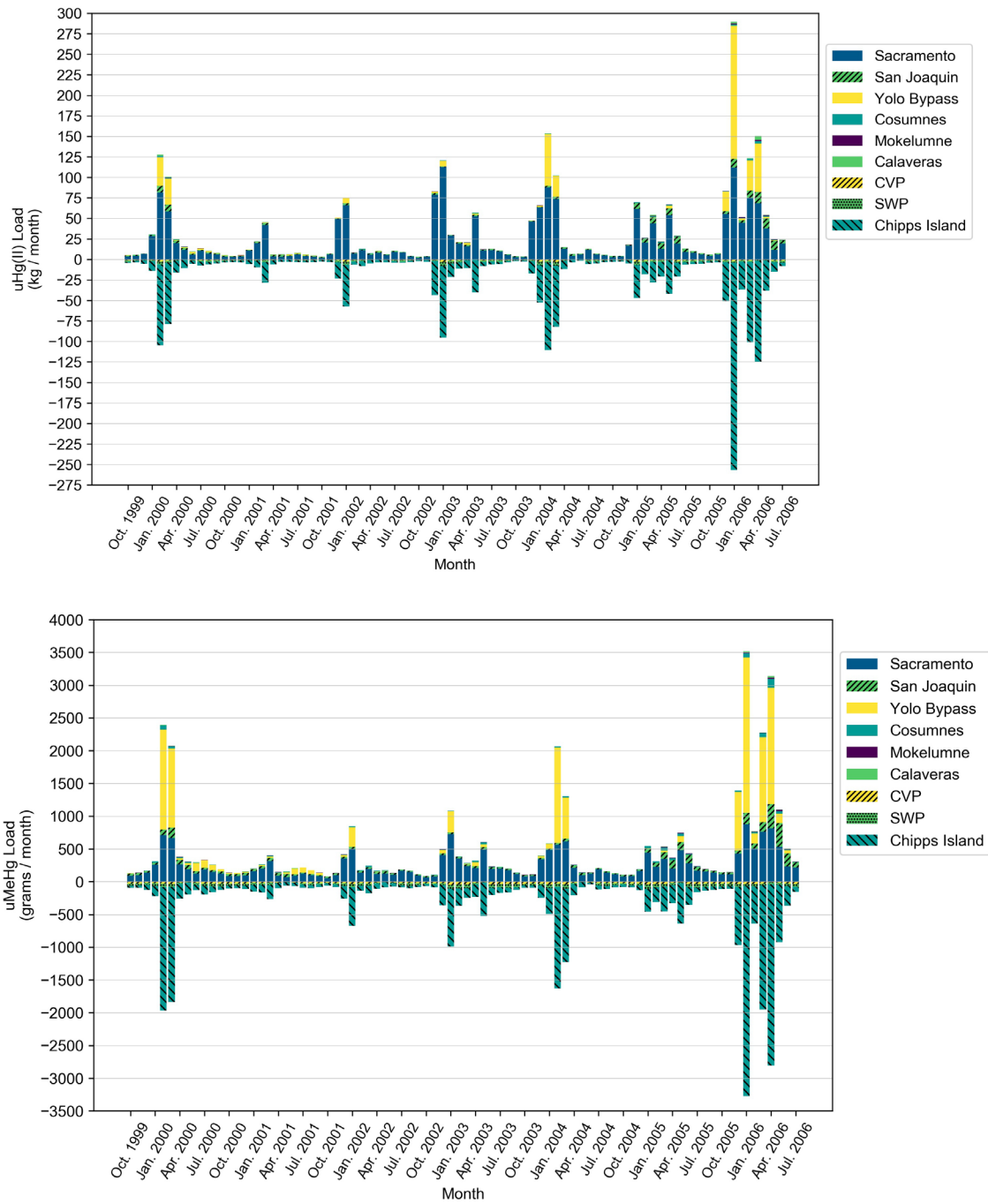
Figure Note: Inflow loads (positive values) are from regressions based on field data. Outflows (negative values) are modeled with DSM2-Hg.

Figure 5-21 Simulated Annual Contributions to the Overall Tributary MeHg Inflow Load for Water Years 2000-2006
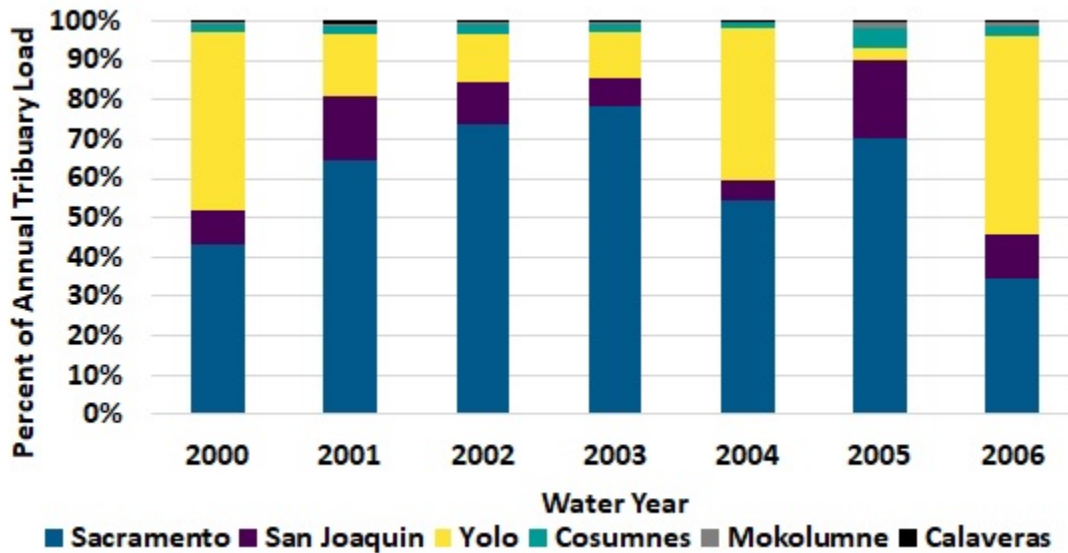
Comparisons to Previous Studies

Model results were compared to values reported by CalFed (Stephenson and others, 2008). Data coverage for the CalFed study spanned a twenty-year hydrologic period (WYs 1984-2003) for Hg and suspended sediment (Louie and others, 2008), and between March 2000 and June 2006 (for MeHg) (Foe and others, 2008), for all major freshwater sources and exports.

Modeled and observed MeHg time periods were similar and although Foe and others, 2008 did not collect samples in every month, average MeHg loads between the two studies generally showed good agreement (Table 5-6). For example, average Yolo Bypass MeHg inputs to the Delta were 1.92 kg/year and 2 kg/year for the observed and modeled results, respectively. The time periods between the two studies for Hg and suspended sediment are not directly comparable, especially given the high year to year variability evident in Figure 5-22.

Table 5-6 Comparison of uHg, uMeHg and Suspended Sediment Loads Reported to CALFED and Average Input Loads from the DSM2-Hg Model

	*CalFED 2008 Report			Delta Mercury Model (DSM2-Hg)		
	THg*	MeHg**	Suspended Sediment	Hg(II)	MeHg	Suspended Sediment
Yolo Bypass Input	[1]167.8 kg/yr	[2]1.92 kg/yr	[1]1107.3 Gg/yr	69 kg/yr	2 kg/yr	382 Gg/yr
Sacramento River Input	[1]182.7 kg/yr	[2]2.54 kg/yr	[1]958.5 Gg/yr	270 kg/yr	3 kg/yr	1548 Gg/yr
San Joaquin River Input	[1]28.3 kg/yr	[2]1.27 kg/yr	[1]236.9 Gg/yr	30 kg/yr	0.6 kg/yr	257 Gg/yr
Total inputs to the Delta	[1]416 kg/yr	[2]5.97 kg/yr	[1]2410 Gg/yr	378 kg/yr	5.6 kg/yr	2207 Gg/yr
Delta export to San Francisco Bay	[1]197.9 kg/yr	[2]3.54 kg/yr	[1]801 Gg/yr	237 kg/yr	3.8 kg/yr	1047 Gg/yr
Annual sedimentation rate	200 kg/yr		1497 Gg/yr	116 kg/yr	1.2 kg/yr	1067 Gg/yr
Annual load contribution from Sacramento River and Yolo Bypass	84%		86%	90%	86%	87%

*Table Note: Full CalFED report Stephenson and others, 2008.

[1]Values adapted from Louie and others, 2008, Table 1, Task 2 (Total Hg and Suspended Sediment). Loads calculated for WYs 1984-2003. Input loads for the Yolo Bypass, the Sacramento River and the San Joaquin were calculated for the Yolo Bypass at Prospect Slough, Sacramento River at Freeport, and San Joaquin River at Vernalis, respectively. See Table 1 for all locations used to calculated total inputs to the Delta. Delta exports to San Francisco Bay calculated at Mallard Island

[2]Values adapted from Foe and others, 2008, Table 4, Task 2 (MeHg). Loads calculated for samples collected intermittently between March 2000-June 2006. Loads are for the Yolo Bypass at Prospect Slough, Sacramento River at Freeport, and San Joaquin River at Vernalis. Total Delta inputs represent the sum of the loads from these three sites plus the Cosumnes River and the Mokelumne River. Delta exports to San Francisco Bay calculated at Mallard Island.

For DSM2-Hg, load estimates represent average values over the simulation period from October 1999 through July 31, 2006. Delta exports to San Francisco Bay calculated at Chipps Island.
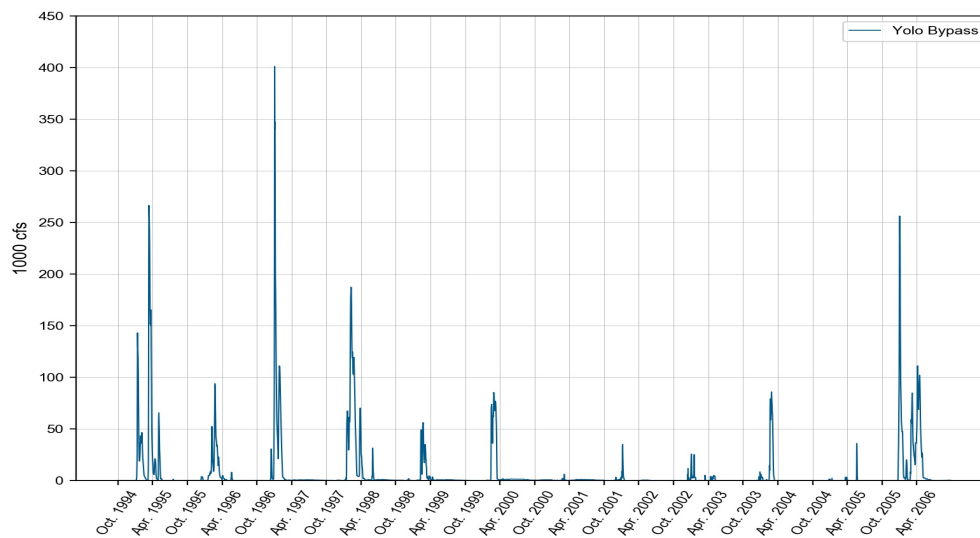
Figure 5-22 Historical Flows for the Yolo Bypass

Figure Note: Flows from DSM2-Hydro using data from CDEC station YBY, Yolo Bypass near Woodland. Data available beginning 1989.

Modeled import and export MeHg loads in g/day were similar to those reported by Foe and others (2008) As shown in Table 5-7, the sum of all modeled tributary imports of MeHg into the Delta totaled 15.7 g/day, while MeHg exports totaled 12.5 g/day. In comparison, between March 2000 and June 2006, total tributary inputs reported by Foe and others (2008) were 16.6 g/day, total exports were 11.3 g/day and exports by the State and Federal water projects to Southern California were calculated at 1.5 g/day (Task 2, Figure 9, Foe and others, 2008). Sediment-water fluxes were similar between the two comparisons, however, as shown by the net sediment flux, the Delta was a net sink for MeHg due to the large settling term and the small sediment-water flux term.

Table 5-7 Comparison of Observed and Simulated MeHg fluxes (g/day) for Selected Locations of Processes

Location	*CalFED 2008 Report	Delta Mercury Model (DSM2-Hg)
Export to SF Bay	-9.8	-10.6
Sum of all Tributary Inputs	16.6	15.7
Sum of S. CA and SF Bay Exports	-11.3	-12.5
Sum of SWP and CVP Exports	-1.5	-1.9
Sedimentation	-4.9	-2.4
Photodegradation	-2.5	-1.4
Open Water Sediment Flux	0.48	0.42
Net sediment-water flux	-4.42	-1.76

*Adapted from Figure 9, Foe and others, 2008

Table Note: Positive values indicate imports into the Delta. Negative values indicate exports out of the Delta. See Table 5-4 for locations used for import and export sites used by DSM2-Hg.

Discussion

Model Development

An existing hydrodynamic model for the Delta, DSM2, was successfully extended to add the capability to simulate Hg cycling in Delta waters and the sediment bed. The model was also enhanced to simulate sediment transport and include the sediment bed as a compartment. These additions were needed for several reasons. First, Hg has a strong tendency to bind to sediments. In systems such as the Delta with significant concentrations of suspended sediment (e.g. >10-20 mg/L), the majority of Hg in surface waters can often be associated with particles. Second, sediment transport and fate become important in terms of determining the remobilization, transport and fate of legacy mercury contamination that occurred in the past. Finally, the surface layer of the sediment bed is important because this is a key zone for the conversion of inorganic Hg into MeHg.

Model Fit to Observations

Overall, the model calibration results reasonably fit observations of suspended solids, uHg and uMeHg in Delta waters. The model simulated suspended sediments well at multiple locations in the Delta (Figure 5-10), both in magnitude and short-term variability over a range of flow conditions. The model fit to observed concentrations of uHg and uMeHg in surface waters was less robust than for suspended

sediments but still reasonable in terms of capturing the magnitude of concentrations on dates when observations were available (Figure 5-14, Figure 5-15). The model demonstrated a higher degree of variability for uHg and uMeHg than observations, often changing quickly in simulations. Given the high observed and simulated variability of suspended sediments in Delta waters (Figure 5-10), and the strong tendency for Hg to bind to particles, at least a part of the explanation for greater variability in simulated concentrations of uHg (and uMeHg) could be related to less field information being available for uHg and uMeHg, potentially at times when short term spikes might occur during high-flow events. It is also not surprising that suspended sediment simulation results are more robust than for Hg given both the availability of high resolution (15-min) continuous field observations for SSC at major tributary inflow locations and additional uncertainties that apply to Hg, including limited information to characterize concentrations and variability in tributary Hg loads, and additional processes affecting Hg cycling in the Delta.

The model was also used to examine spatial trends for suspended solids, uHg(II) and uMeHg in the Delta, and whether any such trends varied with time, e.g. as a function of flow. Spatially, relative to other Delta regions, Davis and others, 2008 and Slotten and others, 2002 observed lower Hg concentrations in fish tissue in the Central Delta. In terms of modeled suspended sediment, a snapshot of the highest flows in the Sacramento River and Yolo Bypass showed high concentrations of suspended sediment on the outer areas of the Delta and lower concentrations in the Central Delta (Figure 5-16), likely due to settling as tributary inflows entered the Delta. This pattern was also observed for modeled uHg(II) in Delta waters, as Hg(II) associated with particles may have followed similar sediment settling trends. This trend was not evident in simulations for uMeHg in the water column or bed sediments in the Central Delta (Figure 5-16, Figure 5-17). Surface water and sediment bed observations for Hg and MeHg concentrations were insufficient to establish the accuracy of spatial variability simulated by the model.

Simulated Hg and MeHg Fluxes

The Sacramento River was the largest estimated source of water, suspended sediments, uHg(II) and uMeHg to the Delta for the simulation period (>50% in all cases) (Figure 5-9, Figure 5-11,Figure 5-18). Estimated tributary loads of suspended sediments, uHg(II) and uMeHg were highly variable with time in simulations at time scales from daily to yearly (Figure 5-12, Figure 5-19, Figure 5-20). This was because (1) flow regimes were highly dynamic and spanned a range of wet and dry years, and (2) estimates of most tributary loads for these constituents were based on regressions that ultimately depended on flow as the independent variable, the exception being Yolo Bypass loads which were estimated with the D-MCM model. Annual tributary loads of uHg(II) and uMeHg were estimated to vary six-fold for water years 2000-2006 (Figure 5-19). There was also a strong seasonality to flows and loads, with greater rates during winter (Figure 5-20). This has important implications when using baseline monitoring data to set targets for future MeHg loading, and when monitoring for compliance. A multi-year perspective is needed.

The relative importance of major tributaries as sources of MeHg also varied among and within years and depended on hydrology. For example the Yolo Bypass represented one third of the overall MeHg load from inflows for water years 2000-2006 (Figure 5-18), but ranged from 3-50% annually (Figure 5-21), with greater importance during wetter periods (expected for a flood control structure). The Delta was simulated to be a sink for suspended sediments, inorganic Hg and MeHg. Exports at Chipps Island were roughly 50% less than inflow loads for suspended sediments, 25% less for uHg, and 13% less for uMeHg for the simulation period.

It is important to note that large tributary sources of uHg and uMeHg do not necessarily lead to higher concentrations. The combination of a high flow and low concentration for a tributary could lead to a source being large relative to other tributary inputs but acting to dilute concentrations in receiving waters. If, for example, measures were taken that reduced the flow of a source with lower than the average MeHg concentration for tributaries, it might not lead to lower concentrations in Delta waters. Additional simulations would be needed to explore this concept, but the key point is that it is important to consider concentrations as well as loads for tributaries when evaluating remedial options.

Key Processes

The model analysis confirmed the key roles of hydrodynamics and sediment transport in terms of affecting mercury cycling in the Delta. Increased flow led to increased tributary loads and increased internal mobilization and transport of sediment and associated Hg and MeHg. The dynamic nature of flow in the Delta (and the Yolo Bypass) resulted in a high degree of variability in simulated concentrations of uHg and uMeHg concentrations, inflowing loads and export rates in the short term (e.g. daily) and longer term (e.g. annually).

Uncertainty

Two common sources of uncertainty for model analyses are data and knowledge gaps. While there have been a range of Hg studies in the Delta, they have been undertaken with a variety of objectives and not necessarily designed to quantify Delta-wide fluxes of MeHg and Hg. Therefore more data is desirable to better quantify fluxes over the Delta The large geographic area included in the Delta, wide range of conditions within it, and the high variability of conditions over short periods of time, also add to the challenge of characterizing concentrations, fluxes and key processes affecting Hg and MeHg in the Delta.

In terms of the state of knowledge of mercury cycling in aquatic systems, this continues to evolve, but gaps remain that contribute to model uncertainty. For example, research is ongoing in the scientific community to identify the pool of mercury available for methylation, and whether some sources of Hg(II) to a system are more bioavailable than others. Of relevance to the Delta, which sometimes has high loads of suspended sediment and particulate Hg(II), is whether Hg(II) on suspended sediments is less available for methylation in the system than dissolved Hg(II) loads. This could affect the relative importance of different sources of Hg(II) to the Delta, in terms of contributing to MeHg production. The effects of vegetation on mercury cycling and MeHg production specifically are also topics of recent research (e.g. Chapter 3 in this study and USGS studies by Windham-Myers and others, (2014) are important for the Delta, in terms of affecting MeHg supply from wetland areas and the Yolo Bypass.

Overall, available data and the state of knowledge of mercury cycling were sufficient for the model analysis to proceed but limited the confidence that could be assigned to simulation results. Future application of DSM2-Hg using PEST++ software will help to better identify sources of uncertainty in the model analysis.

Conclusions

The DSM2 hydrodynamic model for the Delta was extended to included sediment transport and mercury cycling in Delta waters and the sediment bed. The model reasonably fit observations of suspended sediment, inorganic Hg and MeHg concentrations in Delta waters. Simulations indicated that flow and

sediment transport have a strong influence on Hg cycling, supporting the need to include these processes in the model analysis. The Sacramento River was the largest estimated source of water, suspended sediments, Hg and MeHg to the Delta for the Hg simulation period from October 1999-July 2006 (>50% in all cases). Dynamic flows in the Delta led to high variability in fluxes and concentrations of suspended solids, uHg(II) and uMeHg in inflowing tributaries and in Delta waters during simulations. Annual estimated inflow loads of uHg(II) and uMeHg to the Delta varied by six-fold during the simulated period. Simulations were also characterized by variable concentrations and fluxes on shorter time scales, e.g. months and during events. The Yolo Bypass represented one third of the overall uMeHg load from inflows for water years 2000-2006, but ranged from 3-50% among years, with greater importance during wetter periods (expected for a flood control structure). This temporal variability has important implications when using available data to set targets for uMeHg loading, and when monitoring compliance. A multi-year perspective is needed as well as the ability to capture short term dynamics. The Delta was simulated to be a sink for suspended sediments, uHg(II) and to a lesser extent, uMeHg. Spatially, the model analysis simulated lower concentrations of suspended sediments and uHg(II) in the Central Delta, but not uMeHg. Available data were insufficient to support or refute simulated spatial patterns. Overall, available data and the state of knowledge of mercury cycling were sufficient for the model analysis to proceed and provide meaningful results but limited the confidence that could be assigned to the analysis.

Data/Knowledge Gaps and Next Steps

- **Data gaps**: Available field data were limited in terms of characterizing boundary inflow loads, and concentrations within the Delta, for suspended sediments, uHg(II) and uMeHg. This was partly due to the large geographic area involved. This issue was magnified by the dynamic nature of hydrology in the Delta, leading to a high degree of temporal and spatial variability that could not be captured with limited sampling. This constrains the current ability to quantify mercury cycling in the Delta to a coarser perspective rather than a tightly quantified analysis. Additional data are needed to better characterize inflow loads and within-Delta conditions for a range of hydrologic conditions and a range of years. These data include measurements of inorganic Hg and MeHg in filtered, unfiltered and particulate phases in the water column and sediments, as well as ancillary data such as water chemistry and sediment characterization. Concentration data needs to be collected in a manner allowing the estimation of fluxes at key points in the system, in order to confirm which sources of inorganic Hg and MeHg are most important, and when.
- **Model Development:** The current model analysis included the Delta and Yolo Bypass, using separate models and passing outputs from one model to the other. The model analysis indicated that tributary inflows have a strong influence on mercury concentrations in the Delta. Exports from the Delta may also be an important source of MeHg to downstream areas including San Francisco Bay. Consideration could be given to the merits (and cons) of a model analysis extending beyond the legal Delta.
- **Scientific gaps**: There are scientific gaps that also contributed to uncertainty in the model analysis, including:
    - What pool of Hg(II) is available for methylation? This question has persisted for decades and is challenging to resolve but is especially important at sites with legacy Hg contamination.
    - Is mercury on suspended and bed sediments readily exchangeable or are some sources of inorganic Hg more important that others, in terms of supplying MeHg production? The

analysis carried out in this study assumed that Hg on solids is readily exchangeable with the dissolved phase.
- How does vegetation influence MeHg cycling and production? This question is primarily related to loads from the Yolo Bypass, but has important implications for MeHg supply to the broader Delta.

- **Modeling Scope**:
  - MeHg in fish: Given that fish and shellfish MeHg levels are the ultimate end point of interest, the model analysis could be extended to include a food web and bioaccumulation component.
  - Management Scenarios: Time and resources prevented using the developed DSM2-Hg model to evaluate system perturbations to drivers of interest. As approved by the Regional Board, development of the DSM2-Hg model met open water DMCP regulatory requirements, however, future work could apply the model to evaluate how changes to the system would impact MeHg loads and concentrations. Depending on the changes simulated, modifications could be required to the models used and other models may be necessary in order to realistically simulate operational scenarios (discussed further below).
  - Climate change is altering conditions in the Delta that have the potential to affect Hg cycling and bioaccumulation (see for example, Dettinger and others, 2016 and Chapter 6). This issue should be incorporated into future assessments.
  - Sensitivity and uncertainty analyses have not yet been carried out for DSM2-Hg simulations of the Delta, due to time constraints. The future application of DSM2-Hg using PEST++ will provide information on sensitivity and uncertainty, in addition to refining the model calibration.

- **Model Development:** Simulating any changes to operational conditions would require an analysis to estimate Delta inflows and Yolo Bypass operations. Commonly this is done by running the SWP/CVP operations model CALSIM (DWR, 2020c).
  - If Yolo Bypass outflows are used to provide boundary conditions for the Delta model, Delta modeling can only occur during the period and for the management options that have already been run using the Yolo Bypass model. Simulations of different operational scenarios would currently require re-running the proprietary hydrologic model (TUFLOW) and the D-MCM Hg model for the Yolo Bypass. The D-MCM model was also applied to the Yolo Bypass at a coarse spatial resolution. An alternative to these two proprietary models would be to use different simulation software for the Yolo Bypass, for all aspects of the simulations. This could involve using one model for the Yolo Bypass and another (DSM2-Hg) for the Delta, or a single model for the Delta and the Yolo Bypass. Preferably the software would be publicly available software. Within DWR, this platform now exists. If the goal is the long-term use of the Delta model, then consideration should be given to this approach.
  - Model improvements are necessary and important gaps, however, without additional data, the resolution of the model will not improve, therefore it is important that model improvements and increased data gathering efforts happen in parallel.

Program coordination: The ability to quantify and understand sources, sinks, and concentrations of Hg and MeHg in the Delta would benefit from a coordinated Delta-wide program with a specific focus on mercury. In the past and currently, there have been a variety of separate studies, some of which include Delta-wide monitoring for end points of interest such as Hg concentrations in biota (for example the Delta

Regional Monitoring Program), but there is not yet a well-funded, Delta-wide coordinated program to quantify the processes the govern the trends being monitored. The Bay-Delta Hg strategy (Weiner and others, 2003) stated that effective coordination will be crucial for a successful Hg program and suggested that the California Bay Delta Authority recruit or appoint a point of contact on Hg issues. In 2020, this roll could be fulfilled by the Delta Science Program. The coordinating entity would fulfill several duties which include serving as the chief overseer for a Delta-wide effort to identify data and knowledge needs, carry out or oversee studies to address gaps, and create a more robust characterization and understanding of Hg in the Delta and Yolo Bypass.

References

Bay SM, Vidal-Dorsch DE, Lowe S, Gehrts Fetscher AE. 2012. Survey of Sediment Quality in the Sacramento-San Joaquin Delta. Southern California Coastal Water Research Project. Technical Report 686. March 2012.

CEDEN. 2018. www.ceden.org

CNRA, 2020. Methodology for Flow and Salinity Estimates in the Sacramento-San Joaquin Delta and Suisun Marsh, Annual Report prepared by the Department of Water Resources submitted to the State Water Quality Control Board, posted on California Natural Resources Agency website https://data.cnra.ca.gov/dataset/methodology-for-flow-and-salinity-estimates-in-the-sacramento-san-joaquin-delta-and-suisun-marsh. Accessed July 29, 2020.

Davis JA, Greenfield BK, Ichikawa G, Stephenson M. 2008. Mercury in Sport Fish from the Sacrament-San Joaquin Delta Region, California, USA. Science of the Total Environment, Volume 391, Issue 1, Pages 66-75.

Dettinger, M., Anderson, J, Anderson M, Brown LR, Cayan, D., Maurer, D. 2016. Climate Change and the Delta. San Francisco Estuary and Watershed Science, Volume 14, Issue 3, Pages 2-26.

DiGiorgio C. 2018a. Spreadsheet titled DWR_DFW_Yolo Bypass sed sample results_Mar-Apr2015_MLML MeHg & Hg.xlsx. Emailed to R. Harris August 23, 2018.

DiGiorgio C. 2018b. Spreadsheet titled Consolidated datasets.xlsx. Emailed to R. Harris August 23, 2018.

DWR, 2020a. DSM2: Delta Simulation Model II, California Department of Water Resources website https://water.ca.gov/Library/Modeling-and-Analysis/Bay-Delta-Region-models-and-tools/Delta-Simulation-Model-II. Accessed July 29, 2020.

DWR, 2020b. DICU: Delta Island Consumptive Use, California Department of Water Resources website https://water.ca.gov/Library/Modeling-and-Analysis/Bay-Delta-Region-models-and-tools/DICU. Accessed July 29, 2020.

DWR. 2020c. https://water.ca.gov/Library/Modeling-and-Analysis/Central-Valley-models-and-tools/CalSim-3 Accessed August 8, 2020.

Finch R. 2014. Quantitative calibration of DSM2, Chapter 2 in Methodology for Flow and Salinity Estimates in the Sacramento-San Joaquin Delta and Suisun Marsh, 35th Annual 660 Progress Report to the State Water Resources Control Board.

Foe CG. 2003. Mercury Mass Balance for the Freshwater Sacramento-San Joaquin Bay-Delta Estuary. Final report submitted to the CALFED Bay-Delta Program for the project: An Assessment of the Ecological and Human Health Impacts of Mercury in the Bay-Delta Watershed (Task 1A). California Regional Water Quality Control Board, Central Valley Region. Sacramento, CA. Available at: http://islandora.mlml.calstate.edu/islandora/object/islandora%3A7d1c00fc-e68d-4fb1-a683-25b43cf68a11. Accessed July 27, 2020.

Foe C, Louie S, and Bosworth D. Task 2. Methyl Mercury Concentrations and Loads in the Central Valley and Freshwater Delta, August 2008. In Transport, Cycling, and Fate of Mercury and Monomethyl Mercury in the San Francisco Delta and Tributaries: An Integrated Mass Balance Assessment Approach. CALFED Mercury Project Final Report, September 15, 2008. Available at: http://islandora.mlml.calstate.edu/islandora/object/islandora%3A08af4458-e767-4484-9bae-b0608b47852b. Accessed July 27, 2020.

Heim WA, Coale KH, Stephenson M, Choe KY, Gil GA, Foe C. 2007. Spatial and Habitat-Based Variations in Total and Methyl Mercury Concentrations in Surficial Sediments in the San Francisco Bay-Delta. Environmental Science and Technology. Volume 41, Pages3501-3507.

Hsu E, Anderson J, Sandhu P. 2019. DSM2 Sediment Transport Model (GTM-SED). Methodology for Flow and Salinity Estimates in the Sacramento-San Joaquin Delta and Suisun Marsh. 40th Annual Progress Report from the California Department of Water Resources to the State Water Resources Control Board, Chapter 4.

Hsu E, Ateljevich E, Sandhu P. 2014. DSM2-GTM. Methodology for Flow and Salinity Estimates in the Sacramento-San Joaquin Delta and Suisun Marsh. 35nd Annual Progress Report from the California Department of Water Resources to the State Water Resources Control Board, Chapter 4.

Liang L. 2018. Updating the DSM2 Historical Simulation. Methodology for Flow and Salinity Estimates in the Sacramento-San Joaquin Delta and Suisun Marsh. 39th Annual Progress Report from the California Department of Water Resources to the State Water Resources Control Board, Chapter 3.

Liu L. and Sandhu N. 2012. DSM2 Version 8.1 Recalibration. Chapter 3 in Methodology for 683 Flow and Salinity Estimates in the Sacramento-San Joaquin Delta and Suisun Marsh, 33rd Annual Progress Report to the State Water Resources Control Board.

Louie S, Foe C, Bosworth D. 2008. Task 2. Mercury and Suspended Sediment Concentrations and Loads in the Central Valley and Freshwater Delta, August 2008. In Transport, Cycling, and Fate of Mercury and Monomethyl Mercury in the San Francisco Delta and Tributaries: An Integrated Mass Balance Assessment Approach. CALFED Mercury Project Final Report, September 15, 2008. Available at: http://islandora.mlml.calstate.edu/islandora/object/islandora%3A92beb721-5d4b-450f-b26d-c226c71cc458/datastream/OBJ/view. Accessed July 27, 2020.

Morgan-King Tara L, and Wright Scott A. 2013. Computation of Suspended-Sediment Concentration Data, Sacramento-San Joaquin River Delta, California, Water Years 2011-2013: U.S. Geological Survey Data Series Report.

NHC (Northwest Hydraulic Consultants). 2003. Assessment of sediment budget of Sacramento-San Joaquin Delta. Report prepared for the California Department of Water Resources, Sacramento, California, July 2003, 36 pages.

Sandhu P. 2016. "OMG! Yet Another Animator." DSM2 Users Group Meeting, December 2016.

Slotton DG, Ayers SM, Suchanek TH, Weyand RD, Liston AM, Asher C, Nelson DC, Johnson B. 2002. The Effects of Wetland Restoration on the Production and Bioaccumulation of Methylmercury in the Sacramento-San Joaquin Delta, California. Submitted to CALFED, September 25, 2002. 48 pages.

SRWP. 2004. Microsoft Access database that compiles Sacramento River Watershed water quality data collected for the Sacramento River Watershed Program. Database provided by Larry Walker Associates (Claus Suverkropp) to Central Valley Regional Water Quality Control Board (Michelle Wood, Environmental Scientist, Sacramento).

Stephenson M, Foe C, Gill GA, Coale KH. 2008. Transport, Cycling, and Fate of Mercury and Monomethyl Mercury in the San Francisco Delta and Tributaries: An Integrated Mass Balance Assessment Approach, CALFED Mercury Project Final Report, September 15, 2008. Available at: http://islandora.mlml.calstate.edu/islandora/object/islandora%3A4f5a7824-2efa-480f-a9d1-bff55261f59b. Accessed July 27, 2020.

Weiner, JG, Gilmour CC, Krabbenhoft DP. 2003. Mercury Strategy for the Bay-Delta Ecosystem: A Unifying Framework for Science, Adaptive Management, and Ecological Restoration. Final Report to the California Bay Delta Authority. December 31, 2003. 67 pages. Available at: https://www.google.com/search?sxsrf=ALeKk01EPJj-apQZHWVsfYIRL1qUfcQaDA%3A1597078520984&source=hp&ei=-HsxX9HTObO40PEPt9CbMA&q=nrm.dfg.ca.gov%2FFileHandler.ashx%3FDocumentID%3D4071&oq=nrm.dfg.ca.gov%2FFileHandler.ashx%3FDocumentID%3D4071&gs_lcp=CgZwc3ktYWIQAzoKCC4Q6gIQJxCTAjoHCCMQ6gIQJzoHCC4Q6gIQJ1DKFVjKFWCHLmgBcAB4AIABfIgBfJIBAzAuMZgBAKABAqABAaoBB2d3cy13aXqwAQo&sclient=psy-ab&ved=0ahUKEwjRr62PjZHrAhUzHDQIHTfoBgYQ4dUDCAk&uact=5. Accessed August 10, 2020.

Wyndham-Myers, L., M. Marvin-DiPasquale, E. Kakouros, J.L. Agee, L.H. Kieu, C.A. Stricker, J.A. Fleck, and J.T. Ackerman (2014). Mercury cycling in agricultural and managed wetlands of California, USA: Seasonal influences of vegetation on mercury methylation, storage, and transport

Wood, M. L., C. G. Foe, J. Cooke, and S. J. Louie. 2010. Sacramento-San Joaquin Delta Estuary TMDL for Methylmercury, Staff Report. Regional Water Quality Control Board, California Environmental Protection Agency, Central Valley Region, April 2010.

Mercury Open Water Final Report for Compliance with the Delta Mercury Control Program

Chapter 6. Climate Change Impacts on Water Operations and Mercury Biogeochemistry in the Yolo Bypass and Delta

Submitted by the Open Water Technical Work Team

August 31, 2020

The Open Water Mercury Technical Workgroup

California Department of Water Resources
Division of Environmental Sciences
Carol DiGiorgio
David Bosworth

San Jose State University
Moss Landing Marine Laboratory
Wesley Heim, M.S
Mark Stephenson, M.S. (ret.)

Pacific Northwest National Laboratory
Marine Sciences Laboratory
Gary Gill, Ph.D. (ret.)

United States Geological Survey
California Science Center
David Schoellhamer, Ph.D.
Paul A. Work, Ph.D., P.E., D.CE

Acknowledgements

Contents

List of Figures

List of Tables

List of Acronyms and Abbreviations

CVP	Central Valley Project
Delta	Sacramento-San Joaquin Delta system
D-MCM	Dynamic Mercury Cycling Model
DOC	Dissolved Organic Carbon
DSM2	Delta Simulation Model 2
DWR	(California) Department of Water Resources
Hg	Mercury
MeHg	Methyl mercury or monomethyl mercury
RCP	Representative Concentration Pathway
SWP	State Water Project

Introduction

This chapter describes the major climate change impacts that are predicted for northern California and the Sacramento-San Joaquin Delta region and how these impacts might alter the net production of methyl mercury (MeHg) and its behavior fate and transport in the Yolo Bypass and Delta region. The impacts follow the drivers outlined in California's Fourth Climate Change Assessment (Bedsworth and others, 2018). Generalized impacts based on our current understanding of the biogeochemistry of mercury (Hg) and MeHg are described first, followed by site specific predictions for the Delta and Yolo Bypass based on a literature understanding of Hg and MeHg biogeochemistry and studies conducted for this report.

Key Findings

Climate change is anticipated to have significant impacts on the Sacramento-San Joaquin Delta system (Delta) and Yolo Bypass which will manifest in also impacting the behavior and fate of Hg and MeHg (Table 6-1). Due to projected increases in volatility of winter rainfall events and periods of drought, predicting long-term Hg trends is problematic. However, we anticipate that the Yolo Bypass will continue to remain a significant net exporter of MeHg to the Delta. It is possible that MeHg exports could increase, driven principally by increases in water temperatures which boost microbial methylation. Enhanced MeHg production could also occur due to more frequent and intense storms delivering more Hg and organic matter to the Delta, resulting in enhanced Hg methylation. Extended periods of drought may also occur. In these circumstances, net Hg and MeHg exports from the Yolo Bypass to the Delta, when compared to the Sacramento River, may become insignificant, but the buildup of vegetation between subsequent flood periods may provide increased organic material for methylation when floodwaters return. It is unclear whether periods of extended drought would enhance or reduce Hg methylation in the Delta. It is currently not clear what impacts declining snowpack, shifts in runoff timing, and rising sea level will have on MeHg production, behavior, fate and transport in the Delta system.

Major Climate Change Impacts and Potential Mercury Response

This section describes in general terms how Hg and MeHg might respond to predicted climate change impacts. These predictions are based primarily on literature references of our general understanding of the biogeochemistry of Hg and MeHg.

Temperature Impacts

Temperature in California is expected to increase statewide between 2 and 7 °C by the end of the century (Pierce and others, 2018). Because MeHg is biotically produced by microbial organisms, microbial activity and MeHg production will be greatly influenced by temperature. While there are several factors influencing microbial activity, in a very general sense, warmer temperatures tend to lead to greater microbial activity, which manifests in greater MeHg production (Desrosiers and others, 2006; St. Pierre and others, 2014; Yang and others, 2016).

Table 6-1 Climate Change Impacts on the Delta, Yolo Bypass and Implications for Mercury Response

Climate Impact	Expected Trend[1]	Delta and Yolo Bypass Response	Mercury Response
Temperature	Warming ↗	Warmer air & water temperatures	Potential enhanced microbial methylation of mercury
Precipitation	More precipitation as rain ↗ Less precipitation as snow ↘ Interannual variability ↗ Precipitation frequency ↘ Atmospheric River storm frequency and intensity ↗ [2]	Impact on Delta/Bypass affected by upstream reservoir operations; Greater interannual flooding variability. Flooding may be more severe- could lead to prolonged flooding when it occurs.	Prolonged and greater aerial extent of flooding of the Yolo Bypass could result in greater MeHg production
Snowpack	Declining ↘	Higher winter stream flows since more precipitation falls as rain than snow,	Unknown
Runoff	Shifting earlier and increasing with warmer storms. ←	Impact on Delta/Bypass affected by upstream reservoir operations	Unknown
Extreme Storms	Increasing ↗	Greater interannual flooding variability. Higher flood flows. Possible increased frequency and duration of flooding in the Bypass	Winter MeHg exports from the Yolo Bypass will likely increase due to increased flood duration and a greater extent of flooded area.
Droughts	Increasing ↗	Lower freshwater inflows will move the salinity mixing zone upriver. Limited discharge of freshwater from the Yolo Bypass into the Delta.	In the winter, there will be no or limited export of MeHg from the Yolo Bypass to the Delta during drought periods. Periods of drought may increase cumulative vegetation biomass in the Yolo Bypass resulting in greater MeHg production in subsequent flood events.
Sea Level	Rising ↗	Sea level rise could move the salinity mixing zone upriver; Levees could overtop if not heightened, and previously dry land could become submerged; Minimal or no impact on northern portion of the Bypass.	Newly submerged lands could result in enhanced MeHg production as has been observed when new reservoirs are impounded.
Wildfires	Increasing ↗	Runoff from burn areas could increase contaminants in water	Mercury content of forest biomass and soils will be released into local air and watersheds, providing additional substrate for mercury methylation.

[1] Adapted from California's Fourth Climate Change Assessment (Thorne and others, 2018)

[2] Overall there are expected to be fewer rainfall events, but storms may be more intense when it rains.

Precipitation and Extreme Storm Impacts

A recent report by Gershunov and others (2019) predicts that climate change along the west coast of the United States will result in greater precipitation variability and greater total precipitation, but with fewer precipitation events and greater intensity of individual events. California's Fourth Climate Change Assessment predicts mean annual precipitation to increase modestly in the northern part of the state, and year-to-year variability is also projected to increase (Pierce and others 2018). By the end of the century under the Representative Concentration Pathway (RCP)[1] 8.5 (business as usual) scenario, winter precipitation is projected to increase by up to 20%, but spring and autumn precipitation may decrease by up to 20%. Daily extreme precipitation values are projected to increase 5-15% under the RCP 4.5 (medium emissions) scenario to 15-20% under the RCP 8.5 scenario, presenting challenges for storm drainage and flood control.

The increase in total precipitation and intensity of precipitation events could result in more intense and prolonged flooding events in the Yolo Bypass. This will likely also manifest in a greater aerial extent of the Yolo Bypass being flooded during a storm event. Both manifestations could increase the production of MeHg and enhance MeHg export from the Bypass.

It is not clear what impact precipitation increases and increased storm intensity will have on MeHg production and behavior in the Delta.

Snowpack and Runoff Impacts

With warming trends predicted, more precipitation will fall as rain rather than snow, reducing the snowpack, and shifting runoff earlier in the year (Bedsworth and others 2018; and references therein). These predicted trends will clearly affect operation of reservoirs and water delivery systems (e.g. Wang and others 2018; Schwarz and others 2018), but it is unclear how these snowpack and runoff changes will affect the production and transport of MeHg in the Yolo Bypass and Delta system.

Drought Impacts

Drought periods are anticipated to be more frequent and more intense with dryer seasonal conditions, even if precipitation increases (Bedsworth and others 2018; and references therein). Climate projections show that seasonal summer dryness in California may become prolonged due to earlier spring soil drying that lasts longer into the fall and winter rainy season (Bedsworth and others 2018; and references therein). Obviously, if droughts are more frequent, there will be more frequent periods of time when the Yolo Bypass has no flow going through it and will not be contributing MeHg export to the Delta. Drought impacts on agricultural vegetative growth in the Bypass are probably minimal as the majority of agricultural vegetation in the Bypass is irrigated, including a significant proportion of its largest land-use-pasture. Sources of water in the Yolo Bypass include groundwater pumping and surface water.

---

[1] A Representative Concentration Pathway (RCP) is a greenhouse gas concentration (not emissions) trajectory adopted by the International Panel on Climate Change. RCP 8.5 refers to the concentration of carbon that delivers global warming at an average of 8.5 watts per square meter across the planet. The RCP 8.5 pathway delivers a temperature increase of about 4.3°C by 2100, relative to pre-industrial temperatures.

One of the major findings of this report is that submerged vegetation undergoing degradation is a major process contributing to internal MeHg production in the Yolo Bypass (see Chapter 3 and Technical Appendix E). Hence, any process which will affect biomass production will likely also impact MeHg production. Droughts are typically associated with low biomass production. In the Yolo Bypass however, if irrigation water is available, drought periods will likely not significantly reduce the biomass available for methylation. Hence, during extended drought periods, if irrigation water continues to be available, winter biomass could reach peak production levels in areas that floodwaters would normally remove since flooding events will not occur as frequently. Subsequent flood events, following an extended drought period, will thus likely experience enhanced internal MeHg production from the vegetation that has built up during the drought period. If enhanced removal of vegetation occurs during major flood events, then it may take several years for high biomass levels to rebuild in some locations. Hence, vegetation driven MeHg production in the Yolo Bypass could experience boom and bust cycles based on more frequent and intense periods of drought combined with more intense storm flooding events which wipe out the vegetation. In some extreme droughts, biomass levels could also be lower if irrigation water was no longer available or was reduced. It is also possible that in winter, rye grass and other grazing forbs that remains standing in the Yolo Bypass, could change during an extended drought. We currently have no information on the production and release of MeHg from grasses and other vegetation other than rye grass.

Sea Level Rise

Over the last 100 years, there have been 158 island failures resulting in Delta island flooding (Department of Water Resources, 2009) (Figure 6-1). The pressure on Delta levees will increase with rising sea levels on the water side and falling land surface elevations (subsidence) on the land side of the levee. Predictions combining sea level rise and Delta island subsidence indicate that Delta levees may no longer meet the federal levee height standard (PL84-99) in the time frame of 2060-2080 (Brooks and others 2018). This will result in an increased risk of Delta levees being breached and previously dry pasture and farmland becoming submerged, creating newly flooded aquatic habitat, possibly permanently (Dettinger and others 2016). Even without climate change, the calculated probability of at least 10 island failures is estimated to be between 60 and 80% (Figure 6-2).

A rapid inundation of newly flooded land could have significant impacts on MeHg levels in overlying water. It is well known that creation of hydroelectric reservoirs by enlargement of riverine lakes and flooding of adjacent forested land leads to a marked rise in rates of MeHg production by microorganisms in sediments and is manifest in significant MeHg increases in finfish residing in the newly impounded waters (Jackson 1988; Kelly and others 1997; Willacker and others 2016). Moreover, this increase in MeHg production and increase in fish mercury levels can persist for many years to decades (Hall and others 2005; Bodaly and others 2007). It is reasonable to assume that a similar phenomenon will result in the Delta if levees are breached and pasture and farmland is rapidly inundated. This expansion of flooded land and enhanced potential for mercury methylation will be further exacerbated as much of the newly flooded land is highly peat rich, which would be a carbon source for promoting and enhancing microbial activity (Department of Water Resources,1995). The impact of a slow sea level rise to expanding the areas of inundation in the Delta will likely be minimal as levees keep water flow highly channelized. However, while sea level rise is a slow process, it will ultimately result in inundating some low-lying areas increasing the surface area for production of MeHg, in areas where no flooding had previously reached.

Figure 6-1 Photo of Jones Tract Levee Failure (June 4, 2004)

Source: DWR

Figure 6-2 Probability of exceeding a number of simultaneous islands flooding due to high water conditions over a 25-year period (2005-2030)
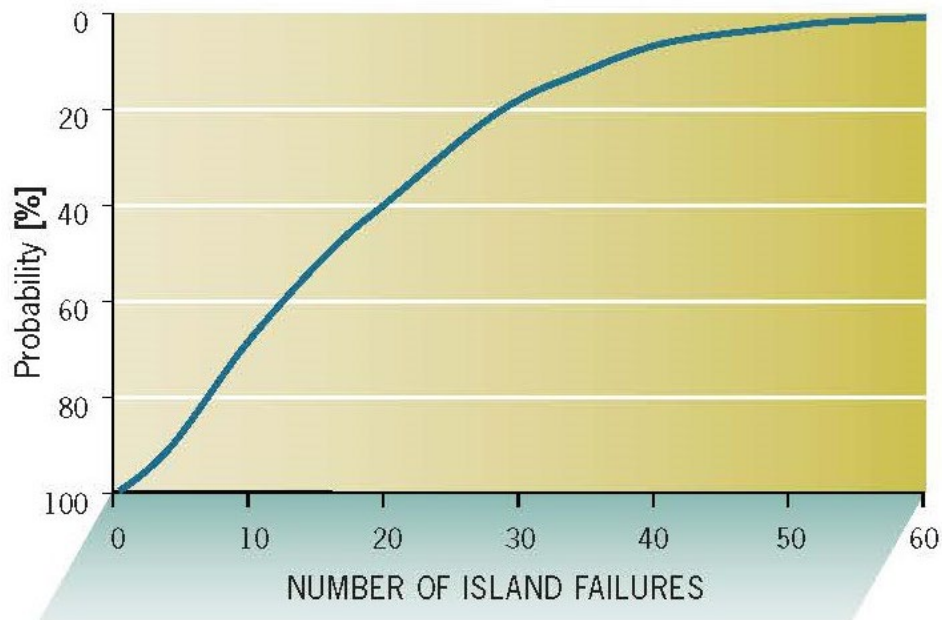
Source: Adapted from Delta Risk Management Strategy (DRMS) Report URS/JBA 2008c, Figure 13-11.

Figure 6-3 Historic Island Flooding in the Delta and Suisun Marsh Since 1900
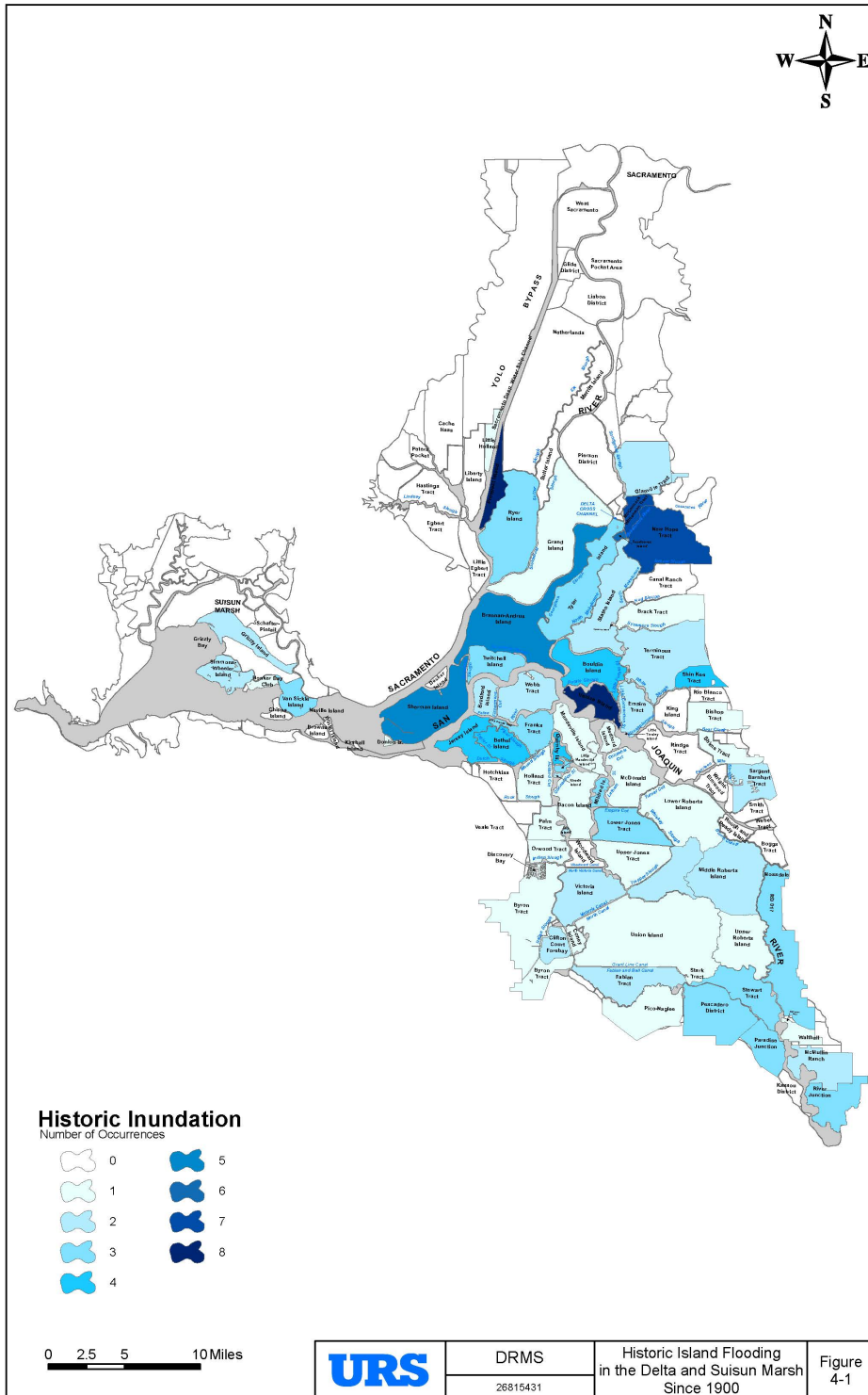
Figure Note: From Technical Memorandum: Delta Risk Management Strategy (DRMS) Phase 1. Topical Area: Levee Vulnerability Final, Figure 4-1, May 2008.

Figure 6-4 Historical Maximum Salinity Intrusions (Approximately 5 Percent Sea Water) Between 1921-1943 Prior to the Building of Shasta Dam
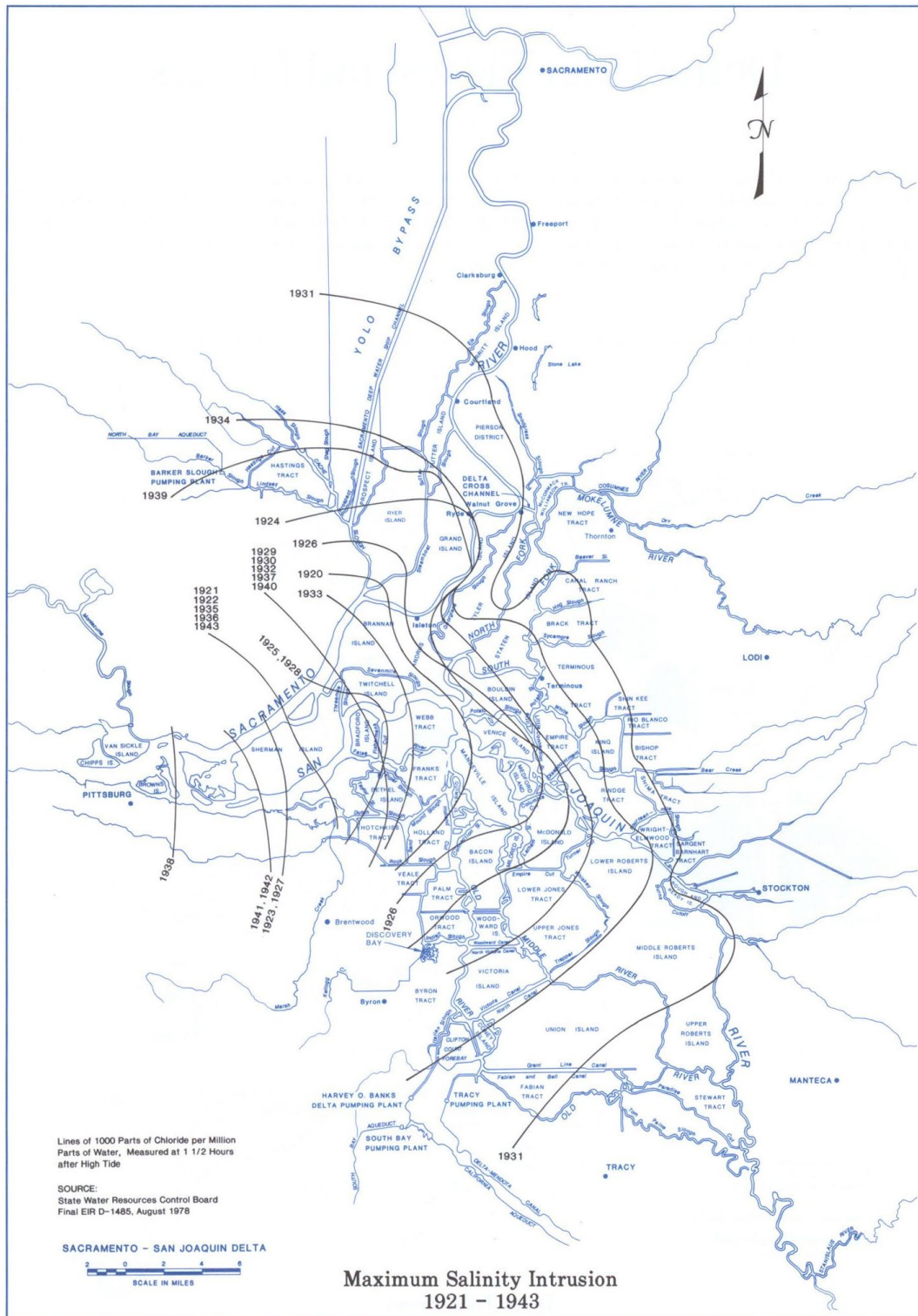
Source: DWR, 1995.

Salinity in the Delta depends on the balance between salt water coming into the Delta from the ocean and freshwater from tributary rivers pushing the saline water toward San Francisco Bay. When freshwater flows are higher, the Delta is less saline. When freshwater flows are lower, salinity intrudes further into the Delta. Under sea level rise, more saline water will flow into the Delta if adequate freshwater releases from upstream reservoirs are not available to keep the salinity in San Francisco Bay. Historically prior to the completion of the Central Valley Project, historical maximum salinity intrusions extended into the southern end of the Yolo Bypass (Figure 6-4) (Department of Water Resources, 1995). How a more saline environment will affect MeHg production is currently unknown.

Wildfire Impacts

Wildfires are predicted to be larger and more frequent in the Western United States, driven by reduced fuel moisture due to warming-induced increases in evaporative demand, reduced snowpack, and reduced warm-season precipitation frequency (Williams and others 2019; and references therein). A recent assessment by Williams and others (2019) found that between 1972 and 2018, California experienced a five-fold increase in annual burned area, mainly due to more than an eight-fold increase in summer forest-fire extent, which was attributed to significantly increasing the atmospheric vapor pressure deficit driven by climate change.

Mercury sequestered in biomass and soils is released during a fire into the atmosphere where a significant portion can be deposited locally in fallout (Biswas and others 2007; Rothenberg and others 2010; Pompeani and others 2018). This locally deposited mercury can enter into waterways and provide additional mercury substrate for methylation in aquatic systems. The impact can be quite significant, Kelly and others (2006) observed a 5-fold increase in whole-body mercury accumulation for rainbow trout in a mountain lake impacted by a forest fire.

Operational Impacts

California's water supply is tightly woven up with climate change. The majority of climate models project that the number and potentially the intensity of atmospheric rivers making landfall in California will increase significantly in the 21st century if greenhouse-gas emissions continue to increase (Dettinger 2011; Warner and others 2015; Hagos and others 2016), potentially resulting in larger peak flows and flood risks in the warming future. However, future changes in precipitation are much less certain than warming and some other changes like sea level rise and declines in surface air humidity (Cayan and others 2008; Dettinger and others, 2016). Climate change warming projections predict that both droughts and floods will increase as the climate warms, with storms becoming more intense, and intervening periods drier, longer, and warmer. Riverine inflows into the Delta will be affected by both shifting precipitation and runoff patterns and management decision on how to operate upstream reservoirs. A greater fraction of runoff generated could pass through the Delta earlier in the year. Warming will likely affect riverine inflows to the Delta, as winter storms warm and become rainier (less snow), and snowpacks melt earlier. As a result, summer salinity in the upper San Francisco Bay and Delta is projected to increase (Knowles and Cayan, 2004; Cloern and others, 2011) if sufficient freshwater releases from upstream reservoirs are not available counteract the salinity intrusion. Decreases in surface air humidity would result in greater potential for evapotranspiration from soil and vegetation, intensifying hydrologic droughts (Dettinger and others, 2016).

Warming temperatures, shifting hydrology, and rising sea levels associated with climate change is anticipated to have significant impacts on reservoir operations, and the State's water systems (Wang and others, 2018). Extra runoff is predicted from early snow melting and a higher percentage of rain in the winter and early spring. This extra runoff will not be conserved in reservoirs, but rather released as flood water in the winter and early spring to become Delta outflow. By mid-century, Delta exports are expected to be reduced by a half million-acre feet and north of Delta carryover storage would diminish by 1.5 million-acre feet. Reservoir dead storage is expected to occur much more frequently. Delta exports would reduce to half of those found in historical droughts while carryover storage would diminish to one-fifth of those found in historical droughts.

How these operational impacts will this effect MeHg behavior is currently unknown.

Major Climate Change Impacts on Methylmercury Biogeochemistry in the Yolo Bypass and Sacramento-San Joaquin Delta system

The previous section provided an overview of the generalized large-scale climate change impacts potentially affecting MeHg production in the Delta and the Yolo Bypass. In this section we relate work summarized in this report to site specific predictions for the Delta and Yolo Bypass based on a literature understanding of mercury and MeHg biogeochemistry.

Yolo Bypass

Another major finding of our vegetation senescence studies is that submerged vegetation undergoing degradation may be a significant contributor to internal MeHg production in the Yolo Bypass (see Chapter 3 and Technical Appendix E). Hence, any process which will affect vegetation biomass production will likely also impact MeHg production. Within the Yolo Bypass there are over 17,400 acres of vegetated pasture (area calculated from the Yolo Bypass D-MCM land use map), the largest land use in the Yolo Bypass. MeHg increases in both the water column and on the particles of vegetation. With increased volatility of rainfall, flooding and drought events, it is reasonable to assume that the Yolo Bypass will experience extended periods of drought. If water deliveries remain relatively "drought-proof," then we can expect to see the same level of biomass for irrigated pasture regardless of the water year type. However, biomass quantities for non-irrigated pasture may increase over successive, non-flood years. Seasonally non-irrigated pasture experiences seed germination with winter and spring rains. Since this vegetation is not irrigated, this vegetation dies during the heat of summer, forming a layer of dead grass material as well as thatch. The cycle repeats each season, resulting in a cumulative year over year build-up of dead vegetated material. Depending on the grazing pressure, this can form a dense build-up of biomass. The return frequency of large-scale inundation events then dictates when most of this vegetation will be removed. The longer the time-period between flood years, the potentially greater biomass from non-irrigated pasture, available for Hg methylation when flood waters return. Hence, vegetation driven MeHg production in the Bypass will experience boom and bust cycles based on more frequent and intense periods of drought combined with more intense storm flooding events which wipe out the vegetation.

Based on these vegetation dynamics, under projected climate change scenarios, our vegetation senescence experiments suggest that the Yolo Bypass will continue to be a net exporter of MeHg to the Delta. The combination of changes in temperature and precipitation, resulting in more precipitation falling as rain rather than snow, and occasional more intense storms, is projected to increase the frequency and

magnitude of floods in the tributaries that feed the Delta, including the Yolo Bypass. With increased flood severity and frequency, overtopping of the Fremont weir and widespread flooding of the Yolo Bypass will potentially increase. When flooding occurs, large acreages of pastureland will continue to be flooded with the potential for more acreage to become submerged if the severity and duration of the floods increases. Large areas of submerged vegetation will thus continue to serve as MeHg sources contributing to MeHg export from the Yolo Bypass.

Sacramento-San Joaquin Delta system

Climate change amounts to an, "additional" stressor in the Sacramento-San Joaquin Delta system. The Delta's climate is characterized by high variability, and climate change is expected to accentuate this variability, resulting in both more extreme flood risks and greater drought risks. Thus, the Delta of the future will be very different than the Delta we know today. Effects on the Delta ecosystem include sea level rise, reduced snowpack, earlier snowmelt and larger storm-driven streamflow's, warmer and longer summers, warmer summer water temperatures, and water quality changes.

It is reasonable to assume that larger and more frequent storm driven stream flows will result in greater erosion of Hg contaminated sediments in the Sierras and Coastal mountain ranges, resulting in enhanced loads of Hg entering the Delta. If this does occur, then there will likely be a greater abundance of Hg available for methylation than in the current case. This is consistent with our current work, where it was observed that as tributary flow into the Yolo Bypass increased during a flood event, the delivery of Hg and MeHg increased as well (see Chapter 3 and Technical Appendix B). Moreover, it is highly likely that most of the delivery of Hg loads to the Delta will occur primarily in the more intense storms, which are predicted to be more frequent under climate change.

It is further reasonable to speculate that climate impacts on the behavior, fate and transport of dissolved organic carbon (DOC) and particles, especially particulate organic carbon, will play a major role in how Hg biogeochemistry responds to climate change impacts in the Delta. This prediction is based on several factors and observations. First, it is well known that dissolved and particulate organic carbon plays a major role in the transport of Hg in aquatic systems (Mierle and Ingram, 1991; Driscoll and others, 1995; Mason and Sullivan, 1998; Schuster and others, 2011; Chiasson-Gould and others, 2014). Second, it is also well known that availability of labile organic matter for microorganism's productivity is one key parameter that strongly influences MeHg production (Lambertsson and Nilsson 2006; Graham and others, 2012; Marvin-DiPasquale and others, 2014). In the Yolo Bypass, Marvin-DiPasquale and others (2014) observed that MeHg production in agricultural and non-agricultural wetlands was not limited by sulfate bioavailability, but rather by the availability of labile organic carbon for microbial respiration. And third, several studies have predicted or observed that when tributary runoff increases (as is predicted for the Delta under climate change) there are often increases in organic carbon concentrations or loading and commensurate increases in Hg concentrations or loading (Shanley and others, 2008; Sebestyen and others, 2009; Dittman and others, 2010; Schuster and others, 2011; Schelker and others, 2011). Hence, if more Hg and organic matter is delivered to the Delta under a changing climate, one could reasonably predict that microbial production of MeHg will also increase. While the prediction that MeHg production is likely to increase under a changing climate in the Delta, the significance and magnitude of the enhancement is currently not known and will likely involve high uncertainty.

Data Gaps and Next Steps

How MeHg production, fate, and transport will change from climate change stressors has not been evaluated for the Yolo Bypass and the Delta Region. While general predictions (increase, decrease, remain the same) can be made based on our current understanding of MeHg biogeochemistry, such assessments have high uncertainty and do not provide magnitude or significance predictions. Modelling efforts and laboratory and field-based investigations (to fill critical data gaps for the modelling efforts) are warranted to test various scenarios regarding climate change impacts on MeHg production, behavior and transport in the Yolo Bypass and Delta. The hydrodynamic and Hg biogeochemistry models described in this report (the Yolo Bypass Dynamic Mercury Cycling Model [D-MCM] and the Delta Simulation Model 2 [DSM2] with mercury module) along with DWR's CalSim model[2] can be used to perform various climate change scenario investigations. Preliminary scenario testing with the above models can be used to identify major climate change drivers affecting MeHg production, behavior, fate, and transport, and to identify gaps in our knowledge that can be filled with laboratory or field-based investigations.

Specific questions to investigate regarding climate change driven alterations in MeHg production, behavior and transport in the Yolo Bypass and Delta include:

- How does the timing and magnitude of changes in tributary run-off influence MeHg production, behavior and transport?
- How does sea level rise (combined with subsidence) influence MeHg production, behavior and transport? What affect will salinity intrusion have on mercury methylation processes?
- How will changes in operations of the water delivery systems (to meet demands) influence MeHg production, behavior and transport?
- How will extended drought conditions influence MeHg production, behavior and transport? Of particular interest is whether MeHg production during a flood event in the Yolo bypass will increase, decrease or remain the same due to climate driven changes in vegetation biomass in pasture lands?
- How will atmospheric input of mercury change from climate impacts?
- Will levees be built-up in response to sea level rise or be allowed to breach and flood?
- How will conversion of primarily freshwater tidal wetlands to more saline tidal wetlands affect MeHg production as a result of sea level rise?
- Will larger and more frequent floods act to deliver fresh new Hg to the Delta from erosion in the Sierras?

---

[2] CalSim is a water resources planning model, jointly developed by the California Department of Water Resources (DWR) and the Mid-Pacific Region of the U.S. Bureau of Reclamation, to simulate operations of the State Water Project (SWP) and the Central Valley Project (CVP) and much of the water resources infrastructure in the Central Valley of California and the Sacramento-San Joaquin Delta region.

References

Bedsworth L, Cayan D, Franco G, Fisher L, Ziaja S. 2018. Statewide Summary Report. California's Fourth Climate Change Assessment. Publication number: SUM-CCCA4-2018-013. Viewed online at: http://www.climateassessment.ca.gov/. Accessed January 6, 2020.

Biswas, A, Blum JD, Klaue B, Keeler, GJ. 2007. Release of Mercury from Rocky Mountain Forest Fires. Global Biogeochemical Cycles, Volume 21, Issue 1, GB1002.

Bodaly, RA (Drew), Jansen WA, Majewski AR, Fudge RJP, Strange NE, Derksen AJ, Green DJ. 2007. Postimpoundment Time Course of Increased Mercury Concentrations in Fish in Hydroelectric Reservoirs of Northern Manitoba, Canada. Archives of Environmental Contamination and. Toxicology. Volume, 53, Pages 379–389. DOI 10.1007/s00244-006-0113-4.

Brooks BA., Telling J, Ericksen T, Glennie CL, Knowles N, Cayan D, Hauser D, LeWinter A. 2018. High Resolution Measurement of Levee Subsidence Related to Energy Infrastructure in the Sacramento-San Joaquin Delta. California's Fourth Climate Change Assessment, California Energy Commission. Publication Number: CCCA4-CEC-2018-003. Viewed online at: http://www.climateassessment.ca.gov/. Accessed January 6, 2020.

Cayan DR, Maurer EP, Dettinger MD, Tyree M, Hayhoe K. 2008. Climate Change Scenarios for the California Region. Climate Change Volume 87, Supplement 1, S21-S42.

Chiasson-Gould SA, Blais JM, Poulain AJ. 2014. Dissolved Organic Matter Kinetically Controls Mercury Bioavailability to Bacteria. Environmental Science and Technology, Volume 48, Issue 6, Pages 3153-3161. https://doi.org/10.1021/es4038484.

Cloern JE, Knowles N, Brown LR, Cayan D, Dettinger MD, Morgan-King TL, Schoellhamer DH, Stacey MT, van der Wegen M, Wagner RW, Jassby AD. 2011. Projected Evolution of California's San Francisco Bay-Delta River System in a Century of Climate Change. PloS One Volume 6, Issue 9, e24465. Viewed online at: https://www.ncbi.nlm.nih.gov/pmc/articles/PMC3177826/. Accessed January 6, 2020.

Department of Water Resources, 1995. Sacramento Delta San Joaquin Atlas. Reprinted July 1995, 121 pgs. Viewed online at http://baydeltaoffice.water.ca.gov/DeltaAtlas/. Accessed November 12, 2019.

Department of Water Resources. 1995. Sacramento-San Joaquin Delta Atlas. Viewed online at: https://mavensnotebook.com/resource-pages/maps-and-diagrams/maximum-salinity-intrusion-1921-1943/. Accessed November 1, 2019

Department of Water Resources. 2009. Delta Risk Management Strategy, Executive Summary. Viewed online at http://www.water.ca.gov/floodmgmt/dsmo/sab/drmsp. Accessed August 1, 2019.

Delta Risk Management Strategy: 2008. Technical Memorandum: Delta Risk Management Strategy (DRMS) Phase 1 Topical Area: Levee Vulnerability Final. Prepared by URS Corporation/Jack R. Benjamin & Associates, Inc. for the California Department of Water Resources, May 15, 2008.

Desrosiers M, Planas D, Mucci A. 2006. Mercury Methylation in the Epilithon of Boreal Shield Aquatic Ecosystems. Environmental Science and Technology, Volume 40, Pages 1540-1546.

Dettinger MD. 2011. Climate Change, Atmospheric Rivers and Floods in California-A Multimodel Analysis of Storm Frequency and Magnitude Changes. Journal of the American Water Resources Association, Volume 47, Pages 514-502

Dettinger, M., Anderson, J, Anderson M, Brown LR, Cayan, D., Maurer, D. 2016. Climate Change and the Delta. San Francisco Estuary and Watershed Science, Volume 14, Issue 3, Pages 2-26.

Dittman JA, Shanley JB, Driscoll CT, Aiken GR, Chalmers AT, Towse JE, Selvendiran P. 2010. Mercury Dynamics in Relation to Dissolved Organic Carbon Concentration and Quality During High Flow Events in Three Northeastern U.S. Streams. Water Resources Research, Volume 46: W07522. doi:10.1029/2009WR008351.

Driscoll CT, Blette V, Yan C, Schofield CL, Munson R, Holsapple J. 1995. The Role of Dissolved Organic Carbon in the Chemistry and Bioavailability of Mercury in Remote Adirondack Lakes, Water Air and Soil Pollution, Volume 80, Pages 499–508.

Gershunov A, Shulgina T, Clemesha RES, Guirguis K, Pierce DW, Dettinger MD, Lavers DA, Cayan DR, Polade SD, Kalansky J, Ralph FM. 2019. Precipitation Regime Change in Western North America: The Role of Atmospheric Rivers. Nature – Scientific Reports, Viewed online at: https://www.nature.com/articles/s41598-019-46169-w.

Graham AM., Aiken GR, Gilmour CC. 2012. Dissolved Organic Matter Enhances Microbial Mercury Methylation Under Sulfidic Conditions. Environmental. Science and Technology, Volume 46, Issue 5, Pages 2715-2723. https://doi.org/10.1021/es203658f.

Hagos SM, L. Leung R, Yoon J-H, Lu J, Gao Y. 2016. A Projection of Changes in Landfalling Atmospheric River Frequency and Extreme Precipitation Over Western North America from the Large Ensemble CESM Simulations. Geophysical. Research. Letters, Volume 43, Pages 1357–1363, doi:10.1002/2015GL067392.

Hall BD, St. Louis VL, Rolfhus KR, Bodaly RA, Beaty KG, Paterson MJ, and Peech Cherewyk KA. 2005. Impacts of Reservoir Creation on the Biogeochemical Cycling of MeHg and Total Mercury in Boreal Upland Forests. Ecosystems, Volume 8, Pages 248–266. DOI: 10.1007/s10021-003-0094-3.

Jackson TA. 1988. The Mercury Problem in Recently Formed Reservoirs of Northern Manitoba (Canada): Effects of Impoundment and Other Factors on the Production of MeHg by Microorganisms in Sediments. Canadian Journal of Fisheries and Aquatic Sciences, Volume 45, Issue 1, Pages 97-121. https://doi.org/10.1139/f88-012.

Kelley EN, Schindler DW, St. Louis VL, Donald DB, Vladicka KE. 2006. Forest Fire Increases Mercury Accumulation by Fishes Via Food Web Restructuring and Increased Mercury Inputs. Proceedings of the National Academy of Sciences, Volume 103, Pages 19380-19385.

Kelly CS, Rudd JWM, Bodaly RA, Roulet NP, St.Louis VL, Heyes A, Moore TR, Schiff S, Aravena R, Scott KJ, Dyck B, Harris R, Warner B, Edwards G. 1997. Increases in Fluxes of Greenhouse Gases and MeHg Following Flooding of an Experimental Reservoir. Environmental Science and Technology, Volume 31, Issue 5, Pages 1334-1344. https://doi.org/10.1021/es9604931.

Knowles N, Cayan, DR. 2004. Elevational Dependence of Projected Hydrologic Changes in the San Francisco Estuary and Watershed. Climate Change, Volume 62, Pages 319-336.

Lambertsson L, Nilsson M. 2006. Organic Material: The Primary Control on Mercury Methylation and Ambient MeHg Concentrations in Estuarine Sediments. Environmental Science and Technology, Volume 40, Issue 6, Pages 1822-1829. https://doi.org/10.1021/es051785h.

Marvin-DiPasquale M, Windham-Myers L, Agee JL, Kakouros E, Kieu L, Fleck JA, Alpers CN, Stricker CA. 2014. Methylmercury Production in Sediment from Agricultural and Non-Agricultural Wetlands in the Yolo Bypass, California, USA. Science of the Total Environment, Volume 484, Pages 288–299. http://dx.doi.org/10.1016/j.scitotenv.2013.09.098.

Mason RP, Sullivan KA. 1998. Mercury and Methylmercury Transport Through an Urban Watershed. Water Research, Volume 32, Issue 2, Pages 321-330. https://doi.org/10.1016/S0043-1354(97)00285-6.

Mierle G, Ingram R. 1991. The Role of Humic Substances in the Mobilization of Mercury from Watersheds. Water, Air, and Soil Pollution, Volume 56, Pages 349-357.

Pierce DW, Kalansky JF, Cayan DR, (Scripps Institution of Oceanography). 2018. Climate, Drought, and Sea Level Rise Scenarios for the Fourth California Climate Assessment. California's Fourth Climate Change Assessment, California Energy Commission. Publication Number: CNRA-CEC-2018-006.

Pompeani DP, Cooke CA, Abbot MB, Drevnick PE. 2018. Climate, Fire, and Vegetation Mediate Mercury Delivery to Midlatitude Lakes over the Holocene. Environmental Science and Technology, Volume 52, Issue 15, Pages 8157-8164.

Rothenberg SE, Matthew EK, Bird BW, DeRose MB, Lin C-C, Feng X, Ambrose RF, Jay JA. 2010. The Impact of Over 100 Years of Wildfires on Mercury Levels and Accumulation Rates in Two Lakes in Southern California, USA. Environmental Earth Sciences, Volume 60, Pages 993–1005.

Schelker JD, Burns A, Weiler M, Laudon H. 2011. Hydrological Mobilization of Mercury and Dissolved Organic Carbon in A Snow-Dominated, Forested Watershed: Conceptualization and Modeling. Journal of Geophysical Research, Volume 116, G01002. doi:10.1029/2010JG001330.

Schuster PF, Striegl RG, Aiken GR, Krabbenhoft DP, Dewild JF, Butler K, Kamark B, Dornblaser M. 2011. Mercury Export from the Yukon River Basin and Potential Response to a Changing Climate. Environmental Science and Technology, Volume 45 Pages 9262–9267. dx.doi.org/10.1021/es202068b.

Schwarz A, Ray P, Wi S, Brown C, He M, Correa M. (California Department of Water Resources). 2018. Climate Change Risks Faced by the California Central Valley Water Resource System. California's Fourth Climate Change Assessment. Publication number: CCCA4-EXT-2018-001.

Sebestyen SD, Boyer EW, Shanley JB. 2009. Responses of Stream Nitrate and DOC Loadings to Hydrological Forcing and Climate Change in an Upland Forest of the Northeastern United States. Journal of Geophysical Research Volume. 114, G02002, doi:10.1029/2008JG000778.

Shanley JB, Mast MA,.Campbell DH, Aiken GR, Krabbenhoft DP, Hunt RJ, Walker JF, Schuster PF, Chalmers A, Aulenbach BT, Peters NE, Marvin-DiPasquale M, Clow DW, Shafer MM. 2008. Comparison of Total Mercury and Methylmercury Cycling at Five Sites Using the Small Watershed Approach, Environmental Pollution., Volume 154, Pages 143–154.

St. Pierre KA., Chételat J, Yumvihoze E, Poulain AJ. 2014. Temperature and the Sulfur Cycle Control Monomethylmercury Cycling in High Arctic Coastal Marine Sediments from Allen Bay, Nunavut, Canada. Environmental Science and Technology, Volume 48, Pages 2680−2687. dx.doi.org/10.1021/es405253g.

Thorne JH, Wraithwall J, Franco G. 2018. California's Changing Climate 2018. California's Fourth Climate Change Assessment, California Natural Resources Agency.

Wang J, Yin H, Reyes E, Smith T, Chung F. (California Department of Water Resources). 2018. Mean and Extreme Climate Change Impacts on the State Water Project. California's Fourth Climate Change Assessment. Publication number: CCCA4-EXT-2018-004.

Warner MD, Mass CF, Salathé Jr. EP. 2015. Changes in Winter Atmospheric Rivers Along The North American West Coast in CMIP5 Climate Models, Journal of. Hydrometeorology, Volume 16, Pages 118–128.

Willacker JJ, Eagles-Smith CA, Lutz MA, Tate MT, Lepak JM, Ackerman JT. 2016. Reservoirs and Water Management Influence Fish Mercury Concentrations in the Western United States and Canada. Science of the Total Environment, Volume 568, Pages 739-748.

Williams PA, Abatzoglou JT, Gershunov A, Guzman-Morales J, Bishop DA, Balch JK, Lettenmaier DP. 2019. Observed Impacts of Anthropogenic Climate Change on Wildfire in California. Earth's Future, Volume 7, Pages: 892–910. https://doi.org/ 10.1029/2019EF001210.

Yang A, Fang W, Lu X, Sheng G-P, Graham DE, Liang L, Wullschleger SD, Gu B. 2016. Warming Increases Methylmercury Production in an Arctic Soil. Environmental Pollution, Volume 214, Pages 504-509.

Mercury Open Water Final Report for Compliance with the Delta Mercury Control Program

Chapter 7. Conclusions-Management Implications

Submitted by the Open Water Workgroup

August 31, 2020

Contents

List of Acronyms and Abbreviations

BMP   Best Management Practice

CCSB   Cache Creek Settling Basin

Delta   Sacramento-San Joaquin Delta system

D-MCM   Dynamic Mercury Cycling Model

DSM2   Delta Simulation Model 2

DWR   (California) Department of Water Resources

fMeHg   Filter-passing Methylmercury

Hg   Mercury

MeHg   Methylmercury

uHg   An unfiltered (aqueous) mercury (sample)

uMeHg   An unfiltered (aqueous) methyl mercury (sample)

Management Implications

Field and Laboratory Results

One of the most important findings associated with our research was identifying the important role decomposing vegetation may play in the production of MeHg in the Yolo Bypass. Independent MeHg load extrapolations of pastureland laboratory results compared favorably with the robust load calculations for the entire Yolo Bypass in the 2017 water year flood season. Although several assumptions went into these extrapolations, the results suggest that mesocosm and laboratory experiments captured mechanisms exhibited under extended flooding in the Yolo Bypass, when most of the MeHg is discharged to the Delta.

Managing vegetation as a key component of reducing winter internal Yolo Bypass methylation has important management considerations and provides a starting point for future open water control studies and development of Best Management Practices (BMPs). However, it is important to note that the (California) Department of Water Resources (DWR) is not a landowner in the Yolo Bypass, therefore any changes in land use practices are outside its jurisdiction and must be pursued and negotiated by the Regional Water Quality Control Board in cooperation with the individual land-owners and agencies. In addition, any changes in land use management does not address the underlying problem of mercury (Hg) delivery via the discharge of Hg laden sediment from upstream abandoned mines. As detailed by Singer and others (2013), major flood events continue to erode legacy Hg-laden sediment. They estimate this process will continue for at least another 10,000 years. Since control studies were not conducted, our research cannot answer specifics on control studies' feasibility, effectiveness, cost, and compliance.

Much attention has been placed on the Cache Creek Settling Basin (CCSB) and its contributions of inorganic Hg and MeHg to the Yolo Bypass. However, our coarse estimates of MeHg mass generated from decaying vegetation suggests that reductions in vegetation biomass could substantially help with the Yolo Bypass load allocation reduction required in the DMCP. However, these mass estimates need to be refined to accurately reflect the true MeHg mass of decaying vegetation,

Additionally, from a management standpoint, the source of the Hg resulting in this vegetative methylation in the Yolo Bypass (whether from the CCSB, over-toppings of the Fremont weir, the atmosphere, or other sources or pathways), requires further evaluation. For example, Bloom (2002) determined that mine derived solids from the Cache Creek watershed were approximately 20 times less bioavailable towards methylation than Hg (II). Focusing on discharges from the CCSB, while not understanding the Hg source behind vegetative methylation and methylation in general in the Yolo Bypass, could lead to management actions that unintentionally have less impact on in-bypass MeHg production than anticipated. It is not clear from our experimental work whether the key influence of vegetation on methylation is via effects on the activity of methylating microbes (e.g., via a supply of labile carbon) or via changes to the concentration of available Hg(II) for methylation (e.g., via increased DOC).

The sections below briefly highlight some of the management implications associated with vegetation and land use management as a possible BMP.

Disking of Pastureland

Disking vegetation into the soil appears to be a promising approach to reduce the internal production of MeHg in the Yolo Bypass. Our vegetation senescence studies clearly showed that disking pasture vegetation into the soil results in less MeHg production over a vegetated soil (see Chapter 3 and Technical Appendix E). However, like any proposed BMP, this approach also needs to be evaluated holistically within the full context of the environment that the BMP would be used. From a livestock perspective, it may be undesirable to disk pastureland. From a climate change perspective, tillage of vegetation is discouraged because of the loss of sequestered carbon in the soil during tillage and the loss of carbon sequestration from standing vegetation (Woodbury and Wightman, 2017). Whether this is an issue for the Yolo Bypass is unknown. From a regulatory perspective, it needs to be determined how a disking requirement would be implemented. Therefore, while disking appears to be a promising BMP, its implementation requires closer examination.

Reduction in Vegetation Biomass

Our vegetation senescence studies suggest that understanding the role of vegetation quantity, quality, and type in the Yolo Bypass may provide approaches to future BMPs. However, management implications of this approach are complicated due to the complex interplay between plant growth and the environment. For example, our experiments had mixed results on MeHg production when plant biomass was reduced by grazing. Complicating this picture were results suggesting that the quality of the vegetation (e.g., new versus old growth), as well as the quantity, influences MeHg production from senescing vegetation (see Chapter 3 and Technical Appendix E). Moreover, the current research focused only on rye grass. It is unknown whether other vegetation types will respond in a similar fashion. These caveats confound the simplistic explanation that less vegetation will equal less MeHg production. Therefore, while an encouraging start, the dynamics between vegetation quality, quantity, and vegetation type requires further investigation before a definitive BMP can be proposed.

It is recommended that before additional studies are conducted, landowners and agencies, such as the Resource Conservation Districts, will need to be consulted to determine if the ecological and cost-benefit impacts, associated with this potential management approach, are reasonable or practical.

Selective Flooding

Selective flooding of pastures in the fall, prior to the winter flood season, may be another approach to reduce or remove the standing biomass of vegetation and reduce methylmercury production from vegetation during a flood event. Throughout the fall, prior to major flooding in the Yolo Bypass, rice fields and seasonal wetlands are intentionally flooded to break-down plant material, leach salts, and provide habitat for migrating waterfowl. Previous work (Heim and others, in prep.) has shown that when flooded in the fall, seasonal wetland MeHg concentrations in water quickly spike after fall flood-up and return to lower levels by early December. Flooding of pasture vegetation in the fall potentially has the advantage of removing vegetation biomass available for microbial respiration prior to major flooding and downstream export and potentially increasing MeHg destruction from photodegradation (Fleck and others, 2014). However, the seasonality of elevated MeHg concentrations in decaying vegetation can be highly variable and requires further study. For example, in a study by Alpers and others (2014), water was applied in mid-November 2007 to a post-harvest white rice field in the Yolo Wildlife Area, resulting in very high concentrations of uMeHg and fMeHg three months later, in February 2008, during region-wide flooding of white rice fields. Therefore, to be considered a useful tool, the timing of fall flood-ups and

draw-downs and vegetation decay rates requires investigation. For this approach to work, it will be critical that most of the vegetation has decayed and been removed from the system prior to winter flooding. Additionally, depending on the timing, holding water may result in elevated mercury exposure to wildlife using the area. Therefore, whether this land management practice is achievable or practical within current pasture management practices will require further investigation and discussion with current landowners.

Liberty Island

Our studies did not evaluate the cause(s) behind the MeHg loads originating from Liberty Island in water year 2017. While not as large a source as the upper reach of the Yolo Bypass, from a management perspective, understanding the sources of MeHg contributions from Liberty Island may require management approaches specific to that area.

Modeling Results

Yolo Bypass

Model sensitivity runs in the Yolo Bypass examined possible management approaches to reduce MeHg supply. These simulations imposed 50% reductions on selected model inputs anticipated to affect MeHg supply, including factors affecting MeHg production in the Yolo Bypass, and tributary loading rates for solids, inorganic Hg and MeHg. The choice of 50% reductions was meant to be large enough to generate a response in the model and was not necessarily intended as a practical real-world scenario in all cases. The sections below briefly highlight some of the management implications associated with the biogeochemical Hg modeling results from the Yolo Bypass D-MCM model. The Delta DSM2-Hg model was calibrated, but due to insufficient time and resources, sensitivity runs were not conducted.

Sensitivity Analyses

Of the sensitivity runs investigated for the Yolo Bypass, those primarily affecting MeHg production in surface sediments had the largest benefit (up to a 20% reduction in the export of MeHg from the Bypass). This suggests potential benefits for management options that reduce MeHg production in the Yolo Bypass sediment bed. Methylation rates in sediments are influenced by a range of factors that can broadly be grouped into two categories: those affecting the activity of microbes that produce MeHg and those affecting the concentration of Hg(II) available for the production of MeHg. Related site conditions potentially include changes in the supply of organic matter (e.g. via vegetation), temperature, water chemistry (DOC or pH) and the rate of supply of Hg(II) to sites of methylation. In terms of practical management options, the supply of organic matter (e.g., from vegetation) and reduced inputs of inorganic Hg(II) to the Yolo Bypass emerge as initial candidates. In the case of vegetation, Figure 7-1, shows the reduction in MeHg production in different land use areas in the Yolo Bypass for a simulation identical to the base case calibration, except with the removal of all vegetation.

Other sensitivity simulations had less effect than initially expected. For example, reducing the load of suspended sediments from the CCSB (and associated Hg(II) and MeHg) had a small effect on MeHg concentrations and export in the Yolo Bypass, despite CCSB being an important source of Hg(II) in the Yolo Bypass budget. Upon closer examination, the 16-year simulation may not have allowed sufficient

time for the effects of this simulation to be fully realized. This points out the need to consider the time for management actions to take effect and the need to understand (via field work and modeling) what controls the rate of response following management actions.

Figure 7-1 Modeled Effect of Net MeHg Production (g/year) due to Removal of all Vegetation by Land Use Type in the Yolo Bypass
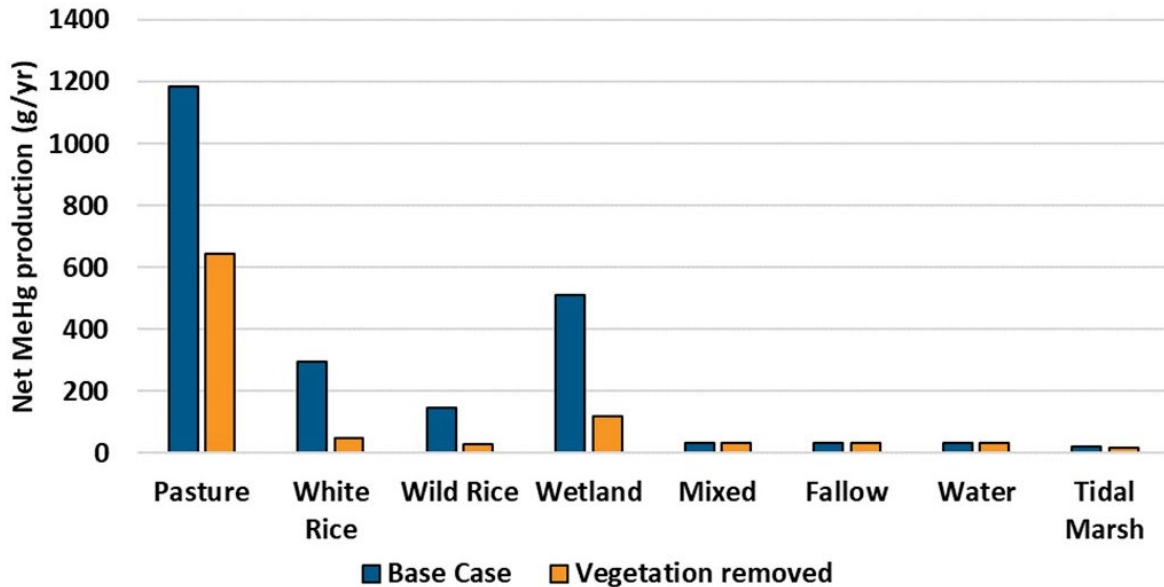
Delta

Based on resource and time constraints, exploration of management implications was limited. However, the Delta mercury model was used to simulate conditions from October 1999 to July 2006. Relative contributions of mercury sources and how those sources vary during wet and dry years can be explored. Given the rapid water throughput in the Delta, tributary loads were important sources of solids, inorganic Hg, and MeHg in simulations. The Sacramento River was the largest tributary source of MeHg to the Delta (roughly half of the total), followed by Yolo Bypass (one third of the total for the full simulation period, up to half in a wet year). The relative importance of different tributary sources varied among years in simulations. For example, the Yolo Bypass was more important as a source of MeHg during wet years. In the future, the model could be used to simulate relative changes in MeHg loads and concentrations in the Delta for various management or source reduction alternatives. Modeling management alternatives would require additional resources and may require running other models (e.g., such as reservoir operations models).

The model analysis also pointed out that seemingly straightforward management options may have multiple effects on hydrology, sediment transport, Hg cycling, and MeHg supply, sometimes in competing directions. For example, tributary loads are the product of concentrations and flows. Some loads could be high as a result of high flows, with relatively low concentrations. A reduction in the supply of water from such a source would indeed reduce the load of a constituent but might not have a

corresponding effect on reducing concentrations in receiving waters. Essentially, a tributary with these characteristics could help dilute concentrations that would occur otherwise. The distinction between lowering loads and lowering concentration could also emerge when recognizing that the food web in the Delta does not bioaccumulate based directly on MeHg loads. Exposure is based on MeHg concentrations. The duration of exposure for fish is the same in wet or dry years, and their uptake is based on concentrations during those periods. Given that the relative importance of MeHg sources to the Delta varied among years in simulations, consideration should also be given to exposure in dry years and sources of MeHg during those periods. This issue was not fully explored during the model analysis but warrants further consideration.

Overall, model results for the Delta and Yolo Bypass illustrated high variability in loads of suspended sediments, inorganic Hg, and MeHg, strongly influenced by the dynamic hydrology of the system. This variability occurred under short and longer time scales (e.g. events to years). This has important implications when estimating present-day baseline loads, assigning load allocations, and monitoring for compliance with regulations in the future. A multi-year perspective is needed, designed to capture year to year variability, but with sufficient resolution to also capture short term variability (or not be biased by it), and show longer term systematic trends that might occur (e.g., via climate change).

References

Alpers CN, Fleck JA, Marvin-DiPasquale M, Stricker CA, Stephenson M, Taylor HE. 2014. "Mercury Cycling in Agricultural and Managed Wetlands, Yolo Bypass, California: Spatial and Seasonal Variations in Water Quality." Science of the Total Environment. Volume 484, Pages 276-287.

Bloom NS. 2002. Solid Phase Hg Speciation and Incubation Studies in or Related to Mine-Site Runoff in the Cache Creek Watershed (CA).,In: Assessment of Ecological and Human Health Impacts of Mercury in The Bay-Delta Watershed. CALFED Bay-Delta Mercury Project Final Report.,

CVRWQCB 2018. The Water Quality Control Plan (Basin Plan) for the California Reginal Water Quality Control Board Central Valley Region, Fifth Edition, The Sacramento River and San Joaquin River Basins. Viewed online at https://www.waterboards.ca.gov/centralvalley/water_issues/basin_plans/sacsjr_201805.pdf. Accessed: Dec. 5, 2019. Last updated: June 13, 2019.

Fleck JA, Gill GA, Bergamaschi BA, Kraus T, Downing BD, Alpers, CN. 2014. "Concurrent Photolytic Degradation of Aqueous Methylmercury and Dissolved Organic Matter." Science of the Total Environment. Volume 484, Pages 263-275. http://dx.doi.org/10.1016/j.scitotenv.2013.03.107.

Heim WA, Weiss-Penzias P, Stephenson M, Negrey J, Litton G, and Coale KH. (in prep). "Using Polishing Ponds to Lower Monomethylmercury Concentration in a Seasonally Inundated Wetland Environment: Results of a Large Scale Replicated Field Experiment."

Marvin-DiPasquale M, Windham-Myers L, Agee JL, Kakouros E, Kieu LH, Fleck JA, Alpers CN, Stricker CA. 2014. "Methylmercury Production in Sediment from Agricultural and Non-Agricultural Wetlands in the Yolo Bypass, California, USA." Science of the Total Environment. Volume 484, Pages 288-299.

Singer MB, Aalto R, James LA, Kilham NE, Higson, JL, and Ghoshal, S. 2013. "Enduring Legacy of a Toxic Fan Via Episodic Redistribution of California Gold Mining Debris. Proceedings of the National Academy of Sciences of the United States of America." Volume 110, Issue 46, Pages 18436-18441.

Woodbury P and Wightman J. 2017. *Soil Carbon Management and Greenhouse Gas Mitigation Opportunities,* Information Sheet #6. Cornell University. Viewed Online at: https://cpb-u.s-e1.wpmucdn.com/blogs.cornell.edu/dist/2/7553/files/2017/09/IS6-Soil-Carbon-Management-Greenhouse-Gas-Mitigation-Opportunities-1nnur5m.pdf. Accessed November 1, 2019.